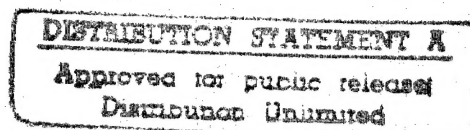


**NASA CONTRACTOR
REPORT**



NASA CR-235

NASA CR-235



**DEVELOPMENT OF A PREDISTRIBUTED
AZIDE BASE POLYURETHANE FOAM
FOR RIGIDIZATION OF SOLAR
CONCENTRATORS IN SPACE**

by N. Jouriles and C. E. Welling

19960502 139

Prepared under Contract No. NAS 1-3301 by
GOODYEAR AEROSPACE CORPORATION
Akron, Ohio

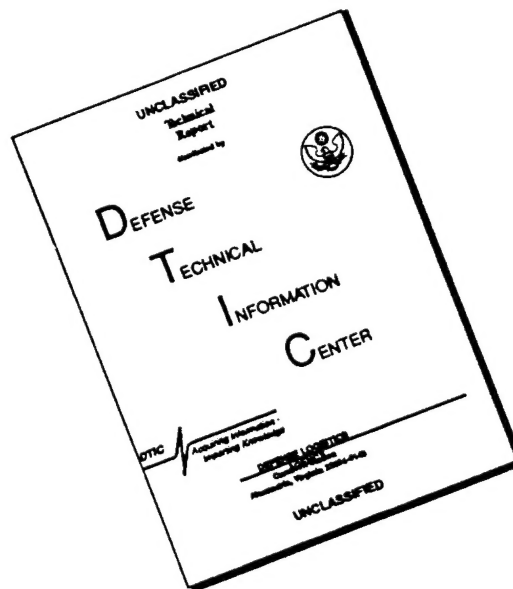
DEPARTMENT OF DEFENSE
PLASTICS TECHNICAL EVALUATION CENTER
PICATINNY ARSENAL, DOVER, N. J.

for
NATIONAL AERONAUTICS AND SPACE ADMINISTRATION • WASHINGTON, D. C. • JUNE 1965

DTIC QUALITY INSPECTED 1

PLASTEC 7278

DISCLAIMER NOTICE



THIS DOCUMENT IS BEST QUALITY AVAILABLE. THE COPY FURNISHED TO DTIC CONTAINED A SIGNIFICANT NUMBER OF PAGES WHICH DO NOT REPRODUCE LEGIBLY.

DEVELOPMENT OF A PREDISTRIBUTED AZIDE BASE
POLYURETHANE FOAM FOR RIGIDIZATION OF
SOLAR CONCENTRATORS IN SPACE

By N. Jouriles and C. E. Welling

DISTRIBUTION STATEMENT A

Approved for public release
Distribution Unlimited

Distribution of this report is provided in the interest of information exchange. Responsibility for the contents resides in the author or organization that prepared it.

Prepared under Contract No. NAS 1-3301 by
GOODYEAR AEROSPACE CORPORATION
Akron, Ohio

for

NATIONAL AERONAUTICS AND SPACE ADMINISTRATION

~~For sale by the Clearinghouse for Federal Scientific and Technical Information
Springfield, Virginia 22151 - Price \$6.00~~

DTIC QUALITY INSPECTED 1

ABSTRACT

This ~~final~~ report covers a successful 14-month effort to develop a predistributed foam material applicable for the rigidization of solar concentrators in space. Seven months of chemical research and development yielded an azide base polyurethane foam formulation that: (1) could be applied as paste on a membrane structure; (2) could be foam activated and rigidized by the application of heat; and (3) could produce a foam product that would meet the design goals of a space solar concentrator.

Twelve azide structures were investigated, and a prepolymerized polyol resin, a blocked isocyanate, a microquartz filler, and various catalysts, surfactants, and plasticizers were examined in the development of the foam formulation. Although a number of limitations were encountered in the development process (e. g., availability of certain azides, purity, synthesizing of azide structures, and effectiveness of azides, plasticizers, catalysts and surfactants), an optimum formulation was developed based on the work accomplished. The foam product, which was produced in vacuum, was also tested in vacuum for physical property values. Tensile ultimate stress values as high as 20 psi and tensile modulus values up to 1385 psi were obtained for foam densities of approximately 4 pcf. Solar concentrators of up to two feet in diameter have been foam rigidized in vacuum. Contour measurements on one model gave less than 0.1 inch deviation from a perfect paraboloid over almost all of the surface area.]

A problem area is the removal of gases from the vacuum chamber during the foaming process (pressure surge). One of the conclusions is that a workable predistributed foam has been developed. Recommendations include advanced development efforts in the production of larger mirrors, and further improvement of the foam quality.

TABLE OF CONTENTS

Section	Page
I INTRODUCTION	1
II SUMMARY	5
A. General	5
B. Foam Formulation	6
C. Physical Property Tests	9
D. Rigidization of Two-Foot Models	9
III FOAM PRODUCT AND PROCESS DEVELOPMENT	11
A. Scope	11
B. Technical Background	11
C. Process Characterization	12
D. Studies of Acid Azides	15
E. Polyol Resins Utilized	24
F. Synthesis and Properties of Hydroxyl - Terminated Prepolymers	27
G. Precoat Formulation for an Isothermal Foaming Process	34
H. Precoat Formulation for an Adiabatic Foaming Process . . .	38
IV PREPARATION OF PHYSICAL TEST SPECIMENS	53
V PHYSICAL PROPERTIES	57
A. General	57
B. Discussion of Test Data and Results	60
VI TWO-FOOT MODELS	121
A. Fabrication	121
B. Rigidization	128
C. Contour Measuring Tool	146
D. Contour Measurements	146

TABLE OF CONTENTS

Section		Page
VII	PROBLEM AREAS	159
VIII	CONCLUSIONS AND RECOMMENDATIONS	161
	REFERENCES	165
Appendix		
A.	TEMPERATURE ANALYSIS TO PRODUCE REQUIRED HEAT SCHEDULE BY SELECTIVE SURFACES	A-1
B.	AZOMETER TEST AND ANALYSIS	B-1
C.	MEASUREMENT OF HEAT RELEASE FROM AZIDE REARRANGEMENT	C-1
D.	SUBLIMATION TESTS	D-1
E.	ORGANIC AZIDE TEST RESULTS - U.S. NAVAL AMMUNITION DEPOT LETTER	E-1
F.	ORGANIC AZIDE TEST RESULTS FOR SHIP- PING CLASSIFICATION	F-1
G.	CONTOUR MEASUREMENTS	G-1
H.	GEOMETRIC CONTOUR MEASURING FIXTURE	H-1

LIST OF ILLUSTRATIONS

Figure		Page
1	Quarter View of Front Surface of Concentrator Showing Concentrating Rays.	4
2	Block Diagram of Rigidizing Process for Precoat Material. . . .	7
3	Temperature History of Precoat Foam Reaction	8
4	Preparation of Six-Inch Disk Test Sample - Precoat Foam on Aluminized Mylar	41
5	Test Sample in Ring Fixture	41
6	Bell Jar Test Facility	42
7	Test Run in Evacuated Bell Jar with Heat Applied	43
8	Removal of Test Sample from Bell Jar	44
9	Heat Distortion Tests - Experimental Prepolymer Formulations .	45
10	Heat Distortion Tests - High Azide Concentration	47
11	Heat Distortion Tests - With Microquartz Added	49
12	Typical Foam Mass	54
13	Typical Foam Mass Section	54
14	Stress-Strain Test Setup	63
15	Sample Plots of Brittle and Ductile Foam Tests	63
16	Tensile Ultimate Stress versus Density	66

LIST OF ILLUSTRATIONS

Figure		Page
17	Tensile Ultimate Stress versus Temperature for Density Range Tested	67
18	Tensile Yield Stress versus Density	68
19	Tensile Yield Stress versus Temperature for Density Range Tested	69
20	Tensile Modulus Stress versus Density	70
21	Tensile Modulus Stress versus Temperature for Density Range Tested	71
22	Strain at Tensile Ultimate Stress versus Density	72
23	Strain at Tensile Ultimate Stress versus Temperature for Densities between 3 and 4.6 PCF	73
24	Compression Yield Stress versus Density	75
25	Compression Yield Stress versus Temperature for Density Range Tested	76
26	Compression Modulus versus Density	77
27	Compression Modulus versus Temperature for Density Range Tested	78
28	Shear Test Setup and Shear Stress Distribution	80
29	Pure Shear	81
30	Typical Shear Load versus Deflection	81
31	Shear Modulus versus Density	85
32	Shear Modulus versus Temperature for Density Range Tested . .	86
33	Shear Yield Stress versus Density	87

LIST OF ILLUSTRATIONS

Figure		Page
34	Shear Yield Stress versus Temperature for Density Range Tested	88
35	Shear Ultimate Stress versus Density	89
36	Shear Ultimate Stress versus Temperature for Density Range Tested	90
37	Setup for Coefficient of Expansion Tests	92
38	Linear Thermal Expansion of Precoat Foam	93
39	Bond Strength Test Specimen.	96
40	Bond Strength Peel Test	96
41	Peel Load versus Temperature	98
42	Peel Load versus Ultraviolet Effect at 75°F	98
43	Fixture for Foam Stability Tests	99
44	Setup for Elevated Temperature Creep Tests	102
45	Predistributed Foam Creep Curves for 50 Percent of Yield and Ambient Temperature	103
46	Predistributed Foam Creep Curves for 50 Percent F_{ty} and 185°F.	104
47	Predistributed Foam Creep Curves for 50 Percent F_{ty} and 240°F.	106
48	Summary of Predistributed Foam Creep Curves for 50 Percent F_{ty} and for 82, 185 and 240°F.	107
49	Thermodynamic Conductivity versus Temperature	109
50	Thermal Conductivity Test Composite	110

LIST OF ILLUSTRATIONS

Figure		Page
51	Reflectance of Vapor Deposited Aluminum on H-Film	112
52	Reflectance of Vapor Deposited Aluminum on Mylar	112
53	Reflectance Measurements - Sample No. 3A.	113
54	Reflectance Measurements - Sample No. 3B.	114
55	Reflectance Measurements - Sample No. 3C.	115
56	Mirror No. 3 Dissected - Face Up	116
57	Mirror No. 3 Dissected - Back View	116
58	Mirror No. 3 Dissected - Cross Section	117
59	Two-Foot Mirror Test Sections	117
60	Film Seam Shear at Room Temperature	122
61	Film Seam Shear at 400°F	123
62	Film Seam Shear at 500°F	124
63	Exposure Limitation of H-Film Adhesive	126
64	Volatility of H-Film Adhesive	127
65	RISEC 918 Mirror - Temperature and Pressure versus Time . . .	130
66	RISEC 918 Mirror - Thermocouple Locations	131
67	RISEC 918 Mirror - Quarter View of Front Surface	132
68	RISEC 918 Mirror - Quarter View of Rear Surface	132
69	RISEC 924 Mirror - Temperature and Pressure versus Time . . .	134
70	RISEC 924 Mirror - Thermocouple Locations	135

LIST OF ILLUSTRATIONS

Figure		Page
71	Mirror Inflated with Back Flap Attached	136
72	Mirror with Double Thickness Precoat Foam Applied to One-Half Mirror Area	136
73	Mirror with Double and Single Thickness Precoat Applied to Mirror Area	137
74	Mirror with Back Flap Attached	137
75	Mirror Set in Vacuum Chamber	138
76	View of Heating Unit in Vacuum Chamber	138
77	View of Surface in Vacuum Chamber with Heating Initiated . . .	139
78	Foaming Action Started	139
79	Foaming Progressing	140
80	Foaming Completed	140
81	Hot Wire Burn-Off Completed	141
82	Vacuum Released - Chamber Opened	141
83	View of Contour Measuring Apparatus	142
84	Mirror (Cut Free), Contour Measuring Apparatus, and Base Plate	142
85	RISEC 929 Mirror - Temperature and Pressure versus Time . .	143
86	RISEC 929 Mirror - Thermocouple Locations	144
87	RISEC 929 Mirror - Front Face	145
88	RISEC 929 Mirror - Rear View	145
89	RISEC 1014 Mirror - Temperature and Pressure versus Time . .	147

LIST OF ILLUSTRATIONS

Figure		Page
90	RISEC 1014 Mirror - Thermocouple Locations	148
91	RISEC 1014 Mirror - Front Face	149
92	RISEC 1014 Mirror - Rear View	149
93	Polar Plot of RISEC 918 Mirror	151
94	Polar Plot of RISEC 924 Mirror	152
95	Polar Plot of RISEC 929 Mirror	153
96	Polar Plot of RISEC 1014 Mirror	154
A-1	Heat Fluxes on Concentrator External Surface	A-6
A-2	Heat Fluxes on Concentrator Internal Surface (End Cap Attached)	A-7
A-3	Precoat Surface Temperature Versus Time (Reversed Orientation)	A-8
A-4	Foam Temperature Versus Time (Reversed Orientation)	A-9
A-5	Foam Temperature Versus Time (Reversed Orientation)	A-10
A-6	Orbital Temperatures (Normal Orientation, End Cap Attached)	A-11
A-7	Orbital Temperatures (Normal Orientation, End Cap Detached)	A-12
B-1	Sketch of Azotometer Apparatus	B-2
B-2	Photograph of Azotometer Apparatus	B-3
B-3	Percent of Azide Decomposition against Time (Azide Structure X at 193°F)	B-6
C-1	Sketch of Heat of Decomposition Apparatus.	C-2

LIST OF ILLUSTRATIONS

Figure		Page
C-2	Heat of Decomposition Apparatus - Disassembled.	C-3
C-3	Heat of Decomposition Apparatus - Assembled	C-4
D-1	Sketch of Sublimation Test Apparatus	D-2
D-2	Closeup of Sublimation Test Apparatus	D-3
D-3	Sublimation Test Apparatus in Bell Jar Installation	D-4
G-1	Contour Comparisons from all Stations Before, During, and After Rigidizing - Mirror No. 1 (RISEC 918)	G-3
G-2	Contour Comparisons from all Stations Before, During, and After Rigidizing - Mirror No. 3 (RISEC 929)	G-4
G-3	Contour Comparisons from all Stations Before, During, and After Rigidizing - Mirror No. 4 (RISEC 1014).	G-5
G-4	Contour Comparisons of Various Runs from one Station - 10.18 Inch Radius - Mirror No. 1 (RISEC 918)	G-6
G-5	Contour Comparisons of Various Runs from one Station - 10.18 Inch Radius - Mirror No. 2 (RISEC 924)	G-7
G-6	Contour Comparisons of Membrane from all Stations in Atmosphere and in Vacuum - Mirror No. 1 (RISEC 918)	G-8
G-7	Contour Comparisons of Membrane from all Stations in Atmosphere and in Vacuum - Mirror No. 3 (RISEC 929).	G-9
G-8	Contour Comparison of Rigidized Mirror from all Stations in Vacuum and in Atmosphere - Mirror No. 1 (RISEC 918).	G-10
G-9	Contour Comparison of Rigidized Mirror from all Stations in Vacuum and in Atmosphere - Mirror No. 3 (RISEC 929).	G-11
H-1	Geometric Contour Measuring Fixture with Contour Calibration Fixture Installed	H-2

LIST OF ILLUSTRATIONS

Figure		Page
H-2	Fixture Schematic Wiring Diagram	H-5
H-3	Typical LVDT.	H-8
H-4	Mirror Ready for Rigidization on Geometric Contour Measuring Fixture	H-12

LIST OF TABLES

Table		Page
I	Properties of Acid Azide Structures I, X, XI, and XII	17
II	Azide Decomposition Rates - Azotometer Measurements . . .	19
III	Subliming Rates of Azides in High Vacuum	20
IV	Properties of Acid Azide Structures II through VIII	21
V	Polyol Resins Utilized	26
VI	Subliming Rates of Certain Resins and an Early Precoat Formulation in High Vacuum	27
VII	Preparation and Properties of Hydroxyl-Terminated Prepolymers with PFR-6 Resin	30
VIII	Preparation and Properties of Hydroxyl-Terminated Prepolymers	31
IX	Preparation and Properties of Hydroxyl-Terminated Prepolymers and Foam Melt Temperature	32
X	Prepolymer Preparations - Three to Four Pound Scale . . .	33
XI	Relationships in Formulating Azides with Polyol Resins	35
XII	Effects of Prepolymerizing	36
XIII	Precoat Formulations and Vacuum Foaming Results	40
XIV	Tests Performed	58

LIST OF TABLES

Table		Page
XV	Tension Test Data for GAC Predistributed Foam	65
XVI	Compression Test Data for GAC Predistributed Foam . . .	74
XVII	Shear Test Data for GAC Predistributed Foam	84
XVIII	Foam to H-Film Peel Test Data (Bond Strength)	97
XIX	Dimensional Stability Data	100
XX	Two-Foot Mirror Test Specimens	118
A-I	Radiation Equilibrium Temperature (End Cap Attached)	A-5
B-I	Azotometer Run of Structure X	B-4

LIST OF SYMBOLS

- A = area (sq in)
E = Young's modulus of elasticity (psi)
F = stress (psi)
G = shear modulus (psi)
K = thermal conductivity (Btu/hr - °F - sq ft/in.)
L = length (in.)
P = load (lb)
T = temperature (F)
U = total energy (in. -lb)
u = unit energy (in. -lb)
V = shear load (lb)
 α = thermal coefficient of expansion (in./in./°F)
 δ = deflection (in.)
 ϵ = strain (in./in.)
 μ = Poisson's ratio
 ρ = density (pci and pcf)
UV = ultraviolet

Subscripts

- c = compression
L = longitudinal direction
s = shear
T = transverse direction
t = tensile
u = ultimate
y = yield

SECTION I. INTRODUCTION

A mechanically mixed polyurethane foam system offers a desirable packaging system for inflating and rigidizing a solar concentrator in space. However, with large size concentrators the reliability of evenly distributing the foam over the back of the mirror surface in space could be problematic. To minimize the problem, Goodyear Aerospace Corporation (GAC) conducted a development program where a material could be "painted" or predistributed" over the back of the solar concentrator and the foaming and rigidizing process activated by an application of heat.

Many foams were considered when GAC initiated its company-sponsored development program in 1962 on predistributed rigidizing materials. A urethane thermally activated foam system was selected because it did not require an auxiliary blowing agent and the urethane technology had already been developed to a high degree. The urethane system also offered flexibility in selecting the foam formulation to produce the desired physical characteristics. Because the urethane system is a two-component system, it is capable of being mixed readily and deployed over large areas. Samples were applied to aluminized Mylar and thermally activated in a vacuum chamber. Good results were obtained. Several samples were folded prior to foaming and no distortion of the foam at the fold line was evident after rigidization. The foam was stable in vacuum conditions.

Upon selection of a urethane system, efforts of the GAC-sponsored development program were concentrated on obtaining a foam that could be used to rigidize expandable structures in space and to eliminate the necessity of using auxiliary mixing equipment. The Curtius arrangement was used to produce isocyanates.

SECTION I

If a diazide is used, a diisocyanate is produced along with two molecules of nitrogen gas. Thus, when terephthalyl azide is heated 1,4-benzene diisocyanate and two moles of nitrogen gas are produced. By mixing 33-percent terephthalyl azide with Plaskons PFR-6 polyester and heating for two hours at 180°F, a rigid urethane foam of approximately 2 pcf is obtained. However, because of the sublimation of the terephthalyl azide at 180°F in a vacuum of 5×10^{-6} mm Hg, the formulation was changed to 40-percent azide and a perforated cover film added before a satisfactory foam was produced in this vacuum.

Several 6-inch diameter miniature solar collectors have been prepared in a vacuum of 10^{-6} mm Hg. The precoat was mixed and then pressed between Teflon sheets into a 6-inch diameter disk to a thickness of 20 to 25 mils. It was transferred to aluminized Mylar and the cover film placed on top. This sandwich was clamped to a hold-down device that had a plexiglass base plate and an inflation inlet. After vacuum was attained, the sample was inflated to a pressure of five inches of water to establish a curvature. (No attempt was made to establish or maintain an accurate contour.) The samples were rigidized by heating with quartz lamps. The temperature on separate experiments was varied from 150° to 180°F, and the time for rigidization varied from 2 to 24 hours. As the temperature was lowered, longer time was required for rigidization.

The work performed in the GAC development program indicated promise in the azide base polyurethane foam, since it could be produced in vacuum with only the application of heat and since it offered a solution to the problem of distributing foam in space. Additional work was needed to advance the state-of-the-art of this new predistributed foam.

The program herein reported upon was needed to investigate azide structures and select the optimum one for use in this application; to develop a foam formulation adaptable for the space rigidizing of solar concentrators; to determine the physical

properties of the foam product and establish its effectiveness in space; and to determine the effects of this rigidizing process on the mirror contour.

This final report on Contract No. NAS 1-3301 represents a 14-month effort in the development and analysis of a predistributed polyurethane foam method of rigidizing solar concentrators in space. The report covers the work accomplished from 30 September 1963 to 1 December 1964. The effort pursued and presented in this final report consists of three main phases:

- (1) Optimization of the predistributed azide base rigidizing foam.
- (2) Experimental and analytical determination of the material properties.
- (3) Demonstration of rigidization of two-foot model solar concentrators in vacuum.

The goals in the development of this predistributed foam material were established for a workable rigidizing process in space. Hypothetically, the conditions of a 300 nautical mile orbit were used. Some of these goals were: (1) a triggering temperature of 175°F, high enough to prevent an inadvertent reaction and low enough to require a minimum heat input; (2) a sublimation tendency of 10 percent or less after 100 hours at 10^{-5} torr in order that the rigidizing process be capable of reacting after a delayed period in orbit; (3) a rate of azide rearrangement of 50 minutes half-life at 175°F in order that the rigidizing process be completed in one orbit or less; (4) a heat release limit of 15 cal/sq in. to minimize adiabatic temperature rise and prevent distortion of mirror surface; (5) speed of reaction of isocyanate to set in 30 minutes (or less) and cure in one hour (or less); and (6) viscosity of 50,000 cp at 190°F to minimize sublimation during the reaction period.

The report discusses the foam formulation development, the production and testing of the foam product; the rigidizing of two-foot models in vacuum (see Figure 1), and the contour measurements of the two-foot models. The report also discusses

SECTION I

briefly the problem areas and presents conclusions and recommendations concerning the over-all program.

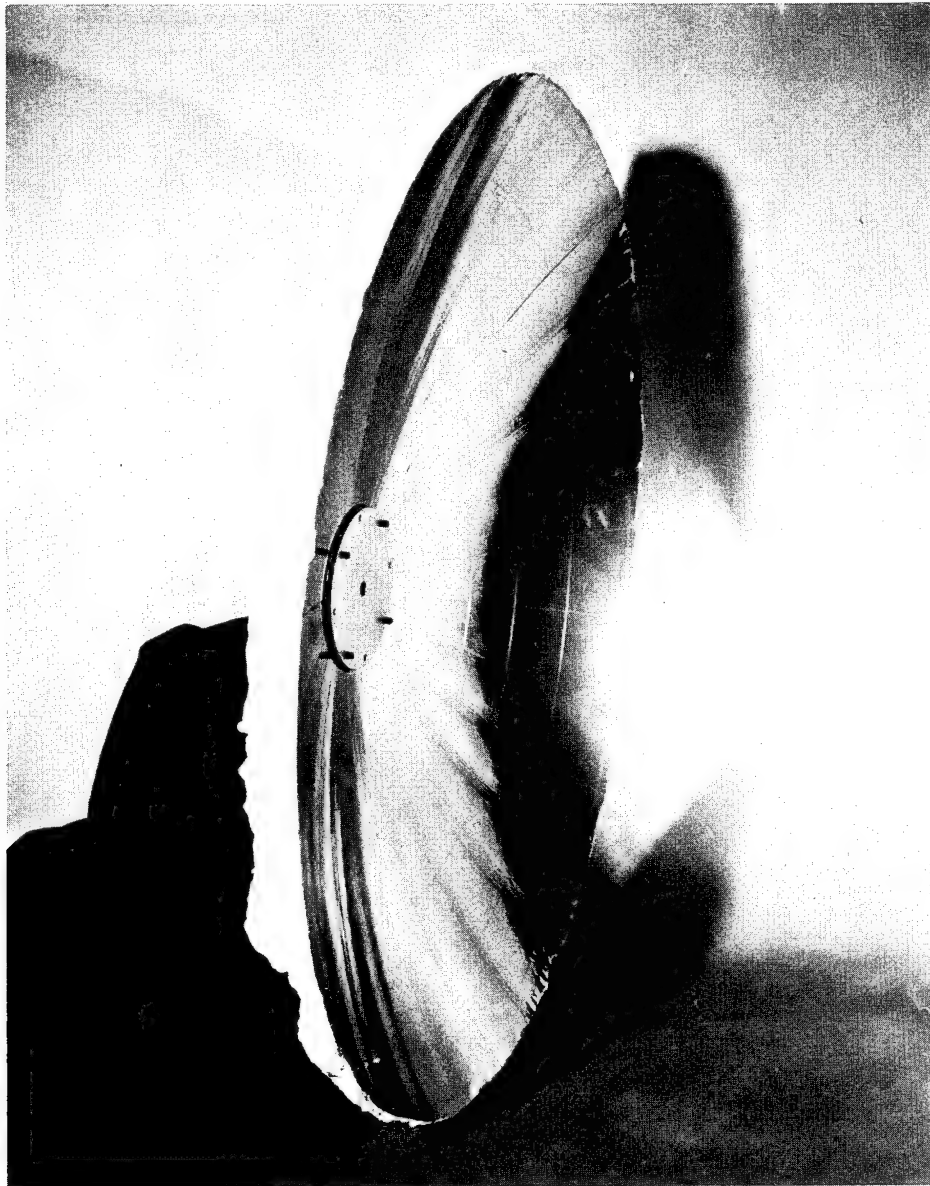


Figure 1. Quarter View of Front Surface of Concentrator
Showing Concentrating Rays

SECTION II. SUMMARY

A. GENERAL

The GAC 14-month effort in the development of a predistributed foam method of rigidizing solar concentrators in space encompassed tasks in three major areas:

- (1) Foam formulation
- (2) Physical property tests
- (3) Rigidizing two-foot models

While the major efforts of the program were the repeatable production of a foam product in vacuum with a rigidizing character applicable to a space solar concentrator, studies were also performed in the areas of substrate materials, new adhesives, selective surfaces, various screening tests, and techniques and procedures in the processing of the new material. Such studies are required to produce a solar concentrator that functions effectively and reliably in the space environment for a specific time period.

The preparation of a solar concentrator and the subsequent space rigidizing process as presently visualized may be summarized as follows. The solar concentrator is inflated and the predistributed material applied as a paste (by troweling) or as segments of a sheeted material. The thickness at various sections of the concentrator may be controlled by varying the weight of predistributed material per unit area. The back flap, which is a loose film placed over the predistributed material and acts as a separator when folding the solar concentrator, is then applied. The solar concentrator is then deflated, folded, and packaged in a container.

The container is fitted into a conveyance vehicle for launching to orbital position. When in orbit the concentrator package is separated from its break-away container

SECTION II

and inflated slowly. When a pressure balance to obtain the desired contour is achieved, heat is applied to the predistributed material. The heat may be applied in several different ways, e. g. , selective surfaces (see Appendix A), hot wires, or pyrotechnics.

The chemical action that takes place is shown in block diagram form in Figure 2 and complemented with the heat schedule of Figure 3. Heat is applied to the predistributed material in such a manner that a temperature rise of approximately 12-1/2 degrees per minute is obtained. At approximately 175°F the azide begins to react as shown in Step 1 of Figure 2, and releases an isocyanate and heat from its own exotherm, which raises the surface temperature to approximately 350°F for a short time period (some nitrogen gas is also released but is lost to sublimation). The heat released from the azide combined with the heat originally supplied is sufficient to unblock the blocked isocyanate as shown in Step 2, thereby releasing more isocyanate. In Step 3 the polyol resin, which is already advanced by prepolymerization, combines with the isocyanate produced by the azide and by the unblocked isocyanate to form the polyurethane foam. The foam then rises and rigidizes.

After rigidizing, the spherical pressure envelope (end cap) is separated from the solar concentrator (e. g. a pyrotechnic fuze) and is jettisoned. The rigidized solar concentrator is then ready for operation.

B. FOAM FORMULATION

The work accomplished in the development of a predistributed foam included research in heat stability, cure time, and control of exothermal reactions. Twelve different organic azide structures, including naphthaloyl and sebacoyl, were investigated for formulation into a precoat foam material. Prepolymers, blocked isocyanates, surfactants, and catalysts were investigated and blended into the predistributed foam material to produce a polyurethane foam product compatible with

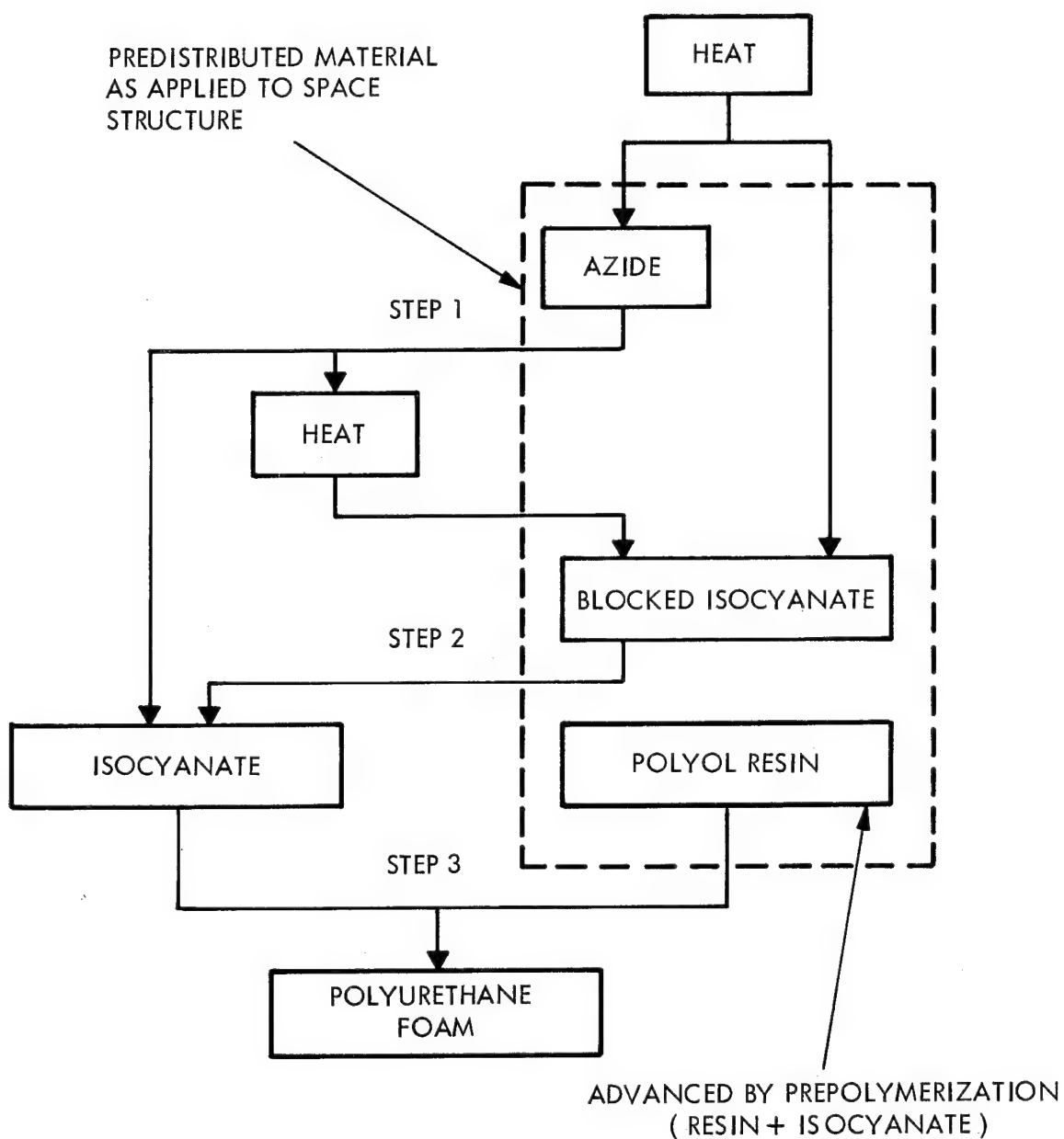


Figure 2. Block Diagram of Rigidizing Process for Precoat Material

SECTION II

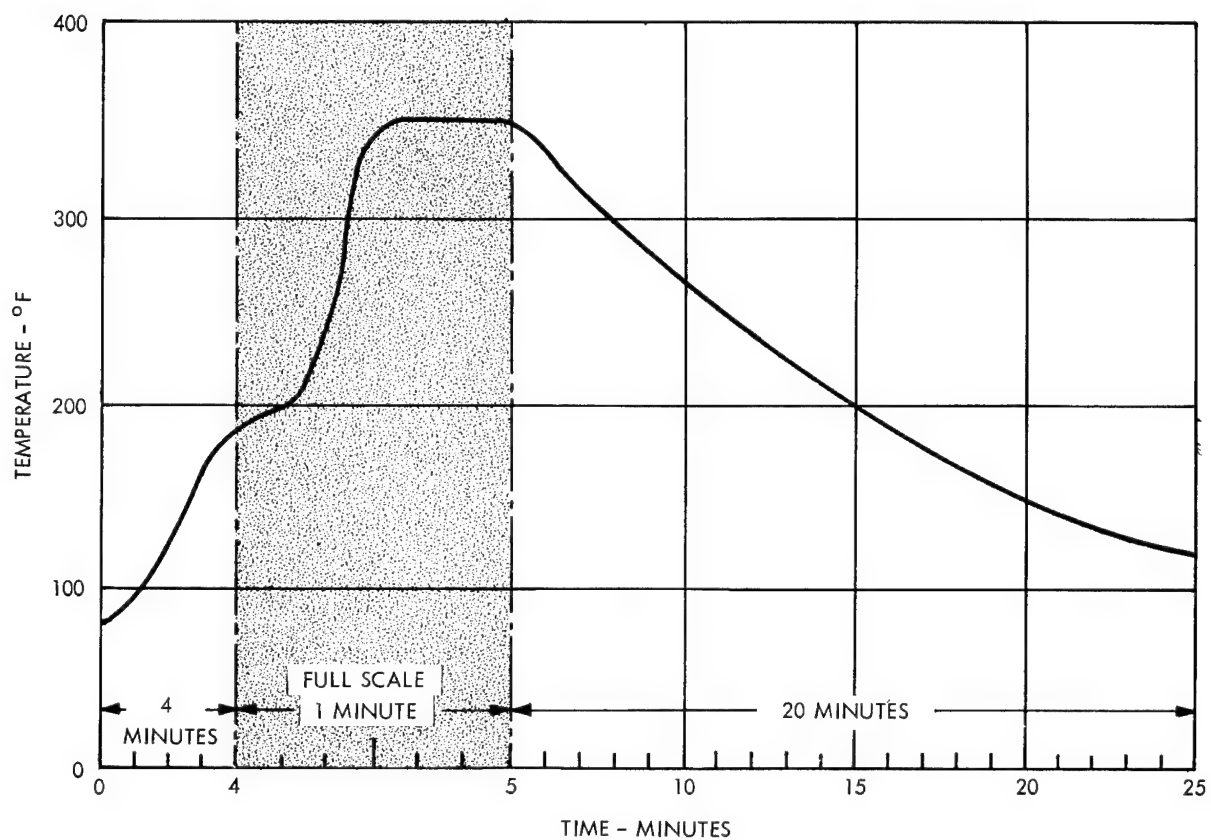


Figure 3. Temperature History of Precoat Foam Reaction

the space mission requirements. Design goals of physical properties set to meet the mission requirements were achieved.

C. PHYSICAL PROPERTY TESTS

A series of physical property tests, including thermal conductivity, linear thermal expansion, stress-strain, shear, bond strength, dimensional stability, ultraviolet effects, and creep, were performed in vacuum. In addition, reflectance measurements and stress-strain measurements of sections taken from the two-foot models were made at atmospheric conditions. Adhesives for H-Film were tested at 400 and 500°F for tensile stress.

D. RIGIDIZATION OF TWO-FOOT MODELS

Four two-foot solar concentrator models were foam rigidized in vacuum. A contour measuring apparatus was fabricated, and contour measurements were made on each of the solar concentrator models. Various means of applying the predistributed foam and various types of back flaps were investigated.

SECTION III. FOAM PRODUCT AND PROCESS DEVELOPMENT

A. SCOPE

The chemical research and development effort described in this section covers the selection of materials for multicomponent storage-stable formulations capable of reacting to form a structurally useful polyurethane foam in a unique heat-initiated process. The foaming process is a somewhat complex assembly of sequential and simultaneous chemical reactions and changes of physical state that is reproducible and subject to control by the methods devised. The process is adapted to meet the dual requirements of operability under the space vacuum and solar radiation conditions of an earth orbit and of production of rigid foam self-bonded to the surface to be rigidized.

B. TECHNICAL BACKGROUND

1. General

The broad class of polyurethane materials is produced from the reaction of active hydrogen in one reactant (which may be present in pendant hydroxyl groups) with an isocyanate group (-NCO) of another reactant. Each reacting molecule must, of course, be at least bi-functional (that is possess at least two reactive points) to permit chain extension and growth into a high polymer.

In the case of the reactants normally used for commercial polyurethane foams, the reaction rates are necessarily high to avoid bubble coalescence and collapse. Starting at room temperature, foam rise and cure usually occurs in about two minutes after mixing the reactants. This typifies the ready reactivity of polyurethane-forming systems. The high reactivity is desirable in foaming, but is a

SECTION III

barrier to obtaining long delayed foaming after mixing. Approaches that have been explored in the past to delay foaming after mixing the reactants have included rapid chilling and holding at quite a low temperature, and the use of marginally stable derivatives of isocyanates (chemically blocked isocyanates) that can be caused to dissociate when desired. Some study has also been made of mixed solid reactants, depending upon the generally low rates of solid-solid reactions and availability of a number of polyisocyanates with melting points covering a range above room temperature.

In principle, in a two-reactant system, one reactant must be inert under storage conditions to yield a storage-stable system of the mixed reactants. Also, for the system to be useful there must be a way to activate the inert reactant.

2. Utility of Acid Azides in Delayed-Action Foaming

The basis of the development reported herein is the prior finding of Goodyear Aerospace laboratories that certain organic compounds carrying two or more acid azide groups ($-\text{CON}_3$) may be employed as the inert ingredient in a mixture of reactants potentially capable of forming a urethane polymer. When exposed to slightly elevated temperatures, such acid azides undergo the Curtius rearrangement. This is the formation of an isocyanate group ($-\text{NCO}$) from each acid azide group with elimination of a molecule of nitrogen. Activation of predistributed mixed material (often termed "precoat" or precoat paste"), which is then capable of reacting to form urethane polymer, thus may be accomplished with limited heating. At the same time nitrogen is produced. The nitrogen then serves to blow the polymer into a foamed physical state.

C. PROCESS CHARACTERIZATION

Appreciable heat releases from azide rearrangement and urethane polymerization are found in the foaming processes. Such heat releases are of particular concern when they occur on the surface of an expanded plastic membrane in space. Obviously

in the space environment the only natural mode of heat rejection is radiation. It is also contemplated that initiation of the foaming process in orbit will come from heating of the precoat ingredients by absorption of solar radiation. Thus both heat absorption and heat rejection must in effect be programmed. The characterization of a foaming process in the light of these and other considerations is made in terms of an isothermal or an adiabatic process. It is not expected however, that either in space or in the laboratory either of the ideal processes will be fully realized.

1. Isothermal Process

It was originally premised that with suitable ingredients a foaming formulation could be so adjusted that a moderate temperature rise of perhaps 15-20°F above the foam initiation temperature of around 160°F would lead to a dynamic temperature balance. This balance would comprise further heating from sunlight, heat release from the foaming reactions, heat rejection by radiation, and the heat capacity of the foaming mixture and structural substrate. It was also contemplated that inert fillers of high heat capacity or volatilizable additives might be used to aid in heat absorption or rejection.

Obviously, an isothermal process becomes more manageable as reaction heat releases are reduced. This consideration led to studies of precoat ingredients and modifications of formulations in the first part of the contract program. However as the problems became better defined the effort was shifted to a study of a new approach involving a nearly adiabatic and much faster foaming process.

2. Adiabatic Process

A new concept was evolved in view of the difficulties encountered with a near isothermal process. The foaming process, now essentially adiabatic, involves heating of the precoat to a temperature ($\approx 180^\circ\text{F}$) above that at which an isothermal balance is possible and a "runaway" rearrangement of azide ensues that is

SECTION III

self-propagating, although slow compared to explosions. The final foam temperature is controlled at some level between 300 and 400°F, primarily by initial azide concentration. The peak exotherm temperature holds in a vacuum environment for less than a minute before cooling by radiation and other processes sets in. The value of this adiabatic process for foaming is in its combination with formulations containing a selected, inert, storage-stable isocyanate derivative that requires a minimum temperature of around 300°F for its rapid activation. (Activation consists in decomposition of the phenol-blocked isocyanate and liberation of the isocyanate as a useful reactant in building the foam polymer.) During the peak of the exotherm and for the first part of the cooling period, urethane polymerization rates are high (and, in addition, are desirably catalyzed) and the final foam product is reasonably well cured.

Advantages gained from modified formulation and the adiabatic process are as follows:

- (1) With isocyanate supplied from an additional initially inert ingredient, it is possible to reduce by half or more the azide requirement (as dictated by the requirement for derived isocyanate for proper foam cure). This is important, since the azide at present is costly and has considerable shock and thermal sensitivity.
- (2) Precoat formulations with the reduced azide content appear indifferent to friction and to shock, such as rifle bullet impact, and if initiated thermally give only a moderate heat release and predictable temperature rise.
- (3) In view of the rapidity of the process, it appears that it should be possible to complete rigidization within the light portion of a single earth orbit.

- (4) The peak exotherm temperature can readily be set high enough to ensure rearrangement of all the azide components. In an isothermal process the rearrangement reaction tends to tail off, extending inordinately the time to complete the reaction. (Reaction rate theory and GAC experiments agree on this point.)

D. STUDIES OF ACID AZIDES

Beginning with the in-house development program and continuing in the program reported herein, GAC has carried out screening studies of acid azides. The objective has been to find the most suitable molecular structures in the acid azide category to implement the development of foaming systems based on azides and the Curtius rearrangement. Screening studies have been complicated by the fact that acid azides of di- or higher functionality are not commercially available, and have been of limited interest to organic chemistry research workers. In consequence, each compound evaluated in the program has required an individual synthesis effort. In some cases the compounds have been new structures, never before made, or at least never reported in literature on the subject.

1. Functional Requirements Placed on Acid Azides

For use in the foaming process, candidate acid azide compounds must meet the following requirements:

- (1) The compound must be at least di-functional.
- (2) The acid azide groups must undergo the Curtius rearrangement smoothly and at least nearly quantitatively in the temperature range of 150-200°F in a few hours or less.
- (3) The di- or polyisocyanate product of the Curtius rearrangement must have suitable reactivity in urethane polymerizations and contribute desirable properties, such as chain stiffness, to the final polyurethane foam.

SECTION III

- (4) Both the azide structure and the isocyanate rearrangement product must have very low vapor pressure.

Other desirable properties in acid azide compounds are:

- (1) A high order of thermal stability in all of the structure exclusive of the azide groups.
- (2) Low shock sensitivity and a minimum heat release per mole of the azide group in the Curtius rearrangement.
- (3) Melting point below room temperature. (This may be incompatible with the cyclic structures that satisfy Item 2 in the list of requirements.)

2. Synthesis of Acid Azides

A comprehensive survey of acid azide chemistry is available (Reference 1). In the present program the acid azides have been produced from the appropriate acid chloride precursor compound by treatment of an acid chloride solution with an aqueous sodium azide solution and precipitation of the organic azide.

3. Measurement of Properties and Chemical Reactivity of Acid Azides

A summary of physical properties and chemical reactivity is presented for four di-functional acid azides in Table I. The synthesis and use of Structure I originated in the in-house development program and was continued in the present program to afford reference points. Structures X, XI, and XII represent attempts to design molecular structures from first principles to satisfy the requirements listed previously. The synthesis of the specified structures was carried out by a subcontractor. Material of satisfactory purity was produced in the case of Structures X and XI. A limited effort to synthesize the quite complex Structure XII produced material of doubtful authenticity and purity, and further effort has been held in abeyance.

Table I. Properties of Acid Azide Structures I, X, XI, and XII

Structure	Azide Name and Mol Structure	Azide Functionality	Isocyanate Produced on Rearrangement	Azide N Content (Wt %)		Azide Melting Point (°F)	Crystal Density of Azide (g/cc)	Half Life** at Stated Temperature (min)	Heat Release on Rearrangement at 275°F (cal/g)	Remarks Pertaining to Azides
				Total	Releasable					
I	Terephthaloyl Azide	2	1, 4 - Benzene Diisocyanate	38.9	25.9	230-232	1.58	28 (prelim) at 196°F †	282	Can be detonated by rapid heating. Shock sensitive. Approximately one percent/month decomposition at 70°F.
	<chem>N#3OC(=O)c1ccc(cc1)C(=O)O#N</chem> Mol wt = 216									
X	4, 4' - Diphenyl Methane Diacyl Azide	2	4, 4' - Diphenyl Methane Diisocyanate Mol wt = 250 Amine eq = 125	27.4	18.3	181-184 (dec)	1.34	30 (prelim) at 193°F	224	Have observed occasional detonation (very mild) on rapid heating. Some shock sensitivity.
	<chem>N#3OC(=O)c1ccc(cc1)C(c2ccccc2)C(=O)O#N</chem> Mol wt = 306									
XI	<chem>N#3OC(=O)c1ccc(cc1)C(=O)O#N</chem>	2	-- Mol wt = 408 Amine eq = 204	18.1	12.1	190-199 (dec)	1.31	24 (prelim) at 196°F †	115	Have not observed detonation on rapid heating.
	<chem>N#3OC(=O)c1ccc(cc1)C(=O)O#N</chem> Mol wt = 464									
XII	<chem>N#3OC(=O)c1ccc(cc1)C(=O)O#N</chem>	4	-- Mol wt = 894 Amine eq = 224	16.7	11.1	--	--	--	--	No authentic material available. Substitution of trimethylolpropane for glycerol in initial esterification step did not solve synthesis problems.
	<chem>N#3OC(=O)c1ccc(cc1)C(=O)O#N</chem> Mol wt = 1006									

** Assuming a unimolecular reaction, the time for 50 percent of the material to undergo rearrangement as measured by nitrogen release.

† Experimental value adjusted for suspected low purity.

SECTION III

The measured values reported in Table I were obtained in the following ways:

- (1) The density of azides was determined on powdered samples with a Beckman air pycnometer and is the crystal density (not bulk density).
- (2) The melting point was determined on a melting point bar or with a polarizing microscope and Kofler hot stage.
- (3) Values for half life in minutes at stated temperature were derived from preliminary runs with an azotometer in which the rearrangement of an azide sample was effected and the concomitant release of nitrogen measured as a function of time. The azotometer technique is described in Appendix B.
- (4) The heat release (calories/gram of azide) for the rearrangement of azide to isocyanate was determined by rapid decomposition in a simple calorimeter at, usually, 275°F. This technique is described in Appendix C.

It should be noted that studies of the rate of azide rearrangement at elevated temperature were not intended to be definitive, but rather to give a preliminary characterization. Some further details are shown in Table II and its accompanying notes.

Only limited measurements of the subliming rates of azide Structures I, X, and XI, as shown in Table III, were necessary to establish that the rates for Structures X and XI were satisfactorily low. This met one of the design objectives for Structures X, XI, and XII - that volatility should be low enough to permit exposure to space vacuum for some hours before foaming. The test method is described in Appendix D.

4. Background on Other Acid Azides

Table IV lists Structures II through VIII that were synthesized, the synthesis attempted, or the synthesis contemplated in the in-house development program.

Table II. Azide Decomposition Rates^(a) - Azotometer Measurements

Structure	I		X		XI	
Temperature (°F)	196	207	193	208	196	208
Time (minutes) for following percent decompo- sitions(b):						
25%	---	---	12	5	---	---
50%	28	13	30	11.5	24	10
75%	---	---	66	23	---	---

(a) For data analysis, the following purities are tentatively assumed from internal and related evidence(c):

Structure I - 83%
 Structure X - 100%
 Structure XI - 85%

(b) Times are read from plotted curves of gas production versus run time; a correction is applied for hold-up in the system, leading to an apparent induction period.

(c) Since making the above azotometer measurements, brief attention has been given the question of whether azide purity can be easily assayed by rearranging the material, dissolved in a solvent, and then employing the n-dibutylamine titration method to determine the amount of isocyanate produced from a known weight of azide material. However, it was found that at least three variables were present simultaneously: (1) azide purity, (2) a question of whether small amounts of azide were lost to non-isocyanate-producing side reactions, and (3) rather frequent occasions in which products of the rearrangement were not completely soluble in the solvent system of the analytical method. It was established that 86 to 93 percent of the theoretical yield of isocyanate could be obtained from Structure I and 90 percent from Structure X. Structure XI gave only slightly soluble products and 5 - 10 percent of theoretical yield of isocyanate, which reflects incompatibility with the assay method.

SECTION III

Table III. Subliming Rates of Azides
in High Vacuum

Hours at 75°F	Percent Weight Loss ^(a) (Accumulated)			
	Structure I	Structure X	Structure XI	MDI ^(b)
17	37	--	--	--
17.5	--	0.3	0.3	--
23	--	--	--	8.1
40.5	--	1.6	0.8	--
84.5	77	--	--	--
132.5	82	--	--	--

(a) Weight losses on three individual samples, exposed simultaneously, are averaged.

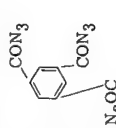
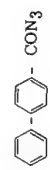
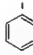

(b) This material, 4, 4'-diphenyl methane diisocyanate, is of interest as it is the diisocyanate resulting from the rearrangement of Structure X.

Attempts at synthesis of Structure VI were continued into the contract program, but without realizing a pure product. However, in retrospect it appears that at the time of deferring the further synthesis effort success had been achieved in establishing a method for synthesizing and purifying the precursor-compound 2, 6 - naphthaloyl chloride with a melting point of 360°F. This conclusion is reached in view of a concurring published melting point value for the chloride that appeared after the effort was concluded (Reference 2).

5. Selection of Most Useful Acid Azide

After consideration of the properties of the various azides, as listed in Tables I

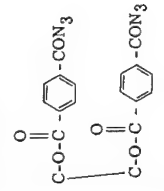
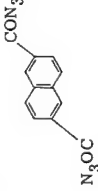
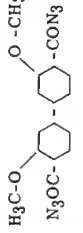
Table IV. Properties of Azide Structures II through VIII

Structure	Azide Name and Mol Structure	Azide Functionality	Isocyanate Produced on Rearrangement	Azide N Content (Wt %)		Azide Melting Point (°F)	Crystal Density of Azide (g/cc)	Half Life** at Stated Temperature (min)	Heat Release on Rearrangement at 275°F (cal/g)	Remarks Pertaining to Azides
				Total	Releasable					
II*	Mesoyl (tri) Azide  N ₃ OC Mol wt = 285	3	1, 3, 5-Benzene Trisocyanate Mol wt = 201 Amine eq = 67	44.2	29.5	174	--	--	--	Extremely shock sensitive. Although too sensitive for serious consideration, its tri-functionality appeared useful in preliminary foaming tests.
III*	Sebacyl Azide N ₃ OC (CH ₂) ₈ CON ₃ Mol wt = 252	2	Octamethylene Diisocyanate Mol wt = 196 Amine eq = 98	33.3	22.2	~75 (literature value 93)	--	--	--	Noticeably thermally unstable at 75°F.
IV*	4, 4'-Diphenoyl Azide  N ₃ OC -  -  - CON ₃ Mol wt = 292	2	4, 4'-Biphenylene Diisocyanate Mol wt = 236 Amine eq = 118	29.8	19.2	259	--	--	--	Perhaps too thermally stable. Diisocyanate is a known carcinogen and undesirable to work with.

*First synthesized and studied on Goodyear Aerospace in-house development program.

**Assuming a unimolecular reaction, the time for 50 percent of the material to undergo rearrangement as measured by nitrogen release.

Table IV. Properties of Acid Azide Structures II through VIII (Continued)

Structure	Azide Name and Mol Structure	Azide Functionality	Isocyanate Produced on Rearrangement	Azide N Content (Wt %)		Azide Melting Point (°F)	Crystal Density of Azide (g/cc)	Half Life** at Stated Temperature (min)	Heat Release on Rearrangement at 275°F (cal/g)	Remarks Pertaining to Azides
				Total	Releasable					
V*	4,4'-Diacyl Azide of Ethylene Glycol Dibenzoate  Mol wt = 404	2	4,4'-Diisocyanate of Ethylene Glycol Dibenzoate Mol wt = 348 Amine eq = 174	20.8	13.9	--	--	--	--	Purity uncertain. Utility in foaming not established but probably good.
VI	2,6-Naphthaloyl Azide  Mol wt = 266	2	2,6-Naphthalene Diisocyanate Mol wt = 210 Amine eq = 105	31.5	21.1	--	--	--	--	Synthesis carried through establishment of procedure for making the precursor di-acid chloride.
VII †	Adipoyl Azide N3OC(CH2)4CON3 Mol wt = 196	--	--	42.8	28.6	--	--	--	--	Synthesis not attempted in view of properties of Structure III.
VIII †	3,3'-Dimethoxy, 4,4'-Diphenoyl Azide  Mol wt = 352	--	--	23.9	15.9	--	--	--	--	Synthesis has not been attempted.

* First synthesized and studied on Goodyear Aerospace in-house development program.

** Assuming a unimolecular reaction, the time for 50 percent of the material to undergo rearrangement as measured by nitrogen release.

† Preparation of this structure contemplated during the Goodyear Aerospace in-house development program.

and IV, and consideration of the properties of the product foam, it was concluded that Structure X best satisfied the over-all requirements. It was definitely the best of the candidates tested in respect to polymer melt temperature of the product foam.

With formulations containing Structure X it has been possible to study the foaming process and product and establish the general feasibility, in many important respects, of foaming in space. It does appear, however, that there are some strong possibilities for structural modifications that will have better properties than Structure X.

6. Purity and Storage Stability of Structure X.

A microchemical analysis of Structure X found 27.50 and 27.75 weight % N in duplicate determinations. The calculated N content is 27.45 percent. Only one mention of the compound is found in the literature; a melting point of 80°C (dec.) is reported in U.S. Pat. 2,865,932. Our melting points are appreciably higher, i. e., 83-84°C.

Infrared studies indicate a low level of contamination with the acid chloride precursor of Structure X, but suggest contamination by the hydrolysis product of the precursor. A study of purification techniques coupled with infrared inspections should afford an effective infrared criterion for purity, but was not carried out in this program.

It should be noted that in the course of the infrared work, measured absorptivities at 2138 cm^{-1} of Structure X as received and approximately one month later differed by an amount indicating a four to five percent decrease in azide concentration during refrigerated storage of the solid material. Indications from other types of work are that the loss of azide function in the solid is somewhat less rapid than that indicated by the infrared work, but perhaps faster in solution. However, definitive work has yet to be done on azide stability and destabilizing factors.

SECTION III

7. Azide Sensitivity Tests

A seventy-five gram quantity of azide Structure X was sent to the U.S. Naval Ammunition Depot at Crane, Indiana to determine the sensitivity of the azide material. A copy of the return letter giving the results of these tests is presented in Appendix E.

The impact sensitivity test consisted of dropping a 2.5-kilogram weight on a 35-milligram sample of the azide from various heights. It was found that when the weight was dropped from a height of 6 cm, the azide would detonate 50 percent of the time. This was established on the basis of 25 drops. This is compared to a highly sensitive rocket fuel tetryl, whose 50 percent height is 24 cm.

The friction pendulum test employed a 3-kilogram weight on the end of a 50 cm pendulum, which was released from a height of 50 cm. After 18 passes, no detonation was observed. In comparison, no detonation was observed with tetryl under the same condition, but positive detonation was observed with lead azide.

A 200-gram quantity of azide Structure X was sent to the Bureau of Explosives to determine the transportation classification of the azide material. A copy of the return letter giving the results of these tests is presented in Appendix F. The dry, undiluted material has been refused a shipping classification because of its thermal instability.

E. POLYOL RESINS UTILIZED

For the polyol resin component of the space-foaming formulation to be developed, a number of resin types were available for consideration and experimentation. It was known that the softening temperature of a polyurethane depended in part upon the nucleus or "starter molecule" of a polyol and upon the length of branches from the nucleus (Reference 3). It seemed desirable to set the goal for softening temperature as the maximum obtainable in order to meet solar reflector design

requirements and perhaps ease design problems. A reasonably high density of cross-links was postulated as necessary, and it was planned to work over a range roughly centered on an M_c value of 500 where M_c = molecular weight/cross-link).

The polyol resins used are reported in Table V with pertinent chemical and physical properties. One resin is an aromatic polyester type (PFR-6); the others are polyethers with aliphatic or heterocyclic nuclei. Since only di-functional azides were available in the program, it was necessary to supply poly-functionality for cross-linking in the resin component. In the resins of Table V, functionality ranges from 3 to 8. Hydroxyl numbers in the range 300 to 500 are required for the M_c values contemplated.

Certain restrictive conditions imposed by the planned use of precoat affect the choice of a resin component. Among these are:

- (1) Reactivity of the hydroxyl groups should be high, at least in the fast, adiabatic process. For this, primary hydroxyls are desirable.
- (2) To avoid vaporization losses in space vacuum exposure before foaming, there should be a minimum of material with molecular weights under about 300. The losses that may occur are illustrated by Table VI.
- (3) Neither a very fluid nor very hard resin would lend itself to compounding a spreadable paste or dough.
- (4) At some point in the foaming process the resin must be foamable. This implies that several conditions, some not too well understood, are met simultaneously.
- (5) In view of the discussion to follow (subsection F) the resin must be convertible into a tractable hydroxyl-terminated prepolymer by reaction with a selected diisocyanate.

The quantitative usage of a resin is discussed in following subsections (F and G).

SECTION III

Table V. Polyol Resins Utilized

Resin Designation:	PFR-6	TP-440	HP-370	PeP-650	Exp. No. 202	Voranol RS-375
Functionality	3	3	4	4	4	8
Nuclear type ⁽¹⁾	--	a ₁	h ₁	a ₂	h ₁	h ₂
Equiv Wt OH(g)	117	139	150	150	144	151
Hydroxyl No.	465 -495	404	370	375	390	375
Density (g/cc)	1.15	--	1.12	--	--	1.14
Brookfield viscosity (cp x 10 ⁻³) at 77°F	70 -80	0.6	30	1.1	--	40

(1) a₁ = Aliphatic initiator (trimethylol propane)

a₂ = Aliphatic initiator (pentaerythritol)

h₁ = Heterocyclic initiator (α - methylglucoside)

h₂ = Heterocyclic initiator (sucrose)

Table VI. Subliming Rates of Certain Resins and an Early Precoat Formulation in High Vacuum

Hours at 75°F	PFR-6 Resin	RS-375 Resin	Precoat ^(b)
1.1	--	--	4.5
17	1.1	0.1	--
23	--	--	6.4
84.5	3.2	0.7	--
90.5	--	--	7.6
132.5	3.4	0.5	--
Plus 72.5 hours at 150°F	13.4	3.9	--

(a) Weight losses on three individual samples, exposed simultaneously, are averaged.

(b) Formulation containing small amount of plasticizing acetone (most volatile component), 20 wt percent Structure I as wetted solids, and the balance viscous low prepolymer of PFR-6 and tolylene diisocyanate.

F. SYNTHESIS AND PROPERTIES OF HYDROXYL-TERMINATED PREPOLYMERS

1. Reasons for Use.

To anticipate the discussion in subsection G of heat release problems encountered in the rearrangement of acid azides in a foaming process, it may be stated that methods have been sought to minimize the azide requirement in a formulation. To a considerable degree this can be accomplished by reacting or "cooking" a polyol resin with some fraction of its equivalent of diisocyanate. The resulting

SECTION III

prepolymer is of low or moderate molecular weight, is certainly branched, and will have reactive hydroxyl groups although all isocyanate will have been reacted into urethane linkages. The -NCO/-OH ratio that can be achieved in the prepolymer is less than the value of the theoretical "gel point." How much less is determined experimentally, and depends upon the prepolymer viscosity desired.

It has appeared desirable in both isothermal and adiabatic foaming processes to have resin or prepolymer viscosity above 10,000 centipoise at 200°F . Viscosities this high generally require plasticizing the formulation (usually with acetone) to obtain handling properties at ambient temperatures.

2. Synthesis Methods

Bulk polymerization of polyol resin with limited amounts of isocyanate may be effected by rapid mixing of reactants to homogeneity and heating for a few hours in the range of 200 to 280°F . Reaction heat generally leads to an exotherm, which must be anticipated and controlled during the original heating up. This operation resembles the well-known preparation of commercial isocyanate-terminated prepolymers. However, the viscosity of hydroxyl-terminated prepolymer is generally very high compared to that of isocyanate-terminated material, and some modifications in technique are required. In the present effort most use was made of tolylene diisocyanate (TDI, normally liquid) or of 4,4' diphenyl methane diisocyanate (MDI, a solid with melting point about 130°F). Some use was made in the early part of the program of a commercial isocyanate-terminated prepolymer (Glidfoam RCR 5043) based on TDI which was cooked with an excess of PFR-6 resin to produce hydroxyl-terminated prepolymer. This was an extension of an approach taken in the earlier in-house development. Consideration of foam strengths versus temperature led to the final selection of MDI.

By bulk polymerization techniques prepolymers having -NCO/-OH ratios ranging from 0.3 to 0.4 have been made. At the high end of the range difficulties with gelation are encountered, but useful prepolymers are obtained at slightly lower ratios.

Some attempts were made to produce prepolymers with -NCO/-OH ratios very close to the theoretical gel point. Polymerizations were conducted in acetone solvent at room temperature and with a tin catalyst. Reaction times were extended to several days and completion of reaction was checked by determining residual isocyanate reactant. The product prepolymers appeared to have high gel contents and were of no use.

3. Summary of Prepolymers Prepared

Tables VII, VIII, and IX list prepolymers made with various reactants to supply material with a range of physical and chemical properties for foaming studies. After a standard foam formulation was adopted that employed No. 382-37 type prepolymer, it was desired to establish the reproducibility of the prepolymer synthesis. This was done with the repetitive prepolymer preparations reported in Table X. At the same time a stock of prepolymer was produced that was used in preparation of foam material for physical test specimens and for rigidization of two-foot model solar collectors.

In the repetitive runs listed in Table X the batch size was scaled up from about one pound to four pounds. This permitted ready measurement of prepolymer viscosity with a Brookfield viscosimeter after the "cook" and without removing the hot resin from the kettle. It is concluded that the prepolymering reaction is reasonably reproducible with respect to viscosity of product and behavior in foaming formulations. However, preparation 382-48 did not reach the viscosity level of the other replicate preparations for an unknown reason. Preparation 382-57 was made approximately four months after the other replicates. It is seen from Table X that its viscosity is in fair agreement with the earlier preparations; however, enough suspended gel was formed to impart a turbid appearance that was not noticed in the earlier products. The performance in foam formulations did not differ.

SECTION III

Table VII. Preparation and Properties of Hydroxyl-Terminated Prepolymers with PFR-6 Resin

Preparation No.	376-9	376-10
Resin Used/Parts by Weight	PFR-6/10	PFR-6/10
Isocyanate Used [*] /Parts by Weight	RCR 5043/2.3	RCR 5043/2.8
-NCO/-OH(Mole ratio of reactants used)	0.21	0.26
Type of Polymerization	Bulk; 3 hr at 210°F; no catalyst.	Bulk; 3 hr at 250°F; no catalyst.
Product Density (g/cc)	1.2	1.18
Product viscosity, Brookfield (cp) at		
194°F	49,500	100,000
212	25,000	85,000
230	14,000	55,000
284	--	8,500

*Isocyanate was supplied as a commercial low viscosity isocyanate-terminated prepolymer (Glidfoam RCR 5043), somewhat branched, and containing free TDI.

Table VIII. Preparation and Properties of Hydroxyl-Terminated Prepolymers

Preparation	59B(a)	60(b)	61(b)	62	63	382-4	382-7	382-10	382-11	382-21	382-25
Resin Used	PFR-6	PFR-6	PFR-6	PFR-6	HP-370	PFR-6	TP-440	PeP 650	HP-370	PeP 650	PeP 650
Diisocyanate Used	TDI	TDI	TDI	MDI	TDI	TDI	TDI	TDI	TDI	TDI	MDI
NCO/OH (Mole Ratio Used)	0.62	0.70	0.75	0.70	0.55	0.24	0.33	0.33	0.33	0.4	0.3-0.4
NCO/OH (Theo. Mole Ratio For Gel Point)	0.72	0.72	0.72	0.72	0.58	0.72	0.72	0.58	0.58	0.58	0.58
Type of Polymerization	Reactants dissolved in approximately 3 times their weight of acetone, mixed, and held in closed container several days at room temperature; 0.1% tin catalyst (D-22) added and never neutralized.					Bulk, no catalyst. Temperature of 120°C for 2 hrs under dry nitrogen atmosphere with stirring.					
Resultant Prepolymer	Firm gel occluding all acetone					Let down with acetone after polymerization					
	Non-uniform					Semisolid at RT. Soluble in hot acetone. Used as 65% solids.	Viscous liquid at RT.	Solid at RT. Melt temp below 100°C. Used as acetone solution.	Solid at RT. Very viscous solution at 100°C.	Solid at RT. Viscous solution at 100°C.	Gel at eqv 0.4. Viscous liquid at 0.3 eqv.
PMT (Dried Acetone Free) or Eqv Wt of Prepolymer	200 to 215°F	---	210 to 230°F	---	~150°F	180(c)	256.5(c)	268(c)	268(c)	372(c)	534 to 624(c)

(a) Run 59 was made with the same reactants and reactants' ratio as shown for 59B, but no solvent was used. The product was an intractable, horny solid, PMT around 225°F, apparently partially cross-linked.

(b) The swollen, rubbery gels from Runs 60 and 61 were not acetone soluble and could be broken down mechanically only with difficulty.

(c) Equivalent wt of prepolymer. Grams of prepolymer needed to react with 1 eqv of isocyanate containing material, e.g., 108 grams Structure I, 153 grams Structure X, etc.

SECTION III

Table IX. Preparation and Properties of Hydroxyl-Terminated Prepolymers and Foam Melt Temperature

Preparation No.	382-28	382-29	382-32	382-37
Polyol Resin Used	PeP 650	PeP 650	HP-370	HP-370
Hydroxyl No. of Resin	374	374	370	370
Diisocyanate Used	MDI ⁽²⁾	MDI	MDI	MDI
Reactants Ratio (-NCO/-OH)	0.40	0.355	0.348	0.30
Reaction Time/Temp	(3)	2 Hrs/120-125°C ⁽⁴⁾	2 Hrs/125°C ⁽⁵⁾	2 Hrs/120°C ⁽⁶⁾
Polymer Melt Temp (°F) ⁽¹⁾	-- --	235-250	--	280-320

(1) When compounded into precoat and foamed.

(2) MDI = 4, 4' diphenyl methane diisocyanate

(3) Reactants gelled after cooking 15 minutes at about 65°C. Product was insoluble. Although NCO/-OH is below theoretical value of 0.58 for gel point, it appears 0.4 is too high to be readily handled experimentally. This confirms results with preparation No. 282-25.

(4) Product soluble and found to have good potential for precoat use.

(5) Product semi-gel when cut with acetone. Unsuitable for use in precoat.

(6) Gave clear, homogeneous solution at 80 percent solids in acetone solution. A superior prepolymer for use in precoat.

Table X. Prepolymer Preparations - Three to Four Pound Scale

Preparation No.	Runs to Determine Scale-Up Techniques			Runs to Establish Reproducibility of Prepolymer Preparations with Product Viscosity as the Criterion										
	382-43	382-44	382-48	382-50	382-51	382-52	382-57							
	Experimental No. 201(1)	HP-370	HP-370	HP-370	HP-370	HP-370	HP-370							
Polyol Resin Used	390	370	370	370	370	370	370							
Hydroxyl No. of Resin	MDI	MDI	MDI	MDI	MDI	MDI	MDI							
Diisocyanate Used	0.31	0.30	0.299	0.30	0.30	0.30	0.30							
Reactants Ratio (-NCO/-OH)	2 Hrs/130-140°C	2 Hrs/120-130°C	2 Hrs/120-126°C	2 Hrs/121-125°C	2 Hrs/123-125°C	2 Hrs/121-125°C	2 Hrs/120-130°C							
Reaction Time/Temp	Viscosity	Viscosity	Viscosity	Viscosity	Viscosity	Viscosity	Viscosity	Viscosity	Viscosity	Viscosity	Viscosity	Viscosity		
	°C	Centi-poise	°C	Centi-poise	°C	Centi-poise	°C	Centi-poise	°C	Centi-poise	°C	Centi-poise	°C	Centi-poise
	131	12,000	126	16,600	124	1,800	124	11,400	123	16,000	141	3,500	124	17,500(3)
	121	13,500	121	21,000	120	2,500	118	17,200	122	18,000	137	5,000	121	13,000
	110	45,000	114	41,000	118	3,500	114	34,800	118	22,000	135	6,500	119	18,500
	93	80,000	108	86,000	115	5,500	112	55,200	115	31,500	133	9,700	115	29,700
	R. T.	Solid	R. T.	Solid	112	6,500	110	54,500	110	54,500	125	17,500	109	51,500
					110	10,500					120	23,500		
											114	38,000	(2)	

(1) Resin supplied by Wyandotte Chemical Corporation

(2) Product prepolymer from run 382-52 was extremely viscous and full of gas bubbles at end of 2 hour cook. Viscosity at end of cook was over 100,000 cp at 124°C. Material was left overnight with heat on, no stirring. In morning, no bubbles present and temperature 141°C. Viscosity measurements were then taken.

(3) A reading or other error is apparently involved at the highest temperature.

REMARKS: Prepolymer viscosity obtained in preparation No. 382-44 is satisfactorily reproduced in No. 382-50, 382-51 and perhaps with 382-52 (see note 2). Preparation No. 382-48 shows a relatively low viscosity; the reason is unknown.

(1) Resin supplied by Wyandotte Chemical Corporation

(2) Product prepolymer from run 382-52 was extremely viscous and full of gas bubbles at end of 2 hour cook. Viscosity at end of cook was over 100,000 cp at 124°C. Material was left overnight with heat on, no stirring. In morning, no bubbles present and temperature 141°C. Viscosity measurements were then taken.

(3) A reading or other error is apparently involved at the highest temperature.

REMARKS: Prepolymer viscosity obtained in preparation No. 382-44 is satisfactorily reproduced in No. 382-50, 382-51 and perhaps with 382-52 (see note 2). Preparation No. 382-48 shows a relatively low viscosity; the reason is unknown.

SECTION III

G. PRECOAT FORMULATION FOR AN ISOTHERMAL FOAMING PROCESS

1. Stoichiometry

Table XI shows weight relationships when azide Structure I, X, or XI is reacted (foamed) with an individual polyol resin or with a prepolymer. In each case, the final ratio of isocyanate to hydroxyl is unity. Knowledge of the heat releases in the rearrangement of the various azides (subsection D) permits calculation of the adiabatic temperature rise to be anticipated in the foam. (The effect of additional heat release from the urethane polymerization is not evaluated.) Values for the quantity of blowing gas released are shown, and are based on the gas yield from the azide. The weight change (loss) between precoat and foam product is indicated. The interrelationships are illustrated between functionality and hydroxyl number of the resins and molecular weight of the diisocyanates from the respective azides that determine M_c values.

2. Heat Release Problems

Particular attention is called to the large magnitude of the calculated temperature rises shown in Table XI, which it was believed would be damaging to the foam and to the membrane to be rigidized if an isothermal process got out of control in space. Since it appeared that a much more elaborate development of azide synthesis than planned for the program would be required to make any large improvement in the direction of reduced heat releases, attention was turned to ways of reducing the azide requirement in formulations. The general character of foam samples produced at $-NCO/-OH$ ratios reduced to 0.75 to 0.9 was discouraging; heat distortion temperatures were found to be low. Attempts were then made to incorporate a maximum of diisocyanate in a prepolymer to reduce that necessarily supplied by azide during foaming.

Efforts to produce prepolymers with $-NCO/-OH$ ratios in the range 0.55 to 0.75

Table XI. Relationships in Formulating Azides with Polyol Resins

Resin	PFR-6 (Hydroxyl No. = 480)		Voranol RS-375 (Hydroxyl No. = 375)		HP-370 (Hydroxyl No. = 370)		Prepolymer from 10 pbw PFR-6 + 2.3 pbw Glidfoam RCR-5043 (Hydroxyl No. = ~304)		
	100(pbw)	100(pbw)	100(pbw)	100(pbw)	100(pbw)	100(pbw)	100(pbw)	100(pbw)	100(pbw)
Azide Component (for -NCO/OH = 1)									
Structure I (pbw) Total Weight	$\frac{92}{192}$	--	$\frac{71.5}{171.5}$	--	$\frac{72}{172}$	--	$\frac{58}{158}$	--	--
Structure X (pbw) Total Weight	--	$\frac{131}{231}$	--	$\frac{101}{201}$	--	$\frac{102}{202}$	--	$\frac{83}{183}$	--
Structure XI (pbw) Total Weight	--	--	--	--	--	--	--	--	$\frac{125}{225}$
Weight after Azide Rearrangement	168	207	153	182.5	235	183	236	143	210
Calculated Mol Wt /Cross Link (M_c)	--	--	308	367	473	459	549	--	--
Vol N ₂ (STP)/Vol Polyurethane Solids (Calculated)*	136	111	116	97	76	119	100	102	87
Adiabatic Temp Rise from Azide Rearrangement - of (Calculated)**	617	565	528	495	300	532	498	457	273

*Assuming for polyurethane solids, $d = 1.2 \text{ g/cc}$

**Based on a heat release of 282 cal/g for Structure I, material weight after rearrangement, and material specific heat of 0.45 cal/g-°C assumed.

SECTION III

Table XII. Effects of Prepolymerizing

Case	1	2	3
Resin	HP-370 Alone	HP-370 Prepolymered to -NCO/-OH = 0.55	HP-370 Prepolymered to -NCO/-OH = 0.25
Wt % Structure X in precoat for final -NCO/-OH = 1	50.5	25.9	36.3
Calculated mol wt/cross- link (M_c)	549*	507*	525*
Calculated adiabatic temp rise from azide rearrange- ment ($^{\circ}\text{F}$)	498	240	345
Polymer melting temp ($^{\circ}\text{F}$)	--	~350	~350

*Variation occurs in the values for M_c because two isocyanates of different molecular weights and in different ratios are being jointly used in Cases 2 and 3.

led to materials with poor solubility and unusably high viscosities, as indicated in Table VIII and related discussion above.

At this point in the program it was possible to analyze the utility of prepolymering as shown in Table XII for three possible cases utilizing HP-370 resin.

The conclusions reached are as follows:

- (1) It can be seen from Table XII that Case 2 offers the best choice with respect to adiabatic temperature rise. This rise of 240°F would occur

from the initiation temperature of about 175°F, giving a final temperature of 415°F. Such a final temperature should be tolerated by aluminized H-Film, but would be severe for aluminized Mylar. No relief can be obtained by going to a higher prepolymer of HP-370, both because the theoretical gel point is at $\text{-NCO/-OH} = 0.58$ and because it is found experimentally that the Case 2 prepolymer is already somewhat too viscous for suitable frothing in a vacuum foaming process. The prepolymer of Case 3 has viscosity properties more suited to vacuum foaming, but at the expense of a 100 degree higher a diabatic temperature rise than Case 2.

- (2) Reduction in cross-link density without non-permissible reduction in heat distortion temperature might be effected by (1) use of an azide yielding a polyfunctional isocyanate; or (2) further search among heterocyclic or aromatic polyols for one that, at equivalent or higher weight than HP-370, would yield a urethane polymer with superior chain stiffness or high glass transition temperature.

3. Conclusions with Respect to an Isothermal Process

The problem of producing a satisfactory foam with so limited an amount of azide that a runaway reaction would do no harm has been discussed in detail above.

Realistic evaluation of a formulation's performance under isothermal processing would require a laboratory setup that would effectively simulate the rates of heat gain or loss that would prevail in orbit.

The process would necessarily be slow to avoid a runaway condition until perhaps half the azide had been rearranged, because of the high temperature coefficient of azide rearrangement rate at 175°F and above. In all probability, several orbits would be required.

SECTION III

A slow foaming process allows time for much drainage of cell walls under gravity and surface tension forces. Foam structure should be better in a weightless situation, but prediction from laboratory experimentation is difficult.

In slow foaming with radiant heating on the back side of the mirror-to-be, the first foam rising tends to form an insulating blanket that isolates unreacted or reacting precoat beneath. This changes the factors that control an isothermal operation. This situation probably occasions most of the difficulties that have been experienced in laboratory vacuum foaming with radiant heating under intended isothermal conditions.

H. PRECOAT FORMULATION FOR AN ADIABATIC FOAMING PROCESS

1. Process Basis

The concept of a fast foaming, adiabatic process has been discussed. The essential elements in formulating and operating the process may be summarized as:

- (1) A prepolymer is chosen on the basis of suitable viscosity at the critical stage in foaming, and structure to yield a final suitable M_c value for resistance to heat distortion.
- (2) The sum of azide and blocked isocyanate is chosen to supply the desired final -NCO/-OH ratio. Isocyanate from azide is generally put around one third to one half of the total supplied.
- (3) The amount of azide is adjusted so that its rapid rearrangement will give an adiabatic temperature rise from 175 - 190°F into the range at which the blocked isocyanate is rapidly "unblocked" (with absorption of heat). At the same time the azide supplies blowing gas.
- (4) Catalysts for the urethane reaction are supplied so that good curing will occur in the short period of time at maximum temperature and thereafter.

- (5) A foaming test is desirably conducted in a well controlled environment. Loss of heat by conduction from the precoat to some contacting part of the equipment, for instance, will quench the foaming reactions.

2. Development of the Process

Some of the experimental work that was required to establish parameters in the formulation is summarized in Table XIII. Primary emphasis here is in the choice of prepolymer. Experimentation at this stage consisted largely in making a number of vacuum foaming runs with close observation of the frothing and rigidizing behavior of each sample. The vacuum bell jar equipment that was used, some of the steps in applying precoat to aluminized film substrates, a foaming run in progress and removal of a sample after foaming are illustrated in Figures 4 through 8.

Further studies led to the conclusion that temperature resistance of the foam would be improved by substitution of MDI for TDI in prepolymers. This work was summarized in Table IX. The prepolymer of formulation 382-37 was adopted for all further work. It is produced by reacting HP-370 resin with a suitable quantity of MDI to give -NCO/-OH ratio of 0.30.

Guidance in formulating to obtain best heat distortion resistance was obtained from routine determinations of polymer melt temperature on a hot bar. Further information was obtained by observing elongation versus time of foam specimens lightly loaded in tension while being heated from ambient at the rate of about 1°F per minute. Behavior of some of the early foams in this test is illustrated in Figure 9.

Experiments demonstrated the need for a urethane polymerization catalyst to advance the cure during the exotherm and immediately thereafter. In the beginning, both a tin catalyst and an amine catalyst were incorporated in the formulations as

SECTION III

Table XIII. Precoat Formulations and Vacuum Foaming Results

Formulation No.	382-9 No. 5	382-14	382-15	382-16 No. 1	382-16 No. 2	382-21	382-23
Type or Basis of prepolymer	TP-440 + TDI	HP-370 + TDI	HP-370 + TDI	PEP 650 + TDI	PEP 650 + TDI	PEP 650 + TDI	Polymer mix of HP-370 + PEP 650 after prepolymerization
Prepolymer -NCO/-OH	0.33	0.33	0.33	0.33	0.33	0.4	0.33
Wt % of prepolymer	48	56.25	51.4	50.5	50.8	57	50.8
Azide Structure	X	I	X	X	X	X	X
Wt % azide	16.7	11.3	15.4	15.9	15.8	16.2	15.8
Wt % blocked isocyanate (a)	28.8	29.6	26.6	27.1	26.8	19.4	26.8
Wt % Surfactant (b)	0.5	0.56	1.54	1.5	1.5	1.7	1.5
Catalyst							
Wt % Dabco (c)	1.5	0.56	1.54	1.5	1.5	1.7	1.5
Wt % D-22 tin (d)	0.5	0.56	0.51	0.5	0.5	0.57	0.5
Wt % Dipropylene glycol	3.0	1.14	3.8	3.0	3.0	3.46	3.0
Maximum measured temp (°F)							
During foaming		Little rise in temp	340	346	325	350	345
Condition of mirror surface		Good	Good	Good to fair	Good to fair	Good	Good to excellent
Foam properties							
Polymer melt temp (°F)		240 - 250	260 - 290	250 - 265	250	215 - 230	270 - 285
Frothing prior to cure	Very fluid mix. Much expansion and collapse.	Rather stiff. Poor foam due to heat on foam before cure.	Slightly more fluid, but a little too stiff.	Rather fluid, but borderline.	Rather fluid, but still borderline.	Still slightly fluid.	Close to ideal. Very slightly stiff.

(a) Blocked diisocyanate used in all cases was the bisphenol adduct of 4, 4'-diphenyl methane diisocyanate, under the commercial designation of Hytlen MP by DuPont.

(b) Surfactant used in all cases was L-5310, Union Carbide Corp.

(c) The amount of Dabco used in all cases was added as a 33% solution in dipropylene glycol, made by Houdry Process Corp.

(d) D-22 tin catalyst is dibutyl tin dilaurate in an inert solvent, made by Union Carbide Corp.



Figure 4. Preparation of 6-Inch Disc Test Sample - Precoat Foam on Aluminized Mylar

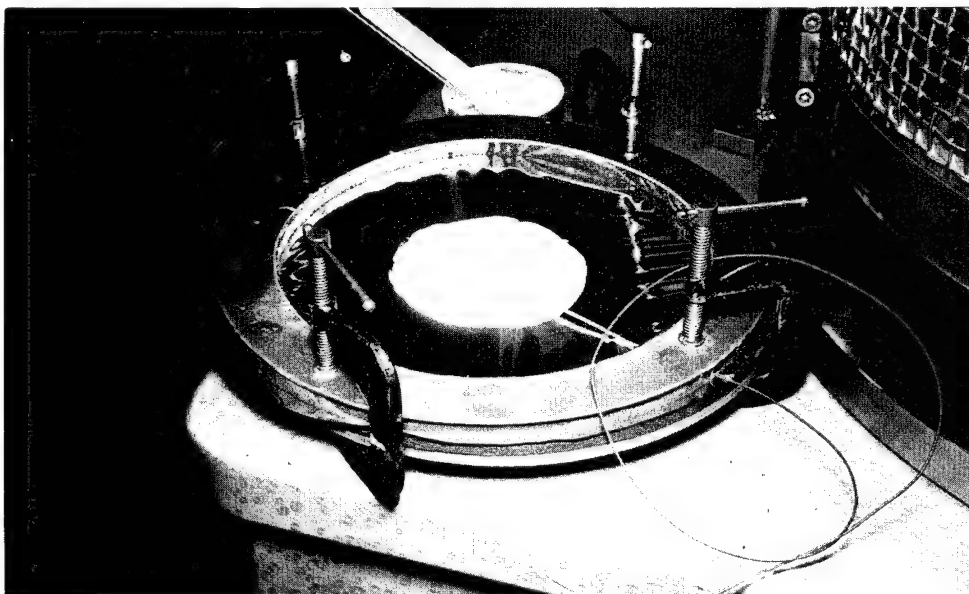


Figure 5. Test Sample in Ring Fixture

SECTION III

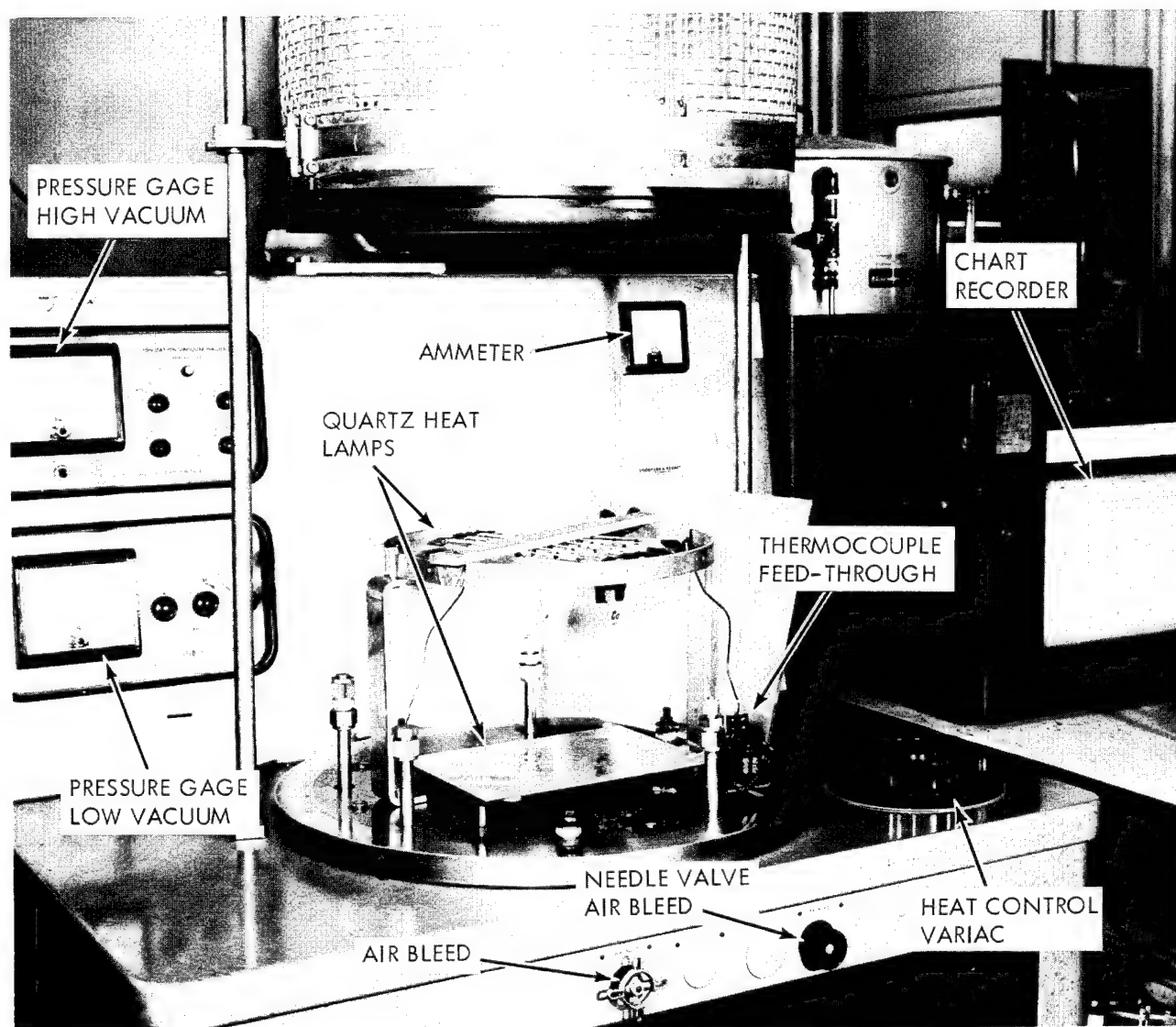


Figure 6. Bell Jar Test Facility

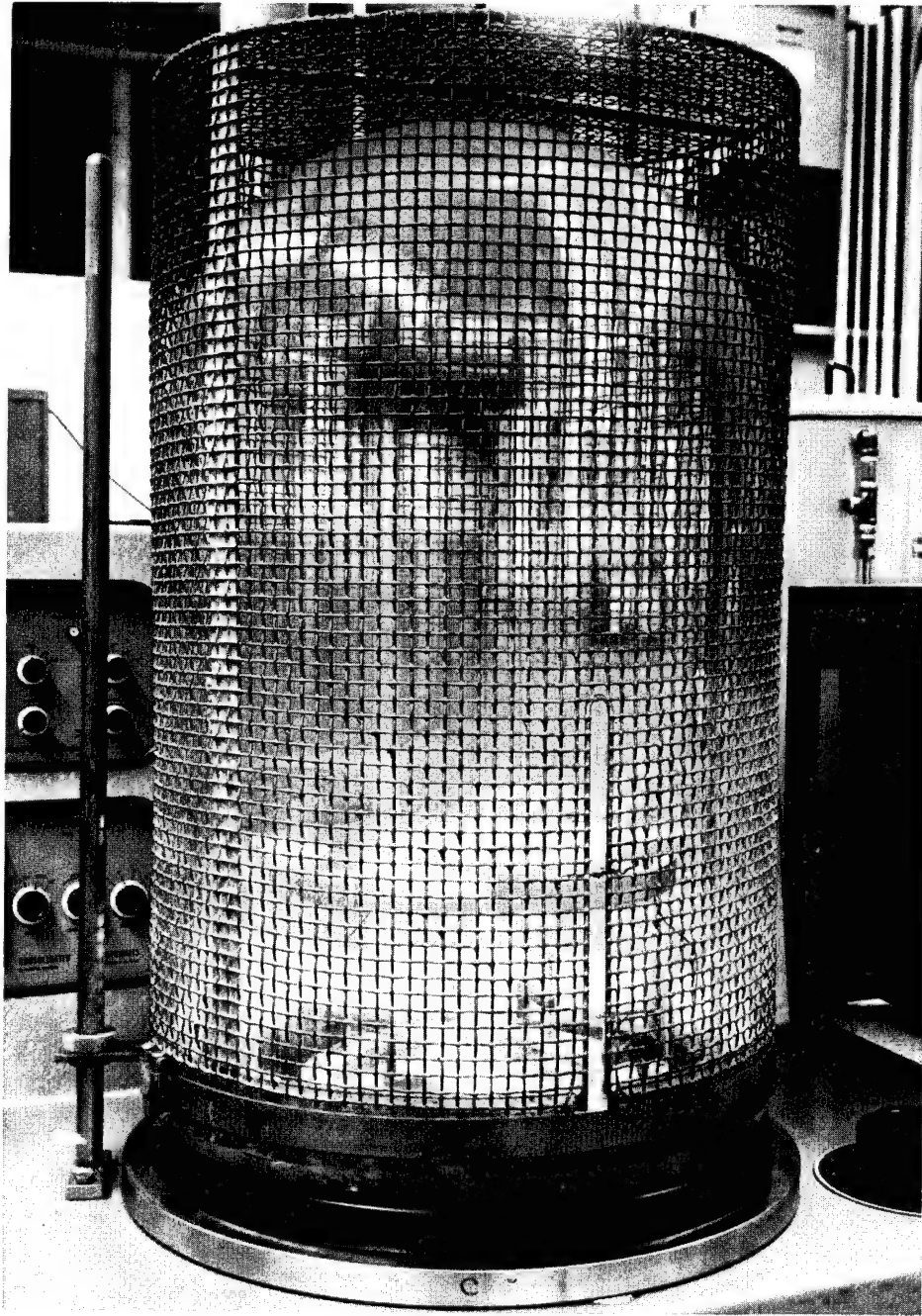


Figure 7. Test Run in Evacuated Bell Jar
with Heat Applied



Figure 8. Removal of Test Sample from Bell Jar

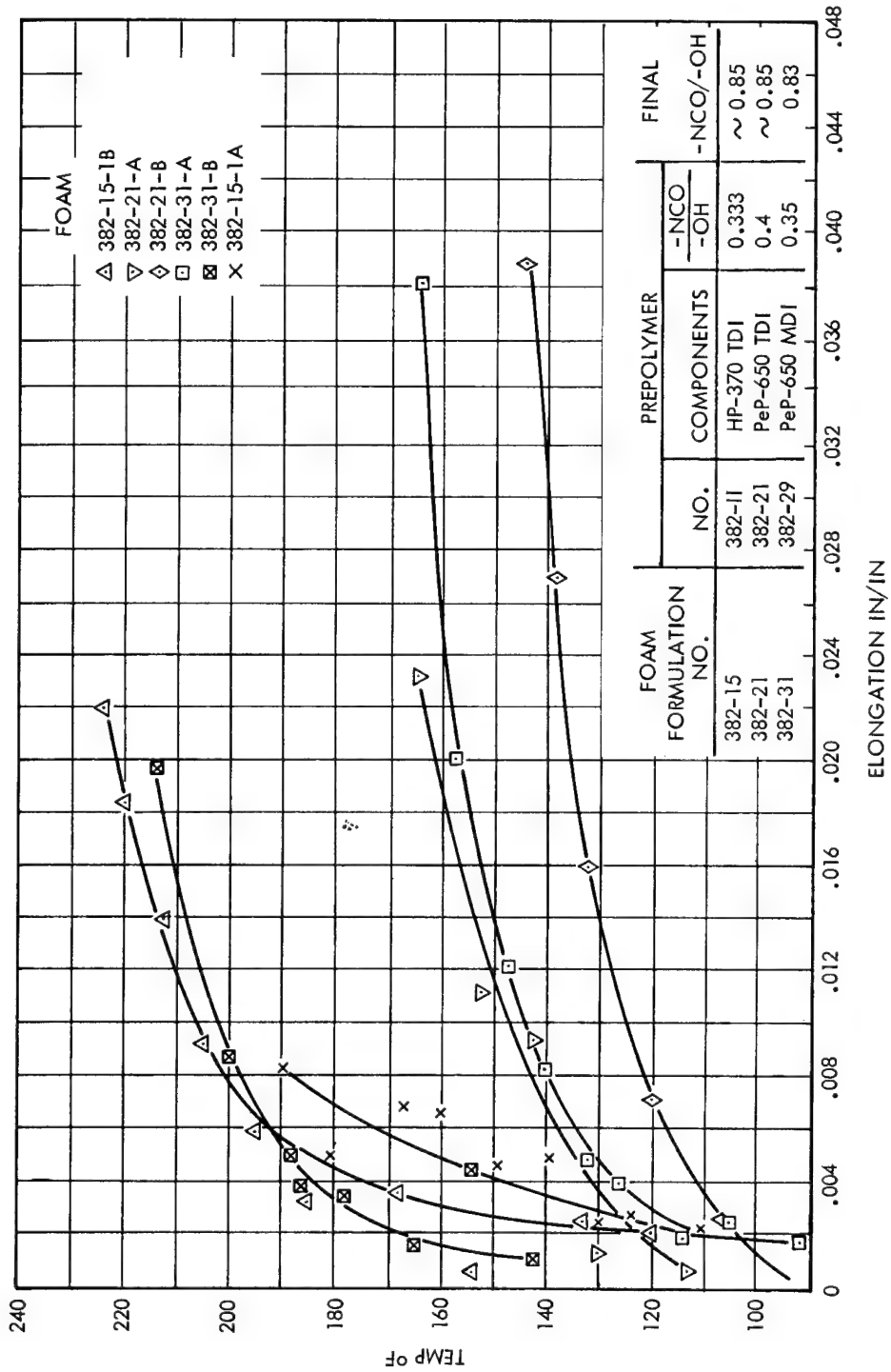


Figure 9. Heat Distortion Tests - Experimental Prepolymer Formulations

SECTION III

indicated in Table XIII. Soon afterward, it was suspected that the amine catalyst impaired the storage stability of the formulations, and its use was discontinued. Experimentation to determine the optimum concentration of a tin catalyst is incomplete due to time limitations. However, the concentration selected is satisfactory.

Some experimental evidence was obtained indicating that the surfactant used in the formulations in Table XIII had a beneficial influence on foam structure. Its use has been continued at the 1.6 weight percent level. However, its influence is not well defined, since again time limitation prevented further investigation in this area.

The original choice of phenol-blocked 4,4' - diphenyl methane diisocyanate for the blocked isocyanate component has seemed satisfactory. In view of other more pressing questions, no further investigation of alternative materials has been found necessary.

In adopting a standard formulation with an exotherm peaking at about 350°F, consideration was given to the effect of the exotherm on a stressed Mylar film substrate. Higher peak exotherms were thought somewhat risky. In consequence, little attention was given to formulations with higher exotherms. However, in earlier work formulation 394-28 was made up with a higher ratio of azide to blocked isocyanate and foamed in vacuum on a H-Film membrane. The peak of the exotherm was 425°F. The heat distortion test results are shown in Figure 10. The heat distortion temperature is indicated to be higher than usual, although the polymer melt temperature of 320°F is in agreement with the polymer melt temperature obtained on many samples made with the standard formulation.

3. Standard Formulation of Precoat

The precoat formulation adopted as standard is made up on a weight basis as shown in the following tabulation, identified as standard precoat formulation No. 382-40.

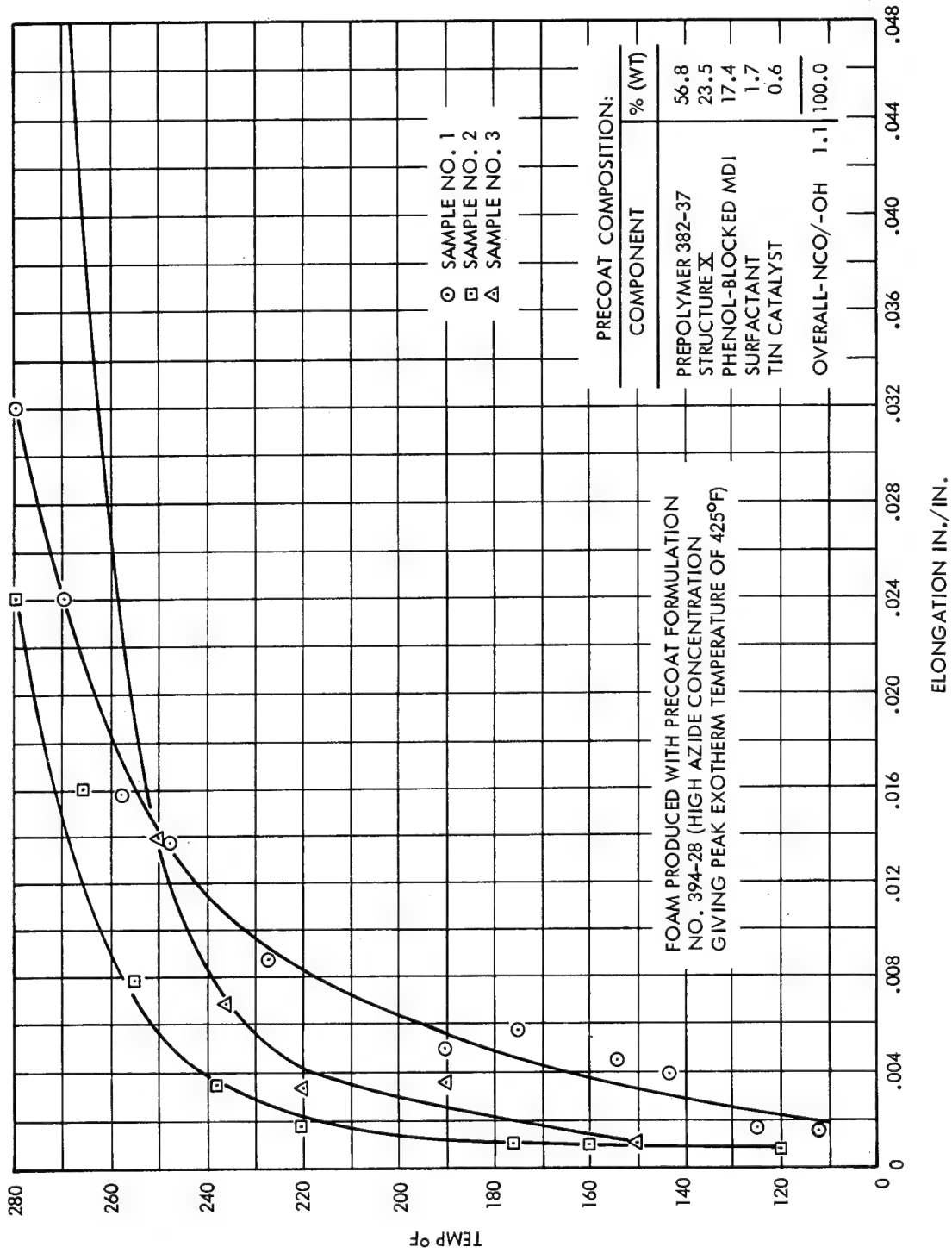


Figure 10. Heat Distortion Tests - High Azide Concentration

SECTION III

<u>Component</u>	<u>Weight (%)</u>
Prepolymer 382-37 (or equivalent) solids	55.4
Azide Structure X	16.5
Biphenol adduct of 4,4'-diphenyl methane diisocyanate (DuPont's Hylene MP)	26.0
Surfactant (Union Carbide's L-5310)	1.6
Tin Catalyst (Union Carbide's D-22)	0.5
	100.0

Some 30 to 40 parts by weight acetone per 100 parts of the above is used as a solvent and plasticizer for mixing and homogenizing the formulation. Spreadable paste is obtained by evaporating (without heating) a portion of the acetone to an acetone content of around 20 weight percent. To obtain a relatively non-tacky sheetable material, the acetone content must be reduced to about the one percent level. In pumping a bell jar down prior to a vacuum foaming, the pressure generally cannot be pulled down below about one hundred microns until the acetone content of a sample to be foamed is reduced to the one percent level.

4. Quartz Fiber Addition to Precoat

It has been found that the addition of a few percent quartz fiber modifies the physical structure of the foam to a considerable degree. Higher densities, strengths, and hardness result from the addition. There also appears to be improvement in heat distortion temperature. Figure 11 shows the resistance to heat distortion displayed by formulation 382-40 to which had been added 5 percent silica fiber.

Although observation of the foaming process indicates that less fluidity develops when fiber is present, it is not clear whether this is the only way in which fiber influences cell size. Nor is it clear as to just how strength-weight ratios and heat distortion temperature are improved by fiber.

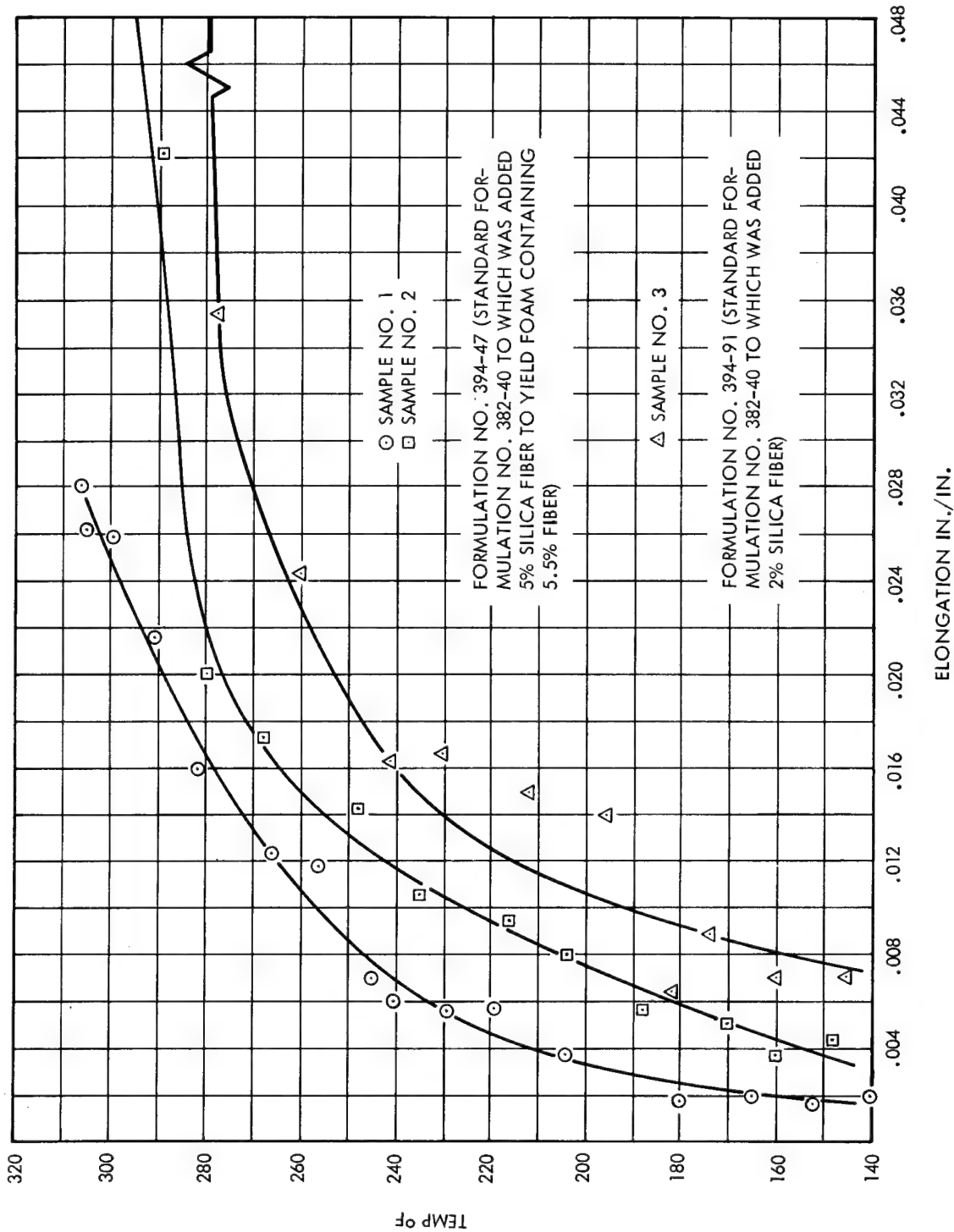


Figure 11. Heat Distortion Tests - With Microquartz Added

SECTION III

On the basis of limited experimentation, it was concluded that the addition of two parts by weight chopped silica fiber (microquartz, 0 - 3 micron diameter) to 100 parts of standard formulation 382-40 would make an over-all improvement in physical properties without increasing density unduly. The modified formulation standard for preparation of physical test specimens is designated 394-91. Results of a preliminary heat distortion test on this material are plotted in Figure 11.

5. Storage Stability of Precoat

De-acetonized precoat spread on Mylar film and stored at room temperature for 44 days has been found to foam satisfactorily. A similar sample stored at room temperature for 137 days did not foam and exhibited no detectable exotherm. A like sample stored for 139 days at about 40°F foamed in the same way as fresh precoat.

Some undesirable stiffening of precoat occurs on long standing that seems unrelated to retention or loss of foaming activity. There has been no opportunity to investigate the phenomenon.

6. Stability of Precoat in Vacuum

The prepolymer that is the basis of the standard formulation is of sufficiently high molecular weight to be quite indifferent to vacuum exposure. The other components may have somewhat higher vapor pressures, but when dispersed within the prepolymer phase their rates of volatilization appear to be very low. Precoat has been exposed to vacuum in the 10^{-4} to 10^{-5} mm Hg range for as long as 60 hours at room temperature without impairment of subsequent foaming behavior.

7. Weight Loss During Foaming

Nitrogen gas is evolved from the azide component and phenol is liberated from the blocked isocyanate component during foaming. Assuming no other volatile components in the precoat, and assuming that nitrogen and phenol are lost to the vacuum,

weight loss on foaming is calculated to be 14.2 weight percent, based on the original acetone-free precoat weight. Calculated yield of foam solids is thus 85.8 weight percent. Experimental foam yields are generally in the 83 to 86 percent range. Modified Kjeldahl nitrogen analysis of foam shows the nitrogen content to be a little below theoretical, suggesting a loss of azide or isocyanate sufficient to reduce foam yield by one to two percent below the theoretical 85.8 percent.

SECTION IV. PREPARATION OF PHYSICAL TEST SPECIMENS

To prepare test specimens for the density, thermal expansion, stress-strain, shear, creep, and dimensional stability tests, foam masses from which 1 x 1 x 4 inch bars, 2 x 2 x 2 inch cubes, etc could be cut were made. Photographs of a typical foam mass are seen in Figures 12 and 13. Precoat material of standard formulation 394-91 with 2 percent microquartz was vacuum-dried to reduce plasticizing acetone to about one percent or slightly less, producing a thin sheet. Three thicknesses of such sheets were pressed in a 5 x 5 inch square mold. The final compacted sheet, weighing about 97 grams, or 3.8 grams/in.², was supported on glass cloth and foamed, one 5 x 5 inch sheet at a time, in a bell jar. Heating rate, with radiant heat from above, was about 3.5°F/minute as measured by a thermocouple embedded in the edge of the sheet. A total of 27 sheets were foamed to produce the material from which specimens were derived.

Specimens for adhesion and ultraviolet exposure tests were prepared from five foam squares prepared according to the following procedure. A five-inch square of standard formulation 394-91 precoat material was centered on a 10-inch diameter circle of H-Film. An amount of precoat was spread to yield a total solids content of 20 grams or 0.8 g/in.² The material was vacuum dried as before. Foaming in vacuum was accomplished with overhead radiant heating at a rate of 8°F/minute in a bell jar. A total of 6 foam squares were thus prepared.

For the thermal conductivity tests, circles 9-1/2 inch in diameter of standard precoat 394-91 were spread on clear Mylar and H-Film and vacuum dried to yield 57 grams precoat solids, or 0.8 g/in.². The samples were foamed in a bell jar using a weighted hoop stretch ring to approximate the stress developed in the film

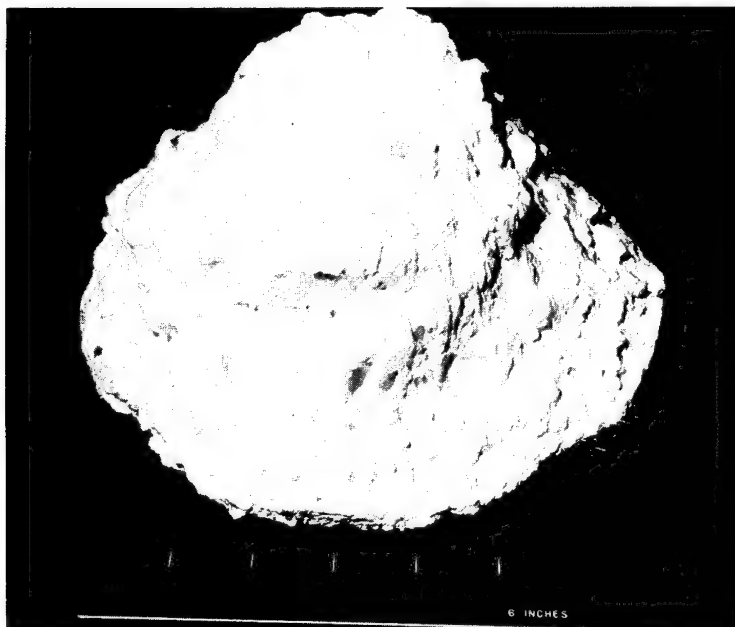


Figure 12. Typical Foam Mass

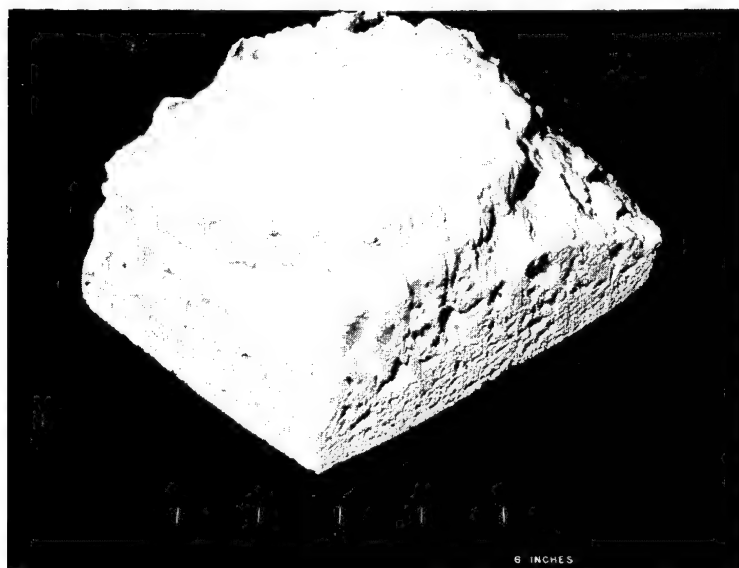


Figure 13. Typical Foam Mass Section

SECTION IV

of the 2-foot models. The samples were heated with radiant heat from above and below at a rate of $12.5^{\circ}\text{F}/\text{minute}$. A total of 8 clear Mylar and 6 H-Film samples were foamed to produce the material from which specimens were cut for the thermal conductivity tests.

SECTION V. PHYSICAL PROPERTIES

A. GENERAL

The results of the testing program conducted to determine the physical properties of predistributed foam are given in Subsection B below. The test program is outlined in Table XIV.

Design of inflatable rigidized structures as solar concentrators for use in the space environment requires that a number of the physical properties of the rigidizing materials be known. Some physical property data is available for foam material produced at atmospheric pressure, but at present there is only one report (Reference 4) available on physical properties of foams generated and tested under vacuum conditions. This referenced report is for a GAC mechanically mixed foam.

Physical property data is needed for a range of foam densities and temperatures. The various foam formulations producing various densities have somewhat different physical properties. The density selected will depend on the properties required. The data for various temperatures is needed because, for example, the temperature in a solar reflector is neither constant nor uniform.

The scope of this contract included a limited test program intended only to yield sufficient physical property data to determine whether the rigidizing foam material has the basic capabilities for application to space solar collectors.

A more comprehensive test program on foams will be required for design calculations in an actual space application if the solar collector is to have predictable performance.

SECTION V

Table XIV. Test Performed

Type of Test (Vacuum Tested)	Specimen Size (inches)	Test Temp (°F)	Density (ρ) Range (pcf)	Strain Rate (in./in./min)	Remarks	Number of Repeats (Subtotals)	Total Tests for Each Type
Thermal Coefficient of Expansion	(1 x 1 x 4)	75 to 300	2.44 to 3.54	--		3	3
Stress-Strain Tension	(1 x 1 x 4)	78	3.25 to 3.82	0.10		3	
	(1 x 1 x 4)	78	4.63	0.25		1	
	(1 x 1 x 4)	78	3.27 to 4.35	0.05		3	
	(1 x 1 x 4)	78	3.32 to 4.34	0.50		3	
	(1 x 1 x 4)	-200	3.56 to 4.18	0.10		3	
	(1 x 1 x 4)	+240	3.51 to 3.72	\approx 0.10		3	
	(1 x 1 x 2.5)	\approx 240	\approx 4.35	0.10		2	18
Stress-Strain Compression	(1 x 1 x 2)	75	2.33 to 4.40	0.10		3	
	(1 x 1 x 2)	240	2.50 to 3.77	0.10		3	
	(1 x 1 x 2)	-200	3.51 to 3.97	0.10		3	9
Shear	2 at (2 x 2 x 3/8)	75	5.00	2.0		1	
	2 at (2 x 2 x 3/8)	75	3.63 and 3.67	20		2	
	2 at (2 x 2 x 3/8)	185	2.57 to 4.10	20		3	
	2 at (2 x 2 x 3/8)	240	3.05 to 3.29	20		3	9
Bond Strength to Mylar versus Temperature	(3/8 x 1 x 5)	75	8.22 to 8.55	(1 in./min)	UV Exposure(hrs) 10 100 1000	4	
	(3/8 x 1 x 5)	185	7.22 to 9.90	(1 in./min)		3	
	(3/8 x 1 x 5)	240	7.15 to 8.27	(1 in./min)		3	10
Bond Strength to Mylar versus Ultraviolet	(3/8 x 1 x 5)	75	7.74 to 8.35	(1 in./min)	10	3	
	(3/8 x 1 x 5)	75	7.71 to 9.48	(1 in./min)	100	3	
	(3/8 x 1 x 5)	75	7.16 to 7.98	(1 in./min)	1000	3	10
Dimensional Stability	(2 x 2 x 2)	75	2.9 to 3.4	--	(Length of Test) 169 to 175 hr	3	3
Creep	(1 x 1 x 4)	75	2 at 3.62	Load=50%F _{ty}	> 500 hr	2	
	(1 x 1 x 4)	185	3.61 and 3.55	Load=50%F _{ty}	> 355 hr	2	
	(1 x 1 x 4)	240	3.91 and 3.87	Load=50%F _{ty}	> 18 hr	2	2(4)*
Tension Tests (2-ft mirror)	(4 x 2 x \approx 1/4)	75	8.4 to 9.0	0.1	(With H-Film)	3	6
	(4 x 2 x \approx 1/4)	75	5.8 to 9.1	0.1	(Without Film)	3	6
Thermal Conductivity	3/8 x 9 dfa	-200 & 100			(With H-Film)	3	3
		-65 & 100 75 & 200 75 & 240			(Without H-Film)	3	3
Reflectance	1 inch discs	75	--	--	1 - aluminized Mylar 1 - aluminized H-Film 3 - from rigid- ized mirror No. 3	--	5

*The column "Density Range" indicates the maximum and minimum density values of the samples tested in that particular series.

The column "Number of Repeats" indicates the number of individual tests performed at the specified condition.

Predistributed foam with densities ranging from approximately 3 to 4.5 pcf were vacuum tested to determine their basic physical properties within the temperature range expected on an orbiting solar concentrator (-200 to +240°F).

The types of tests conducted and the physical properties yielded by each test are as follows:

- (1) Tensile stress-strain tests
 - (a) Tensile ultimate stress, F_{tu}
 - (b) Tensile yield stress, F_{ty}
 - (c) Tensile modulus, E_t
 - (d) Strain at tensile ultimate stress, ϵ_{tu}
- (2) Compression stress stress-strain tests
 - (a) Compression yield stress, F_{cy}
 - (b) Compression modulus, E_c
- (3) Shear tests
 - (a) Shear ultimate stress, F_{su}
 - (b) Shear yield stress, F_{sy}
 - (c) Shear modulus, G
- (4) Thermal coefficient of expansion tests (α)
- (5) Creep tests
- (6) Bond strength tests (with ultra-violet effects) (bond of foam to film)
- (7) Dimensional stability tests
- (8) Thermal conductivity tests (K)
- (9) Reflectance tests

SECTION V

B. DISCUSSION OF TEST DATA AND RESULTS

1. General

The various physical property tests actually performed for the predistributed foam are listed in Table XIV.

The following pages contain a description of each test. Each discussion starts with the test setup and lists the problems encountered and the limitations imposed. Also included are general discussions of the data, curves, and basic results, with suggestions of possible methods for improving the test procedures and methods of data analysis for future tests.

2. Data Reduction

a. Method. For the stress-strain and shear tests there were usually only three tests run at one temperature and at one load rate, with the densities of these specimens varying from approximately 3 to 4-1/2 pounds per cubic foot (pcf). With this limited amount of test data and with the added effects of void size variation with respect to specimen size, it was necessary to select a method for obtaining the best curve fit for these conditions. The method selected was the method of least squares as applied to a linear curve. An example of this method as applied to the tensile ultimate (F_{tu}) at 78°F is shown below. There were ten data points available for this example, but the procedure would be the same for any number of test points greater than two. In the case of the shear curves, they are expected to be nearly linear and to pass through the origin. This was accomplished by assuming an additional large number of test points of zero density having zero shear properties.

b. Example - Least Squares Method (Linear)

Straight line equation:

$$Y = a + b X \quad (1)$$

where

$$a = \frac{N_a}{D} \quad (2)$$

$$b = \frac{N_d}{D} \quad (3)$$

$$D = \begin{vmatrix} \Sigma N & \Sigma X \\ \Sigma X & \Sigma X^2 \end{vmatrix} = [\Sigma N \times \Sigma X^2] - [\Sigma X]^2 \quad (4)$$

$$N_a = \begin{vmatrix} \Sigma Y & \Sigma X \\ \Sigma XY & \Sigma X^2 \end{vmatrix} = [\Sigma Y \times \Sigma X^2] - [\Sigma X \times \Sigma XY] \quad (5)$$

$$N_d = \begin{vmatrix} \Sigma N & \Sigma Y \\ \Sigma X & \Sigma XY \end{vmatrix} = [\Sigma N \times \Sigma XY] - [\Sigma X \times \Sigma Y] \quad (6)$$

X and Y are individually related variables and N is the number of X, Y variables or test points.

From table below, $N = 10$; $\Sigma X = 37.1693$; $Y = 115.40$; $\Sigma X^2 = 140.778$; and $\Sigma XY = 457.048$.

<u>F_{tu} at 78°F</u>				
N	X = ρ (pcf)	X ²	Y = F _{tu} (psi)	XY
1	4.6310	21.446	19.50	90.316
1	3.2486	10.553	8.00	25.989
1	3.2141	10.330	3.50	11.249
1	3.8189	14.584	11.95	45.636
1	3.6461	13.294	13.30	48.493
1	4.3546	18.963	19.10	83.173
1	3.2659	10.666	5.55	18.126
1	3.3178	11.008	7.90	26.211
1	4.3373	18.812	19.10	82.842
1	3.3350	11.122	7.50	25.013
10	37.1693	140.778	115.40	457.048

SECTION V

Using with Equations 4, 5, and 6 above, $D = 26.22$; $N_a = 742.4$; and $N_d = 281.14$.

Equation 2: $a = \frac{N_a}{D} = -28.31$

Equation 3: $b = \frac{N_d}{D} = 10.7223$.

From Equation 1, $Y = a + bX$, or $F_{tu} = -28.31 + 10.7223\rho$. Since the curve is a straight line only, two points are needed to plot F_{tu} versus ρ for this foam at 78°F .

(1) At $F_{tu} = 0$, $\rho = 2.64$.

(2) At $\rho = 5$, $F_{tu} = 25.30$ psi.

3. Stress-Strain Tests

The test setup for the tension and compression tests is shown in Figure 14 (also see References 4 and 5). All tension and compression tests were conducted on an Instron Universal Testing Machine. Test temperatures were obtained with an R. D. Brew vacuum oven. Values of load versus elongation were recorded on the Instron strip-chart recorder.

A complete list of the stress-strain tests is shown in Table XIV. There were a total of 18 tensile and nine compression tests. These tests included three temperature levels (-200 , 75 , and 240°F) and basically one strain rate (0.10 in./in./min) except for the tensile tests at 75°F , where strain rates of 0.05 , 0.25 and 0.50 in./in./min were also tested. Increased strain rates usually result in higher strength and modulus values for ductile material. However, for the limited number of tests at the three strain rates used, these differences could not be detected. There were two primary reasons for this.

- (1) The GAC predistributed foam was of the brittle variety (see Figure 15) at 78°F . For brittle materials, variable strain rates produce much smaller effects, which are difficult to detect.

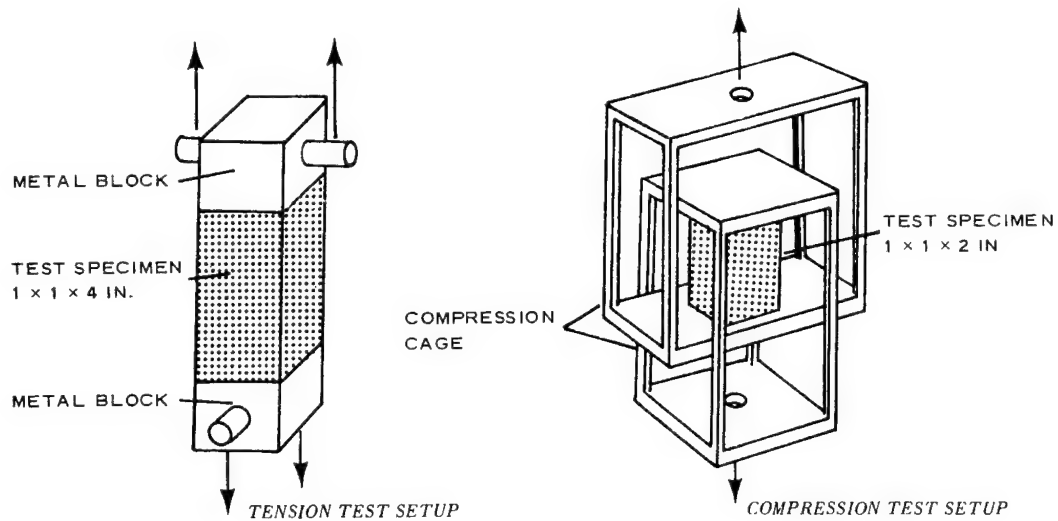


Figure 14. Stress-Strain Test Setup

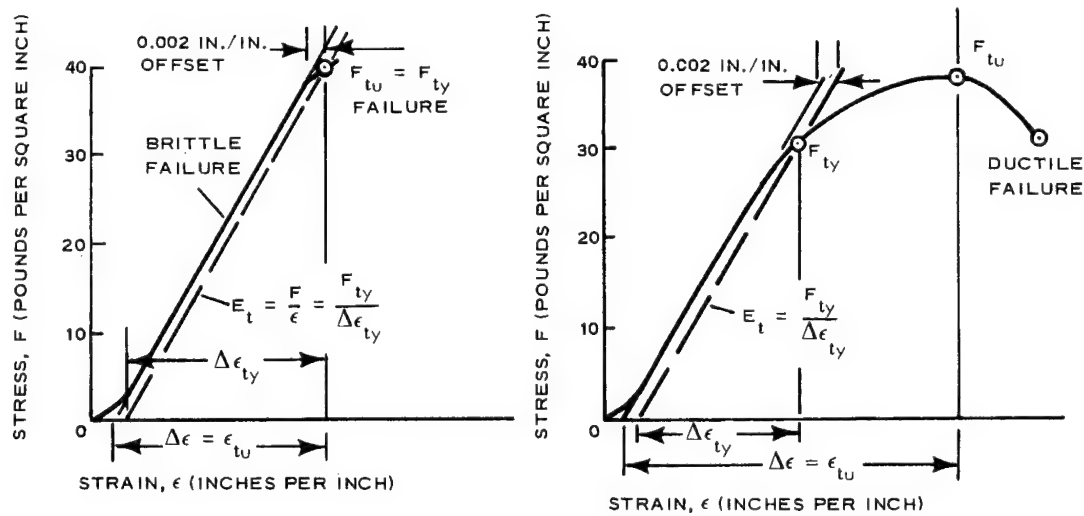


Figure 15. Sample Plots of Brittle and Ductile Foam Tests

SECTION V

- (2) The effect of data scatter was in general larger than the effect of variable strain rates, which increased the difficulty of distinguishing between the two effects.

The area of data scatter, its causes, and effects is one of the prime areas where further work is recommended in the foam development field.

When a large volume of foam is produced, local effects or voids and variations in cell sizes may be negligible. When supposedly representative specimens are cut from this larger mass, however, small voids and cell size variation may no longer be negligible within the limited dimensions of the specimen. Although obviously poor specimens can be discarded, small voids and cell size variation within the specimens and the differences between specimens of the same and different density foams seem to be the main factors contributing to data scatter and the resulting confusion in interpreting data.

The test data and data reduction (exclusive of least squares calculations for curve fitting) for all the recorded stress-strain tension and compression tests are given in Tables XV and XVI.

Tensile and compressive strength, stiffness, and elongation data are plotted by the method of least squares against density for the density range tested. These curves are then cross plotted for foam properties versus temperature for increments of foam density. The tensile and compression curves are shown in Figures 16 through 27.

The predistributed foam is brittle (see Figure 15) from -200 to 78°F , and becomes somewhat ductile at 240°F . However, even at 240°F the strain at ultimate stress is only about twice what it is at 78°F (see Figure 23).

GAC mechanically mixed foam (Reference 4) and ambient polyurethane foams (Reference 6) have comparable tensile and compressive properties. In comparison,

GAC predistributed foam has tensile properties that on the average are approximately 10 to 25 percent as good in the density range from 3 to 4.5 pcf respectively, and compression properties which on the average are approximately 20 to 25 percent as good in the same density range.

These results would indicate that although GAC predistributed foam has significant and useful tensile and compression properties for application in the rigidization of solar collectors, its main advantage still lies in its unique method of application.

Table XV. Tension Test Data for GAC Predistributed Foam

Specimen No.	Temp (°F)	Total Wt		Density		Strain Rate		Pressure (mm of hg)	Specimen Size (in.)	F _{tu} (psi)	F _{ty} (psi)	E _t (psi)	ε _{tu} (in./in.)
		G	Lb	PCI	PCF	In./Min	In./In./Min						
394-122 No. 2	78	4.8577	0.01071	0.00268	4.6310	1.0	0.25	--	1 x 1 x 4	19.5	19.5	1025	0.0200
394-124B No. 3	78	3.4113	0.00752	0.00188	3.2486	0.40	0.10	9.8 x 10 ⁻⁵	1 x 1 x 4	8.0	6.5	360	0.0270
394-126 No. 2	78	3.3813	0.00745	0.00186	3.2141	0.40	0.10	9.8 x 10 ⁻⁵	1 x 1 x 4	3.5	2.7	316	0.0196
394-121 No. 2	78	4.0109	0.00884	0.00221	3.8189	0.40	0.10	8.2 x 10 ⁻⁵	1 x 1 x 4	11.95	11.95	585	0.0217
394-124B No. 2	78	3.8227	0.00843	0.00211	3.6461	0.20	0.05	9.2 x 10 ⁻⁵	1 x 1 x 4	13.3	11.9	530	0.0296
394-122 No. 1	78	4.5752	0.01009	0.00252	4.3546	0.20	0.05	8.8 x 10 ⁻⁵	1 x 1 x 4	19.1	19.1	853	0.0238
394-126 No. 1	78	3.4358	0.00757	0.00189	3.2659	0.20	0.05	8.3 x 10 ⁻⁵	1 x 1 x 4	5.55	5.55	318	0.0190
394-124B No. 4	78	3.4826	0.00768	0.00192	3.3178	2	0.5	9.0 x 10 ⁻⁵	1 x 1 x 4	7.9	7.6	405	0.0225
394-122 No. 3	78	4.5590	0.01005	0.00251	4.3373	2	0.5	8.8 x 10 ⁻⁵	1 x 1 x 4	19.1	19.1	886	0.0230
394-126 No. 3	78	3.4990	0.00771	0.00193	3.3350	2	0.5	8.8 x 10 ⁻⁵	1 x 1 x 4	7.5	7.5	405	0.0205
394-122 No. 4	-195	4.3901	0.00968	0.00242	4.1818	0.4	0.10	8.0 x 10 ⁻⁵	1 x 1 x 4	20.6	20.6	1385	0.0155
394-124D No. 2	-200	3.8698	0.00853	0.00213	3.6806	0.4	0.10	8.0 x 10 ⁻⁵	1 x 1 x 4	12.9	12.9	929	0.0155
394-126C No. 2	-205	3.7444	0.00825	0.00206	3.5597	0.4	0.10	6.0 x 10 ⁻⁵	1 x 1 x 4	12.35	12.35	903	0.0144
394-124C No. 3	241	3.8925	0.00858	0.00215	3.7152	0.25	0.0625	2.8 x 10 ⁻⁴	1 x 1 x 4	3.50	3.35	126	0.0386
394-124D No. 2	239	3.8475	0.00848	0.00212	3.6634	0.40	0.10	1.7 x 10 ⁻⁴	1 x 1 x 4	4.0	3.90	152	0.0297
394-121	240	3.6784	0.00811	0.00203	3.5078	0.40	0.10	1.3 x 10 ⁻⁴	1 x 1 x 4	4.95	4.10	150	0.0434
394-122 1X	250	2.8595	0.006304	0.00252	4.3546	0.25	0.10	3.0 x 10 ⁻⁴	1x1x22.5	11.8	8.0	372	0.0450
394-122 3X	240	2.8494	0.006282	0.00251	4.3373	0.25	0.10	2.4 x 10 ⁻⁴	1x1x22.5	13.85	9.5	470	0.0403

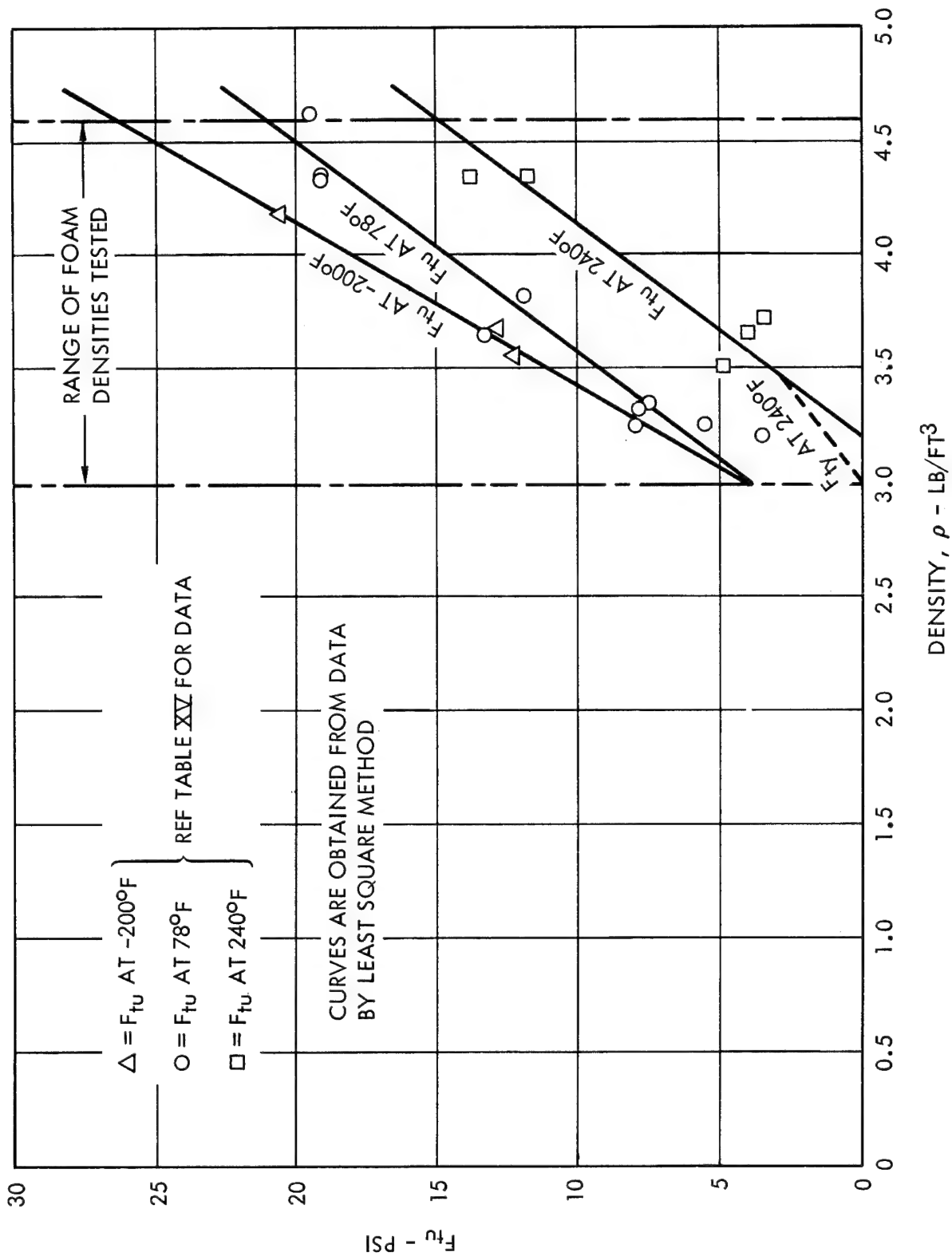


Figure 16. Tensile Ultimate Stress versus Density

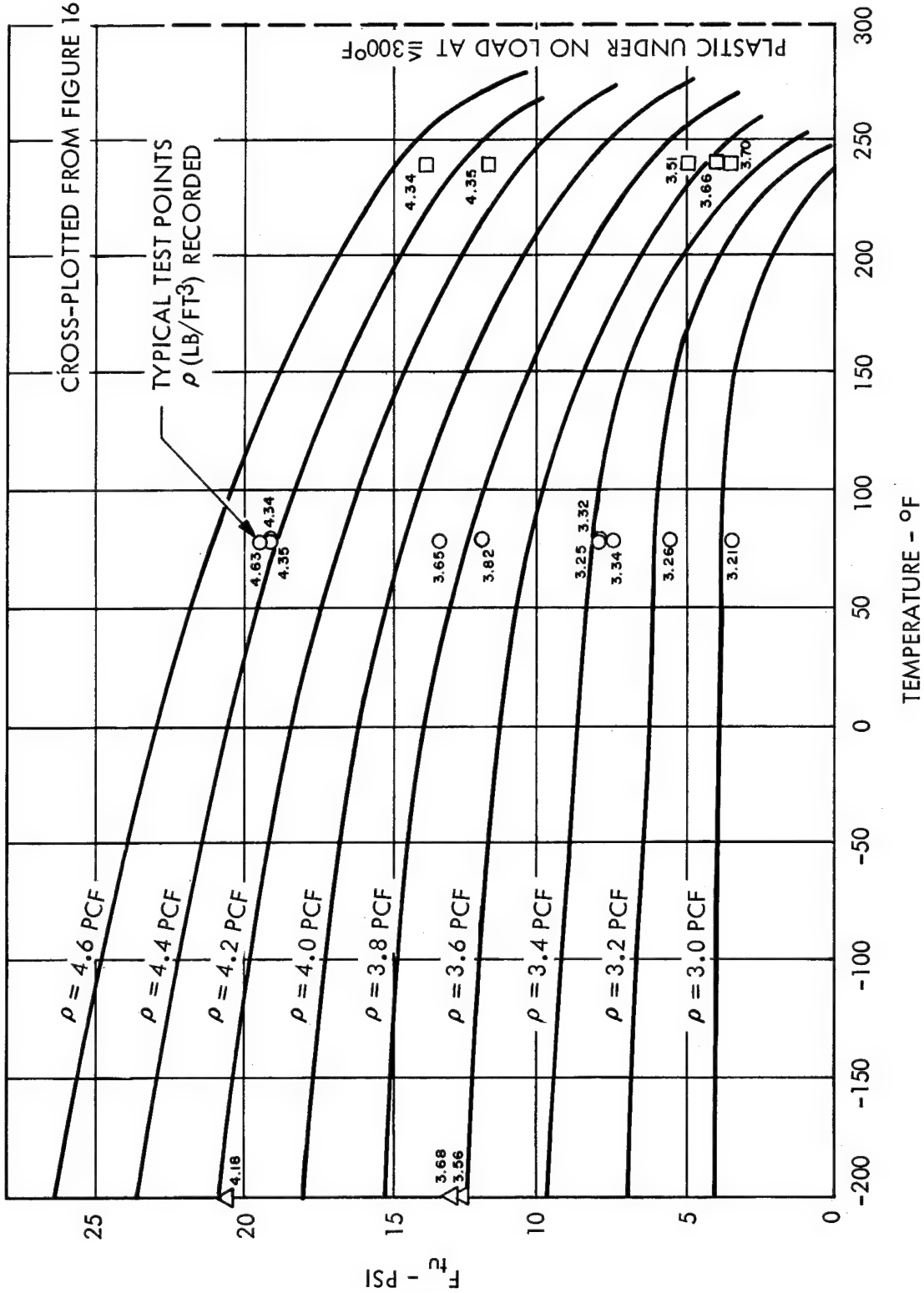


Figure 17. Tensile Ultimate Stress versus Temperature for Density Range Tested

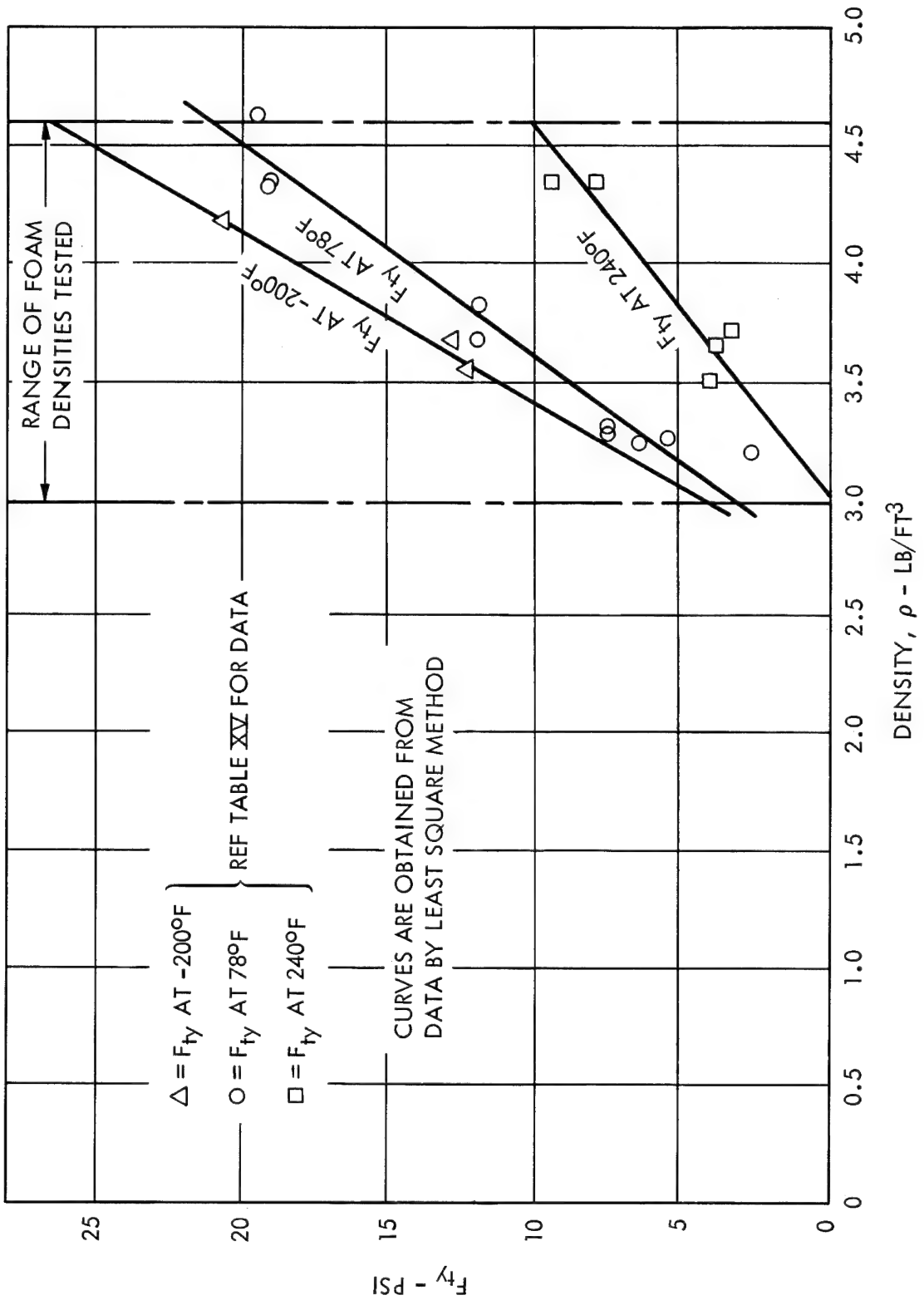


Figure 18. Tensile Yield Stress versus Density

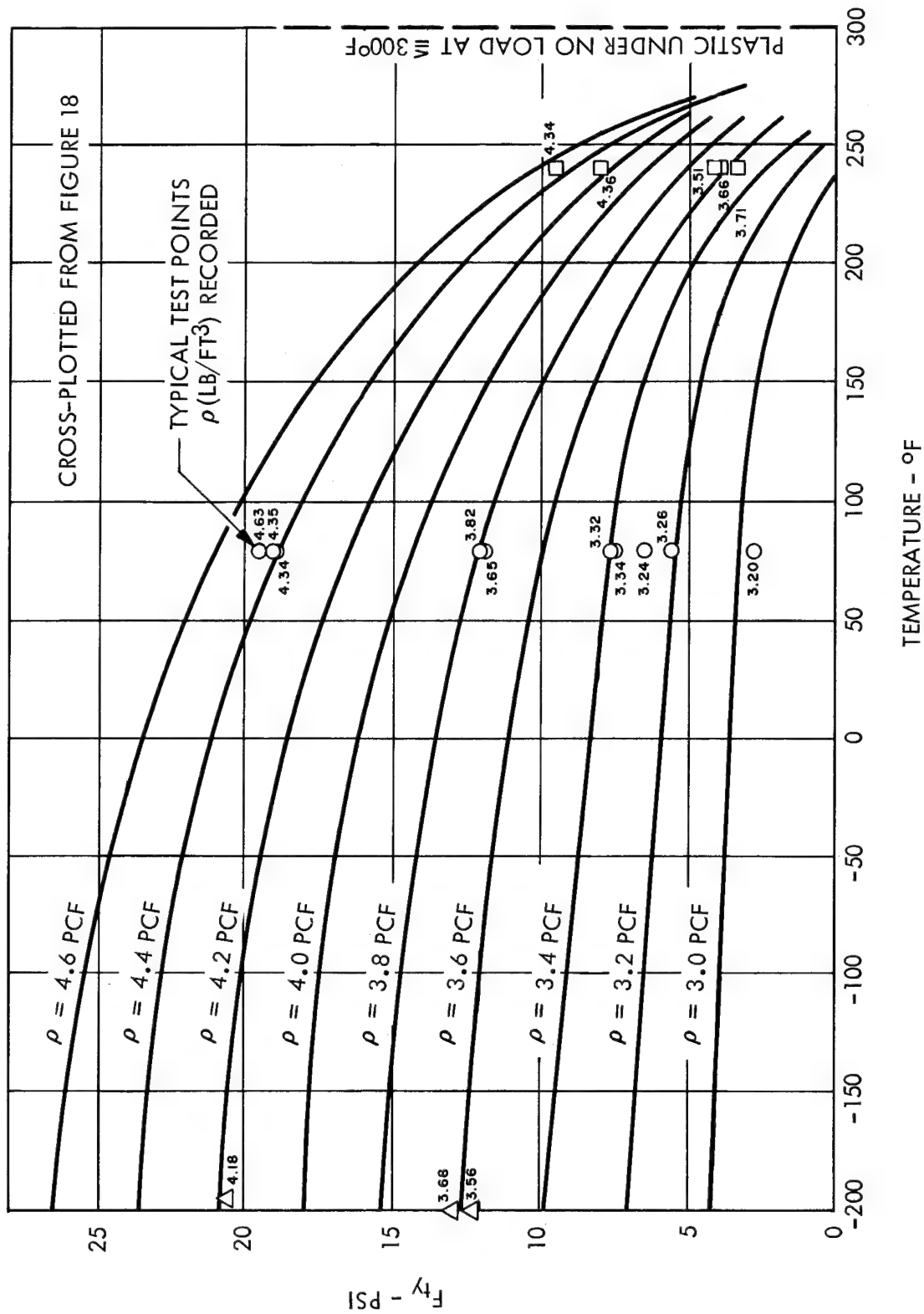


Figure 19. Tensile Yield Stress versus Temperature for Density Range Tested

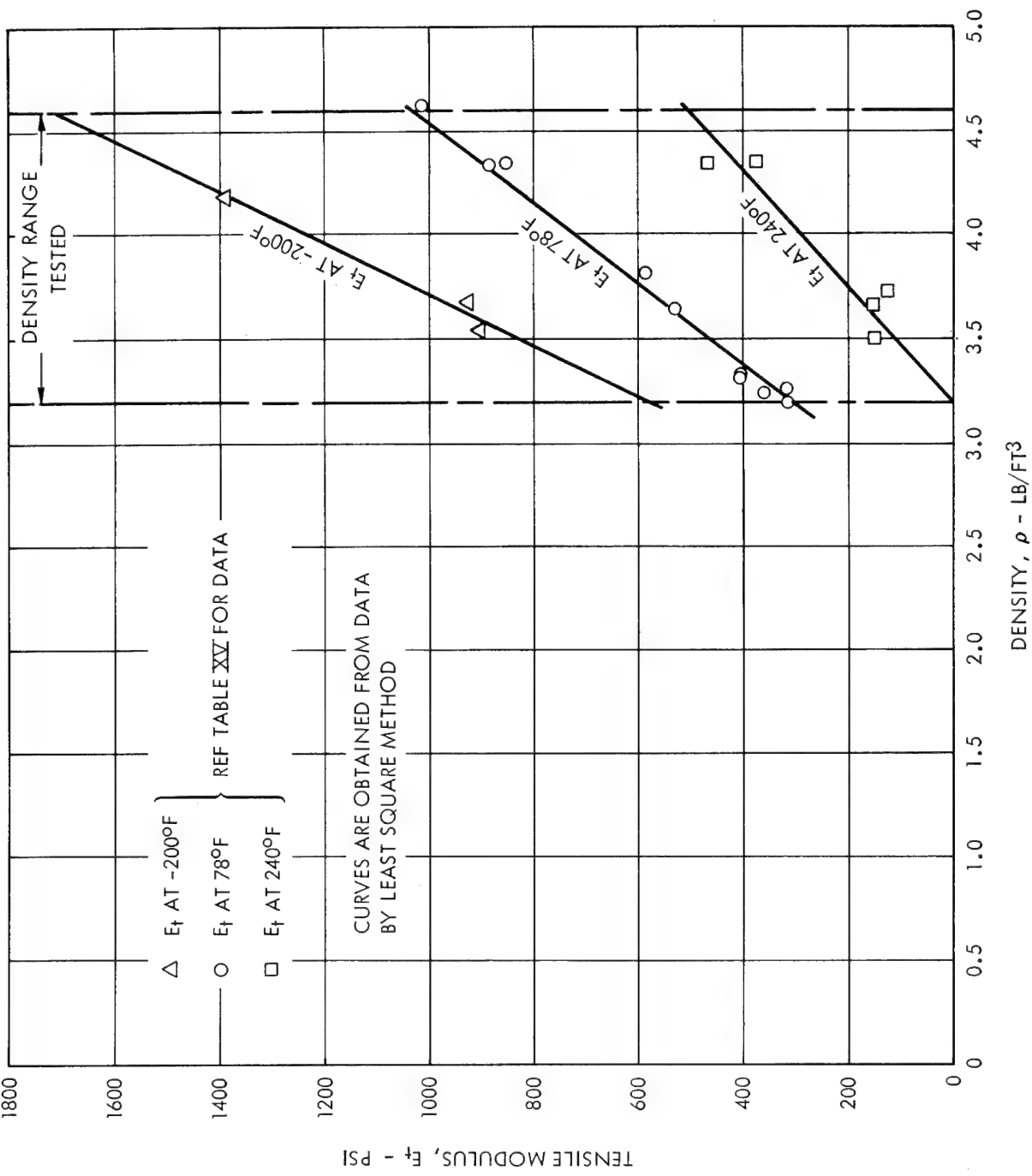


Figure 20. Tensile Modulus Stress versus Density

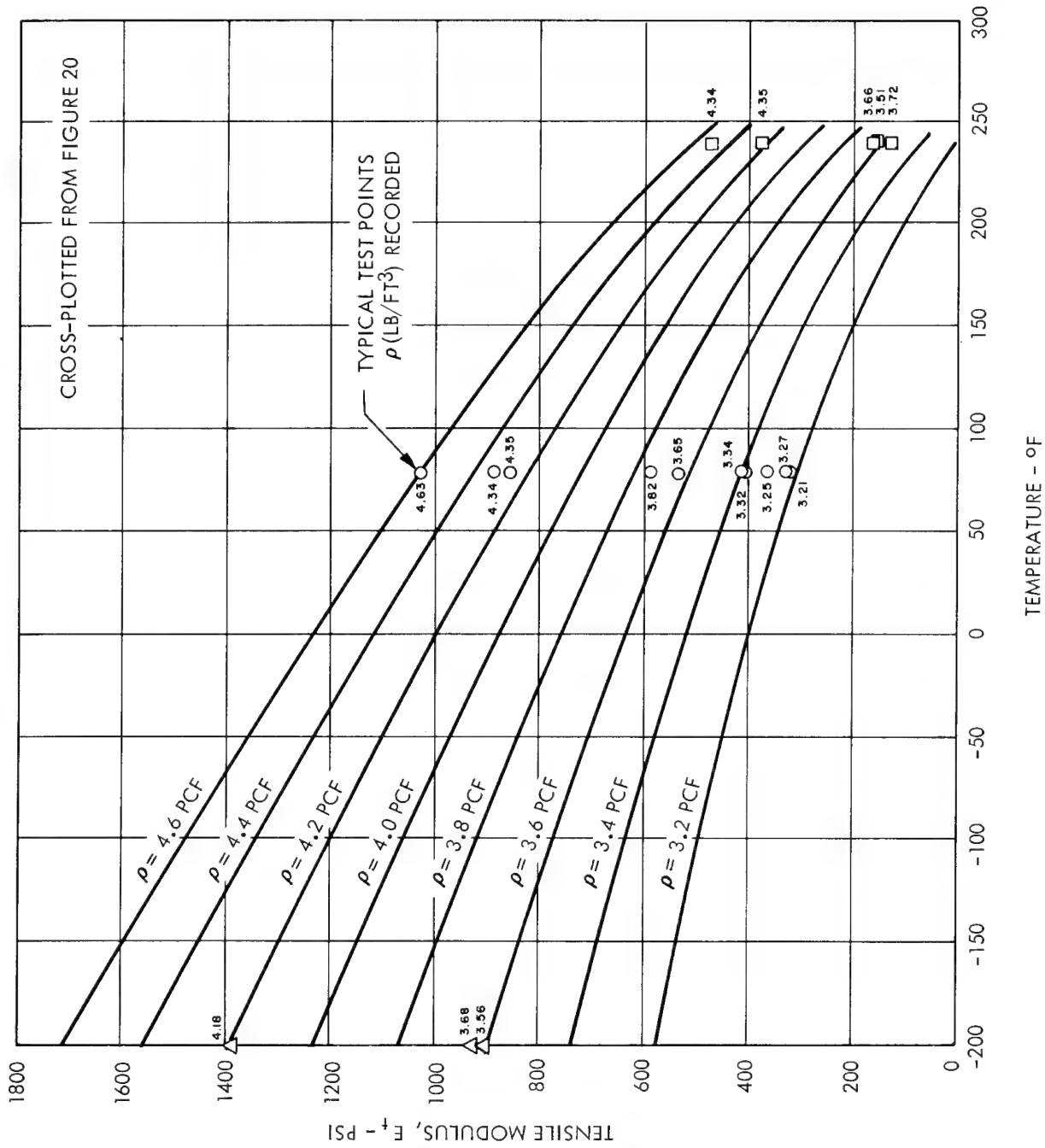


Figure 21. Tensile Modulus Stress versus Temperature for Density Range Tested

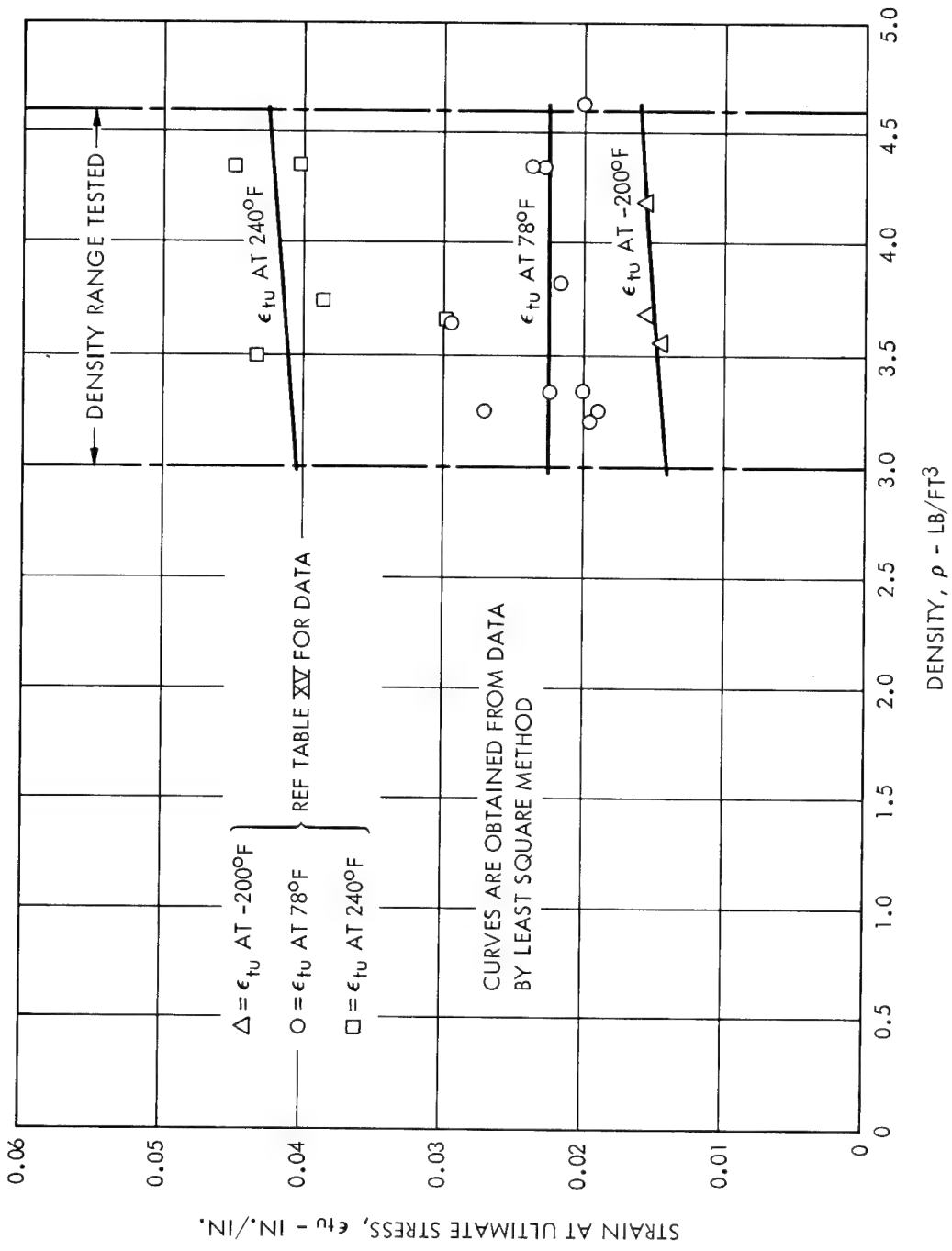


Figure 22. Strain at Tensile Ultimate Stress versus Density

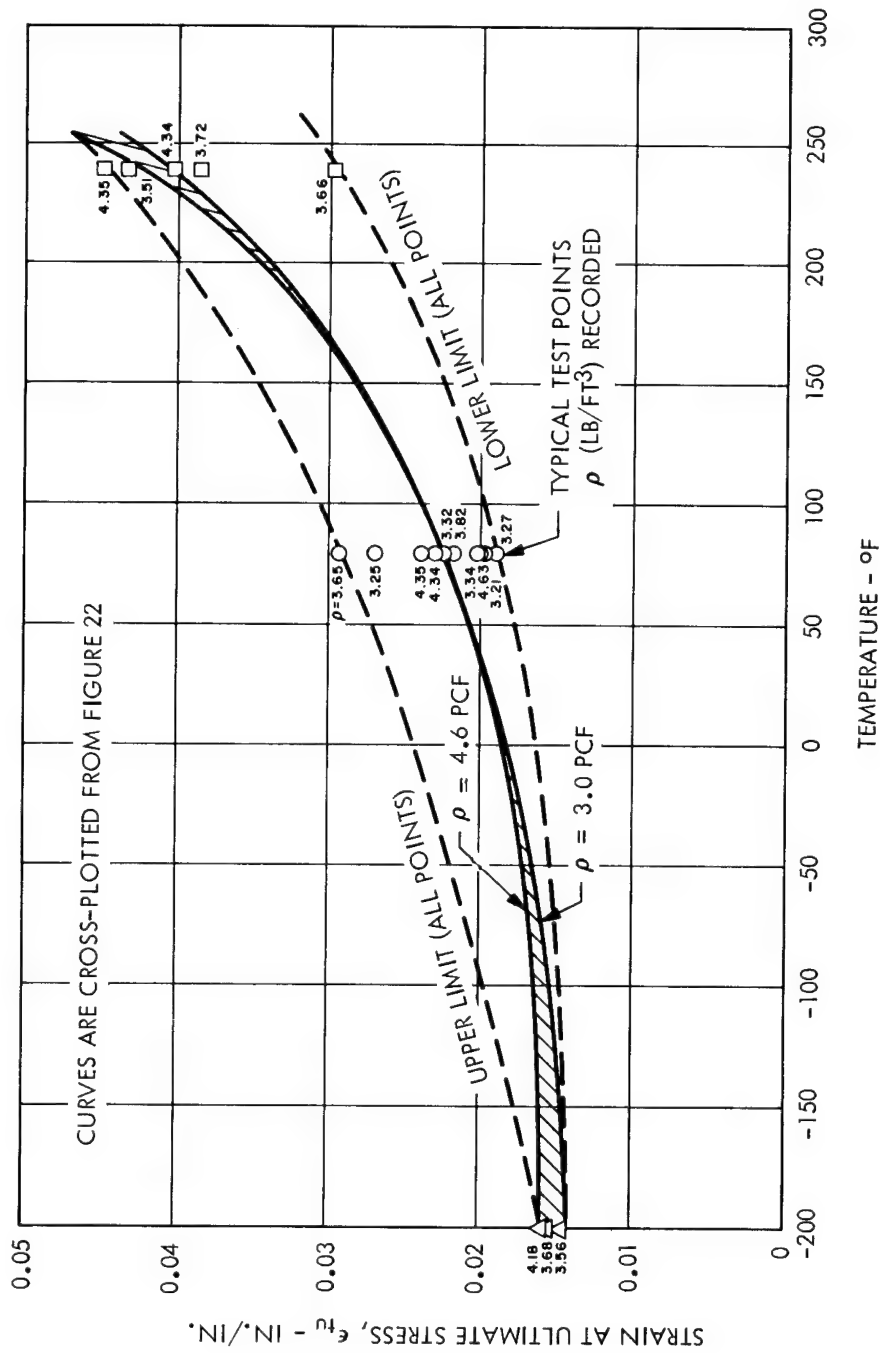


Figure 23. Strain at Tensile Ultimate Stress versus Temperature for Densities between 3 and 4.6 PCF

Table XVI. Compression Test Data for GAC Predistributed Foam

Specimen No.	Temp (°F)	Total Weight		Density		Strain Rate		Pressure (mm of Hg)	Specimen Size (in.)	F _{cu} (psi)	F _{cy} (psi)	F _c (psi)
		G	Lb	PCI	PCF	(In./Min)	(In./In./Min)					
394-92A No. 1	75	2.3109	0.00509	0.002545	4.4017	0.2	0.1	9.0 x 10 ⁻⁵	1 x 1 x 2	35.0	16.2	883
394-92B*	75	1.2223	0.00269	0.001345	2.3282	0.2	0.1	4.0 x 10 ⁻⁵	1 x 1 x 2	9.1	3.0	25
394-1266 No. 1	75	1.7969	0.00396	0.001980	3.4227	0.2	0.1	6.2 x 10 ⁻⁵	1 x 1 x 2	12.5	7.3	475
394-92B	240	1.6562	0.00365	0.001825	3.1547	0.2	0.1	9.0 x 10 ⁻⁵	1 x 1 x 2	5.4	4.3	92
394-92A	240	1.9796	0.00436	0.002190	3.7707	0.2	0.1	6.3 x 10 ⁻⁵	1 x 1 x 2	5.3	3.4	163
394-92B	240	1.3115	0.00289	0.001445	2.4981	0.2	0.1	5.5 x 10 ⁻⁵	1 x 1 x 2	2.3	0.9	42
394-124 No. 1	-200	2.0832	0.00459	0.002295	3.9680	0.2	0.1	8.6 x 10 ⁻⁵	1 x 1 x 2	21.6	18.3	800
394-126 No. 2	-200	1.8443	0.00407	0.002035	3.5129	0.2	0.1	9.0 x 10 ⁻⁵	1 x 1 x 2	21.0	15.0	575
394-124C No. 1	-200	1.8543	0.00409	0.002045	3.5320	0.2	0.1	8.8 x 10 ⁻⁵	1 x 1 x 2	19.4	11.6	454

*Poor specimen - too spongy and offered little resistance to loading.

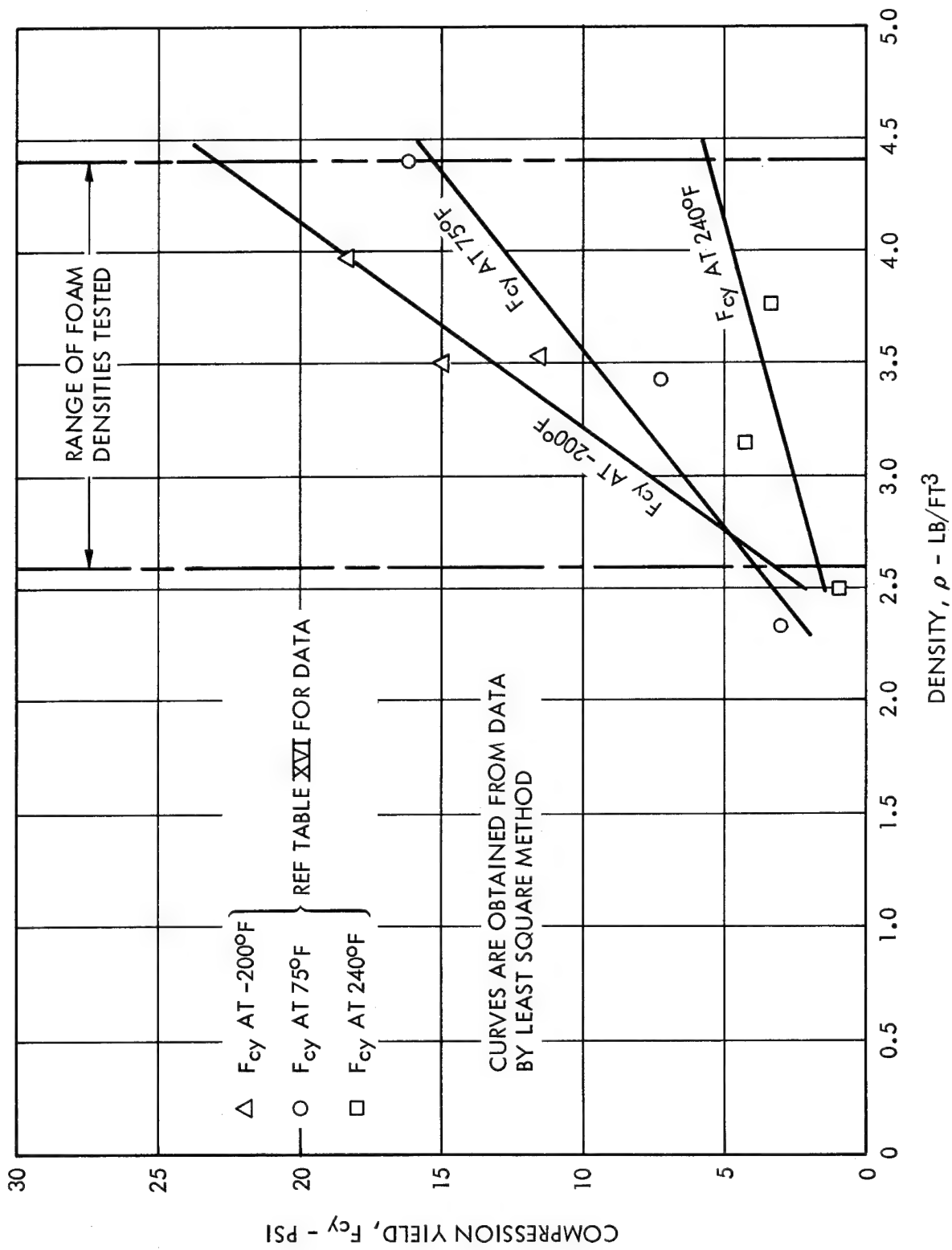


Figure 24. Compression Yield Stress versus Density

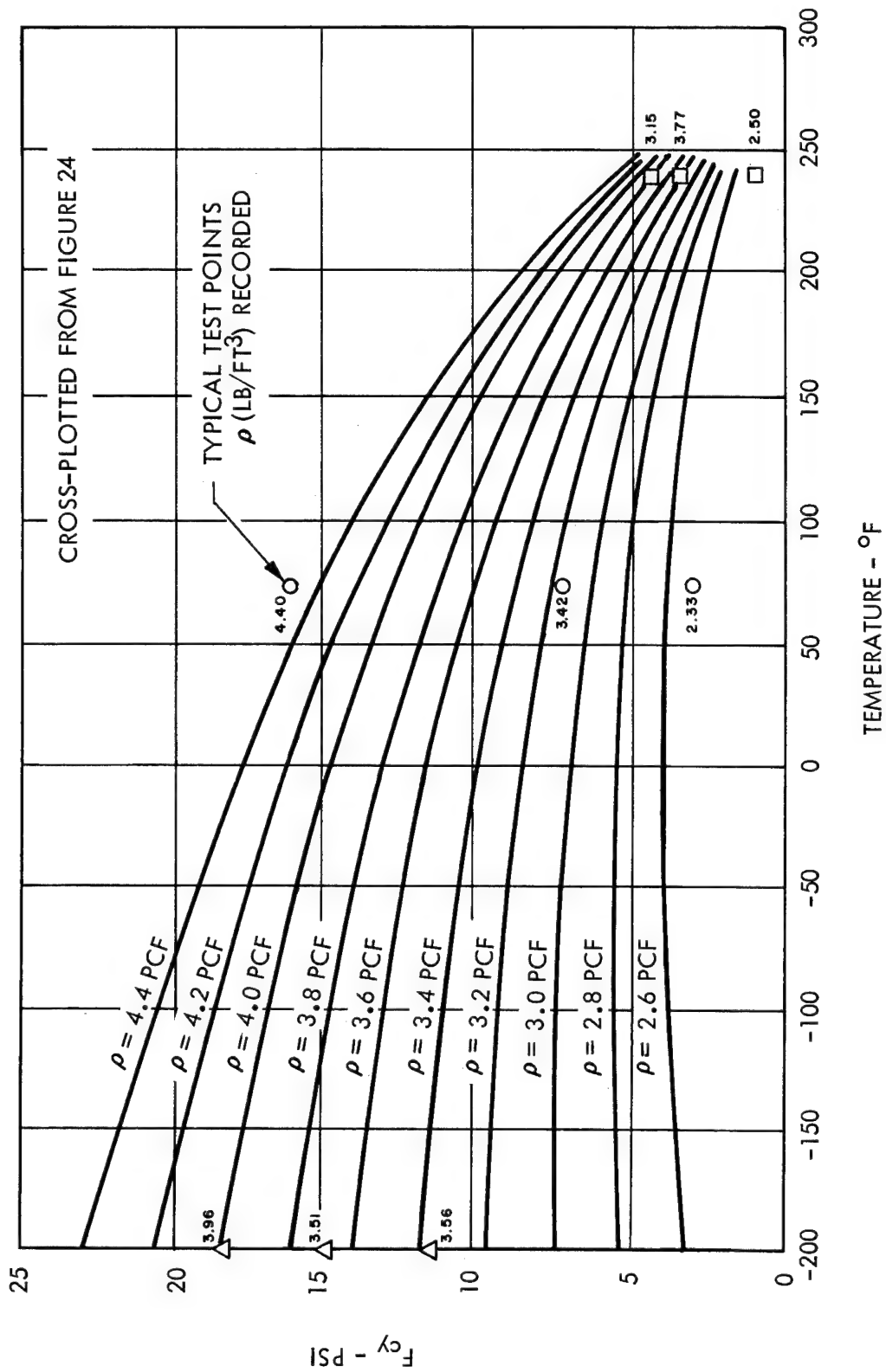


Figure 25. Compression Yield Stress versus Temperature for Density Range Tested

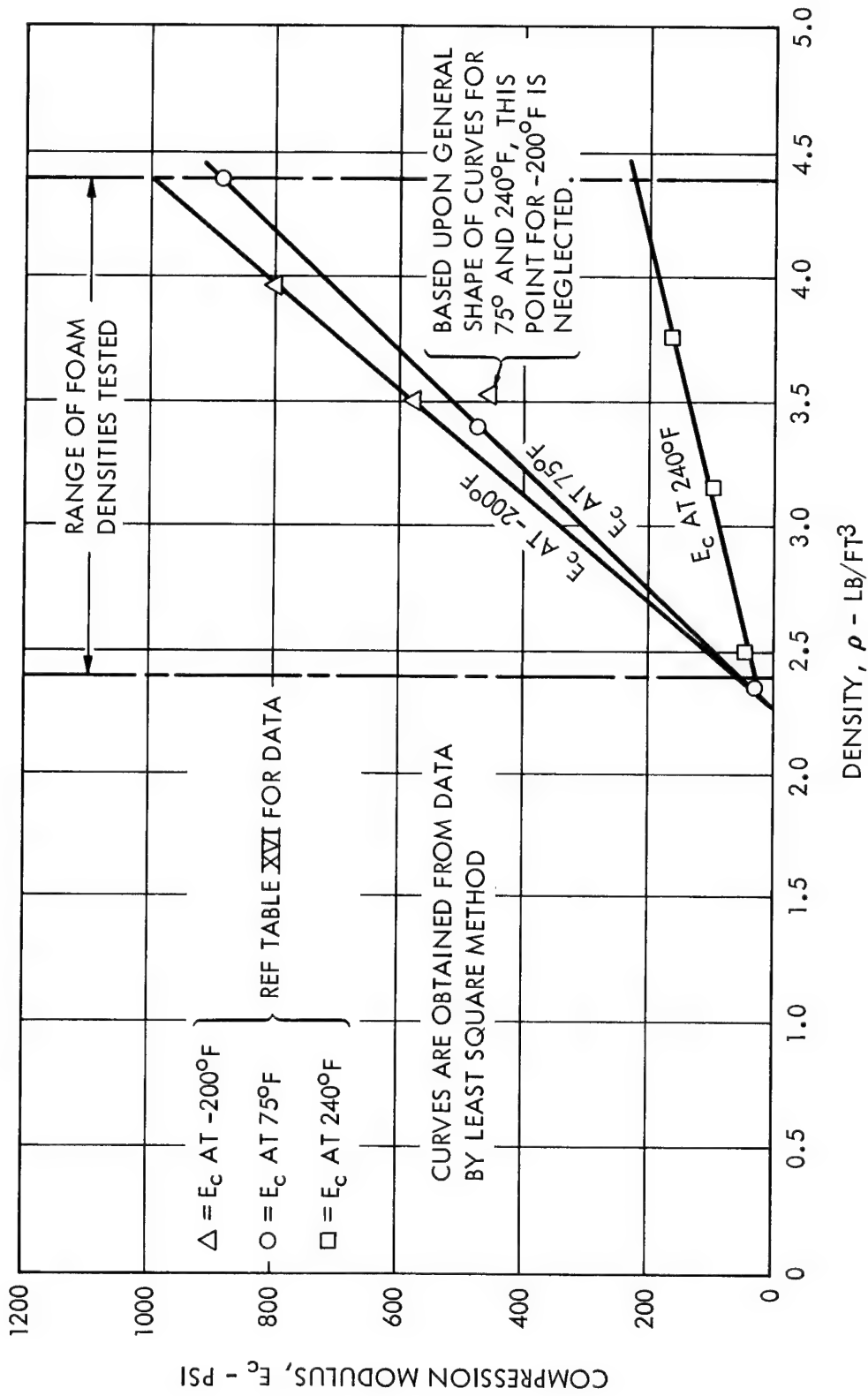


Figure 26. Compression Modulus versus Density

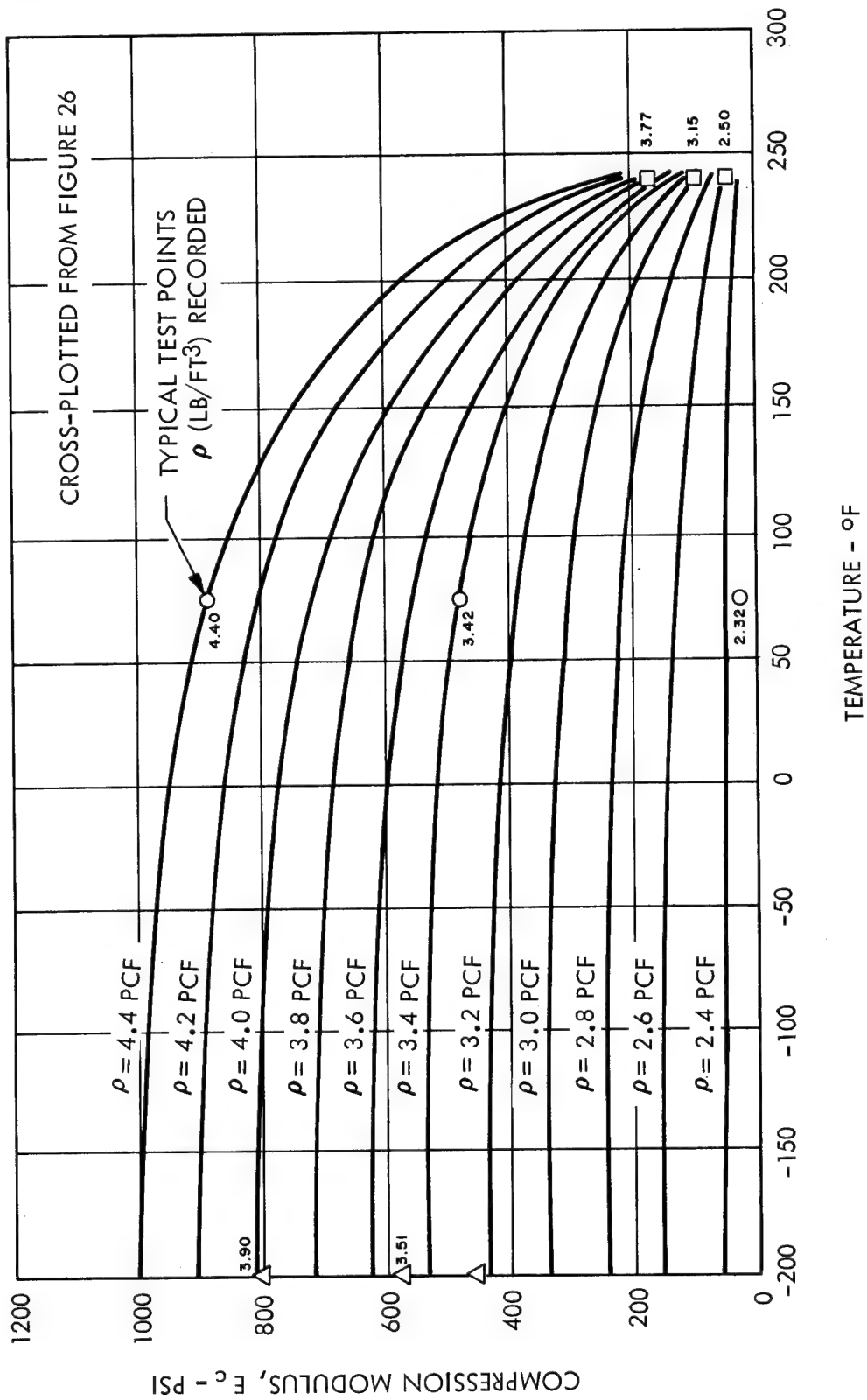


Figure 27. Compression Modulus versus Temperature for Density Range Tested

4. Shear Tests

The shear test setup (for tests performed in a vacuum) is shown in Figure 28. The test was intended to determine the ultimate shear stress (F_{su}) and the shear modulus (G). In a pure shear test, F_s is the shear stress, and the shear modulus, $G = F_s L / \delta_s$, where $F_s = P_s / A_s$ (see Figure 29).

Ideally, the shear stress distribution is uniform and there is no bending. However, pure transverse shear is very difficult to achieve, and some bending stress is nearly always present. These bending stresses lower the apparent yield and ultimate strengths by causing the shear load-versus-deflection curve (Figure 30) to bend over more and sooner than a true pure shear test. This is because the elastic stress distribution is not uniform (see Figure 28 and also Reference 7, pages 50 and 51). Since F_s varies across the section, it is not accurate to solve for G from

$$G = \frac{F_s L}{\delta_s}.$$

The following procedure is used to obtain an accurate relationship involving G from the shear distribution shown in Figure 28 (Figure 28 also shows the geometry and k curve).

The unit energy, u , is given by:

$$u = \frac{F_s^2}{2G}.$$

Therefore, the total energy, U , is given by:

$$\begin{aligned} U &= \int_{x=0}^{x=L} \int_{y=-h/2}^{y=h/2} (du) \\ &= \int_{x=0}^{x=L} dx \sum_{y=-h/2}^{y=h/2} \left(\frac{F_s^2}{2G} \right) b dy. \end{aligned}$$

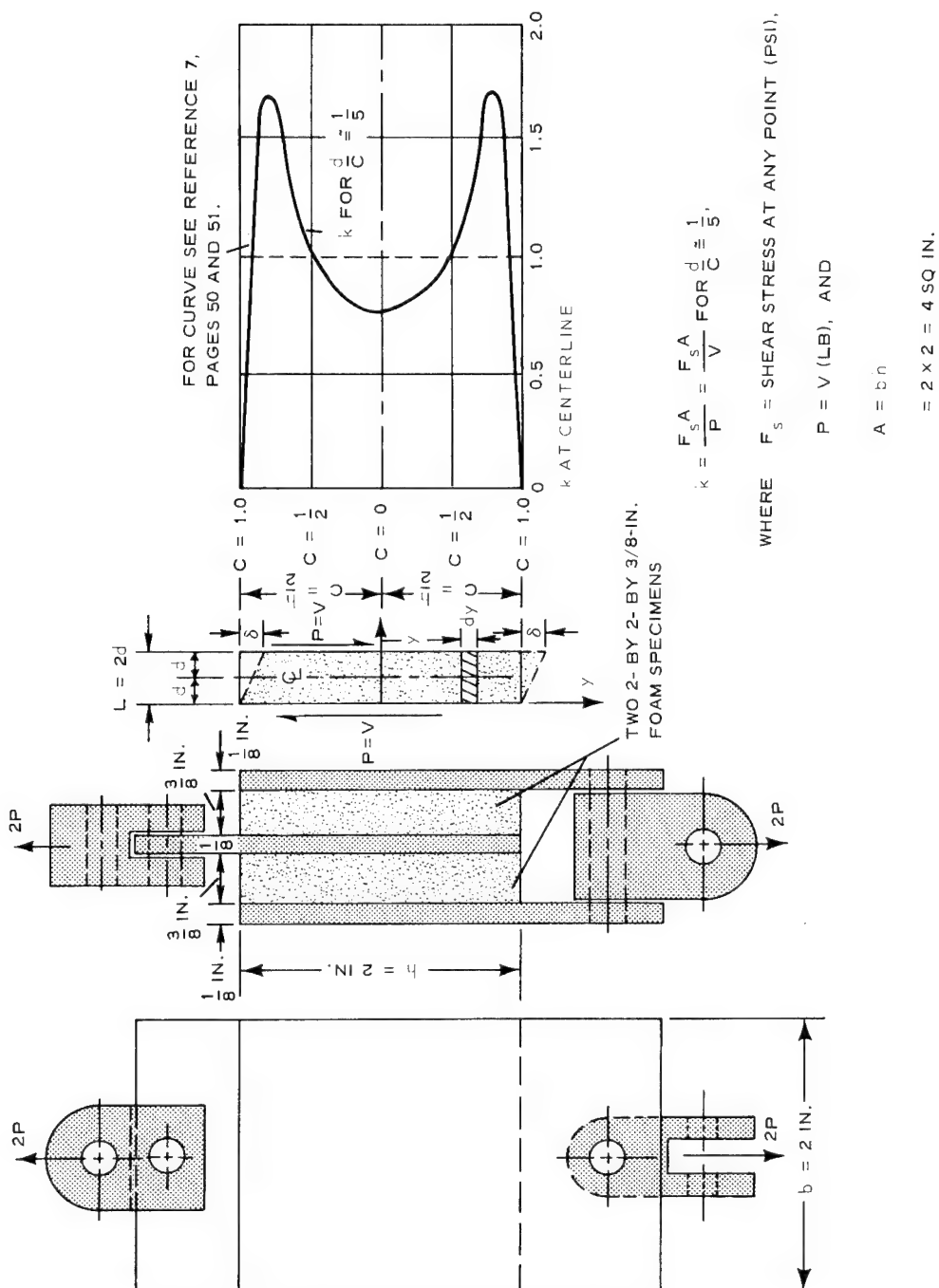


Figure 28. Shear Test Setup and Shear Stress Distribution

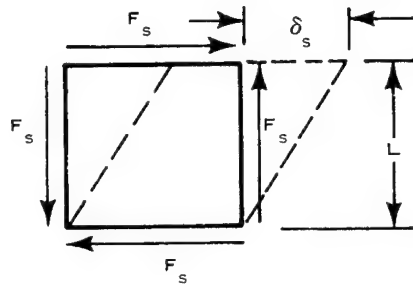


Figure 29. Pure Shear

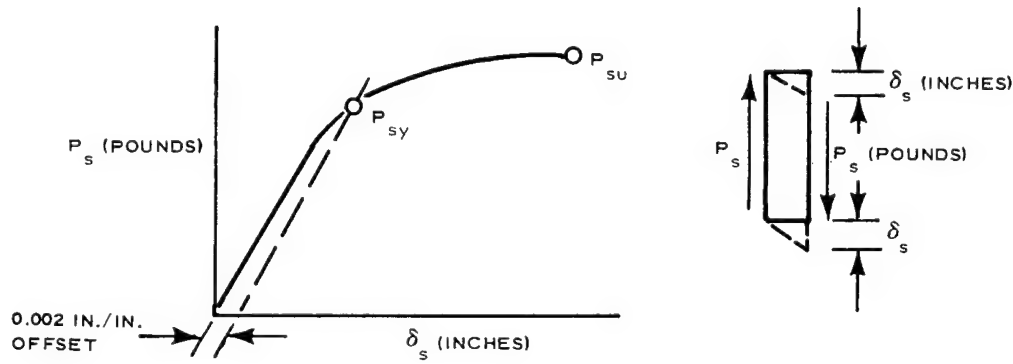


Figure 30. Typical Shear Load versus Deflection

Since $F_s = kV/A = kV/bh$,

$$U = \frac{Lb}{G} \sum_0^{y=h/2} \left(\frac{kV}{bh} \right)^2 dy$$

$$U = \frac{LV^2}{Gbh^2} \sum_0^{y=h/2} k^2 dy.$$

SECTION V

Using 20 equal increments of dy ($dy = h/20$), the average k values for each dy increment are obtained from the k curve and squared. Then,

$$U = \frac{LV^2}{20Gbh} \sum_0^{h/2} k^2,$$

and

$$\begin{aligned} \sum_0^{h/2} k^2 = & (0.435)^2 + (1.58)^2 + (1.65)^2 + (1.42)^2 + (1.13)^2 + (0.945)^2 + \\ & (0.86)^2 + (0.82)^2 + (0.795)^2 + (0.78)^2. \end{aligned}$$

Solving,

$$\sum_0^{h/2} k^2 = 12.247.$$

Substituting the above value into the equation for U ,

$$\begin{aligned} U &= \frac{12.247}{20} \frac{LV^2}{Gbh} \\ &= \frac{12.247}{20} \frac{LV^2}{GA}. \end{aligned}$$

For a cantilever beam, $U = P \delta/2$, or $\delta = 2U/P$, and $P = V$. Therefore,

$$\delta = \frac{2U}{P} = \frac{2U}{V} = \frac{2}{V} \left(\frac{12.247}{20} \right) \frac{LV^2}{Gbh} = 1.2247 \frac{LV}{Gbh},$$

or

$$\delta = 1.2247 \frac{LV}{GA}.$$

Then,

$$G = \frac{1.2247LV}{\delta A}$$

$$= \frac{1.2247LV}{\delta bh}$$

Because this equation holds within the elastic limit of the material, δ_{sy} will be used for δ in the above equation. And since only one-half of the total load (P_{sy}) at δ_{sy} goes through each of the two (2- by 2- by 3/8-in.) specimens in each test, $V = P_{sy}/2$. Also, $A = bh = 2 \times 2 = 4$ sq in., and $L = 3/8$ in. Therefore,

$$G = \frac{1.2247LV}{\delta A}$$

$$= \frac{(1.2247)(0.375)}{(\delta_{sy})(4)} \left(\frac{P_{sy}}{2} \right),$$

or

$$G = 0.057408 \frac{P_{sy}}{\delta_{sy}} \text{ psi,}$$

where P_{sy} = total load (pounds) applied during the test at δ_{sy} (inches). Values of G so obtained and average values of F_{su} and F_{sy} (P_{su}/A and P_{sy}/A) for the density range of the foams tested are given in Table XVII.

As was explained in the discussion on data reduction earlier in this section (subsection B-2), a linear least squares method, which forces the curves through the origin (when plotting F_{su} , F_{sy} , or G versus density), was used in plotting the shear data.

Shear modulus (G), shear ultimate [$F_{su}(\text{avg})$], and shear yield [$F_{sy}(\text{avg})$] are plotted against density for the density range tested. These curves are then cross plotted with these foam properties versus temperature for increments of foam density. The resulting shear data curves are found in Figures 31 to 36.

Table XVII. Shear Test Data for GAC Predistributed Foam

Specimen No.		Temp (°F)	Pressure (mm of Hg)	Cross- Head Speed (in./min)	Chart Speed (in./min)	Weight			Density Based on Failed Specimen (pcf)†	P _{su} (lb)	P _{sy} (lb)	P _{su} 8 (psi)	P _{sy} 8 (in.)	δ _{sy} (in.)	P _{sy} δ _{sy} (lb/in.)	≈ G [‡] = 0.057408 (P _{sy} /δ _{sy}) (psi)
A	B†					A	B†	Avg*								
394-124D No. 1	394-132 No. 2	75	9.4 x 10 ⁻⁵	0.20	2.0	1.2965	1.9700	1.6198	0.004343	287	287	35.9	35.9	0.035	8,200	471
394-132 No. 9	394-132 No. 5	75	9.2 x 10 ⁻⁵	0.20	20.0	1.4764	1.4444	1.4604	0.003185	174	135	21.8	16.9	0.0195	6,920	397
394-132 No. 11	394-132 No. 4	75	9.9 x 10 ⁻⁵	0.20	20.0	1.4439	1.4307	1.4373	0.003155	3.634	195	150	24.4	0.0203	7,389	424
394-132 No. 7	394-132 No. 1	185	9.2 x 10 ⁻⁵	0.20	20.0	1.5283	1.6148	1.5716	0.003560	0.002373	4.101	185	135	0.0187	7,219	414
394-124A No. 1	394-124A No. 2	185	9.4 x 10 ⁻⁵	0.20	20.0	1.0950	1.0106	1.0528	0.002228	0.001485	2.567	105	70	0.0162	4,321	248
394-132 No. 12	394-132 No. 13	185	9.0 x 10 ⁻⁵	0.20	20.0	1.4055	1.4018	1.4037	0.003090	0.002060	3.561	180	130	0.0198	6,566	377
394-132 No. 6	394-122 No. 2	240	9.8 x 10 ⁻⁵	0.20	20.0	1.3628	1.2970	1.3299	0.002859	0.001906	3.294	145	110	0.0204	5,392	310
394-132 No. 8	394-122 No. 1	240	9.9 x 10 ⁻⁵	0.20	20.0	1.2434	1.2003	1.2219	0.002646	0.001764	3.048	133	93	0.0176	5,284	303
394-132 No. 3	394-132 No. 10	240	8.8 x 10 ⁻⁵	0.20	20.0	2.1095	1.2571	1.6833	0.002772	0.001848	3.193	133	97	0.0167	5,808	333

*Average Weight of the two (columns A and B) 2 x 2 x 3/8-inch specimens.

**Average stresses.

†G (Reference Pages 79 through 83)

‡Based upon specimen that actually failed.

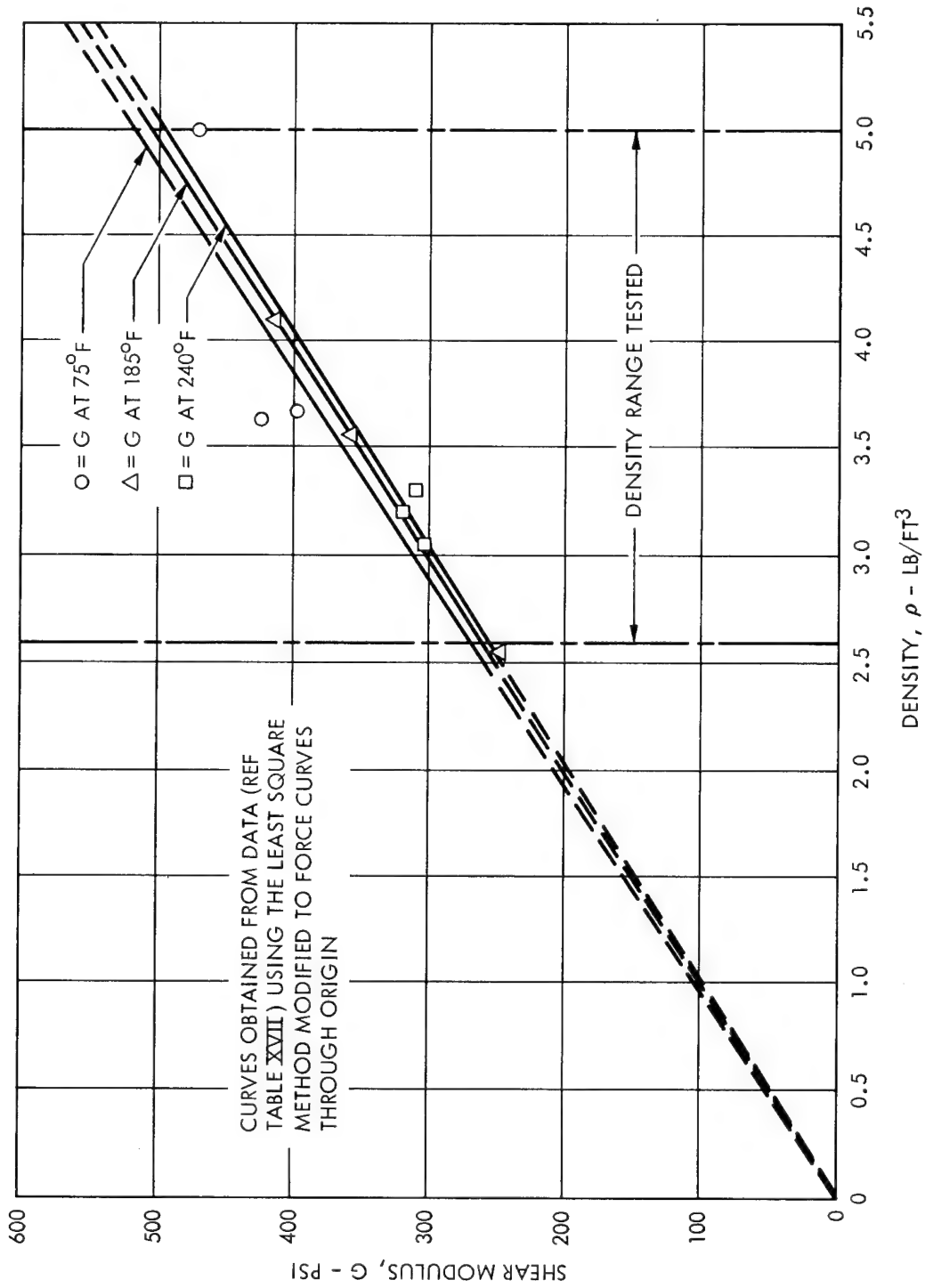


Figure 31. Shear Modulus versus Density

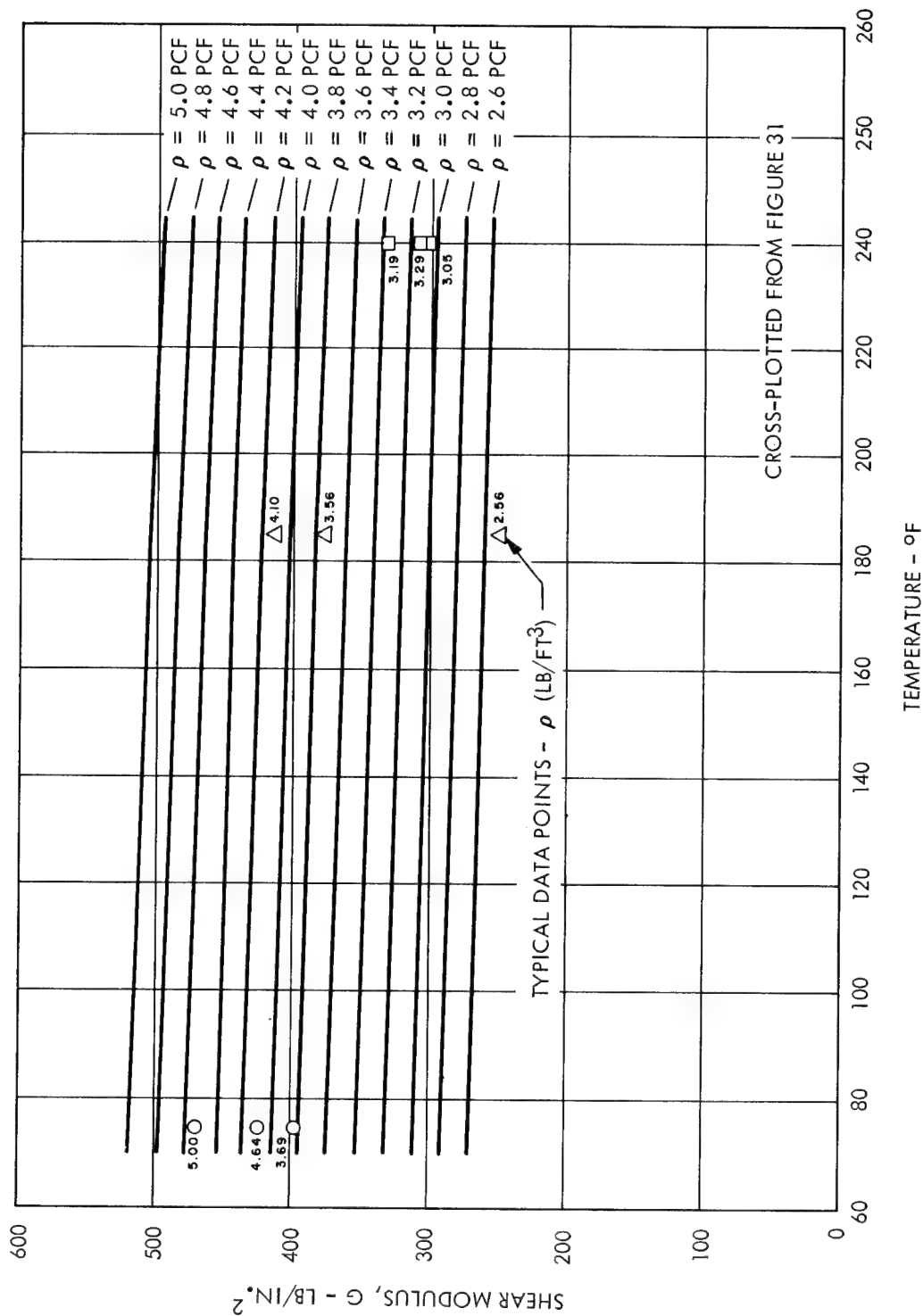


Figure 32. Shear Modulus versus Temperature for Density Range Tested

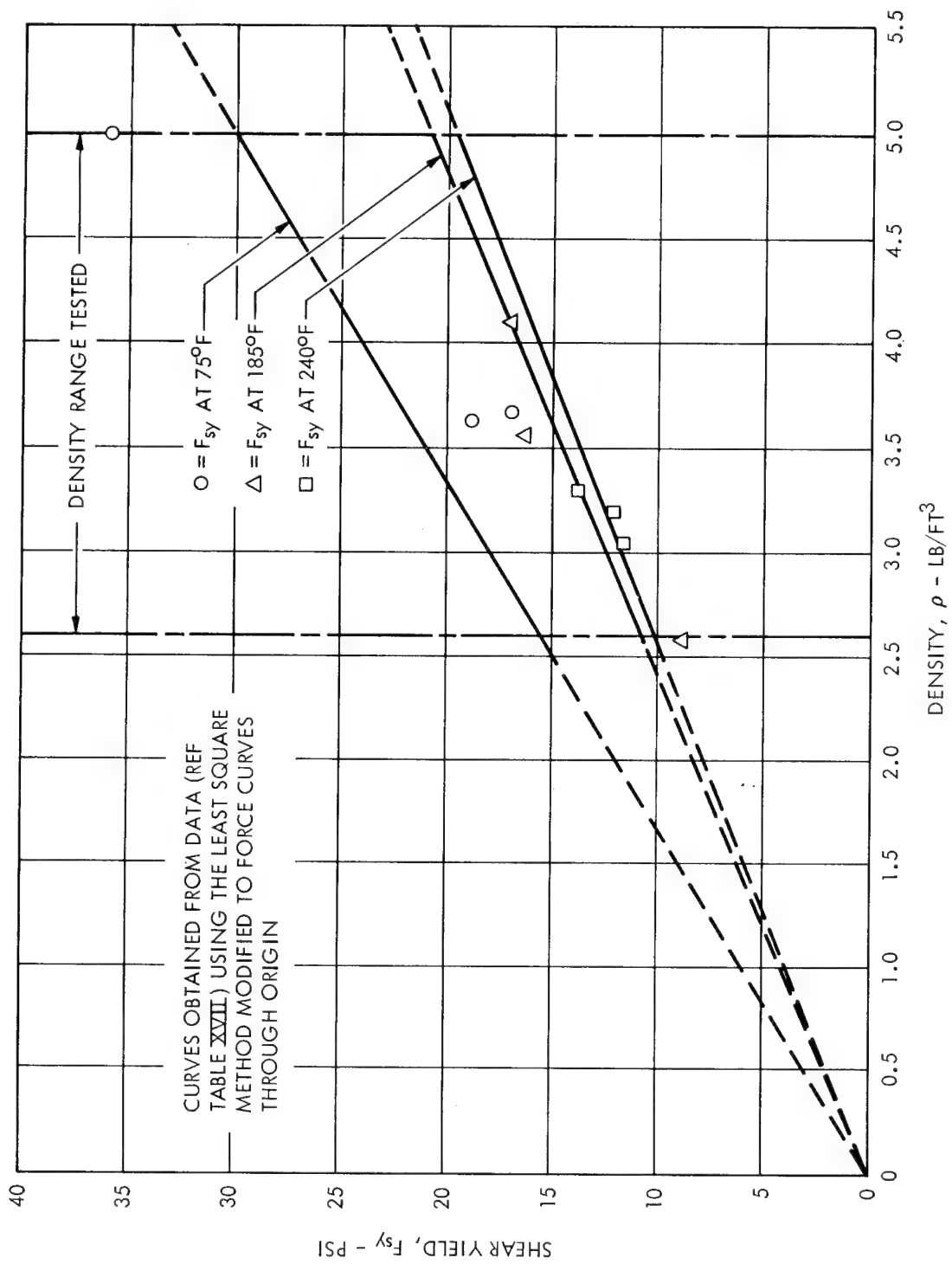


Figure 33. Shear Yield Stress versus Density

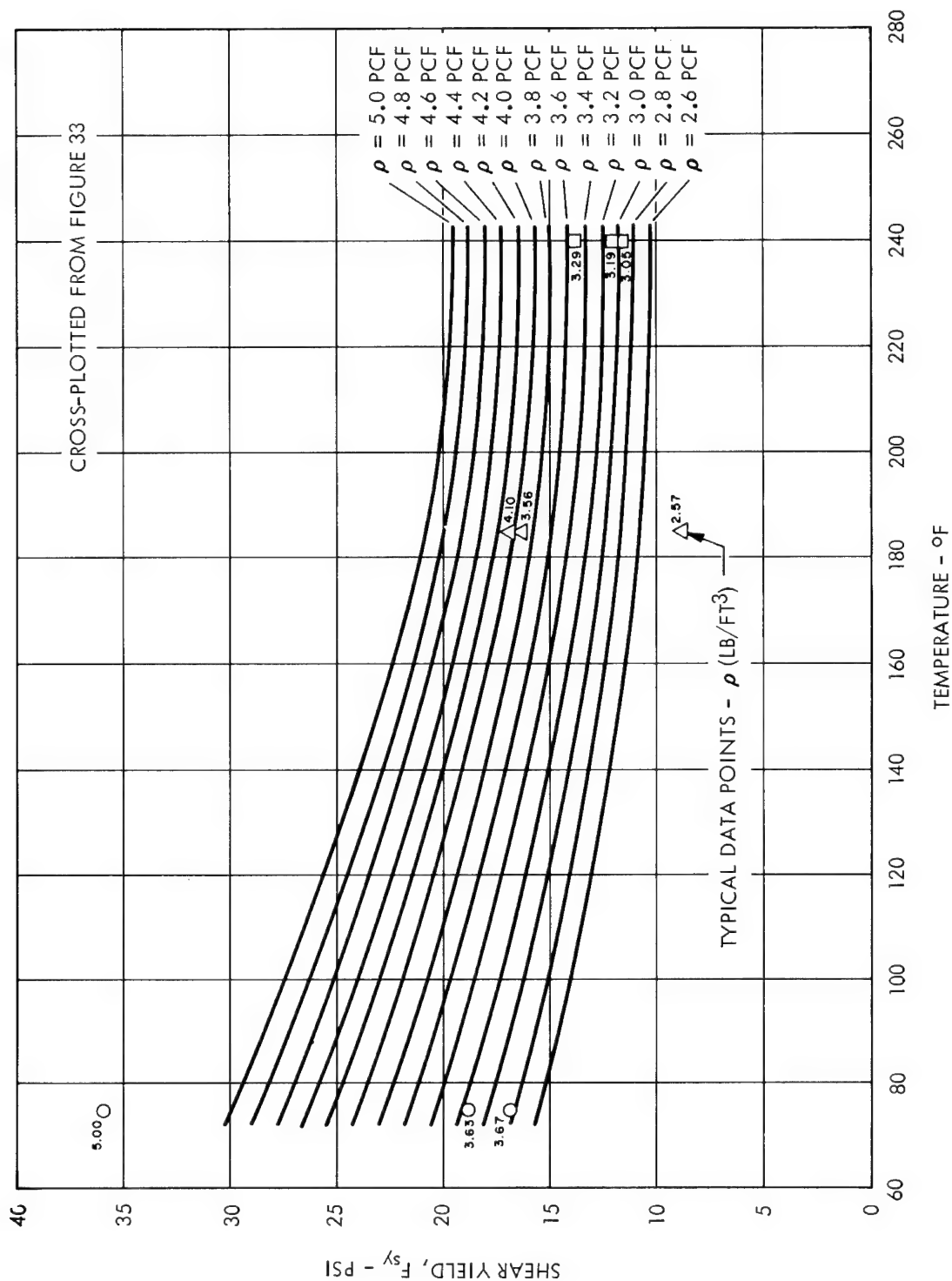


Figure 34. Shear Yield Stress versus Temperature for Density Range Tested

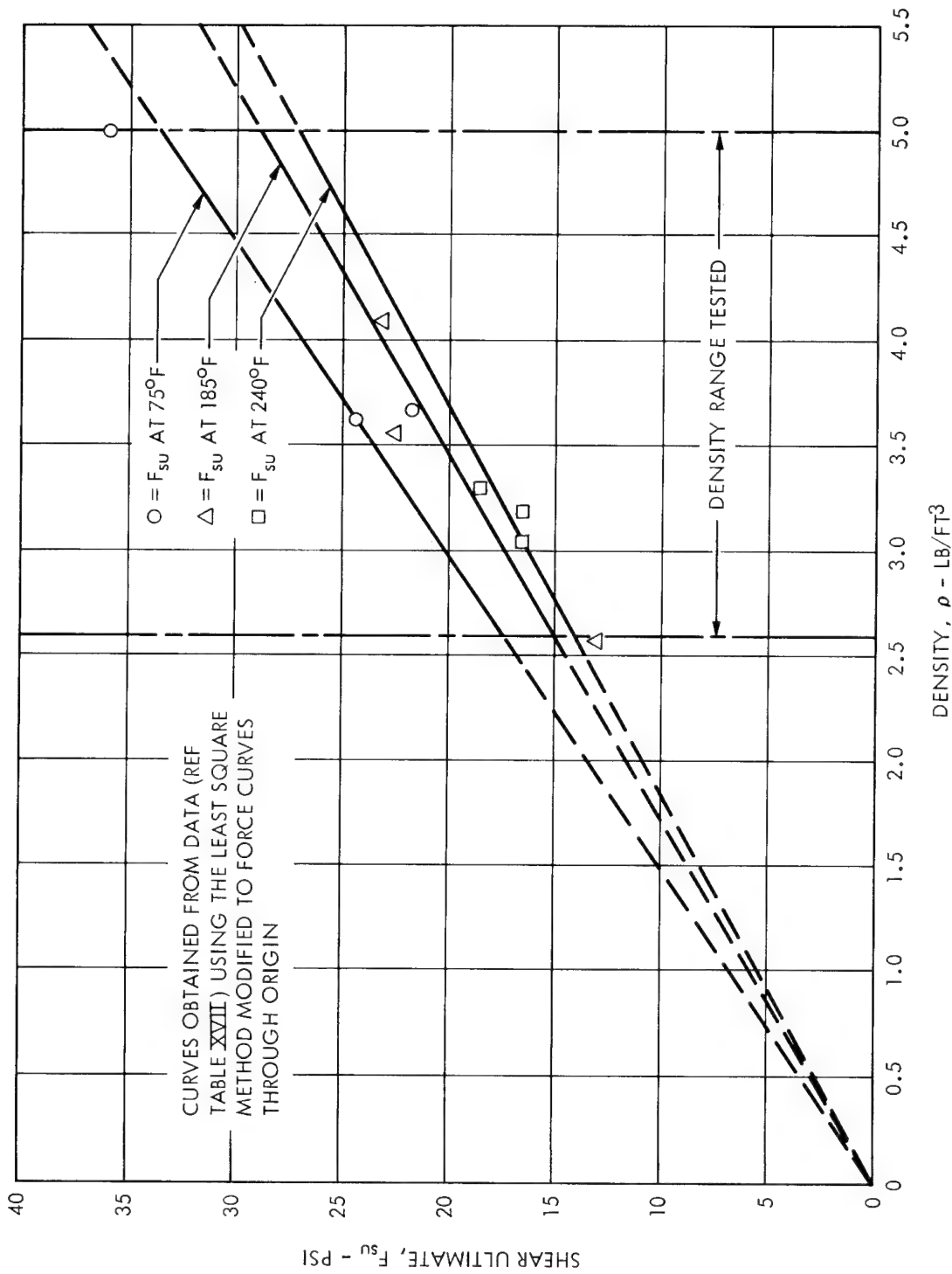


Figure 35. Shear Ultimate Stress versus Density

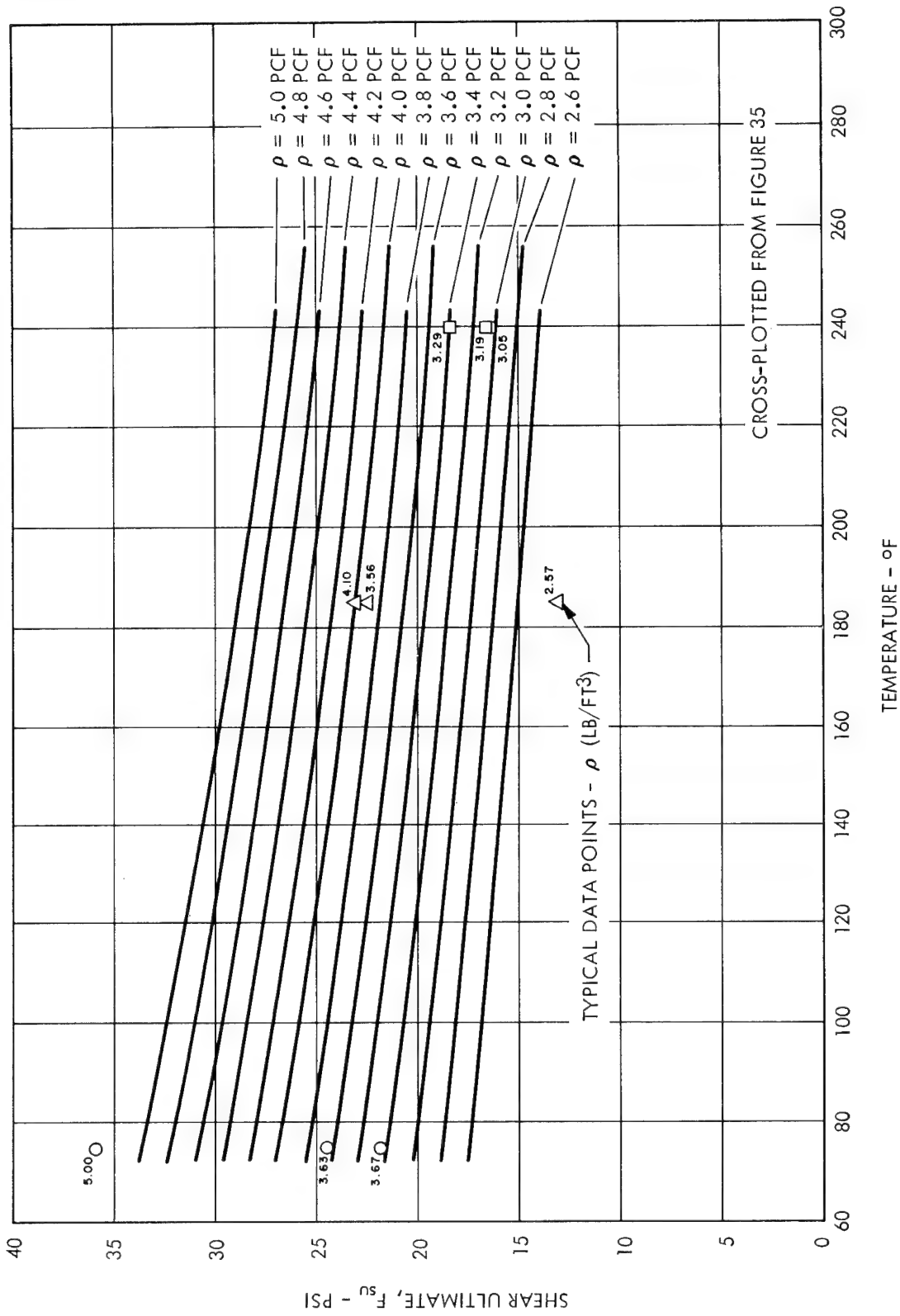


Figure 36. Shear Ultimate Stress versus Temperature for Density Range Tested

GAC mechanically mixed foam (Reference 4) and ambient polyurethane foams (Reference 6) have comparable shear properties. In comparison GAC predistribution foam has shear properties that are approximately 50 percent as high within the 3 to 4.5 pcf density range tested. These shear properties increase directly as a function of density and are approximately constant with respect to temperature.

5. Linear Thermal Expansion Tests

The linear thermal expansion tests were conducted on 1 x 1 x 4 inch specimens (the same as for tensile tests) of predistributed foam in a bell jar under vacuum conditions (see Figure 37).

The gage length was established with two gage points. One gage point was located at the lower part of the upper end block and the other was located approximately three inches below the first, with a 0.020-inch diameter pin placed in the specimen. Then, as the specimen temperature was increased with quartz-tube infrared lamps, the new length between the gage points was measured at specific temperature increments with a cathetometer. The resulting data (elongation versus temperature) were plotted on Figure 38. From this data the coefficient of expansion of the material for any desired temperature increment could be found.

On the basis of the information obtained from these tests the coefficient of thermal expansion cannot be accurately determined. However, the data does indicate that the coefficient of thermal expansion is low; it is not negative; and it is not zero.

It is suspected that the swing in the negative direction may be caused by bending or by contraction due to the evaporation of moisture or other volatiles during the pump-down period. Possible corrections to eliminate negative values may be:

- (1) To make linear measurements from all four sides of the sample.
- (2) To condition the sample in a high vacuum environment until contraction (or expansion) is stabilized.

SECTION V

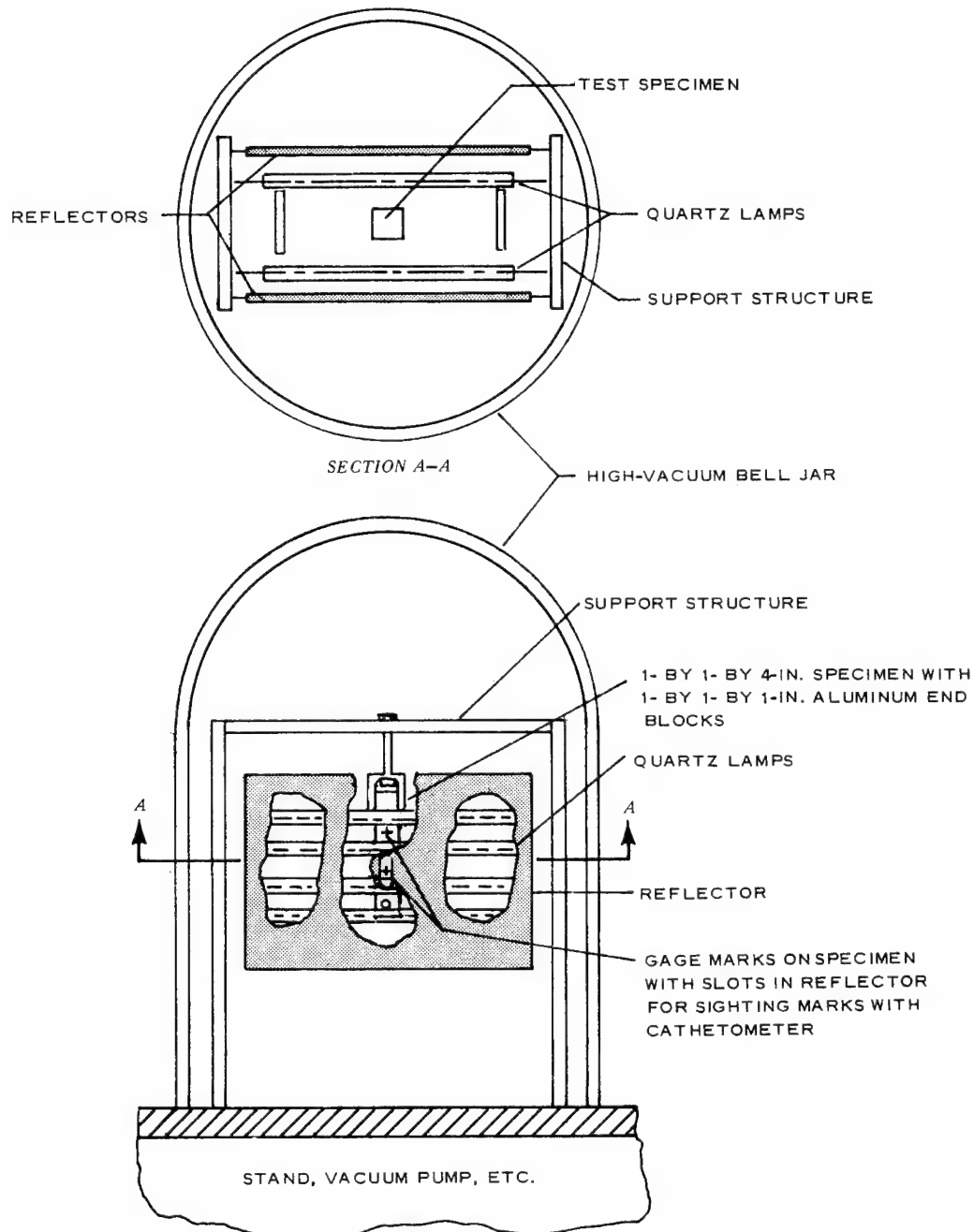


Figure 37. Setup for Coefficient of Expansion Tests

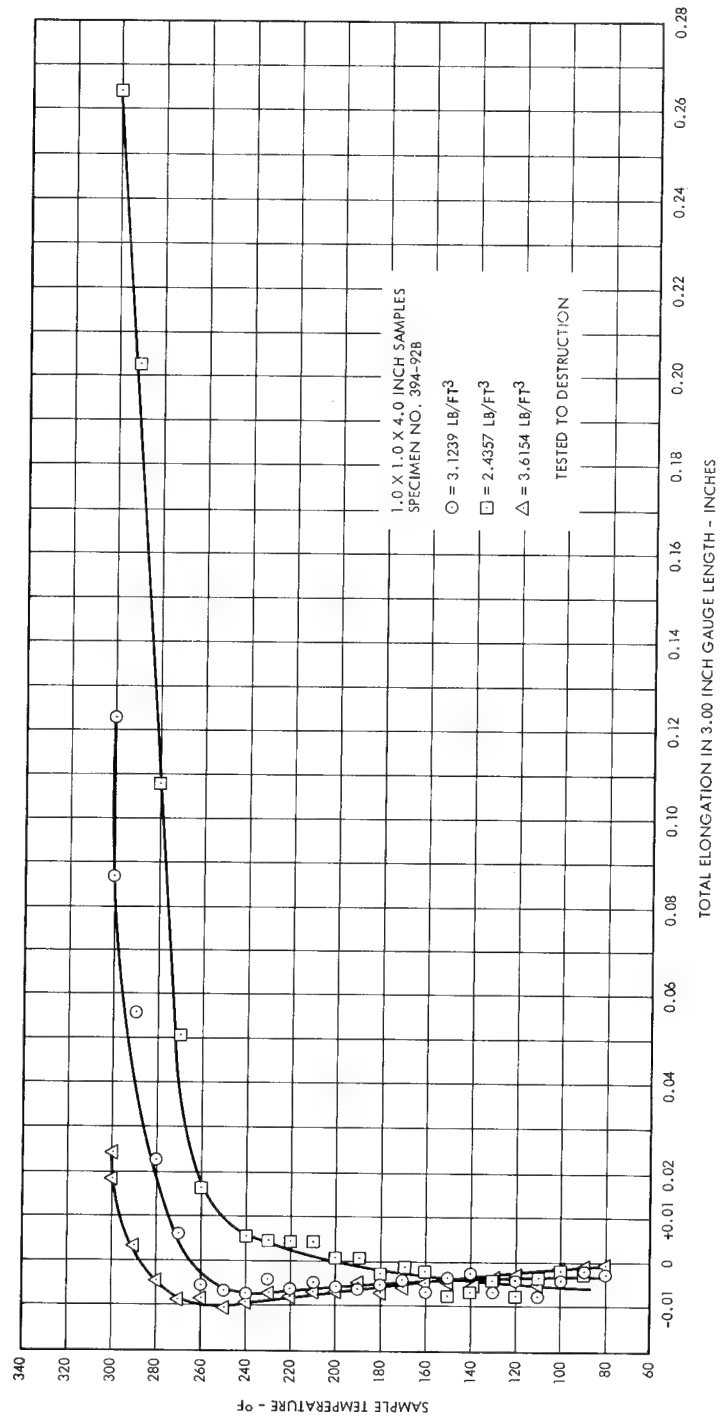


Figure 38. Linear Thermal Expansion of Precoat Foam

SECTION V

A close examination of the data points (see Figure 38) reveals that the 2.4357 lb/ft³ density material (square points) describes almost a straight line curve between the temperature values of 120° and 240°F. This gives a coefficient of expansion value of 3.7×10^{-5} in./in./°F. This value is found to be comparable to that of the mechanically mixed foam that was produced and tested in vacuum (the coefficient of thermal expansion for a 2.4 density material at a temperature of 120°F is 4.05×10^{-5} in./in./°F and at 240°F is 8.2×10^{-5} in./in./°F).

Since the precoat material has a filler of microquartz, its coefficient of thermal expansion is expected to be reduced and its heat distortion temperature is expected to be increased. Also, the trends of foam materials (tested in vacuum) indicate that lower values of thermal coefficient of expansion are characteristic with the higher densities. Therefore, it can safely be assumed that the coefficients of thermal expansion for the two higher density test samples (Figure 38) have lower values than 3.7×10^{-5} in./in./°F.

6. Poisson's Ratio

It was found that a mechanically mixed foam has a Poisson's ratio of approximately one third (Reference 4). Reference 4 also notes the difficulties that are encountered in obtaining this physical property with foam materials. Since the test program for the predistributed foam was limited in scope, it was decided not to attempt Poisson's ratio tests, but to determine this value from the classic relationship for homogeneous materials:

$$\mu = \frac{E}{2G} - 1$$

where,

μ = Poisson's ratio

E = Young's modulus

G = Shear modulus

Since this material is neither homogeneous nor isotropic, unrealistic values resulted when attempts were made to apply the equation to the foam material.

Reference 8 (page 7) indicates that for foams of the subject type with randomly-disposed threads (cell wall junctions), Poisson's ratio takes the value of one-fourth, independent of density. This value is in close agreement with the one-third value for the mechanically mixed foam.

7. Bond Strength (versus Temperature and Ultraviolet)

The bond strength test specimen dimension and bond peel test setup is shown in Figures 39 and 40.

Three specimens each were tested at 75⁰, 185⁰, and 240⁰F. The data obtained from these nine tests are listed in Table XVIII. Figure 41 is a plot of the load at first peeling versus temperature.

Three specimens each were also tested for bond peel strength after undergoing ultraviolet (UV) exposure times of 1, 10, 100, and 1000 hours. The results of this data are also listed in Table XVIII. Figure 42 is a plot of the load at first peeling versus exposure time.

The bond peel strength data indicates that the load at first peeling decreases with increased temperature or ultraviolet exposure except for the 1000-hour UV specimens. However, even the minimum values obtained are considered more than adequate for solar concentrator applications where only very small peeling forces are expected.

8. Density and Dimensional Stability

The test setup for the dimensional stability checks is shown in Figure 43. It consists of measuring the dimensional changes on three axes of a two-inch cube in a vacuum at controlled temperature for 30 or more days. For all three specimens tested the volume change while under vacuum conditions was less than one-half of one percent (refer to Table XIX).

SECTION V

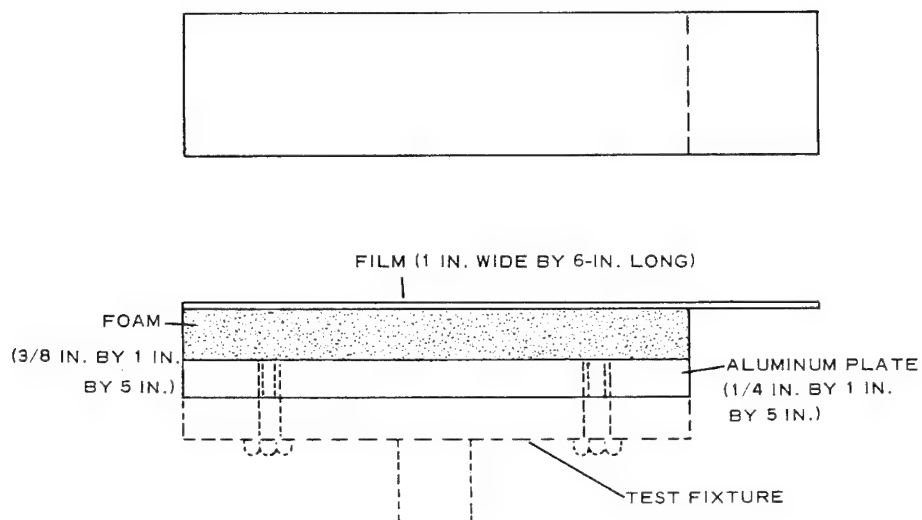


Figure 39. Bond Strength Test Specimen

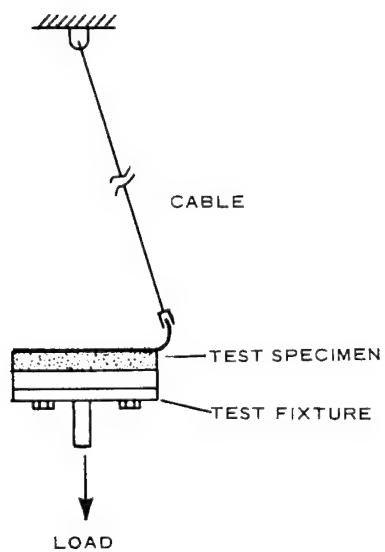


Figure 40. Bond Strength Peel Test

SECTION V

Table XVIII. Foam to H-Film Peel Test Data (Bond Strength)

Specimen No. *	Exposure (UV) (hrs)	Test Pressure (mm of Hg)	Test Temp (°F)	Max Load (lb)	First Peel Load (lb)	Foam Specimen		Failure Comments
						Weight (g)	Density (pcf)	
394-130A No. 4	0	8.8×10^{-5}	75	0.60	0.60	2.6977	8.22	Repeat from opposite end
394-128 No. 1	0	10.0×10^{-5}	75	1.42	1.32	2.8060	8.55	
394-128 No. 1	0	9.6×10^{-5}	75	0.78	0.38	2.8060	8.55	
394-129B No. 2	0	8.6×10^{-5}	75	2.00	2.00	2.7203	8.29	
Avg	0	9.25×10^{-5}	75	1.20	1.075	2.7575	8.40	
394-129A No. 3	0	9.0×10^{-5}	185	0.74	0.46	3.2520	9.90	H-Film ripped.
394-130A No. 5	0	9.0×10^{-5}	185	1.14	0.58	2.3683	7.22	H-Film ripped.
394-129B No. 4	0	9.6×10^{-5}	185	≥ 3.0	0.80	2.7476	8.36	
Avg	0	9.20×10^{-5}	185	1.627	0.613	2.7893	8.50	
394-130 B No. 3	0	9.6×10^{-5}	240	0.90	0.52	2.7136	8.27	H-Film ripped.
394-129B No. 3	0	9.8×10^{-5}	240	0.88	0.48	2.6383	8.04	H-Film ripped.
394-130B No. 3	0	8.4×10^{-5}	240	0.74	0.46	2.3451	7.15	H-Film ripped.
Avg	0	9.27×10^{-5}	240	0.840	0.487	2.5657	7.82	
394-130B No. 2	1	8.8×10^{-5}	75	0.86	0.46	2.6096	7.95	
394-128 No. 2	1	8.4×10^{-5}	75	0.78	0.46	2.7304	8.32	
394-128 No. 3	1	9.4×10^{-5}	75	0.62	0.48	2.6912	8.20	
Avg	1	8.87×10^{-5}	75	0.754	0.467	2.6771	8.18	
394-129A No. 2	10	8.6×10^{-5}	75	0.80	0.30	2.7437	8.35	
394-130A No. 3	10	8.8×10^{-5}	75	1.30	0.92	2.5409	7.74	
394-130A No. 2	10	9.4×10^{-5}	75	1.42	0.42	2.5177	7.68	
Avg	10	8.93×10^{-5}	75	1.173	0.547	2.6008	7.92	
394-130A No. 1	100	10^{-5}	75	0.78	0.28	2.6200	7.98	H-Film ripped.
394-128 No. 4	100	10^{-5}	75	0.98	0.46	2.5283	7.71	
394-129A No. 1	100	10^{-5}	75	1.60	0.46	3.1092	9.48	
Avg	100	10^{-5}	75	1.12	0.40	2.7525	8.39	
394-129 No. 1	1000	10^{-5}	75	1.72	1.72	≈ 2.620	7.98	
394-129B No. 1	1000	10^{-5}	75	1.06	0.32	≈ 2.350	7.16	
394-126	1000	10^{-5}	75	2.16	2.16	≈ 2.510	7.65	
Avg	1000	10^{-5}	75	1.647	1.40	≈ 2.493	7.60	

*Sample Foam Dimensions = 1 x 1/4 x 5 inches. Load Rate = 1 in./min (cross-head speed)

SECTION V

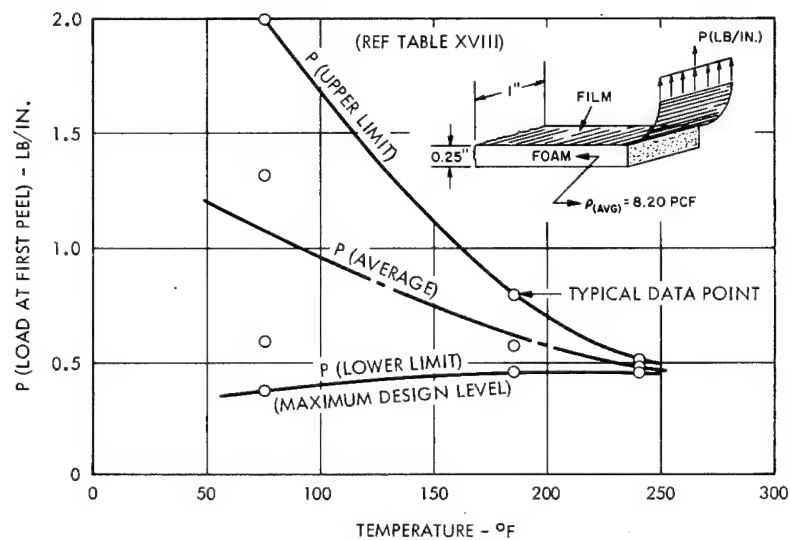


Figure 41. Peel Load versus Temperature

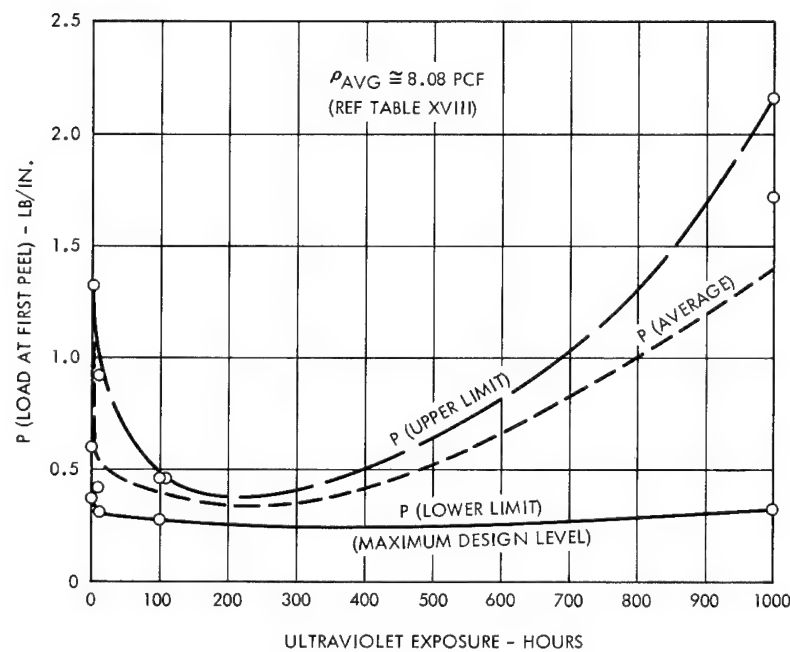


Figure 42. Peel Load versus Ultraviolet Effect at 75°F

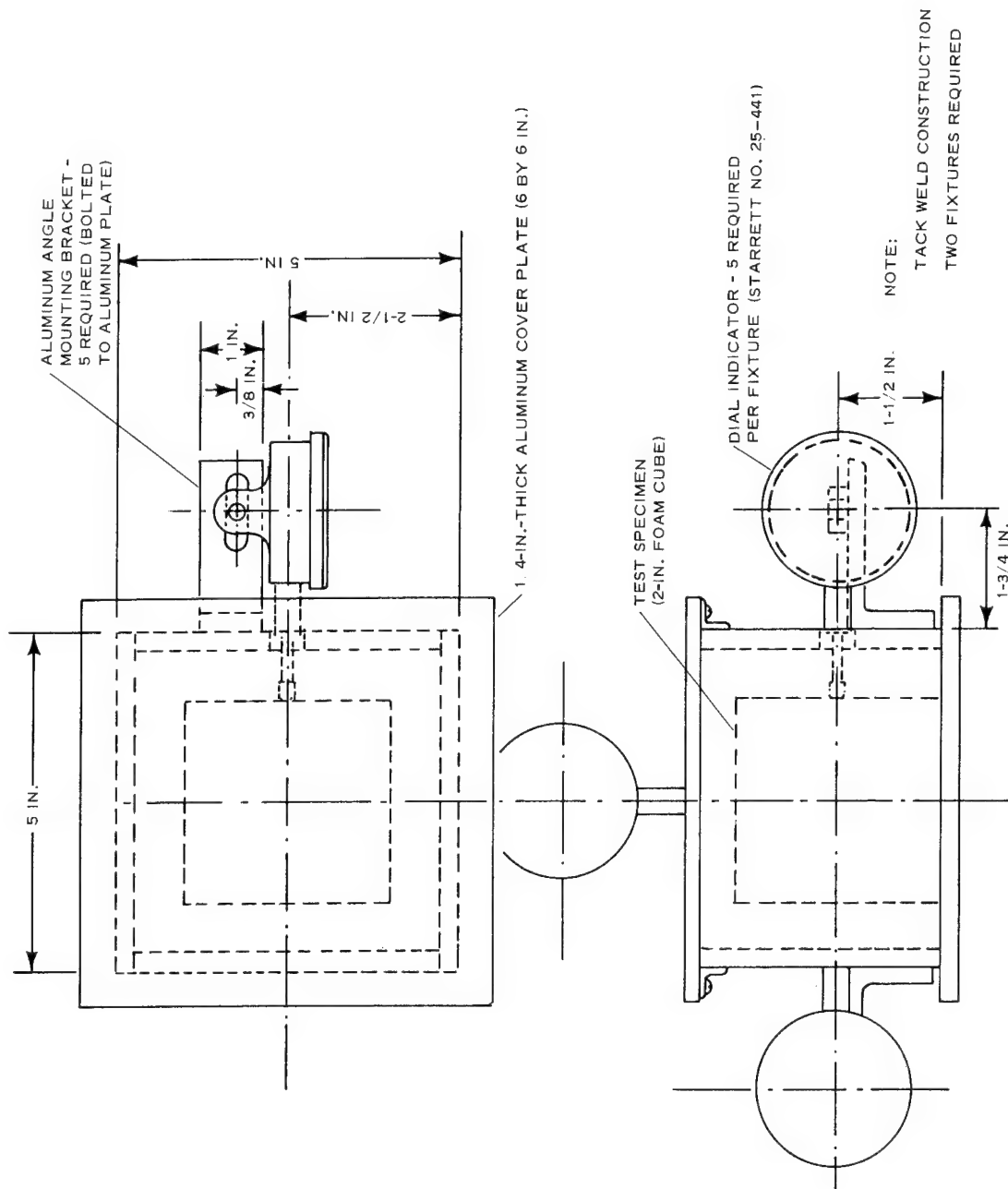
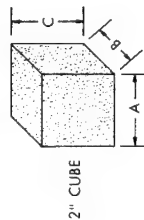


Figure 43. Fixture for Foam Stability Tests

Table XIX. Dimensional Stability Data

Specimen 394-132A Size $\approx 2 \times 2 \times 2$ in. ; Temp = 75°F Density ≈ 3.425 pcf						Specimen 394-132C Size $\approx 2 \times 2 \times 2$ in. Temp = 75°F Density ≈ 2.888 pcf						Specimen 394-132B Size $\approx 2 \times 2 \times 2$ in. ; Temp = 75°F Density ≈ 3.100 pcf					
Hours	Pressure (mm of Hg)	A (in.)	B (in.)	C (in.)	Volume (in.) ³	Hours	Pressure (mm of Hg)	A (in.)	B (in.)	C (in.)	Volume (in.) ³	Hours	Pressure (mm of Hg)	A (in.)	B (in.)	C (in.)	Volume (in.) ³
0	Ambient	2.017	1.994	2.005	8.064	0	Ambient	1.991	1.996	2.006	7.952	0	Ambient	2.003	2.006	2.024	8.132
0.58	1×10^{-1}	2.013	1.989	2.004	8.024	0.5	10^{-1}	1.988	1.993	2.004	7.940	4.0	10^{-5}	1.996	2.002	2.024	8.088
0.75	7.9×10^{-5}	2.013	1.989	2.004	8.024	24.0	10^{-5}	1.988	1.993	2.004	7.940	69.5	10^{-6}	1.996	2.002	2.024	8.088
3.75	10^{-6}	2.012	1.989	2.004	8.020	97.0	10^{-6}	1.986	1.991	2.004	7.924	169.5	10^{-6}	1.995	2.002	2.023	8.080
20.08	10^{-6}	2.012	1.989	2.004	8.020	163.0	10^{-6}	1.986	1.991	2.004	7.924						
51.75	10^{-6}	2.011	1.984	2.003	7.992	521.5	10^{-6}	1.985	1.991	2.0035	7.917						
117.75	10^{-6}	2.011	1.984	2.003	7.992	834.5	10^{-6}	1.985	1.991	2.0035	7.917						
476.25	10^{-6}	2.011	1.984	2.003	7.992	858.5	Ambient	1.985	1.991	2.0035	7.917						
789.25	10^{-6}	2.011	1.984	2.003	7.992	1074.5	Ambient	1.988	1.994	2.0035	7.942						
813.25	Ambient	2.011	1.984	2.003	7.992												

Specimen:



Based on this data, GAC concludes that this foam is probably well suited for a space environment from the dimensional stability standpoint for normal temperature ranges. However, it is suggested that more tests of this type be performed at a wider range of temperatures and densities.

9. Creep Tests

The creep test setup is shown in Figure 44. The specimens are 1 x 1 x 4 inches and are loaded to approximately 50 percent of the tensile yield strength. Six specimens were tested for their creep characteristics, two at 82°F, two at 185°F, and two at 240°F.

The 82°F creep specimen curves (Figure 45) indicate very little primary creep for this foam. After the initial creep phase, a malfunction in the temperature control mechanism caused the temperature to rise to 110°F for a period of time. At this temperature the five-lb load on each of the specimens represented much more than 50 percent of the tensile yield, and at this temperature the creep rate is higher than it is for 82°F.

Consequently, as a result of this 110°F rise in temperature the creep curves jumped upward by ≈ 0.26 in./in. strain. However, once the temperature was again stabilized at ambient the creep curves leveled off and the specimens exhibited no significant creep for the remaining 515 hours that the test was in operation (see Figure 45).

The 185°F creep specimen curves (Figure 46) for a constant 50 percent of yield load indicate that the secondary creep becomes negligible after 75 hours. However, one of the specimens did exhibit 0.011 inch per inch primary creep strain during the first 75 hours as compared to an elastic strain of 0.007 inch per inch due to the three-pound loading (≈ 50 percent F_{ty}). However, when comparing the creep strain with respect to time and load level, the over-all creep characteristics of this foam at 185°F are considered to be very good.

SECTION V

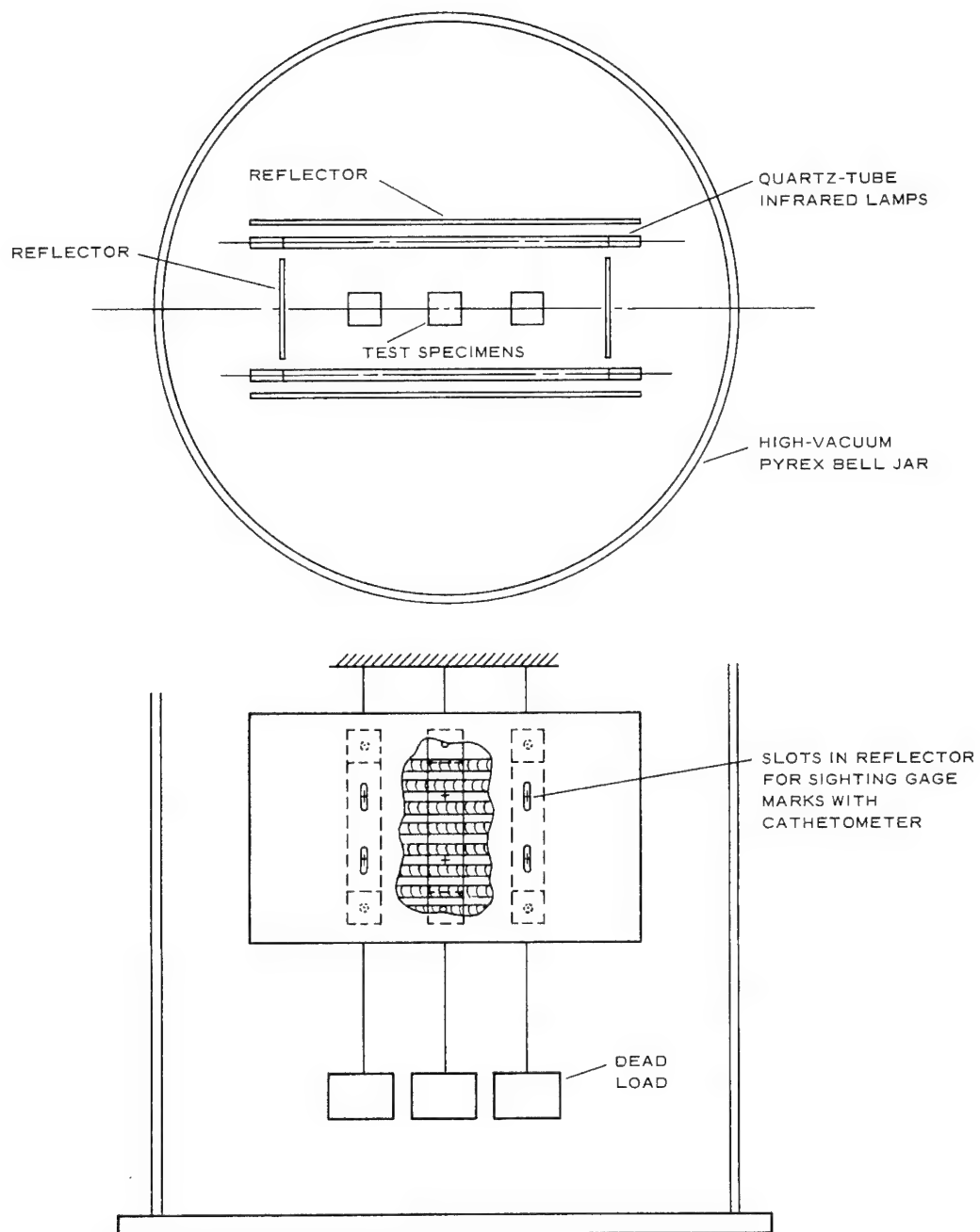


Figure 44. Setup for Elevated Temperature Creep Tests

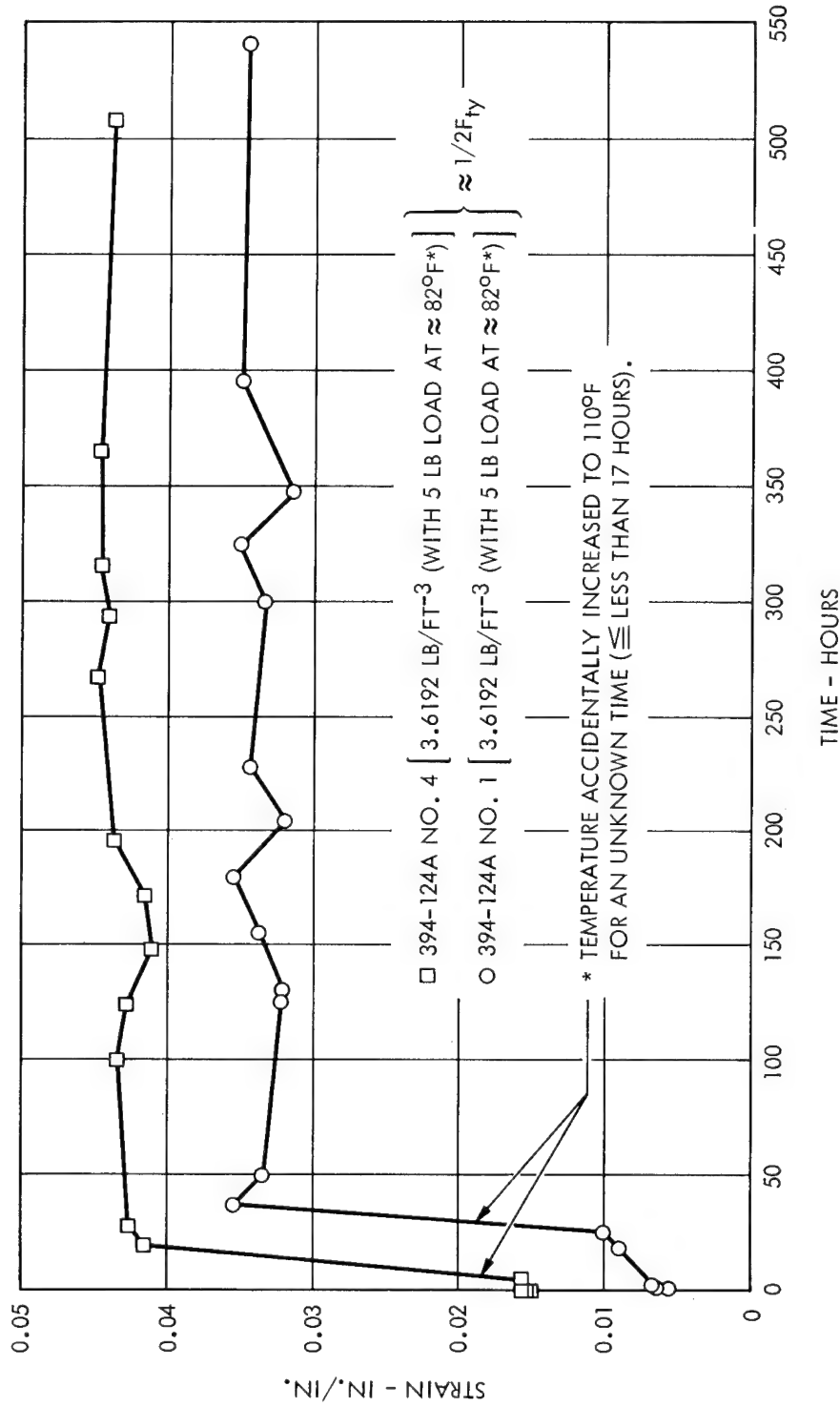


Figure 45. Predistributed Foam Creep Curves for 50 Percent of Yield and Ambient Temperature

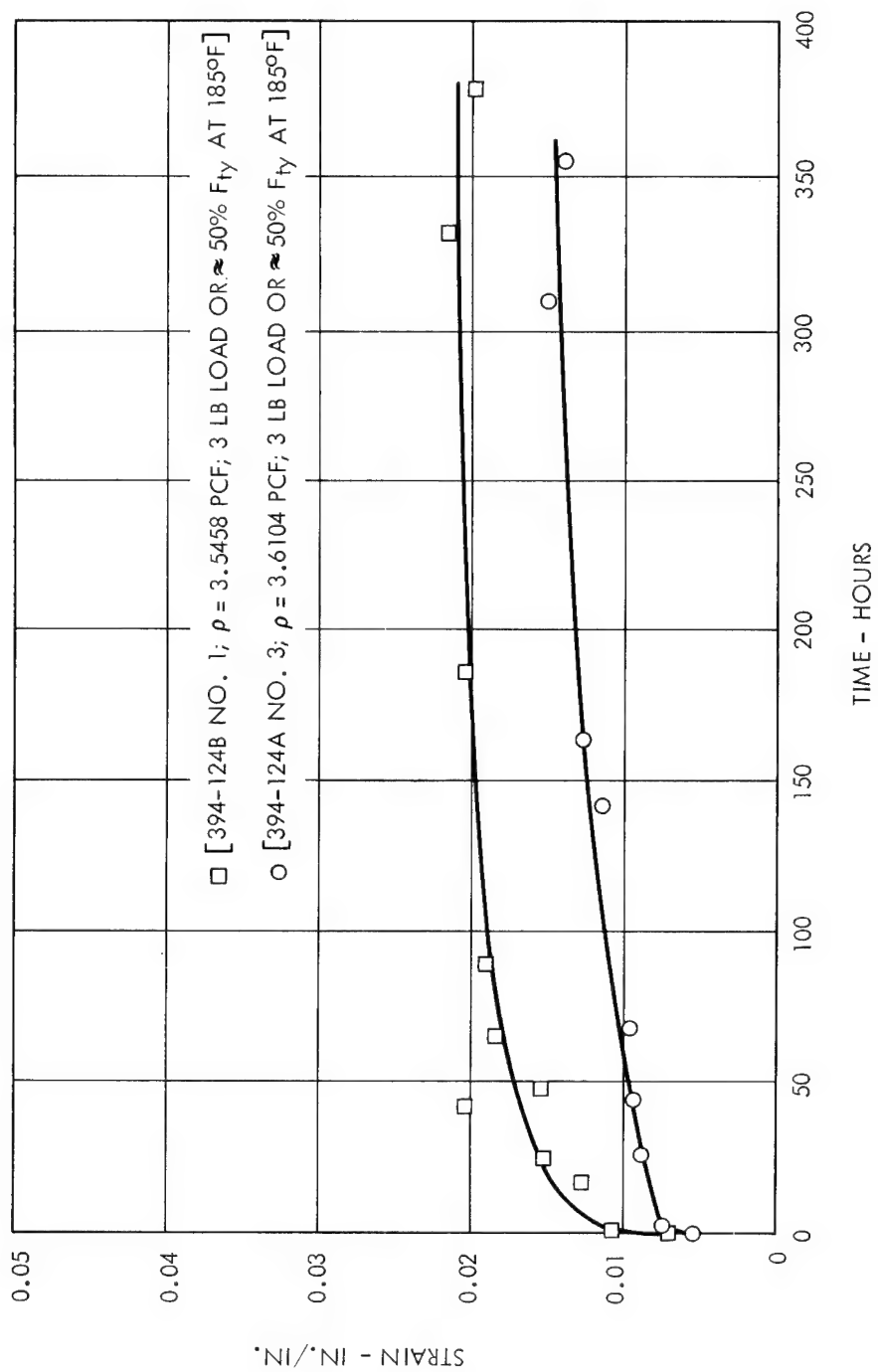


Figure 46. Predistributed Foam Creep Curves for 50% F_{ty} and 185°F

The creep specimen curves for 240°F at a constant load of 50 percent of yield are shown on Figure 47. Both specimens failed between 26 and 91 hours, with creep data available for only 18 and 27 hours. Both specimens had elastic strain of approximately 0.004 inch per inch with the three-pound loading. One specimen had a primary creep of 0.014 inch per inch within two hours, but then leveled off to a very low creep rate. The second specimen had only 0.004 inch per inch creep strain in the first two hours, but then continued to creep at a very high creep rate, with total creep strain of 0.030 inch per inch at 27 hours. The 240°F creep tests indicate that this foam has poor creep characteristics at 50 percent of yield. At lower stress levels the creep rates may be tolerable, but it is doubtful that this foam has the required creep stability at temperatures approaching 240°F .

Figure 48 gives a comparison of the primary and secondary creep characteristics at 50 percent of yield load for this foam at 82°F , 185°F , and 240°F . If the creep strain of 0.026 inch per inch (due to the accidental temperature rise during the 82°F tests) is subtracted from the 82°F creep tests, the comparison curves show the increase in creep strain rates and strain levels as the temperature level is increased to 185°F and 240°F .

10. Thermal Conductivity

The thermal conductivity of a structural material is a significant physical property in solar concentrator design. Since only one side faces the sun, the differences in heat fluxes on opposite sides may be quite large at the different orbital positions. Differences in heat fluxes and temperatures cause thermal deflections. In order to determine the extent of the thermal deflections the thermal conductivity of the material must be known.

In general, a lightweight foam (3 to 4 lb/ft³) has a thermal conductivity of about 0.05 BTU-in./ft²-hr- $^{\circ}\text{F}$ in vacuum. Of the three modes of heat transfer - radiation, conduction, and convection - gas conduction and convection are neglected in a

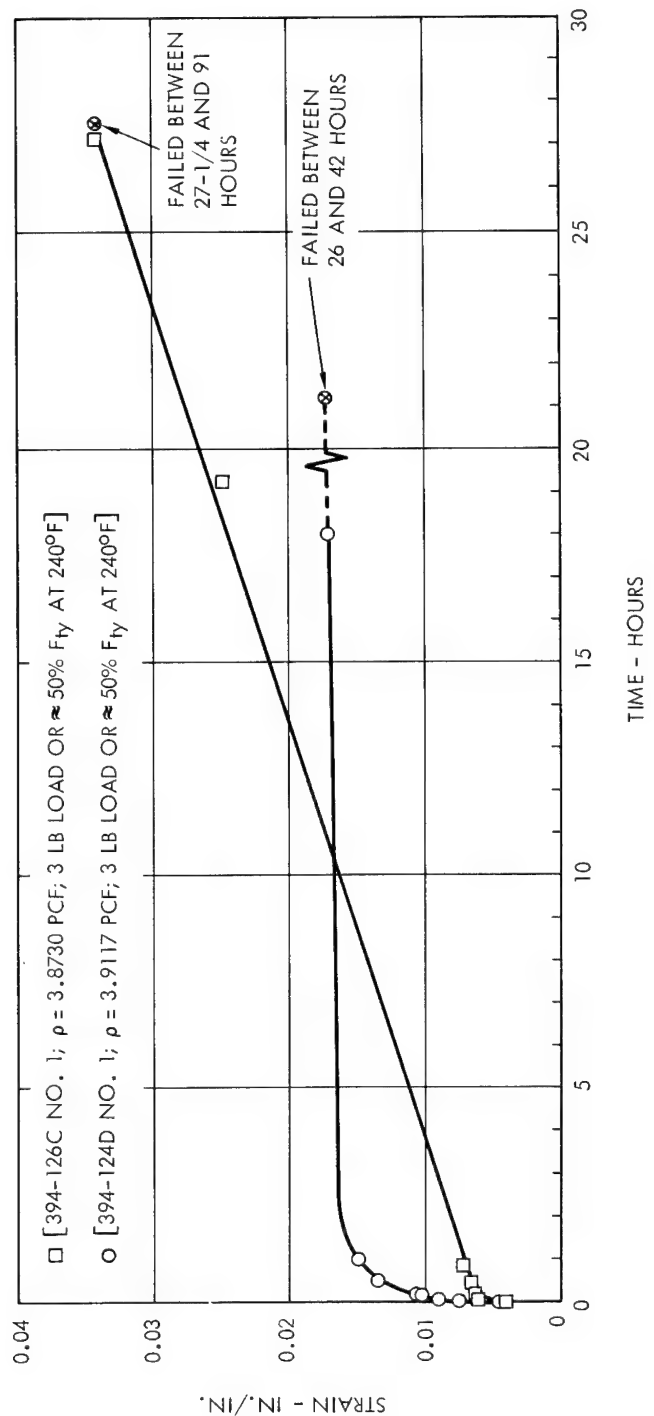


Figure 47. Predistributed Foam Creep Curves for 50% F_{ty} and 240°F

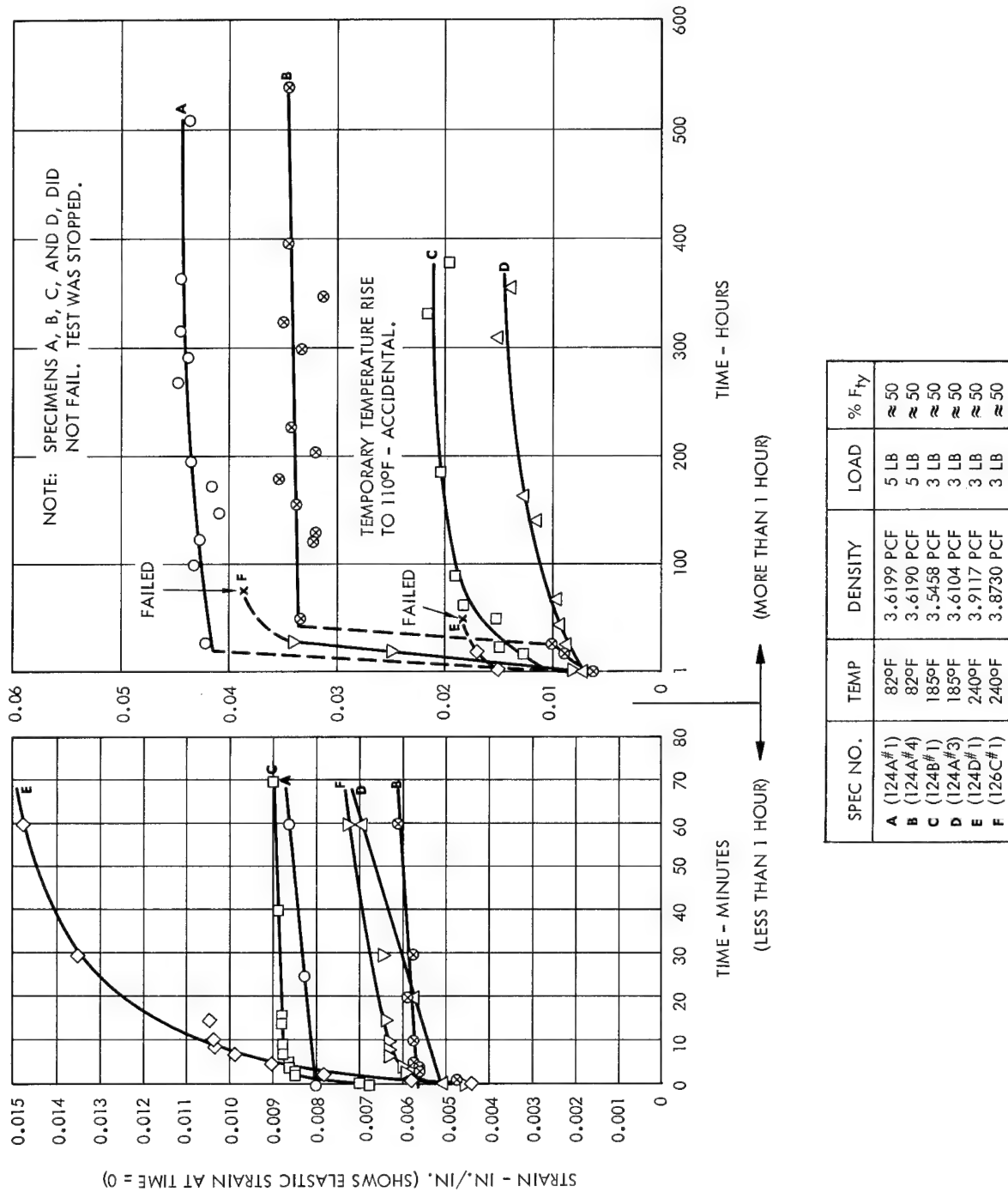


Figure 48. Summary of Predistributed Foam Creep Curves for 50% F_{ty} and for 82, 185, and 240°F

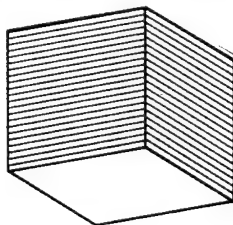
SECTION V

vacuum since it is assumed that all the interstitial gas is gone. The radiation heat transfer in a multibarrier (cellular) wall is proportional to ϵ/n , the material's total emittance over the number of radiation barriers. For small temperature differentials the apparent K_a for radiation is

$$K_a \doteq \frac{\sigma\epsilon}{n} T_{\text{avg}}^3,$$

which is plotted in Figure 49 for two layers, $n = 2$ per inch, and 200 layers, $n = 200$ per inch. For a large number of barriers as would exist in cellular foam, the predominant mode of heat transfer should therefore be conduction.

A typical building element that would construct a multi-cubicle cellular material would consist of a common three-sided orthogonal element as shown:



This means that approximately 67 percent of the material is conducting in any one direction, and since most plastic materials have a solid thermal conductivity of 1 to 2 BTU-in./hr-ft²-°F, the foam thermal conductivity in the absence of radiation and interstitial gas should be a function of the material solidity. Lightweight foam would therefore be about 3 to 4 percent solid and would have a thermal conductivity of 0.02 to 0.06 plus any small amounts of radiation and gas conduction that could remain.

The foam tested on this program was placed in a guarded hot plate where the heating element was sandwiched between two nine-inch diameter by 0.38 inch-thick slices of foam, which were in turn sandwiched between two cold plates (see Figure 50). The four interfaces for this five-ply composite were coated with a highly conductive paste to eliminate or minimize any contact resistance that would exist in



Figure 49. Thermal Conductivity versus Temperature

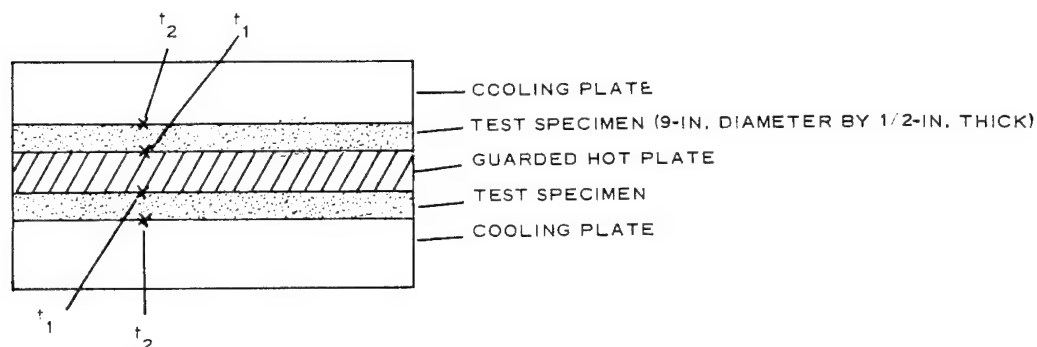


Figure 50. Thermal Conductivity Test Composite

this test setup. It should be noted, however, that due to the irregularity of this type of foam there were still large areas that did not contact the cold plates.

Figure 49 is a plot of a set of test points. The standard apparent thermal conductivity (K_a at 70°F) is about 0.0575 BTU-in./ft²-hr-°F and varies with temperature as would be expected. The data was for foam having a density of about 4 lb/ft³ in a vacuum of 10⁻⁴ mm Hg with temperature differentials ranging from 100 to 300°F. Figure 49 represents six samples being tested. These samples are about twice the density of a mechanically mixed foam which was tested a year ago on another program (the 2-lb foam in Figure 49); also, it was more homogeneous and had a better contact area against the hot plate than the predistributed foam. The surface irregularity of the predistributed foam could also explain the curve displacement of the six specimens tested (see Figure 49). The upward curvature is as would be expected, since the conductivity of the solids increases with temperature and any radiative heat transfer that may be included also follows this trend. Any effects that may be caused by the H-Film are not discernible in the scatter of the test data.

11. Reflectance

Reflectance measurements were integrated over the solar spectrum. Measurements were made on vacuum-deposited aluminum on Mylar and H-Film surfaces and on foam-backed aluminized H-Film surfaces.

The solar reflectance of aluminized H-Film was 83 percent (see Figure 51) and for aluminized Mylar it was 88 percent (see Figure 52). H-Film, like Mylar, can be readily vacuum-metallized. Its surface is not as smooth as Mylar, and consequently its reflectance is not quite as high. The H-Film samples tested were pilot plant (or prepilot plant) production runs. This suggests an improvement in quality when formal production is under way.

Reflectance measurements of three samples, taken from the third rigidized solar concentrator, are shown in Figures 53, 54, and 55. The comparatively low values of these three samples may be attributed to orange peel and double curvature as indicated by the large diffuse component; grease and grime accumulated from handling; a yellow discoloring, noted on samples 3A and 3B, probably due to some chemical action on the aluminum.

The application of a top coat is expected to prevent any great loss of reflectance due to handling. No serious reflectance problem is anticipated, since one unprotected sample measured only eight percent less than the maximum value.

12. Stress-Strain Tests of Model Specimens.

The two-ft model solar concentrator (No. 3) was dissected to obtain reflectance and stress-strain test specimens (Figures 56, 57, and 58). This model was constructed of 1-mil aluminized H-Film, approximately one-fourth inch of foam, and a loose fitting 1/2-mil Mylar back flap.

Six specimens, 4 x 2 inches, were cut in the meridional direction of the mirror. The H-Film was removed from three of these specimens (Group A), while the

SECTION V

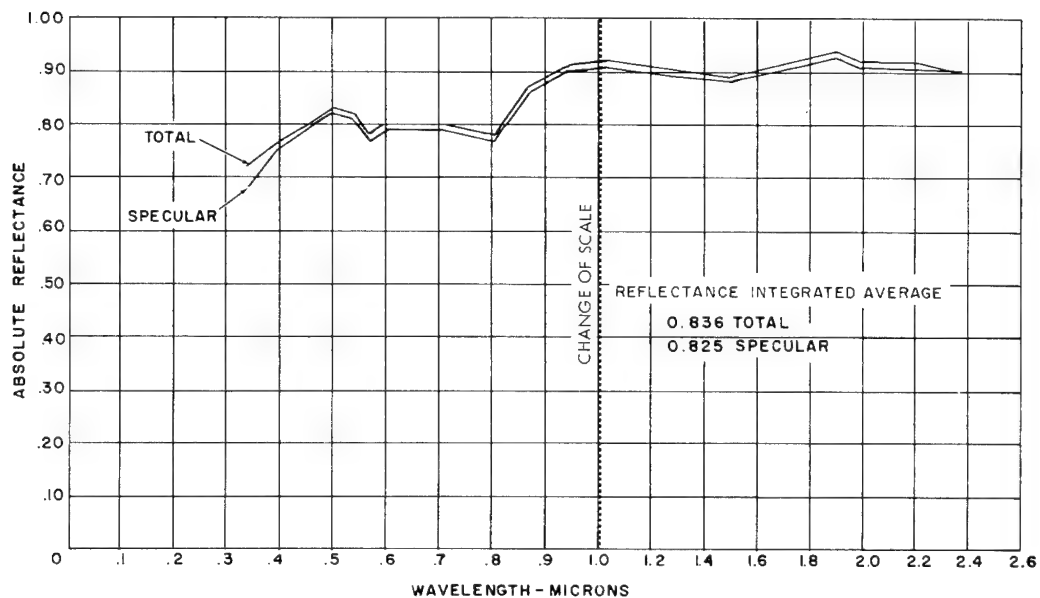


Figure 51. Reflectance of Vapor Deposited Aluminum on H-Film

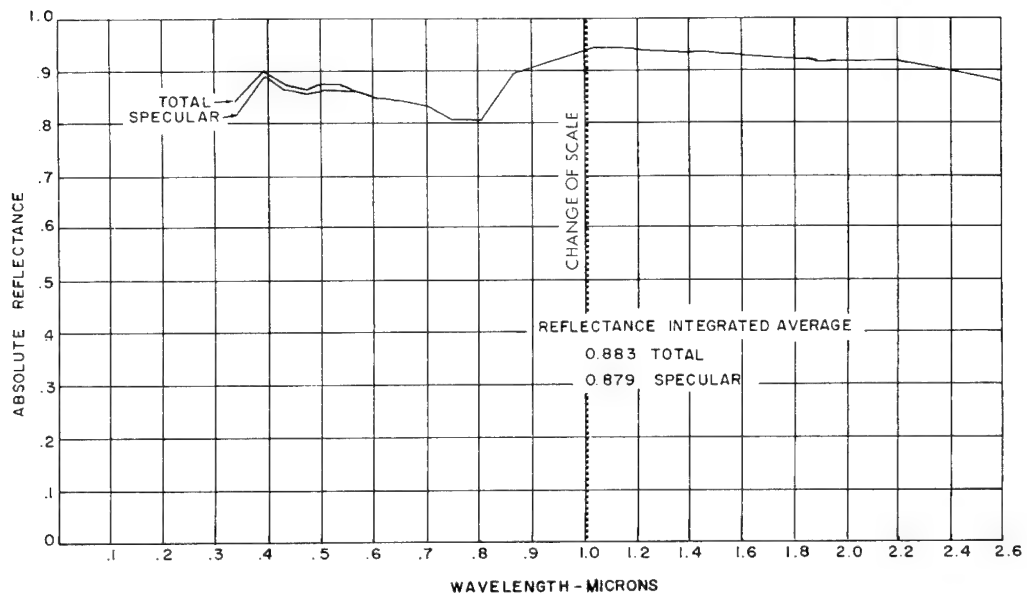


Figure 52. Reflectance of Vapor Deposited Aluminum on Mylar

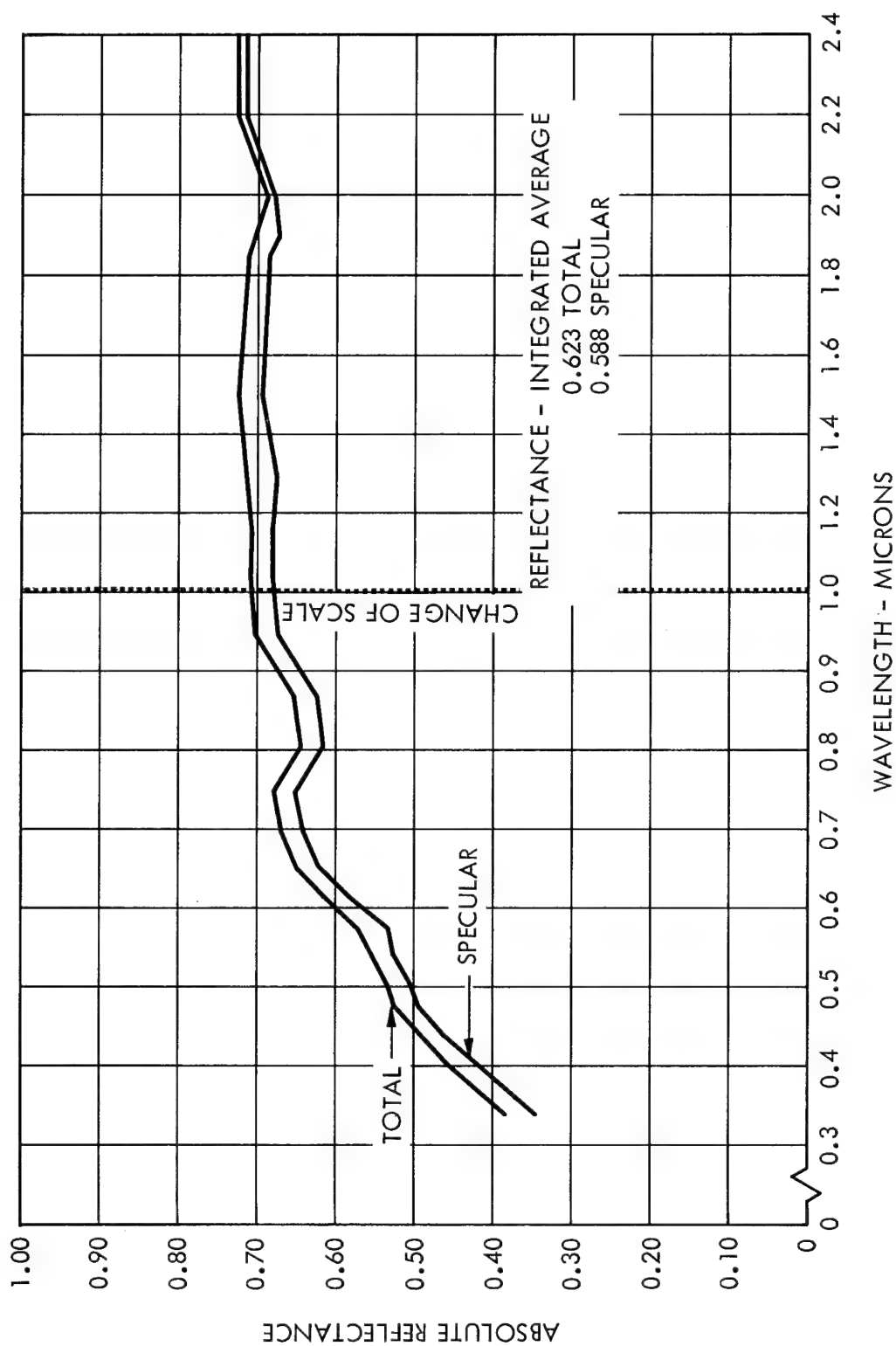


Figure 53. Reflectance Measurements - Sample No. 3A

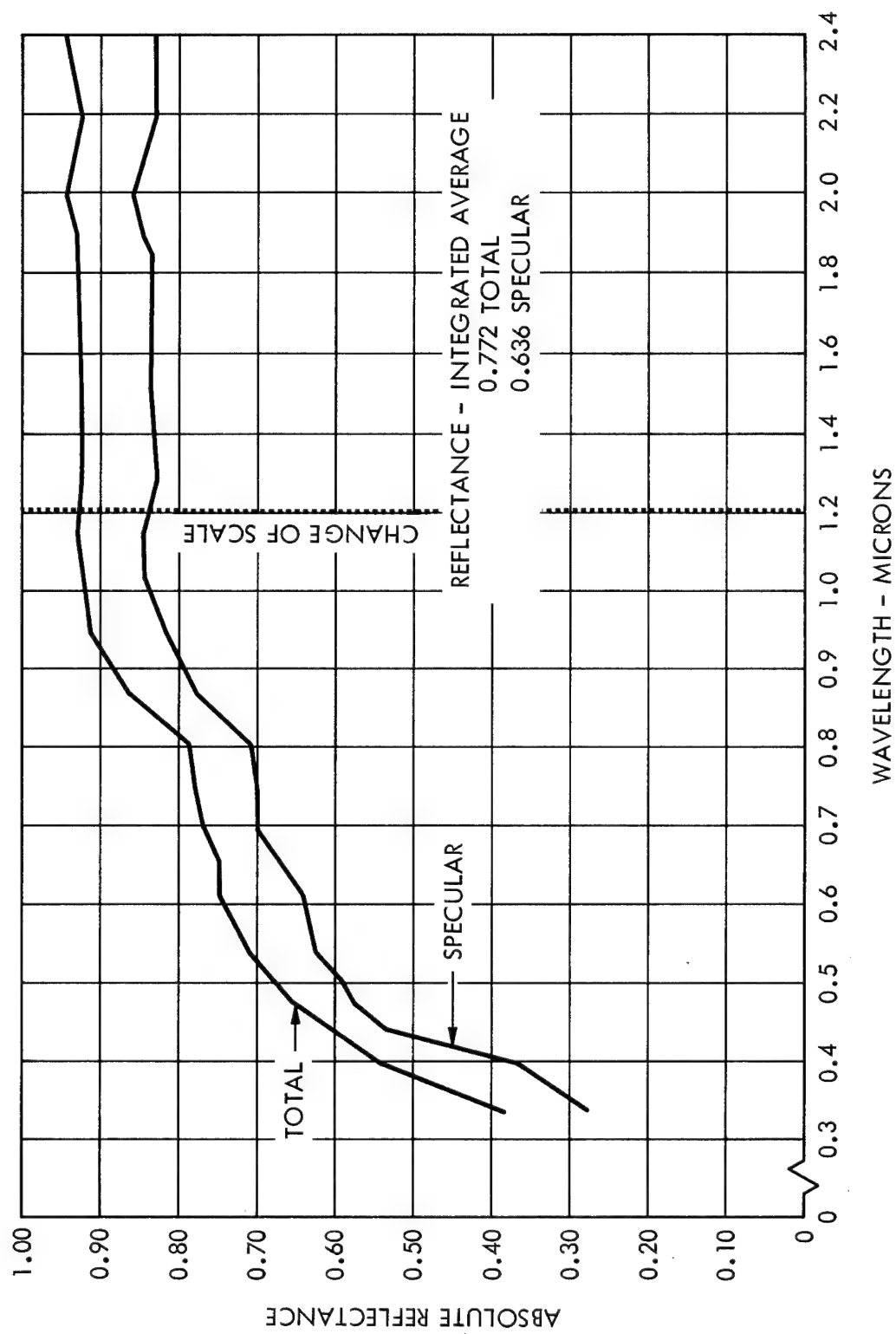


Figure 54. Reflectance Measurements - Sample No. 3B

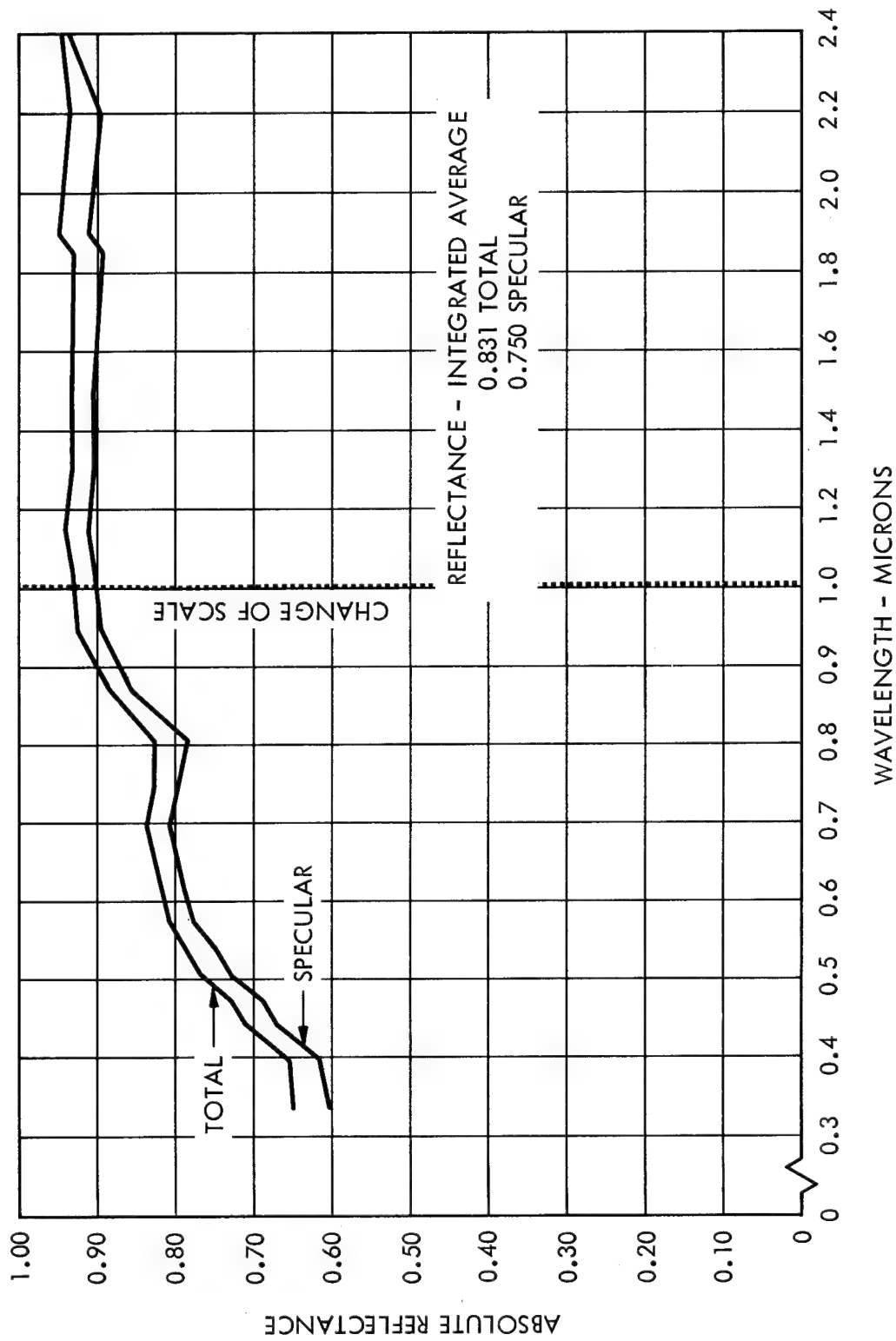


Figure 55. Reflectance Measurements - Sample No. 3C

SECTION V

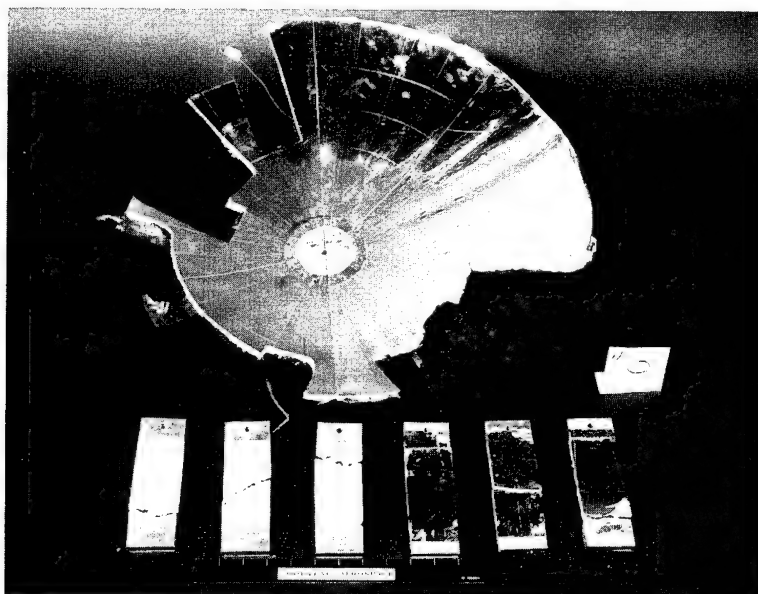


Figure 56. Mirror No. 3 Dissected - Face Up

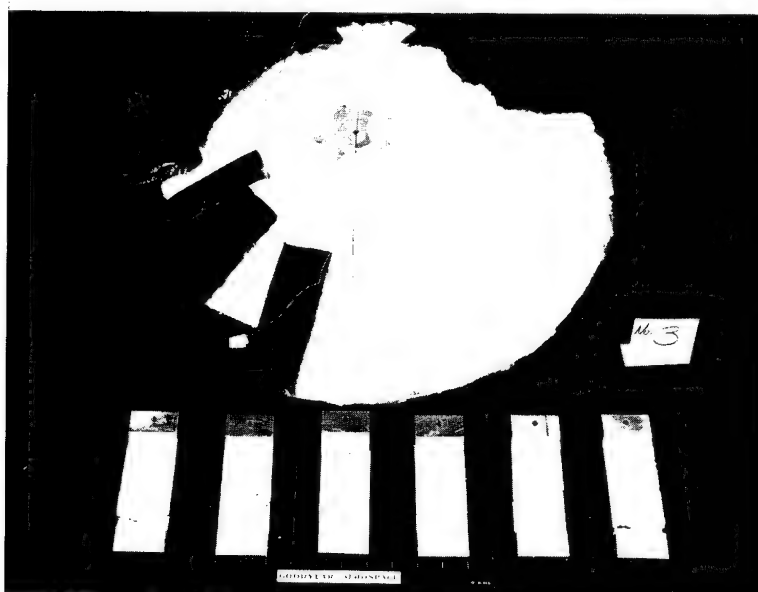


Figure 57. Mirror No. 3 Dissected - Back View

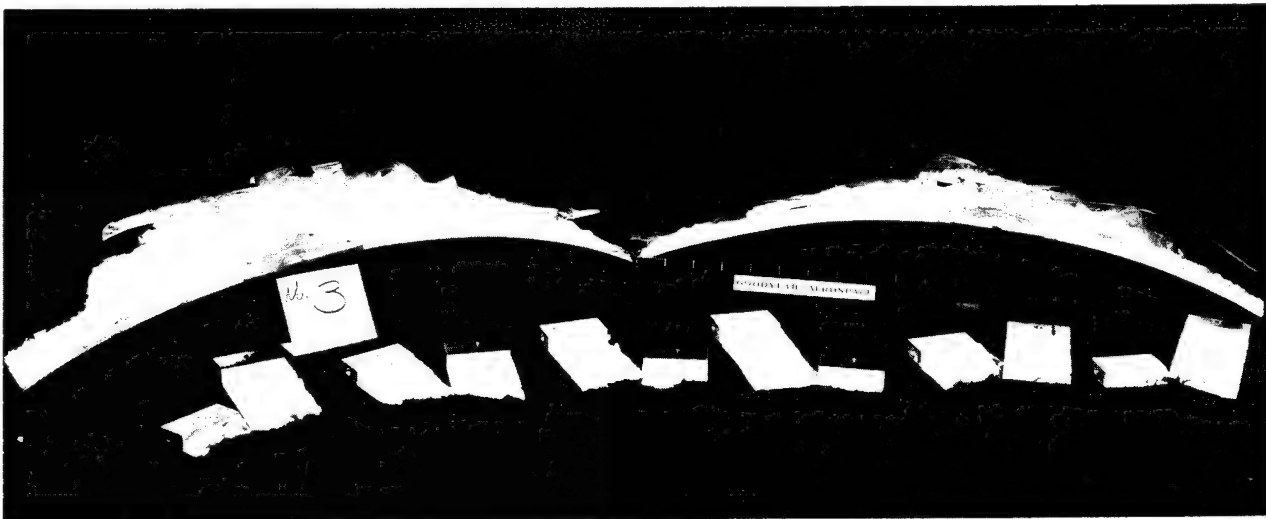


Figure 58. Mirror No. 3 Dissected - Cross Section

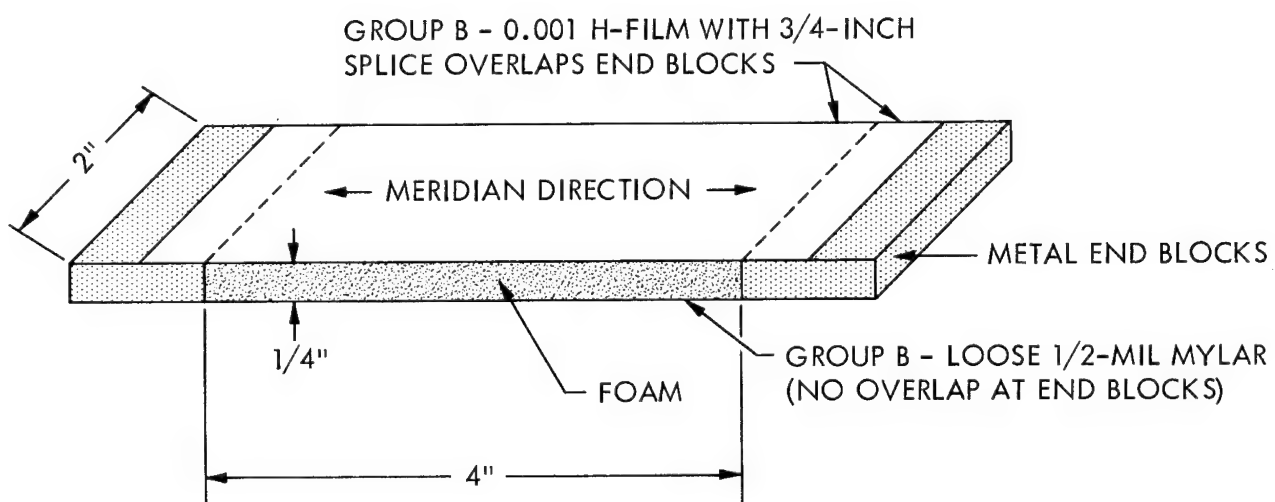


Figure 59. Two-Foot Mirror Test Sections

Table XX. Two-Foot Mirror Test Specimens

Specimen Groups (A & B)	Temp (°F)	Pressure (mm of Hg)	Foam Dimensions (inches)	Foam Volume (in. ³)	Foam Weight* (gm)	Foam Density (~lb/ft ³)	Strain Rate (in./in. min)	Foam Cross Section Area (in. ²)	P _{tu} Total (lb)	P _{ty} Total (lb)	Foam Only			ε _{tu} Total (in./in.)
											F _{tu} (psi)	F _{ty} (psi)	E _t (psi)	
A-1	74	10 ⁻⁵	4 x 2 x 0.214	1.712	4.0894	9.100	0.10	0.428	14.4	13.5	33.64	31.54	2785	0.0130
A-2	74	10 ⁻⁵	4 x 2 x 0.237	1.896	3.1305	6.299	0.10	0.474	9.5	8.2	20.04	17.30	1403	0.0154
A-3	74	10 ⁻⁵	4 x 2 x 0.236	1.888	2.8690	5.789	0.10	0.472	8.3	7.8	17.58	16.53	1107	0.0176
B-1	74	10 ⁻⁵	4 x 2 x 0.298	2.384	5.1477	8.226	0.10	0.596	74.0 19.0†	65.0 10.0†	31.88†	16.77†	2372†	0.0336
B-2	74	10 ⁻⁵	4 x 2 x 0.286	2.288	5.3947	8.982	0.10	0.572	64.0 9.0†	62.5 7.5†	15.73†	13.11†	1808†	0.0208
B-3	74	10 ⁻⁵	4 x 2 x 0.206	1.648	3.6311	8.394	0.10	0.412	79.0 24.0†	66.3 11.3†	58.25†	27.42†	2830†	0.0386
Average (Foam Only)						7.80			14.0	9.7	29.5	20.4	2050	

*Actual Foam Weight (1/2-mil Mylar and if applicable 1-mil H-Film subtracted;
Density of H-Film = 23.27 g/in. ³, 0.0513 lb/in. ³, or 88.646 lb/ft³)

Foam properties reduced from composite section based on H-Film properties; E = 415,000 psi and P_{tu} = 35 lb per specimen.

other three specimens retained the H-Film which included a three-fourths, inch 1-mil H-Film gore seam (Group B, See Figure 59).

The specimens were bonded to metal end blocks. Group B specimens had a one-half inch overlap of H-Film (sufficient to develop the film strength), which was bonded to the sides of the end block (see Figure 59). The ultimate H-Film strength is $\geq 20,000$ psi or 20 lb/in. for 1-mil film. With 2-inch wide film and three-fourths inch splice, the H-Film alone is good for $(20 \times 2-3/4)$ 55 lb. Therefore, any load in excess of 55 pounds in Group B can be attributed to the foam, since the one-half mil Mylar is loose and has no end overlap which would be required to develop its strength.

The test data is tabulated and reduced in Table XX. The Group B (composite sections of H-Film and foam) data was reduced to obtain equivalent foam properties F_{tu} , F_{ty} , and E_t based upon H-Film properties of $E = 415,000$ psi and $F_{tu} \leq 20,000$ psi, which is equivalent to 55 lb/specimen.

The two-foot mirror tests show that the H-Film retained its original strength and that the actual mirror foam had an average density of 7.8 pcf. The average properties of the foam are:

$$F_{tu} = \text{tensile ultimate} = 29.5 \text{ psi.}$$

$$F_{ty} = \text{tensile yield} = 20.4 \text{ psi.}$$

$$E_t = \text{tensile modulus} = 2050 \text{ psi.}$$

These properties are approximately twice those of the prepared specimens (refer to Table XX) having approximately one-half the density of the mirror specimens. This shows that the mirror foam properties are definitely in line with the original prepared specimen's properties as would be indicated on an extension of tension stress-strain data curves.

SECTION VI. TWO-FOOT MODELS

A. FABRICATION

The 2-foot models were fabricated as gored paraboloids. The gores were butted and seamed together with a lapping tape. H-Film was used as the mirror film and a skirt of Mylar extended out to a diameter of four feet. The Mylar was drawn over a four-foot diameter plexiglass disk. Sealing compound was applied between the Mylar and the plexiglass. A clamping ring around the Mylar retained gas tightness between the Mylar and the plexiglass. A contour measuring apparatus was attached to the hub inside the pressure envelope.

The first model was without a back flap. The second model had a back flap made up of unseamed gores with none, one, two, and three slits per gore in each quadrant. The third and fourth models had back flaps made up of overlapping unseamed gores with a fold at the hub and at the rim to permit longitudinal expansion. The latter arrangement seemed to make the most suitable back flap.

The selection of H-Film as a solar concentrator material brought on the problem of finding a suitable adhesive. A number of adhesive materials were selected for test. Seams were made on one-inch wide strips of H-Film. After curing, the strips were subjected to tensile testing at room temperature (see Figure 60 for results). The test strips were then exposed to a temperature environment of 400°F and tensile tested (see Figure 61 for results). Adhesives that demonstrated effectiveness at an environmental temperature of 400°F were subjected to 500°F and tensile tested. The seams that did not fail were those of samples numbered 23, 26, 32, 33, 34, and 38 (see Figure 62). The adhesive application method of sample number 38 was selected for the fabrication of the 2-foot model solar concentrators.

SECTION VI

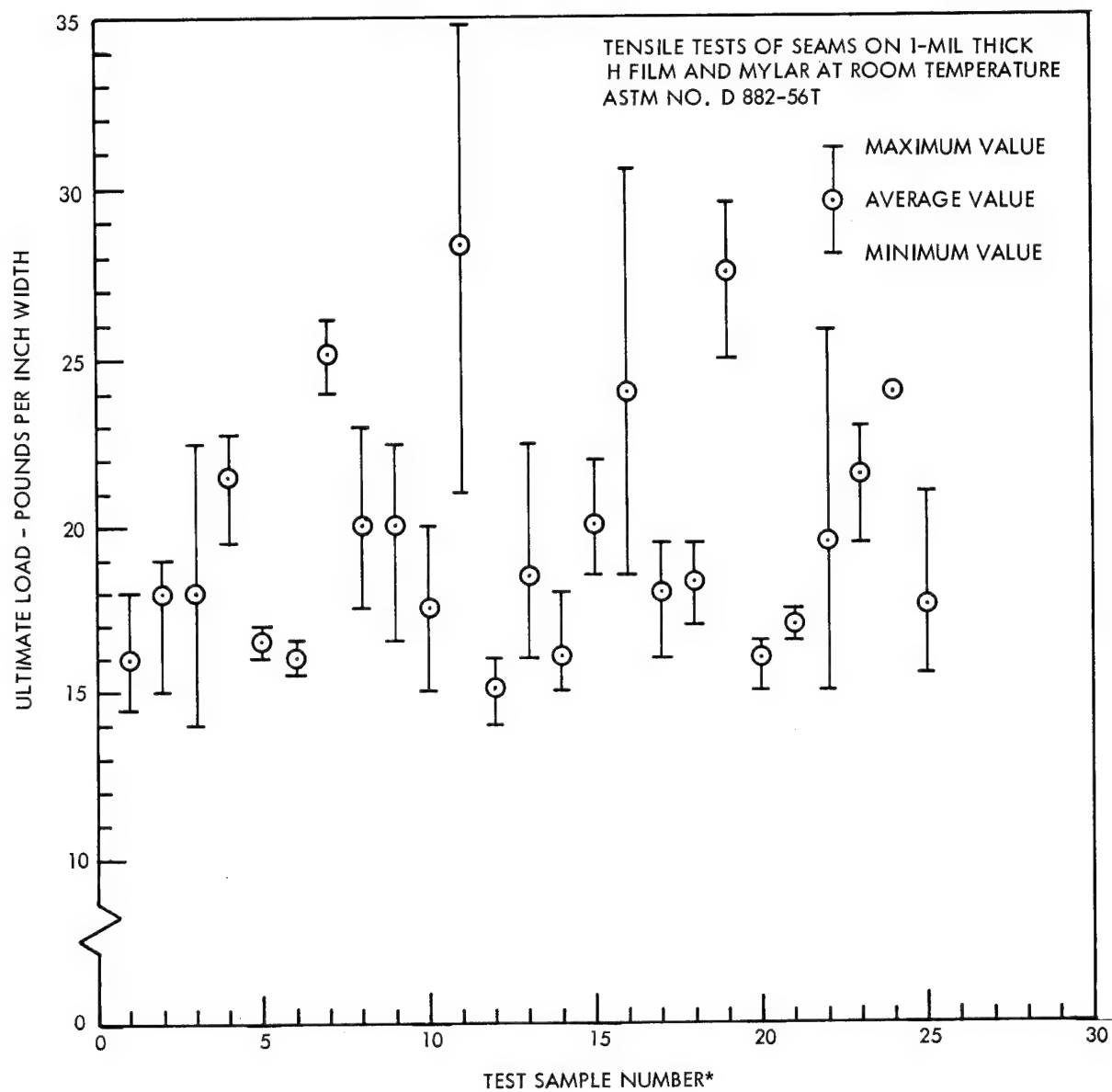


Figure 60. Film Seam Shear at Room Temperature

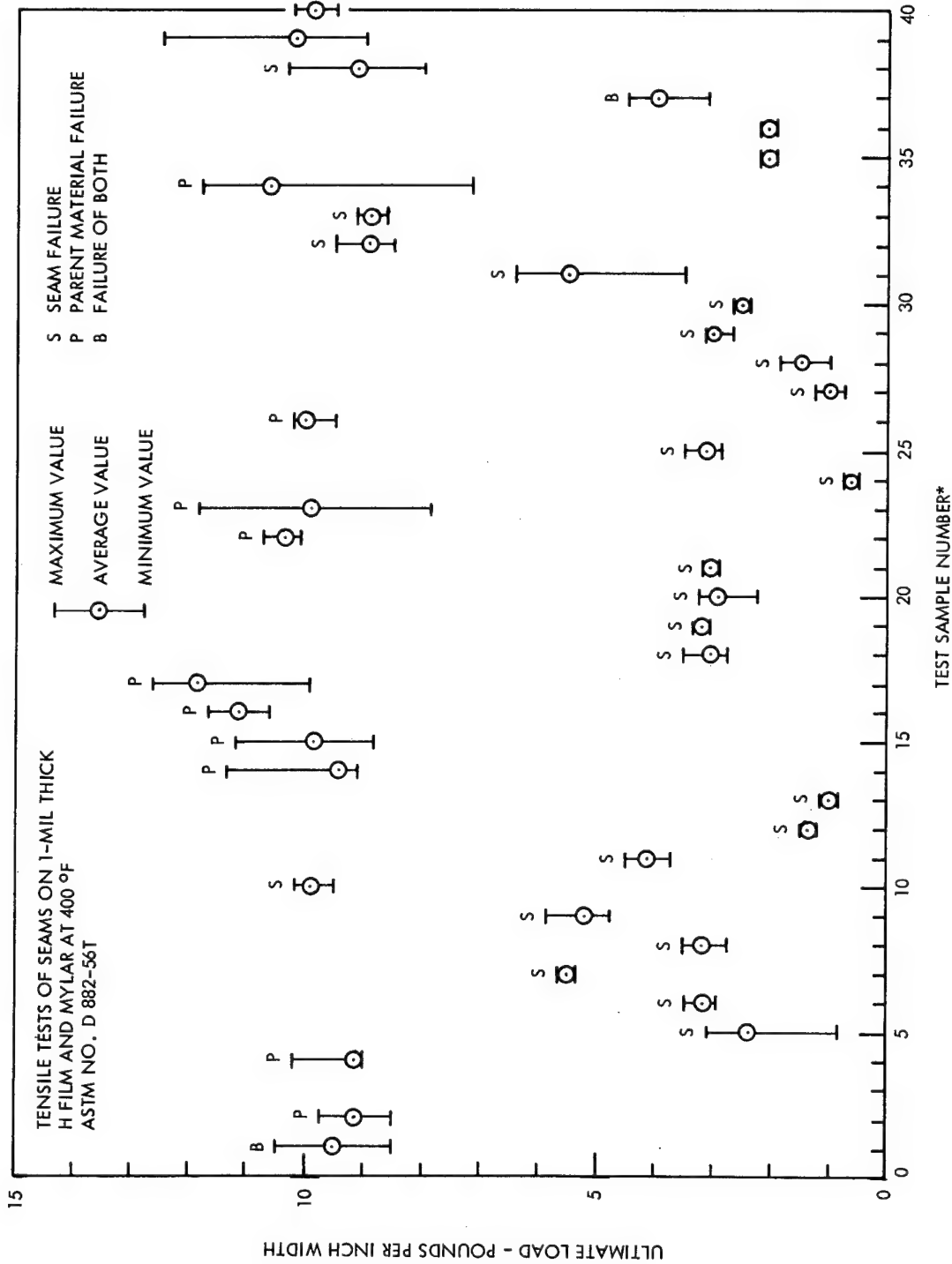


Figure 61. Film Seam Shear at 400°F

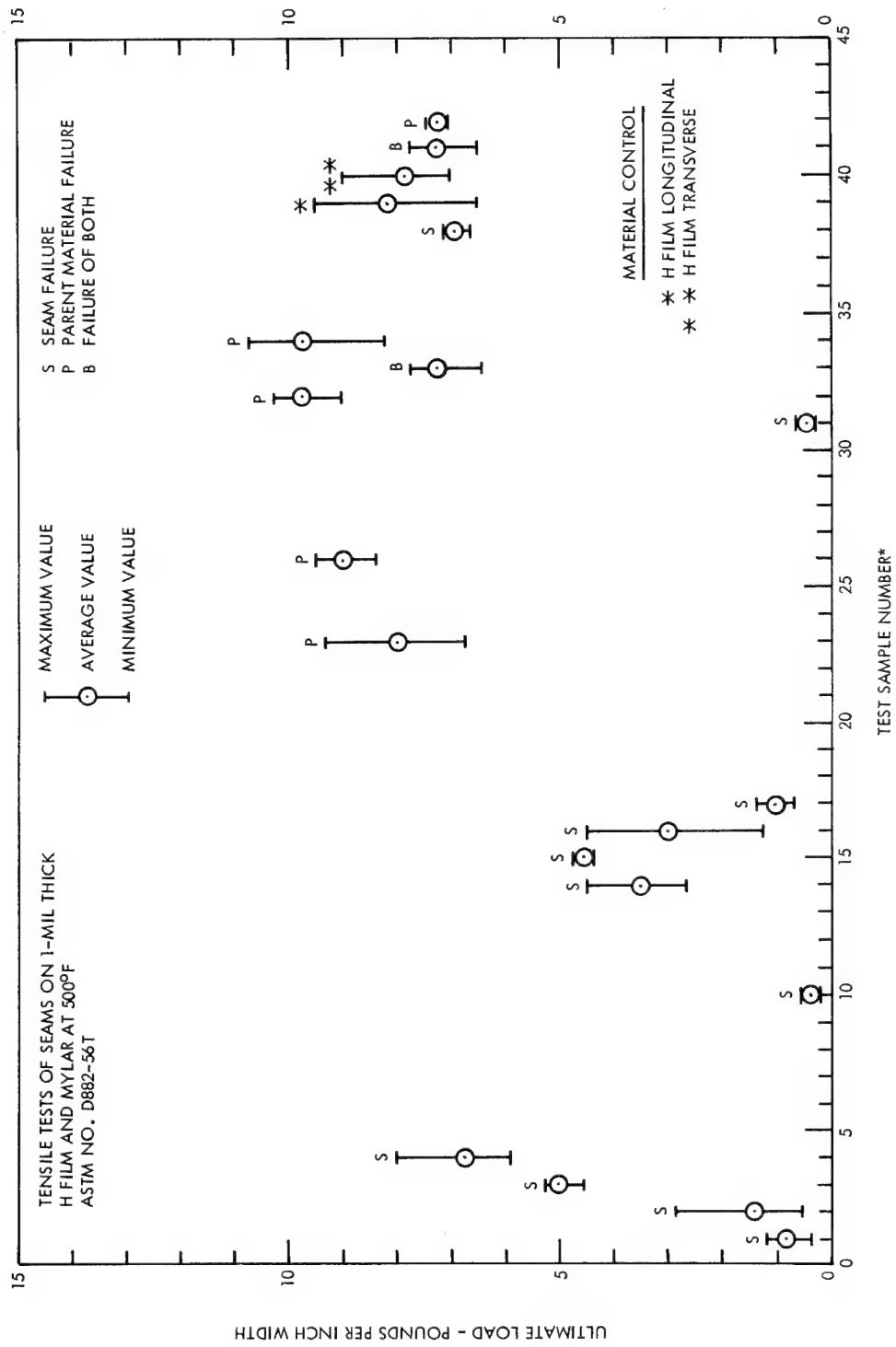


Figure 62. Film Seam Shear at 500°F

An investigation was performed to determine the time limit that a prepared batch of the adhesive may be exposed to laboratory conditions (in an open container) before detrimental effects would appear. Exposures were made up to an eight day period. Seams were tested at 500°F. It was found that seam failures appeared after exposures of seven days (see Figure 63). Exposure limitations (pot life) of up to six days are recommended as a specification.

To test the volatility of H-Film adhesive, seams were prepared with strips of H-Film one inch wide and ten inches long. The H-Film adhesive was applied between the strips. These strips were then attached to a microbalance within a bell jar. The bell jar was then evacuated to the 10^{-5} torr range. A zero reading was taken of the material at this point. Pressure and weight loss were recorded continuously with respect to time. Each followed the same general weight loss pattern. The total weight of one sample was 584 mg at the start and leveled off at 581.8 mg after approximately 3 hours in a vacuum range of 10^{-5} - 10^{-6} torr. Each of the tests was run until the rate of weight loss was down to 0.1 mg per hour or less (see Figure 64). It was concluded that the volatility of the H-Film adhesive was sufficiently low to make it highly compatible with the space environment.

Prior to applying the precoat foam material, one two-foot model was pressurized to 7 inches of H₂O and subjected to a temperature of 350°F for 5 minutes. Several seams were marked so that any movement or slippage of the seams could be determined.

As the pressurized model was placed in the oven which was preheated to 350°F the pressure immediately rose to 10.5 inches of H₂O. After one minute, the pressure control device brought the pressure down to 9.5 inches of H₂O. After two minutes the pressure was down to 7.5 inches of H₂O. After 2-1/2 minutes, the pressure was down to 7 inches of H₂O, where it was maintained to the end of the 5-minute exposure period.

SECTION VI

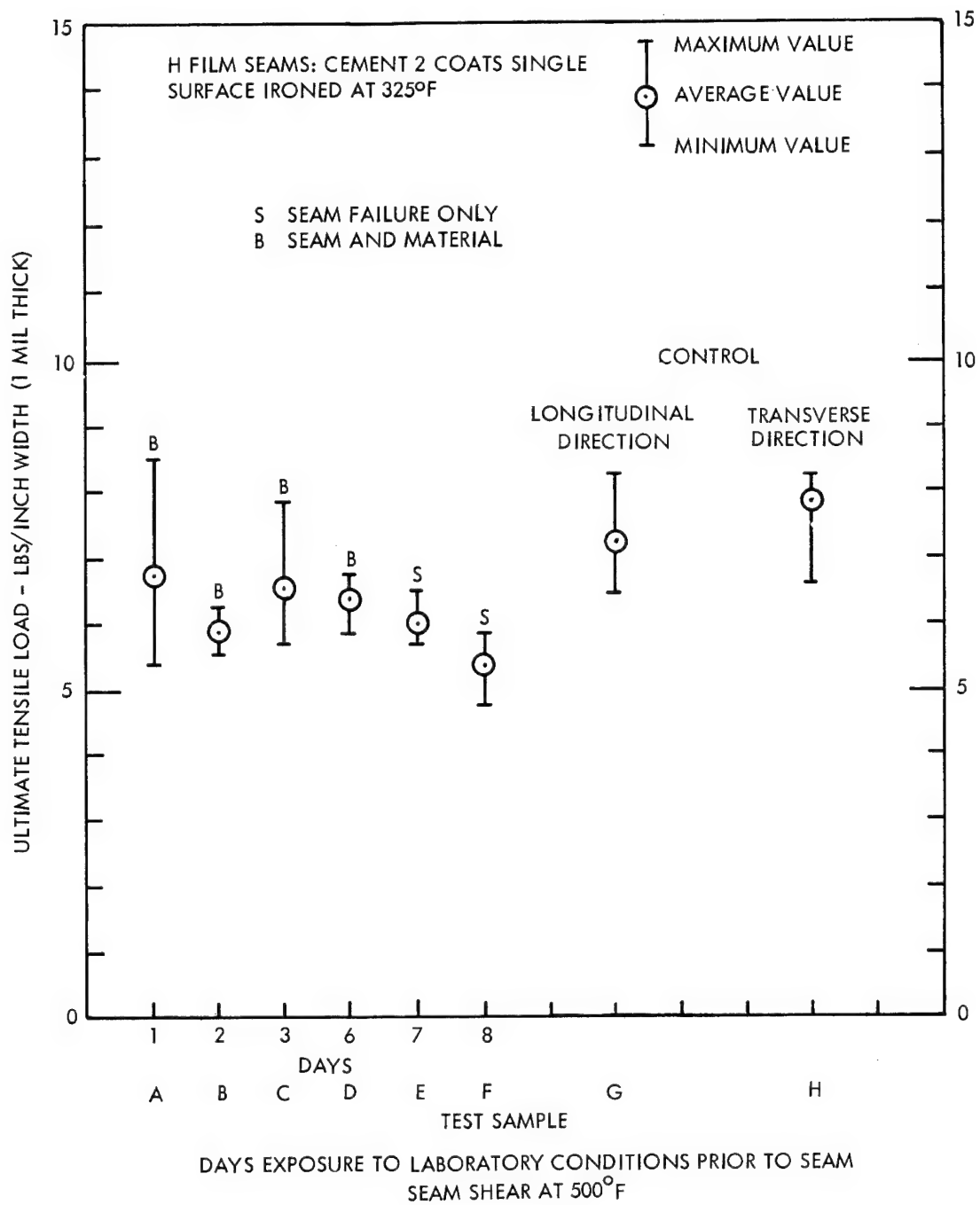


Figure 63. Exposure Limitation of H-Film Adhesive

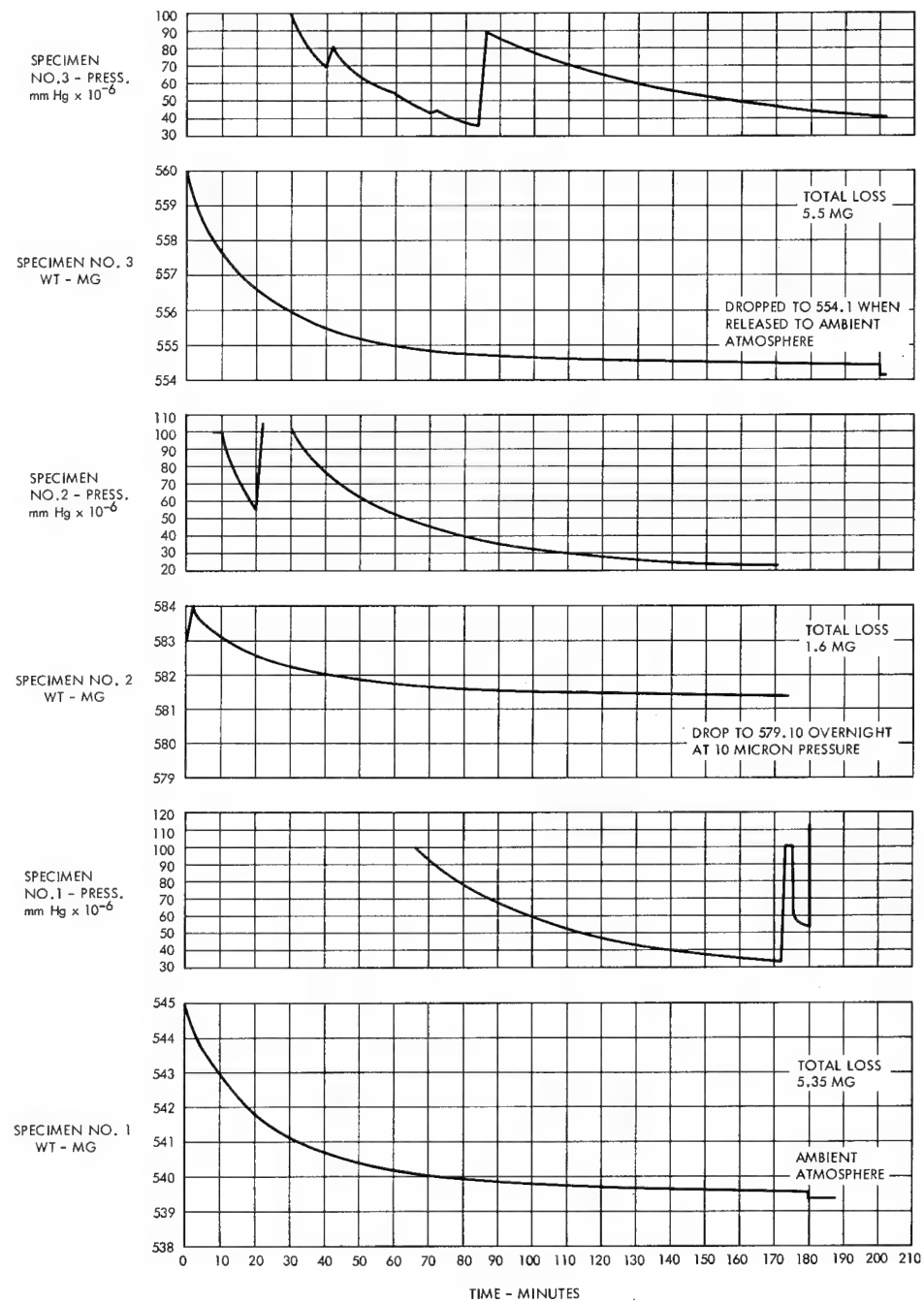


Figure 64. Volatility of H-Film Adhesive

SECTION VI

As the model was removed from the oven, the pressure immediately dropped due to cooling, but recovered in a few minutes. It was noted that the tape separated approximately 0.01 inch. No leakage was detected. All seams appeared in good condition.

The simplified pressure control device used during the heat exposure test did not have sufficient pressure relief capabilities to maintain constant pressure. The effect of the heat on the seams, even with the higher pressure, was negligible. The test run indicated that these seams were well suited for the precoat foam application.

B. RIGIDIZATION

Five rigidization runs were performed. Descriptions and results are as follows:

1. First Run

The first run involved a check on the heat distribution of the heating coil. The heating coil (see Figure 76) consisted of a spiral winding of two parallel circuits of 12-gage heating wire (Haskins Alloy 875) having a resistance of 0.134 ohms per foot. The spiral had a thirty-inch diameter; a spacing of one inch was maintained between the wires. Each circuit required 18 feet of wire. The arms described the same contour as the solar concentrator. All leads were silver-soldered to the heating wires. The heat output was controlled by a 20-ampere variac. Ten squares (3 x 3 inches) of H-Film were prepared and precoat material was spread over a 2 x 2 inch area. These were located at various positions over the back of the solar concentrator. Thermocouples were imbedded in each sample as well as at the hub, at the rim, and at several mid-way positions. The chamber was then evacuated, heat was applied, and the foaming actions occurred satisfactorily in each sample indicating that the heat distribution from the coil was adequate.

2. Second Run

The second run (first mirror model RISEC 918) involved a check on the effectiveness

of a pressed material over a "spread on" material. The same model as that of the first run was used. The pressed material is described as a ball of the precoat material placed in a press where it is pressed into a thin sheet; the sheet is then cut to a pattern and placed on the back of the solar concentrator. The "spread on" material is the precoat material taken from a jar in a paste-like form and spread on the back of the solar concentrator with a small stick or trowel. One-half of the model was covered with the pressed material and the other half was covered with the "spread on" material.

The foaming action resembled that of some of the small models in the bell jar. Large cells presented themselves and a maximum rise of approximately one inch was attained. Average thickness throughout seemed to be about one-half inch. See Figure 65 for temperature and pressure against time, and Figure 66 for location of thermocouples. The mirror surface was reasonably smooth, all seams were intact, and the contour described a fair degree of geometrical perfection. The difference between the "spread on" and the pressed backing was small; the pressed material seemed to have a little more of the larger cells (see Figures 67 and 68).

3. Third Run

The third run (second mirror RISEC 924) included an investigation of the back flap design and variation of the thickness of the "spread on" foam. The back-flap consisted of unseamed gores of clear Mylar, each quadrant having a different number of slits in each gore, ranging from no slits to three slits per gore. The center half of the mirror surface was covered with a precoat consistency (0.8 gm of precoat per square inch of surface) designed to give twice the thickness of the precoat material applied to the outer half of the mirror surface (0.4 gm of precoat per square inch.)

The foaming action was normal. A greater input of heat to follow the described heat schedule for foam reaction was required. The thermocouples revealed a slower rate of heat build-up and cooling over the thicker foam section. A hot wire was used to burn off the Mylar end cap after cool-down. The variation of thickness was produced according to design. Contour measurements indicated that this mirror

SECTION VI

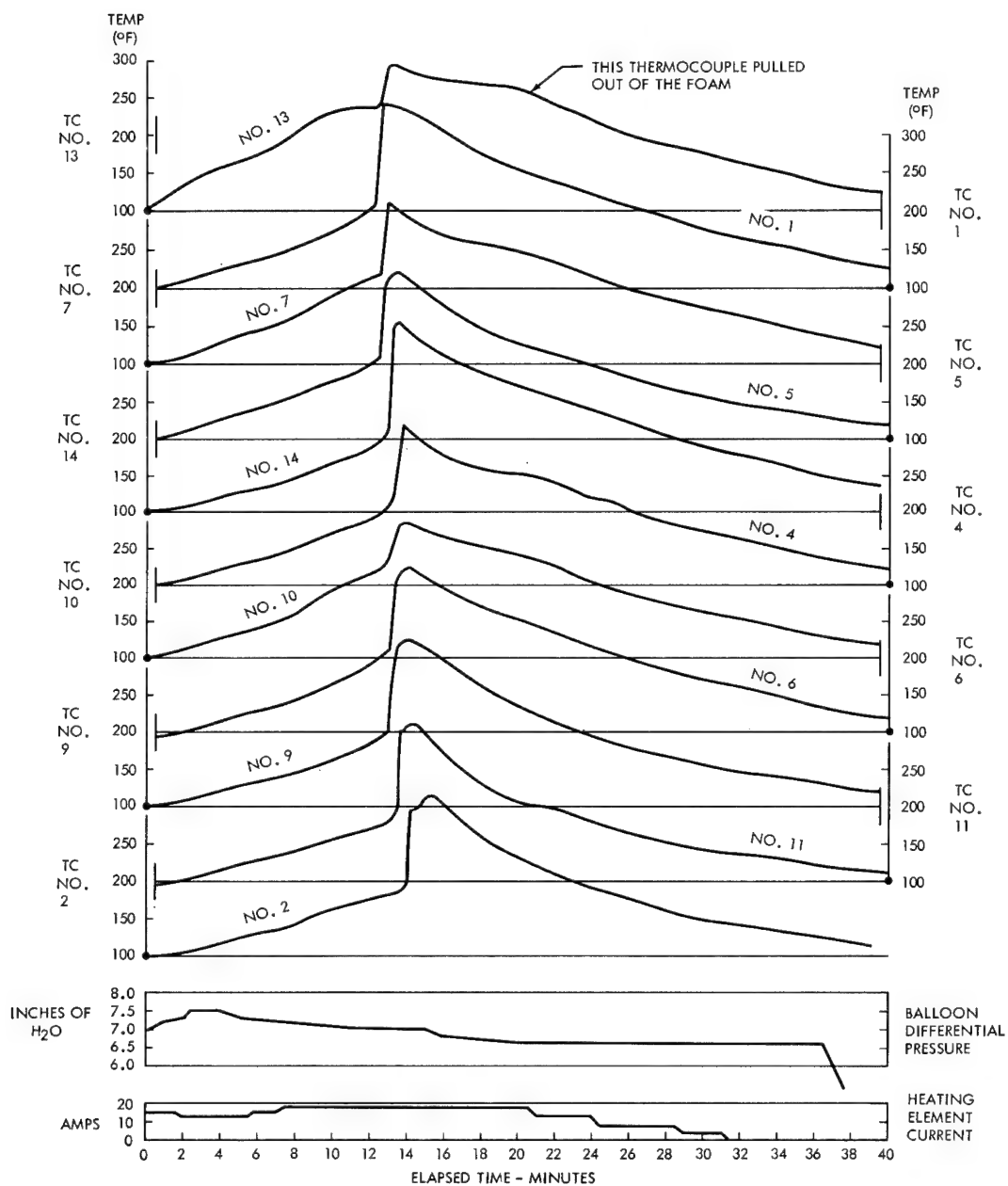


Figure 65. RISEC 918 Mirror - Temperature and Pressure versus Time

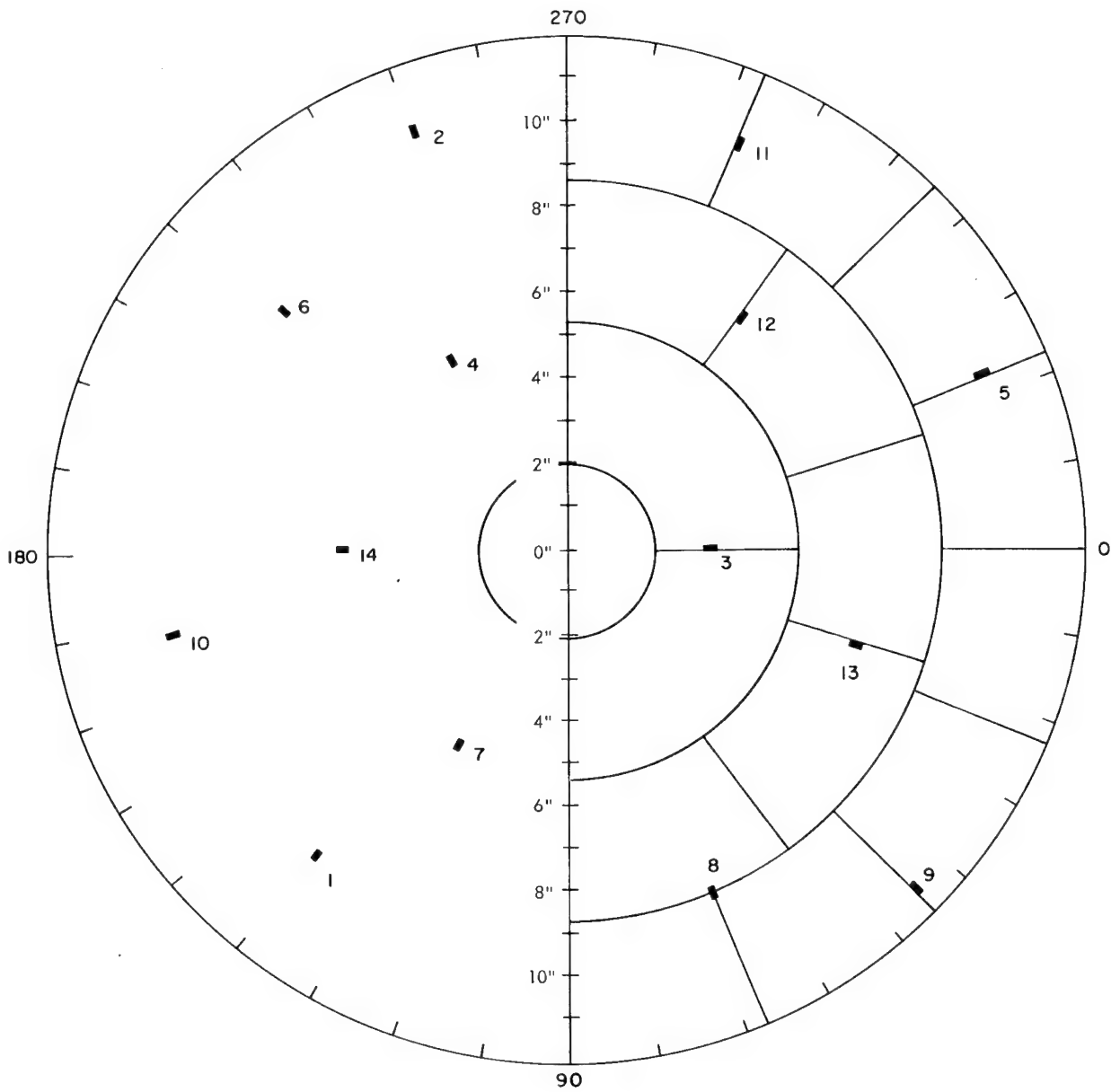


Figure 66. RISEC 918 Mirror - Thermocouple Locations

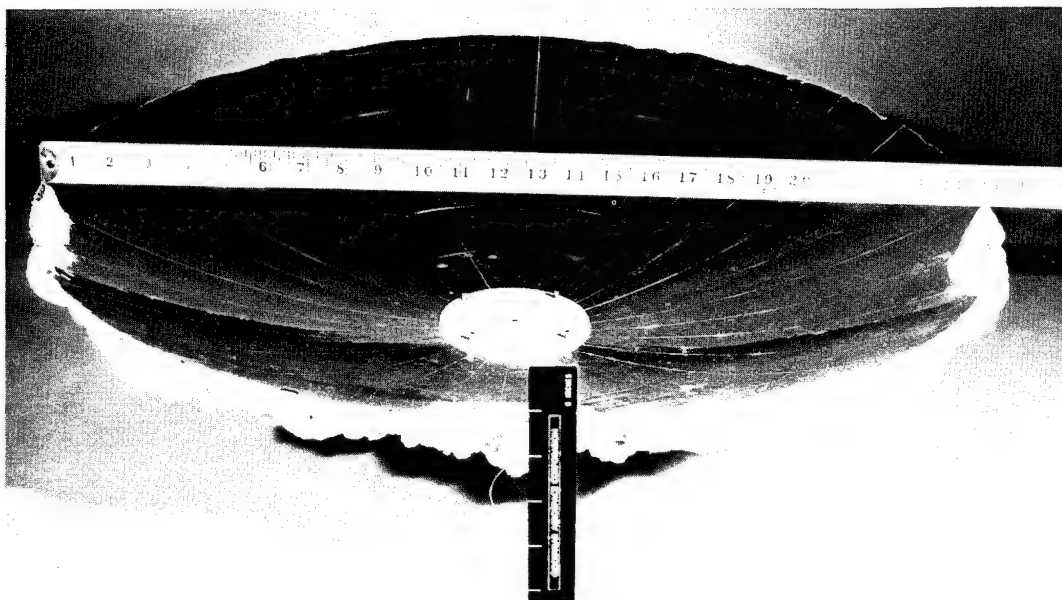


Figure 67. RISEC 918 Mirror - Quarter View of Front Surface

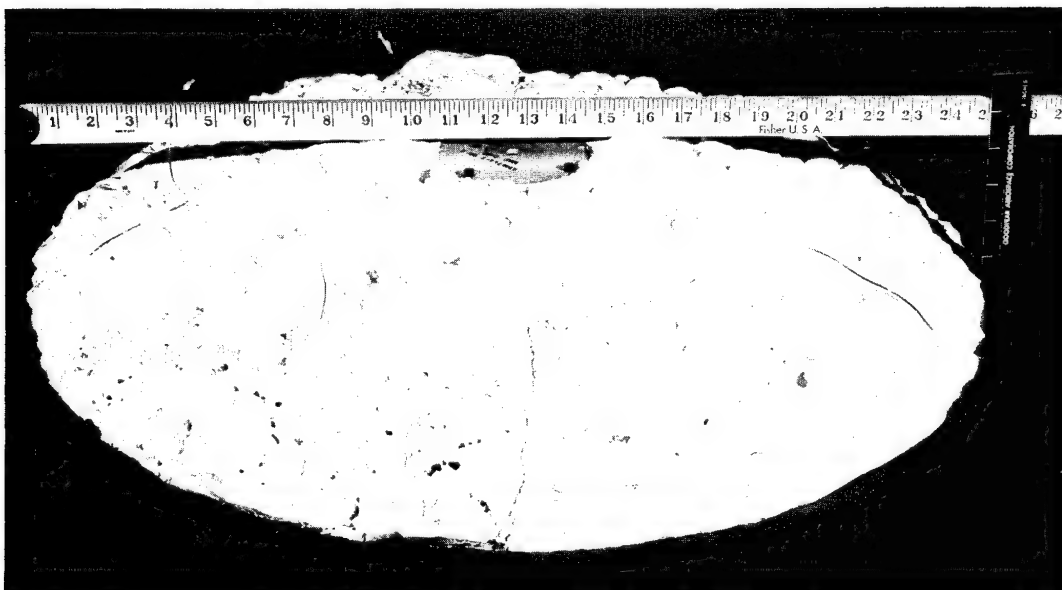


Figure 68. RISEC 918 Mirror - Quarter View of Rear Surface

opened up more than the previous one. (This was the model subjected to the 350°F for a five-minute period.) See Figure 69 for temperature and pressure against time and Figure 70 for location of thermocouples.

Some pits were noted along the seams of the mirror surface (see Figure 84). Figures 71 through 84 show the sequence of rigidizing this mirror.

4. Fourth Run

The fourth run (third mirror RISEC 929) involved a modified back flap design, the two thicknesses of the spread on-foam and a slightly higher internal pressure to improve contour. The back flap consisted of unseamed gores overlapping each other with a fold at the hub and another at the rim to allow for the foam rise. The two thicknesses of foam were applied in the same manner as the preceding run.

The foaming action was normal. Again, due to the back flap, more heat input was required to follow the heat schedule. The variation of thickness was produced according to design. The back flap design appeared satisfactory. See Figure 85 for temperature and pressure against time and Figure 86 for location of thermocouples. Contour measurements indicated that this mirror opened up more (became flatter) than the other two; this was traced to a mounting imperfection. Again, pits appeared along the seams on the mirror surface (more than in the previous mirror). See Figures 87 and 88.

5. Fifth Run

The fifth run (fourth mirror RISEC 1014) involved two thicknesses of foam; a back flap made up of unseamed overlapping gores with folds at the hub and rim to allow for foam rise, and a slightly higher internal pressure. Special care had been taken with the seaming and handling to eliminate any imperfections at the seams and to minimize any markings on the mirror surface.

During the heating period a partial loss of pressure occurred in the mirror envelope. The foaming action was normal. After the setting of the foam, the mirror

SECTION VI

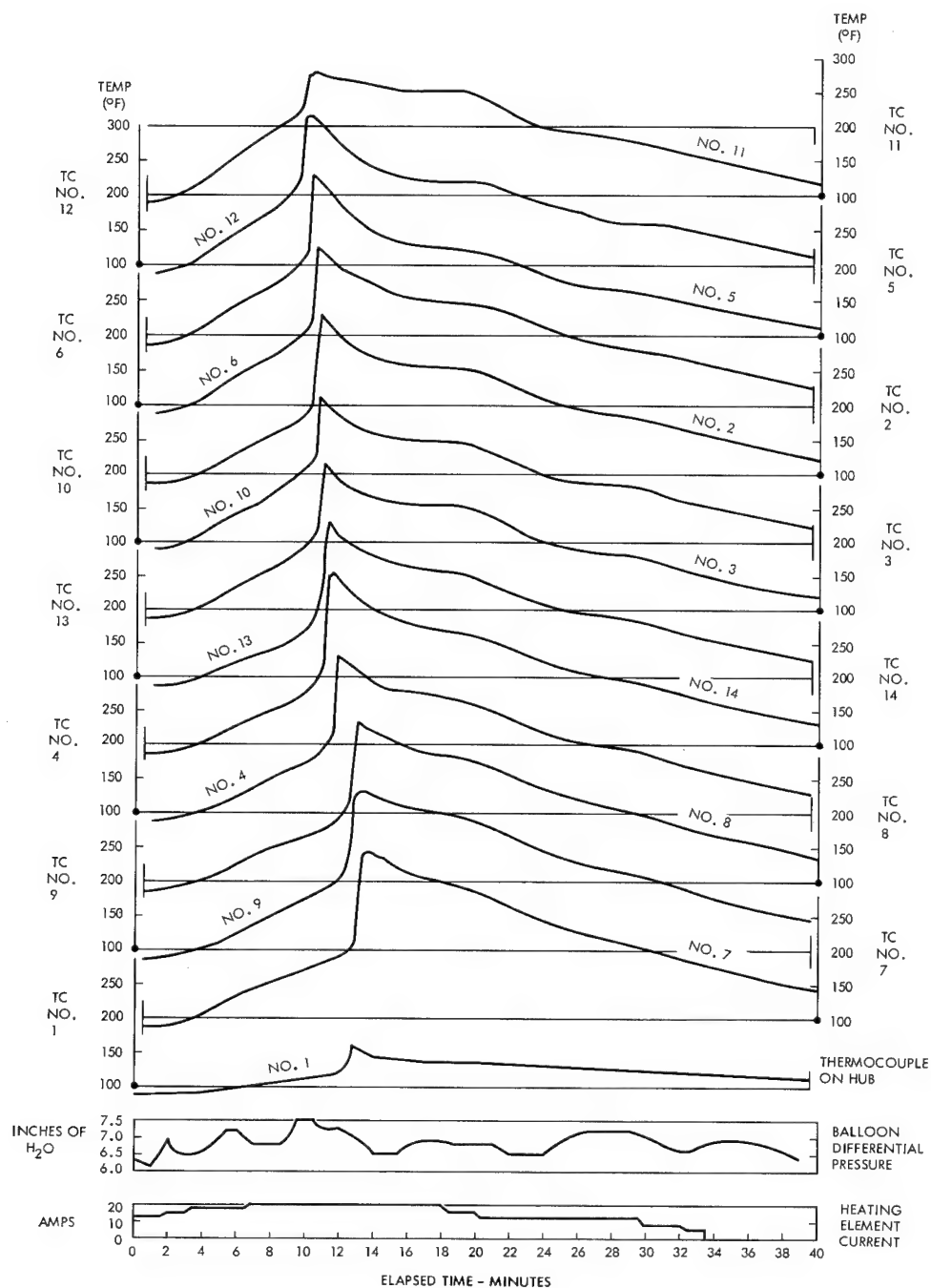


Figure 69. RISEC 924 Mirror - Temperature and Pressure versus Time

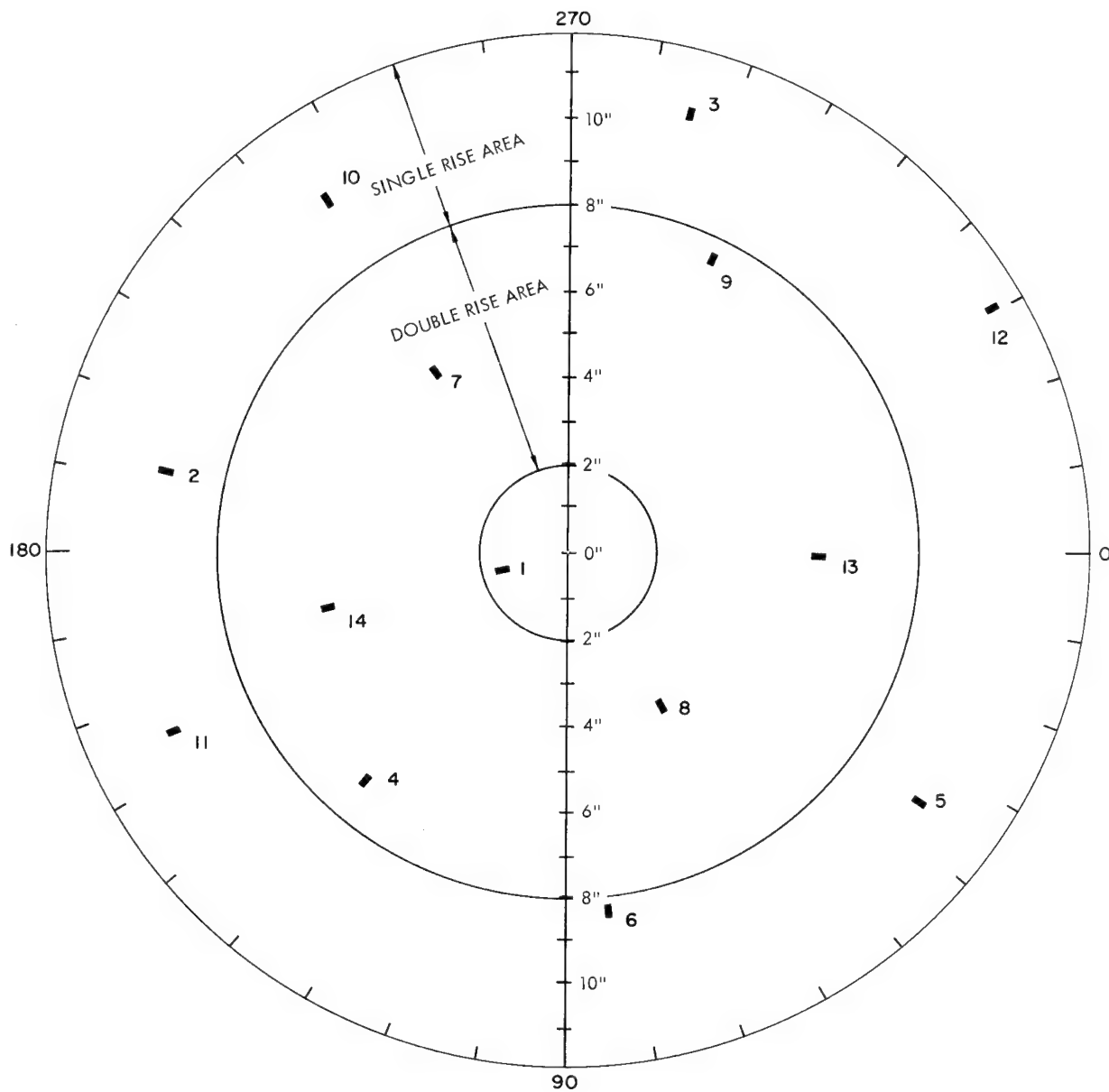


Figure 70. RISEC 924 Mirror - Thermocouple Locations

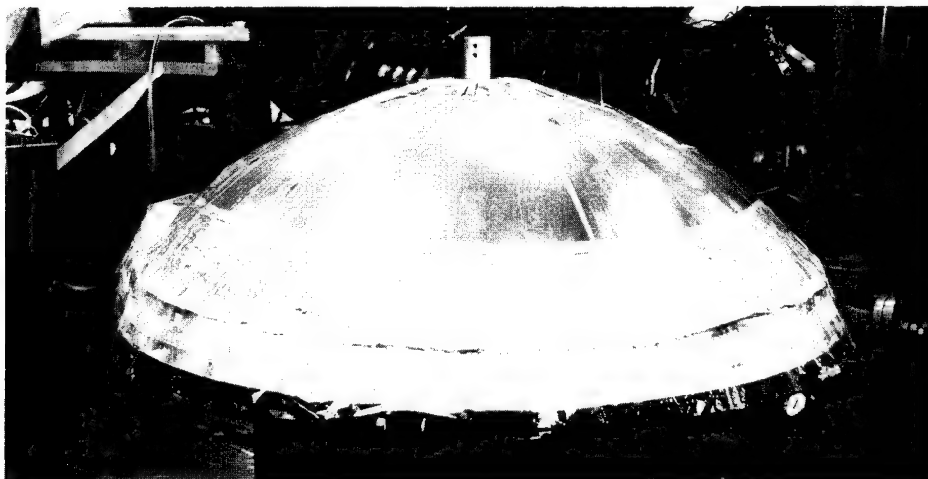


Figure 71. Mirror Inflated with Back Flap Attached

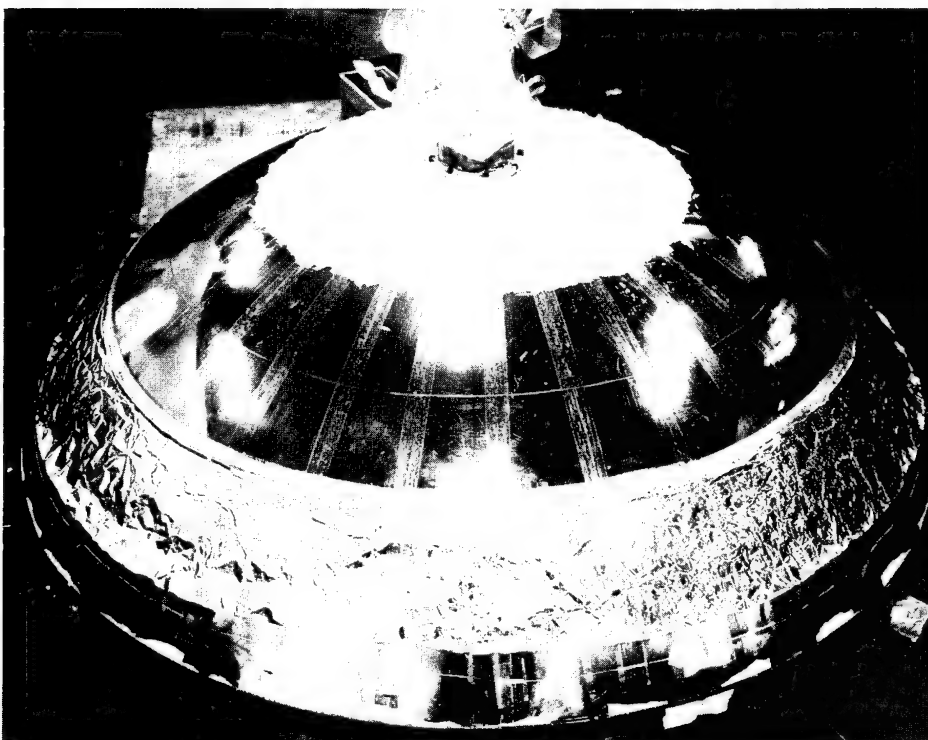


Figure 72. Mirror with Double Thickness Precoat Foam Applied to One-Half Mirror Area

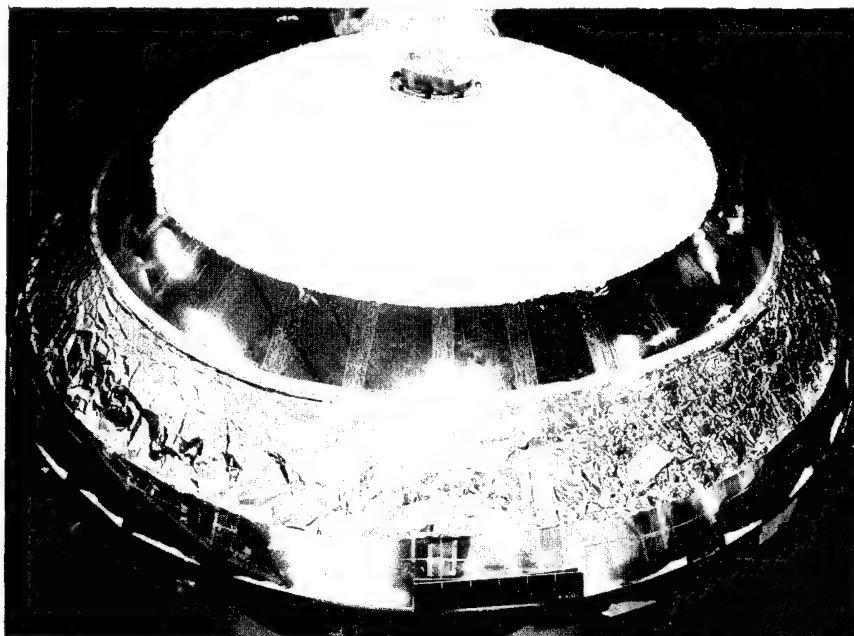


Figure 73. Mirror with Double and Single Thickness Precoat Applied to Mirror Area



Figure 74. Mirror with Back Flap Attached

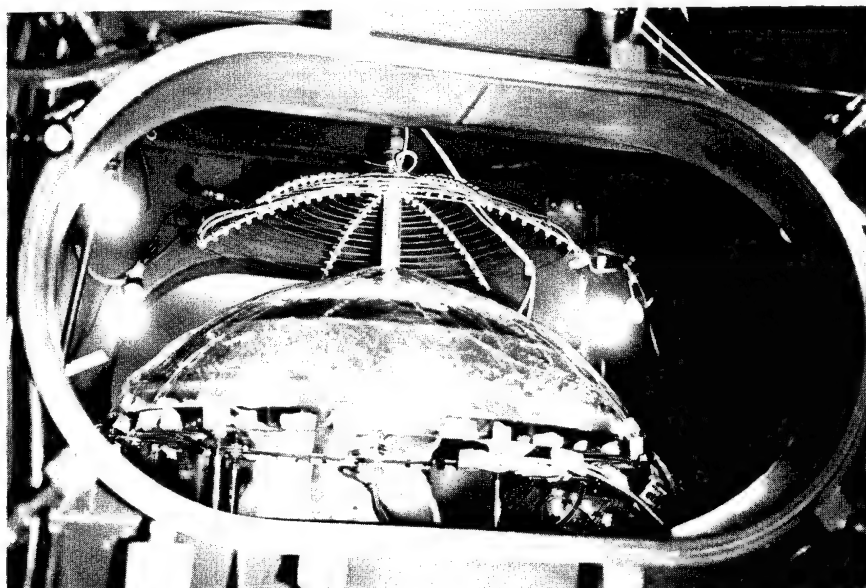


Figure 75. Mirror Set in Vacuum Chamber

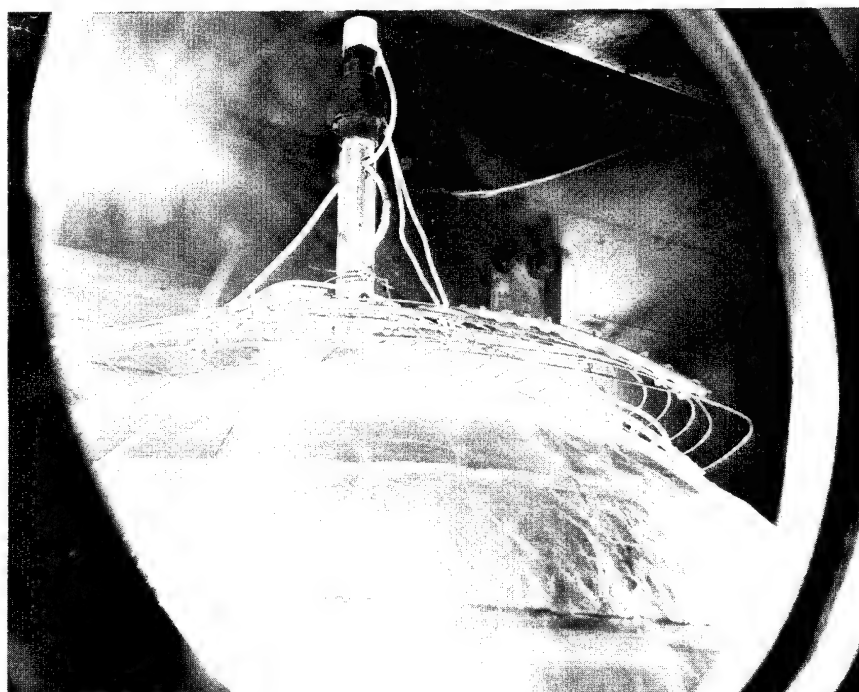


Figure 76. View of Heating Unit in Vacuum Chamber

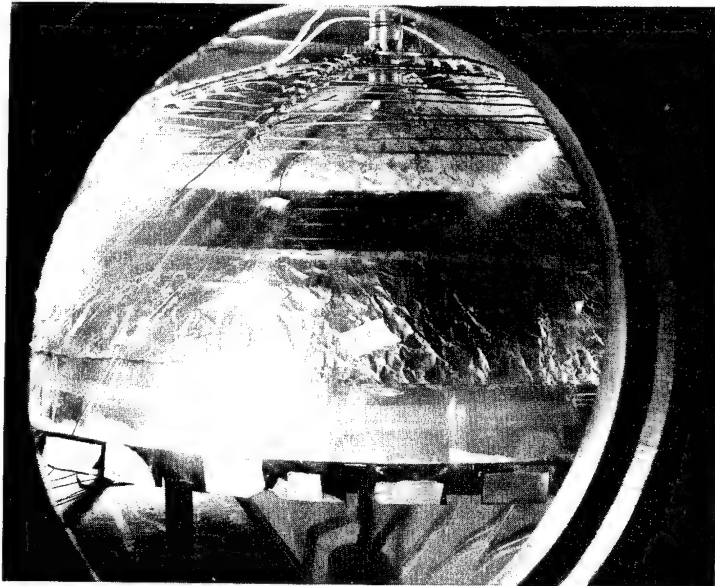


Figure 77. View of Surface in Vacuum Chamber with Heating Initiated

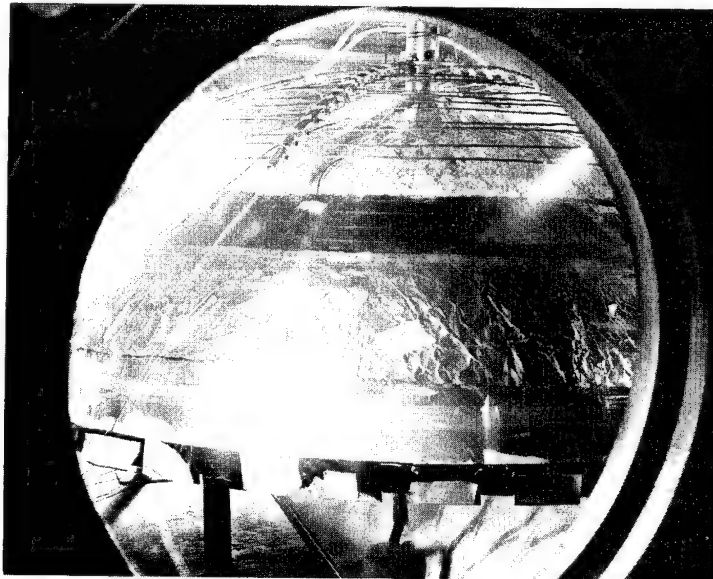


Figure 78. Foaming Action Started

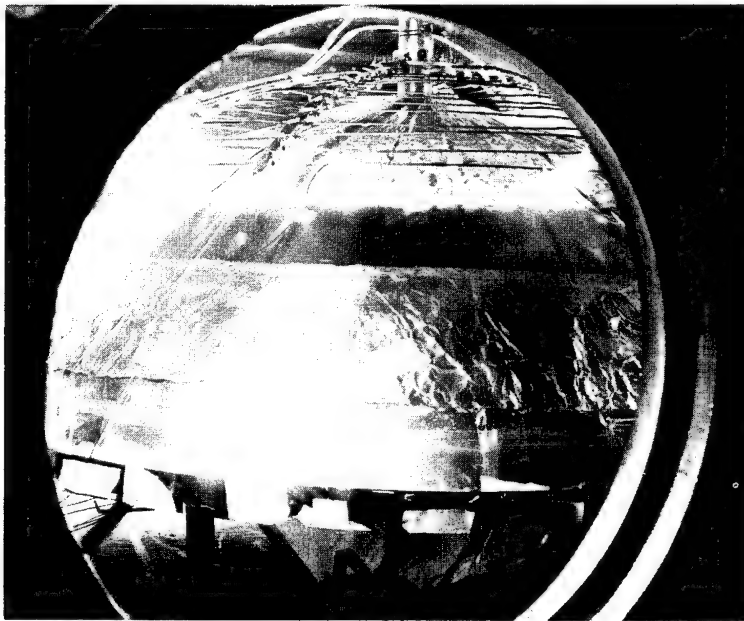


Figure 79. Foaming Progressing

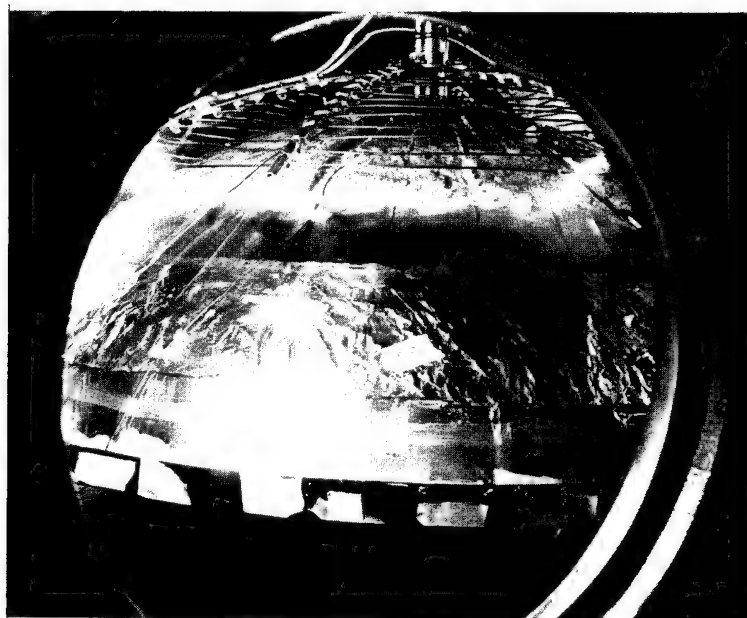


Figure 80. Foaming Completed

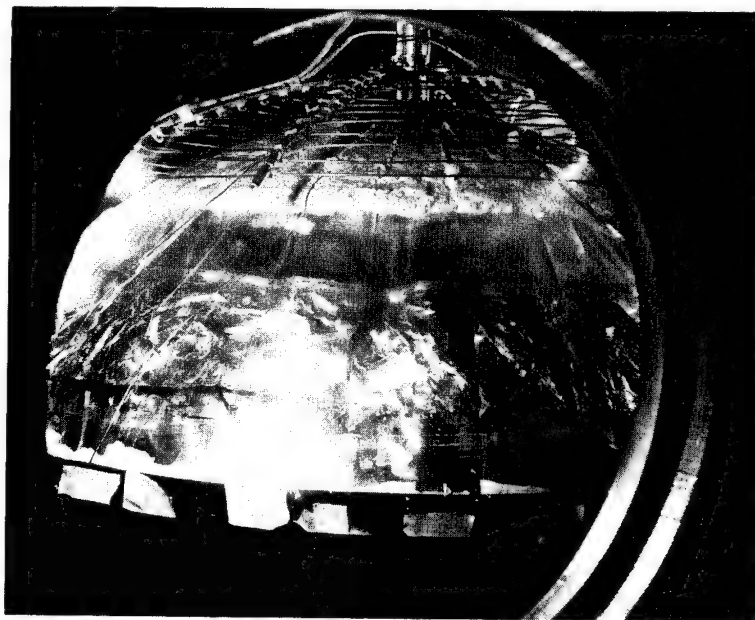


Figure 81. Hot Wire Burn-Off Completed

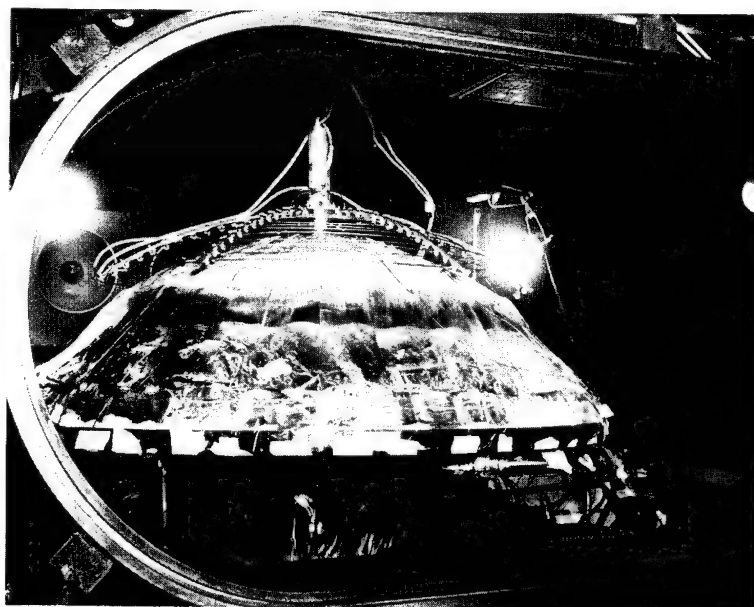


Figure 82. Vacuum Released - Chamber Opened

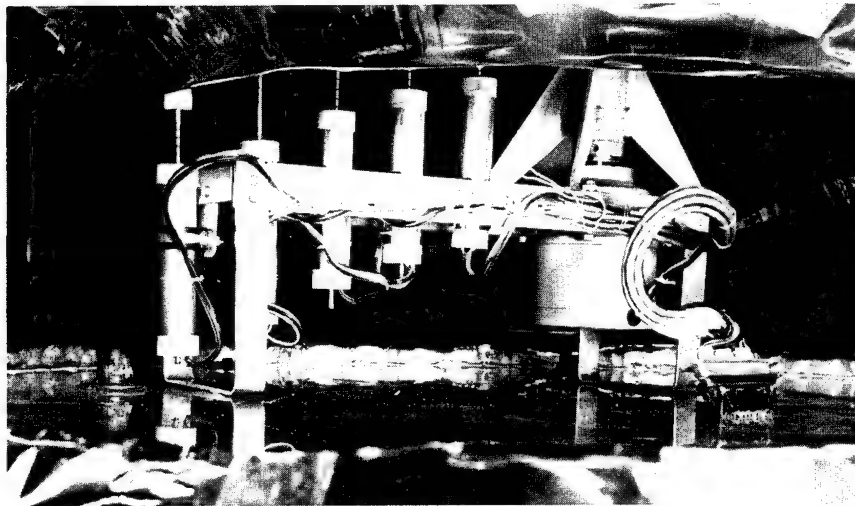


Figure 83. View of Contour Measuring Apparatus

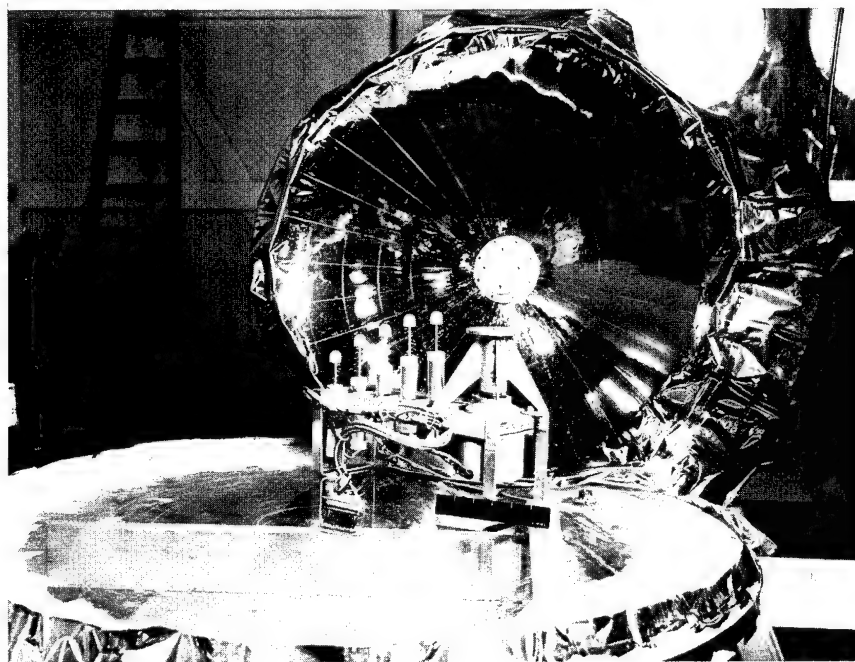


Figure 84. Mirror (Cut Free), Contour Measuring Apparatus, and Base Plate

SECTION VI

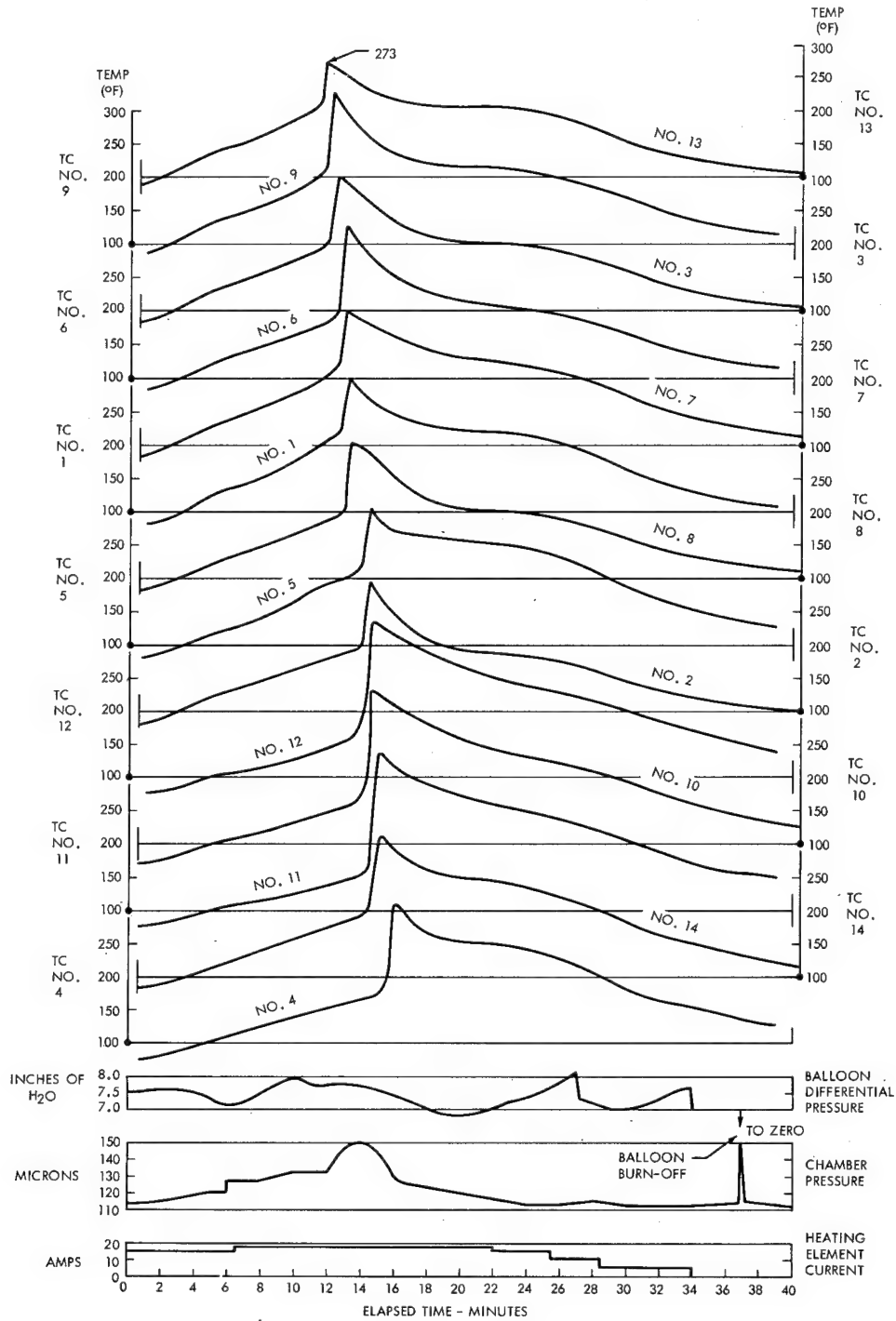


Figure 85. RISEC 929 Mirror - Temperature and Pressure versus Time

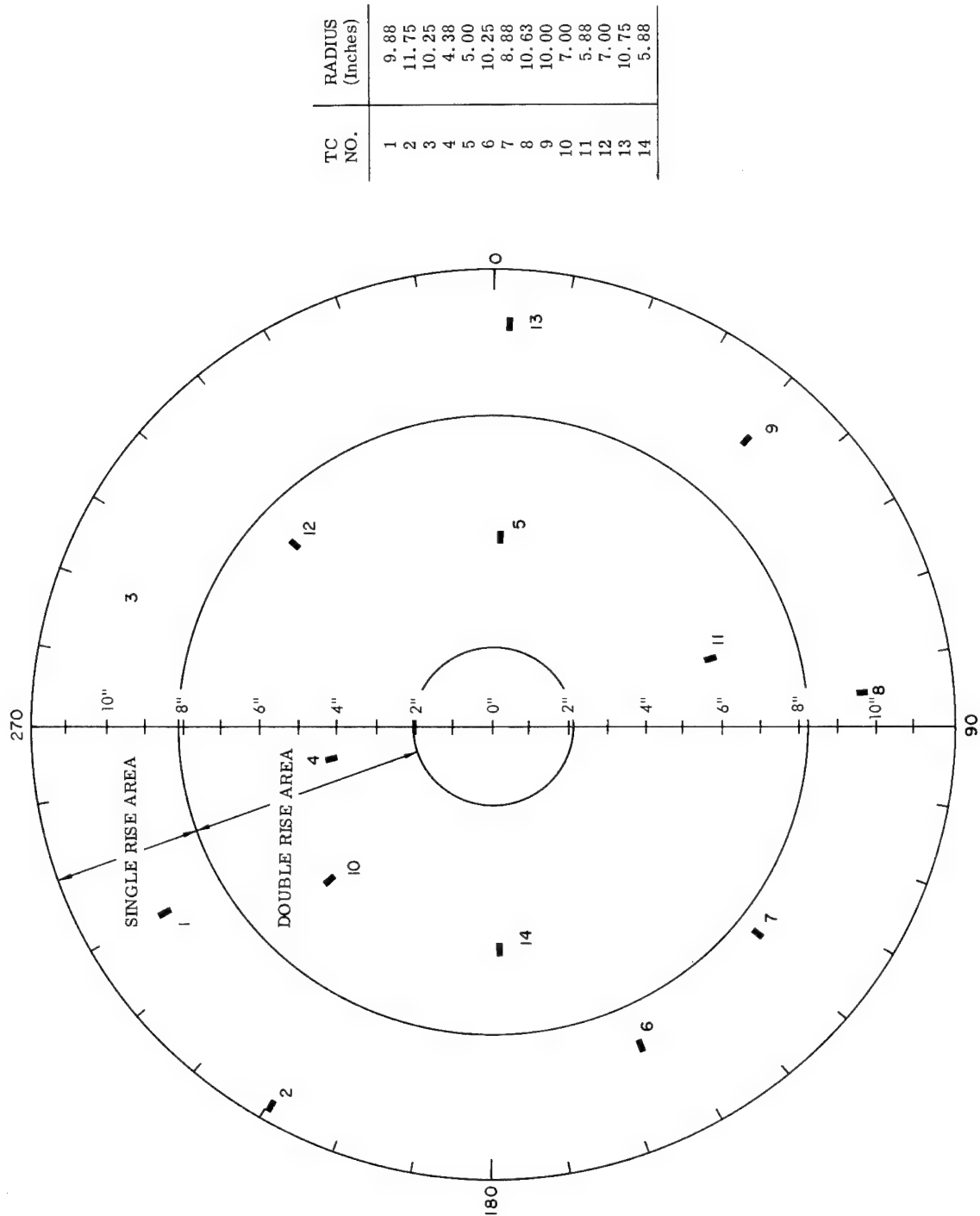


Figure 86. RISEC 929 Mirror - Thermocouple Locations

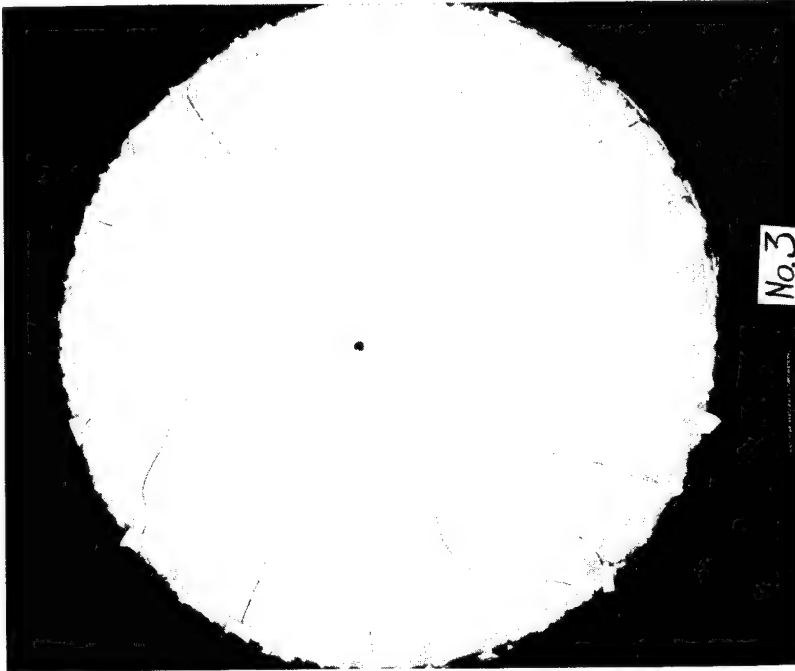


Figure 88. RISEC 929 Mirror - Rear View

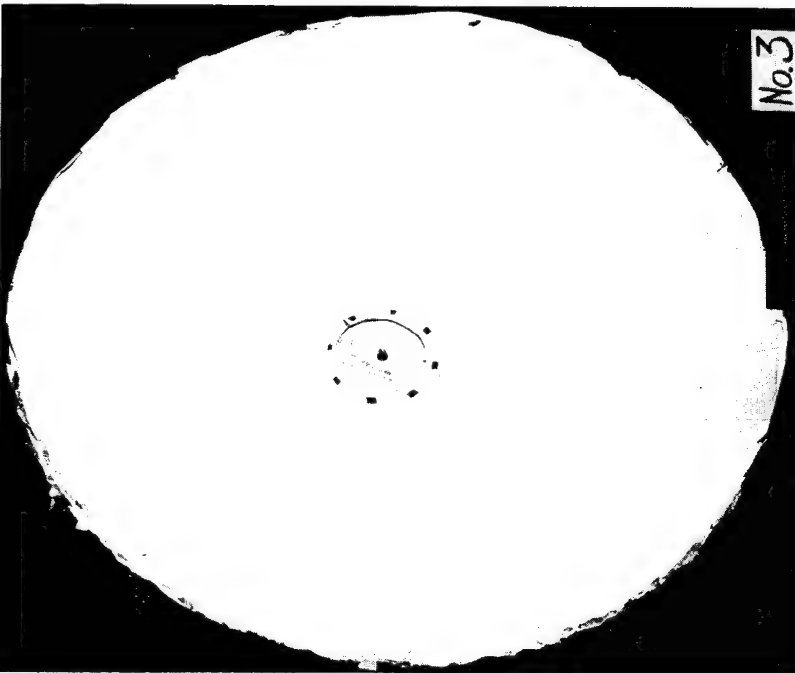


Figure 87. RISEC 929 Mirror - Front Face

SECTION VI

envelope again began to retain a normal pressure. See Figure 89 for temperature and pressure against time and Figure 90 for thermocouple locations. Contour measurements indicated that a good contour was obtained. Seam separation occurred in at least two gores. The seams revealed the most excessive pitting of any of the mirrors rigidized. (See Figures 91 and 92.)

C. CONTOUR MEASURING TOOL

A contour measuring tool for the measurement of a two-foot model solar concentrator was fabricated. The contour measuring instrumentation is similar to that described in appendix H (also see Figures 83 and 84). There are five Linear Variable Differential Transformers (LVDT's) located at specific radii along a rotating arm. As this arm rotates through 360 degrees, the LVDT's measure the difference between the parabolic shape of the mirror and a true parabola. Prior to measuring the mirror, these LVDT's are calibrated against a tool that is machined to the desired parabolic shape. Power for these transformers and their output is controlled by individual demodulators mounted in the control console. The output of these demodulators in turn is fed to an oscillograph for continuous recordings of the deviations. Rotation of the measuring arm is controlled manually at the control console, or semi-automatically by limit switches. Details of circuitry and operation are described in Appendix H.

D. CONTOUR MEASUREMENTS

Contour sweeps were exercised at the following stages of the rigidizing process:

<u>Run No.</u>	<u>Rigidizing Stage</u>
1	Membrane pressurized in atmosphere
2	Membrane pressurized in evacuated environment
3	When precoat temperature is approximately 165°F
4	During the foaming process (temperature \approx 350°F)

SECTION VI

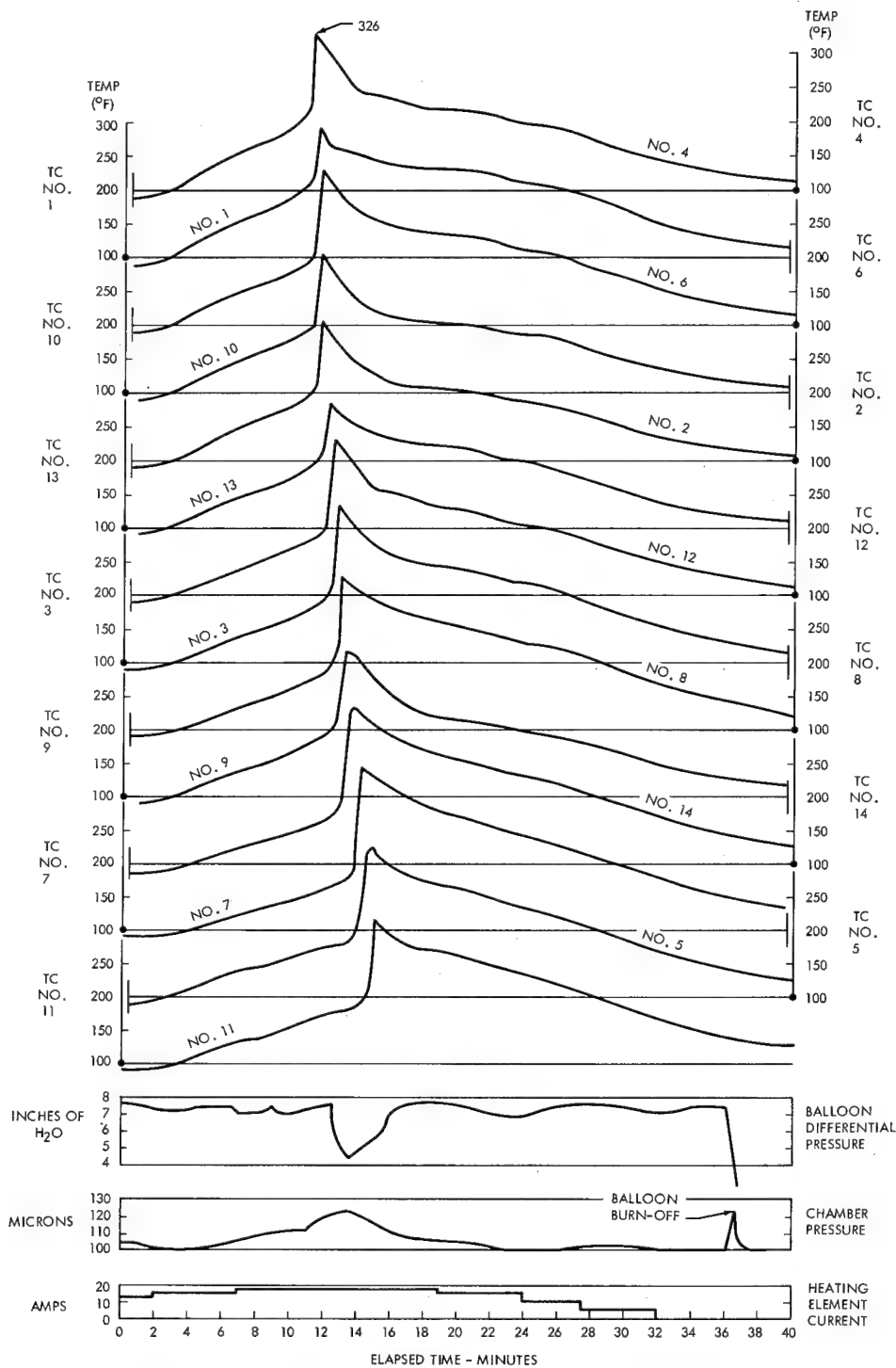


Figure 89. RISEC 1014 Mirror - Temperature and Pressure versus Time

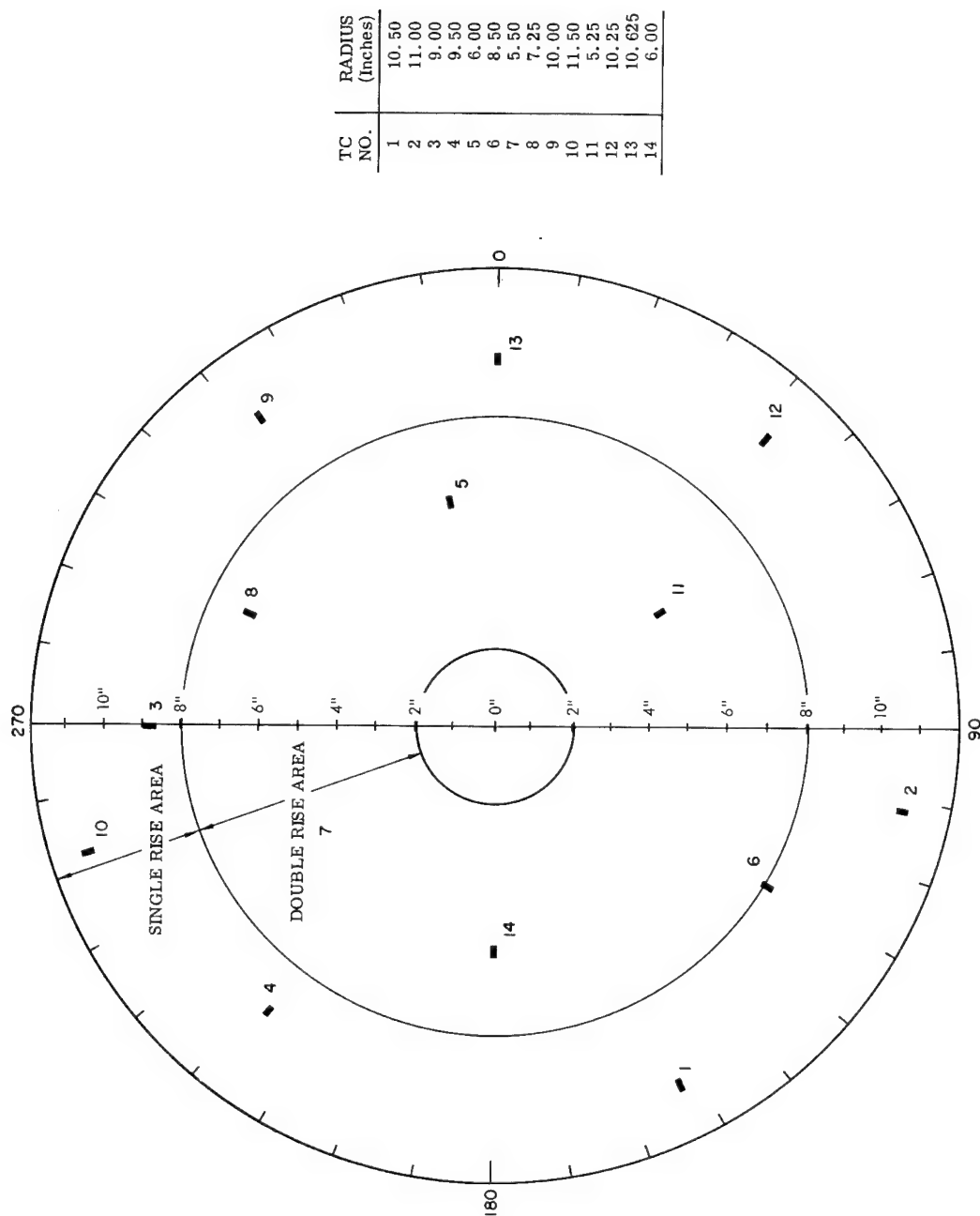


Figure 90. RISEC 1014 Mirror - Thermocouple Locations

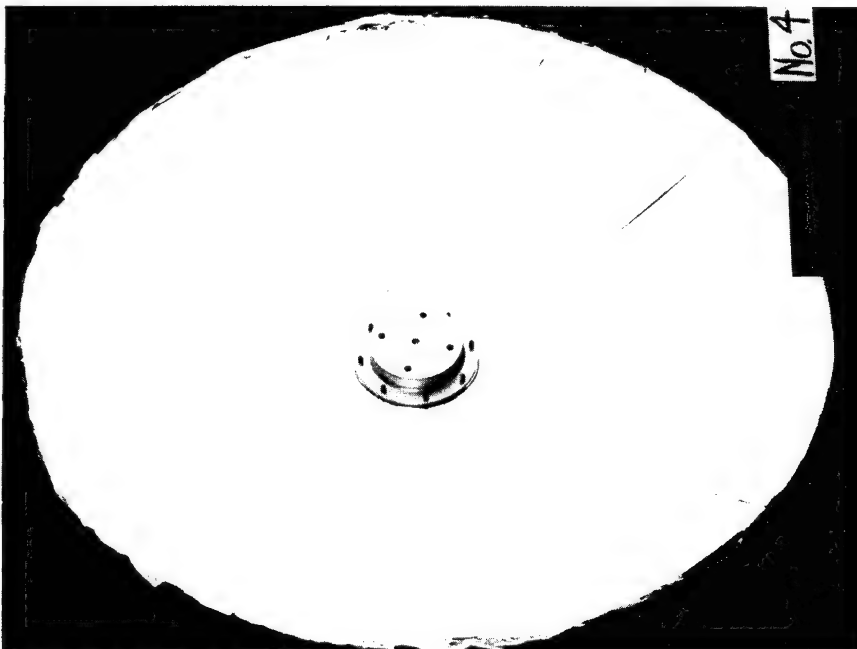


Figure 91. RISEC 1014 Mirror - Front Face

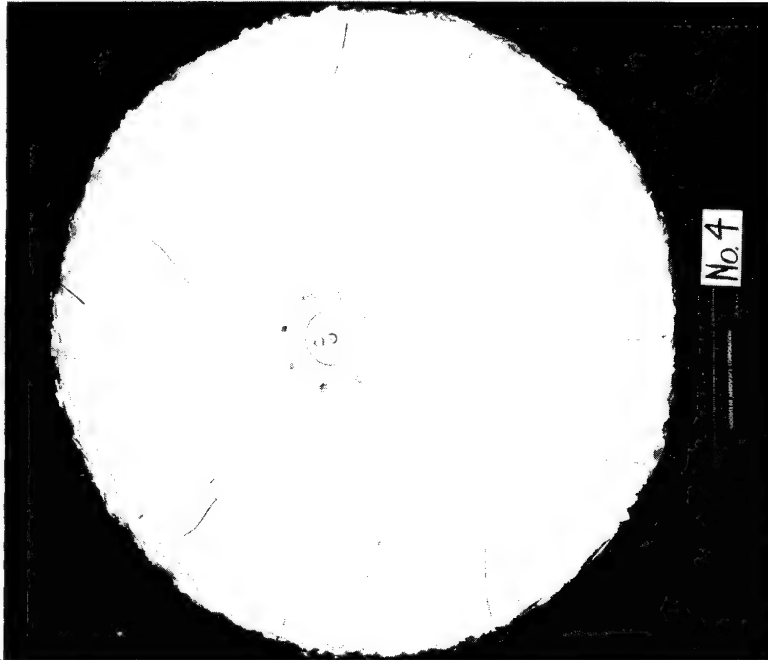


Figure 92. RISEC 1014 Mirror - Rear View

SECTION VI

<u>Run No.</u>	<u>Rigidizing Stage</u>
5	During cooling process (temperature $\approx 200^{\circ}\text{F}$)
6	During cooling process (temperature $\approx 150^{\circ}\text{F}$)
7	After equalization of pressure (vacuum)
8	After release of vacuum

This procedure enabled all necessary changes in contour to be recorded. These variations were analyzed and adjustments made to perfect the contour.

Runs No. 2 and 8 for each mirror were plotted on polar graphs, Figures 93, 94, 95, and 96. Cross sections of the paraboloid were measured at 0, 48, 96, 132, 180, 228, 276, and 312 degrees. Measurements were made at radii of 4.00, 6.09, 8.06, 10.18, and 12.18 inches.

On close inspection of the data it is found that mirror No. 1 (RISEC 918) has the most accurate final geometric contour. Its polar plot (see Figure 93) shows a balance in positioning, an average deviation of less than 0.1 inch and a maximum deviation of slightly more than 0.1 inch. From the hub through the 10.18 inch radius, the deviation is almost entirely within 0.1 inch. Maximum deviation appears at the rim. Though not significant, it may be noted that the side with the minimum deviation was that with the "pressed" precoat material.

Next in accuracy of final geometric contour was mirror No. 4 (RISEC 1014). Its polar plot (Figure 96) shows a balance in positioning, an average deviation of less than 0.1 inch, and a maximum deviation of less than 0.2 inch. Unlike mirror No. 1, mirror No. 4 had good adherence to contour at the hub and at the rim; its maximum deviation was at the 8.06 and 10.18 inch radii. This may have been caused by the seam failures.

On mirror No. 2 (RISEC 924) an LVDT malfunction was experienced on the rim (12.18 inch radius) contour indicator. Measurements from only four radii were available.

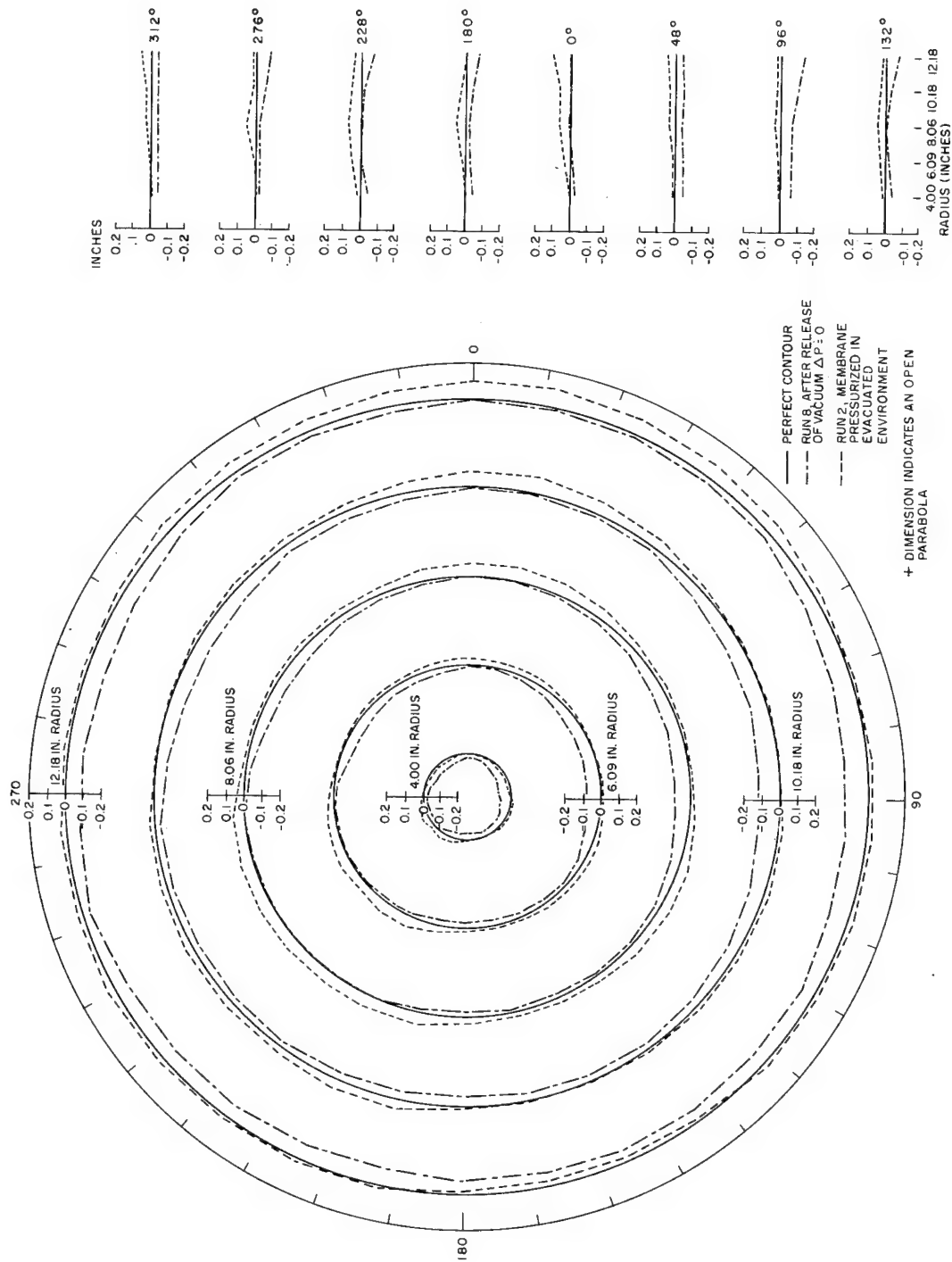


Figure 93. Polar Plot of RISEC 918 Mirror

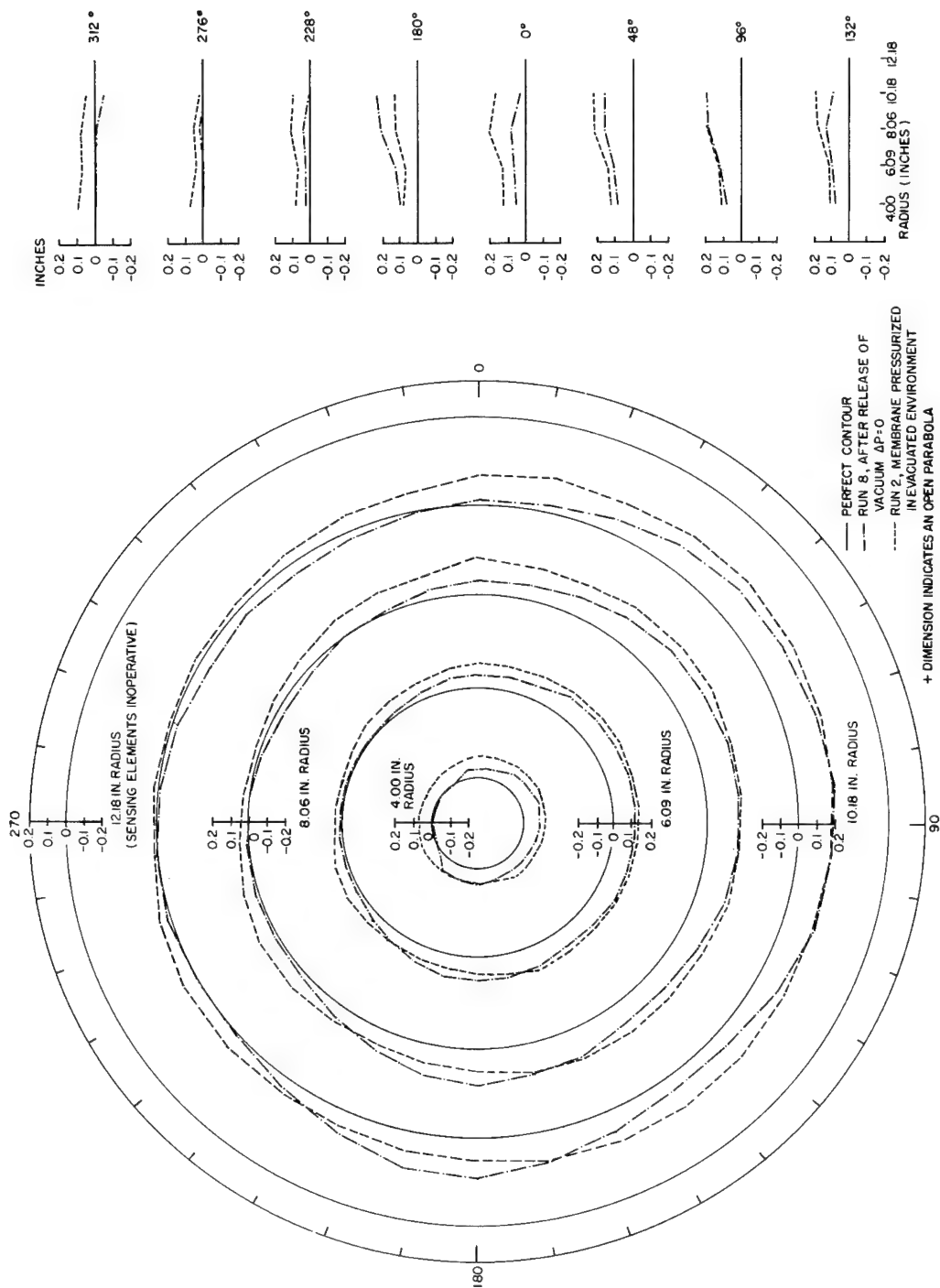


Figure 94. Polar Plot of RISEC 924 Mirror

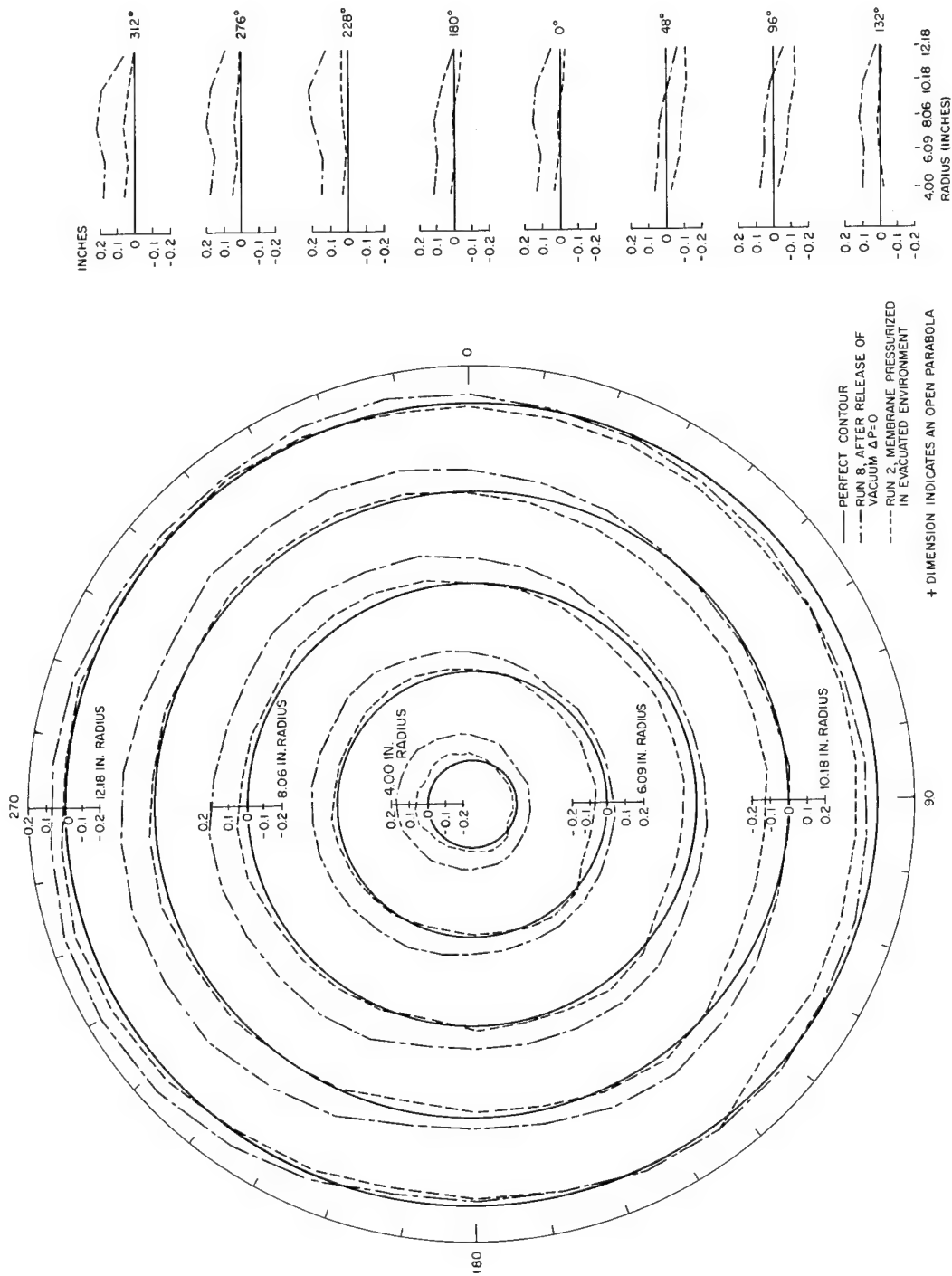


Figure 95. Polar Plot of RISEC 929 Mirror

SECTION VI

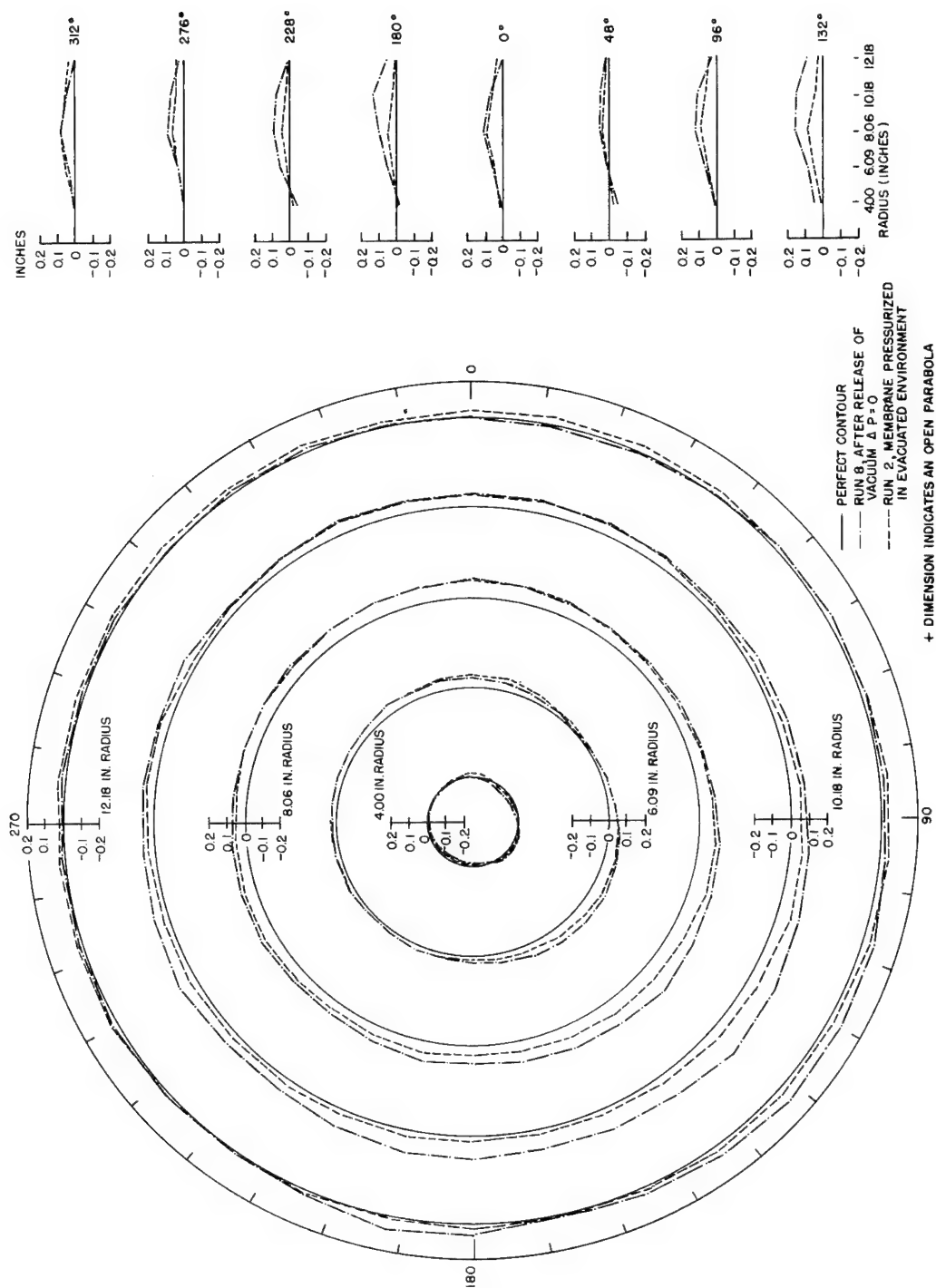


Figure 96. Polar Plot of RISEC 1014 Mirror

The polar plot (Figure 94) indicated a definite unbalance of positioning, average deviation was greater than 0.1 inch, and maximum deviation measured was 0.2 inch. Indications are that the rim contour indicator would have measured deviations greater than 0.2 inch. Minimum deviations appeared at the hub and maximum deviations appeared at the rim.

Mirror No. 3 (RISEC 929) resembled mirror No. 2. Its polar plot (Figure 95) indicates an unbalance in positioning, an average deviation of approximately 0.1 inch, and a maximum deviation of greater than 0.2 inch. Minimum deviations appear at the rim and maximum deviations appear at each of the shorter radii.

A number of other contour measurements at various stages of the rigidizing process are included in Appendix G. Some observations from these data are:

- (1) The contour pattern changes to a more open paraboloid as the temperature is increased and to a more closed paraboloid as the temperature is decreased (refer to Figures G-1, G-2, G-4, and G-5).
- (2) Maximum change is between contour at exotherm and final contour.
- (3) A similar pattern is observed at each of the five radii.
- (4) A closing of the paraboloid is experienced in changing from an equalized pressure in vacuum to an equalized pressure at atmosphere (Appendix G, Figure G-9).

Circumferential bowing in the gores is caused by a difference in strain of the material at the seams and the material between the seams. (Some bowing could also result from the inaccurate cutting of gores, but this is usually very small and any large values would be readily detected). The critical period where the conditions for bowing are greatest is during the exotherm, when the H-Film is exposed to a temperature of $\approx 350^{\circ}\text{F}$. At this increased temperature the tensile strength decreases and the elongation increases (see Reference 9). The pressure, however, is held constant.

SECTION VI

Shortly after the rise in temperature, the foam begins to set. At this time maximum strain is the resulting effect on the gore section and some bowing may be retained after rigidizing. A minimum of bowing may be obtained with a reduction in pressure during exotherm.

Maximum deviations between center of gore and center of seam were found to be 0.030 in. (at 8 in. radius). The average deviation was 0.010 inch. These average and maximum values of bowing in the gores tested (58 values in mirror No. 1 and 55 values in mirror No. 4) indicate a negligible geometric error due to the bowing effect. In all the models tested, the foremost discrepancy was that produced by the misalignment in positioning of the mirror with respect to the contour measuring apparatus. Next and quite small was the discrepancy of pressure control which caused oversizing and undersizing. Last and least was the discrepancy of gore bowing between the seams.

Perhaps the reasons why mirror No. 1 described the most accurate contour are that (1) it was accurately positioned (mirrors No. 2 and 3 were not accurately positioned with respect to the hub, and although their contours may actually be more accurate than indicated here, their misalignment was a factor in their contour measurements); (2) the seams were free from any pitting or separations (mirrors No. 2, 3, and 4 experienced pitting at the seams and mirror No. 4 experienced seam separation at three places which certainly would affect the contour).

Pitting in the seams first appeared in mirror No. 2. The cause was expected to be in the fabrication process. Then when mirror No. 3 was fabricated the temperature of the heat irons (used in applying tapes) was checked and each seam was made at the same rate. The pitting appeared again on mirror No. 3. Tapes were then subjected to high vacuum and to high vacuum with heat combined but no pitting appeared. For the fabrication of mirror No. 4 the adhesive was prepared 24 hours in advance to minimize any aging effect; the tapes were dried at 150°F to remove

all solvents; and special care was taken to keep it free from dust and fingerprints. Even after all this, pitting appeared again in mirror No. 4 after rigidizing. The cause of the pitting is not known. Isolation of each of the variables in each of the steps of the seaming process will be required to determine the cause.

SECTION VII. PROBLEM AREAS

The problem area encountered in the course of this program was primarily the outgassing spurt during the exotherm stage of the rigidizing process.

The outgassing produced by the exotherm stage of the rigidizing process is such that it affects chamber size and pumping capability. It has been determined that 15 percent (by weight) of the precoat material evolves into a gas during the foam rigidizing process. Most of this occurs within a short time period (four minutes on a 2-foot model). A survey of the vacuum facilities throughout the country indicates that some loss of vacuum would occur with any currently available chamber in the rigidizing of a 10-foot diameter solar concentrator. The retention of a high vacuum condition throughout the rigidizing process is a difficult and expensive endeavor. A practical approach would be to establish a limiting pressure rise based on the pumping capacity of the available vacuum chamber facility.

The simulation of the zero g condition to demonstrate foam rigidizing in space is a difficult and expensive undertaking with contemporary facilities. A practical approach to this problem is to foam rigidize a mirror face up and another face down simulating a -1 g and a +1 g condition. However, this approach is limited in the degree to which it reveals the actual behavior of the predistributed foam during the rigidizing process.

SECTION VIII. CONCLUSIONS AND RECOMMENDATIONS

A. CONCLUSIONS

On the basis of the work accomplished in this 14-month effort the following conclusions were reached:

- (1) A workable predistributed foam material capable of rigidizing solar concentrators in space has been developed. With the materials available and the known techniques and procedures used in blending them to satisfy the space requirements, this predistributed foam represents the optimum material known.
- (2) The optimum membrane material to be used with this predistributed foam is H-Film. Because of the peak temperature that the film experiences in the rigidizing process, Mylar may distort and is not desirable for a solar concentrator application.
- (3) Due to the tackiness of the predistributed foam, a back flap would be required as a separator in packaging. The overlapping gore type described in this report is the optimum back flap arrangement conceived to date.
- (4) The predistributed foam can be initiated in space with selective surfaces.
- (5) The foam product has useful structural strength and stiffness in a vacuum condition at temperatures approaching 240° F for densities greater than 3 lb/ft^3 . This material is primarily brittle, but a small amount of ductility is present at temperatures in excess of 100° F.

SECTION VIII

- (6) The limited amount of test data indicates that the tensile, compression, and shear properties (for foams having densities between 3 and 5 lb/ft³) increase with increasing density and decrease with increasing temperature.
- (7) The bond of the foam to the H-Film with temperature and ultraviolet effects is more than adequate.
- (8) The thermal coefficient of expansion tests for the foam were somewhat inconclusive, but they did indicate a relatively small value for this function. The tests also indicated that the thermal expansion value decreases with increasing density.

B. RECOMMENDATIONS

The work accomplished in this effort has opened up new areas of consideration for the improvement of predistributed foam and for broader developments in the application of this type of foam in large flight-type solar concentrators. In regard to these objectives the following recommendations are made:

- (1) That an effort be made to improve the present predistributed foam material. New materials and newly developed techniques and procedures offer a high potential for an improved predistributed foam.
- (2) That the present foam material be used to rigidize larger solar concentrators.
- (3) That various initiator systems be investigated.
- (4) That packaging and deployment systems be investigated.
- (5) That a greater effort be made in the development of an H-Film adhesive. The limited effort undertaken here still left discrepancies in the seams.

- (6) That a greater effort be made in test data interpretation. Due to the nature of the predistributed foam material, its inhomogeneity, and its large cells, test data could be misinterpreted.
- (7) That a more comprehensive test program be undertaken on the foam material before a space flight is attempted.

REFERENCES

1. Smith, P.A.S., "The Curtius Rearrangement," in Organic Reactions, Vol. 3, Chap. 9; John Wiley and Sons, New York; 1946.
2. Journal of Polymer Science, Part A2, 1147; 1964.
3. Dark, Gemimhardt, and Saunders, I & EC Product Research and Development, 2, 194-199; 1963.
4. GER-11529, Solar Reflector Foaming Technology Development - Part 2 - Foam Materials Properties, Goodyear Aerospace Corporation, Akron, Ohio, May, 1964.
5. GAP-2003, Proposal for Rigidized Inflatable Solar Energy Concentrators, Goodyear Aerospace Corporation, Akron, Ohio; 10 April 1963.
6. Stengard, R. A., Properties of Rigid Urethane Foam, E. I. duPont de Nemours and Co., Wilmington, Del.; 21 June 1963.
7. Timoshenko, S. and Goodier, J. N., Theory of Elasticity, Second Edition, McGraw Hill Book Co., Inc., 1951.
8. Fisher, F. R., Foamed Plastics, U.S. Dept. of Commerce, Office of Technical Services, PD 181576, Washington, D.C.; 1963.
9. Tatum, W.E.; Amborski, L.E.; Gerow, C.W.; Heacock, J.F.; and Mallouk, R.S.; H-Film - DuPont's New Polyimide Film, AIEE T-153-3, presented at the Electrical Insulation Conference, 17 September 1963, at Chicago, Illinois.

APPENDIX A. TEMPERATURE ANALYSIS TO PRODUCE REQUIRED HEAT SCHEDULE BY SELECTIVE SURFACES

A thermal analysis was performed to evaluate the precoat concept of foam rigidizing solar concentrators. Under this concept the following sequence of events is desired:

- (1) The concentrator with gas bag is deployed at approximately room temperature. A layer of precoat is between the front and back flaps of the concentrator.
- (2) The paste temperature is to be increased by thermal radiation absorption to 195°F within ten minutes. At this temperature a self-sustaining chemical reaction is initiated within the paste.
- (3) The paste will leaven into a foam in approximately two minutes. The chemical energy released by this process will increase the foam temperature to approximately 350°F.
- (4) The foam is to be maintained at a temperature in excess of 150°F and preferably near 350°F for a minimum of fifteen minutes to allow stabilization and rigidization of the foam.

The following system parameters are established or assumed for this analysis:

Orbital Attitude	300 Miles
Orientation	Free to have back or front side of solar concentrator facing sun
Density: precoat	75 Lbs/Ft ³
foam	6 lbs/Ft ³
Thickness: precoat	0.04 Inch
foam	0.5 Inch

APPENDIX A

Specific heat: precoat foam	0.45 BTU/Lb-°F
Thermal Conductivity:	
pressurized foam	0.26 BTU-In/Hr-Ft ² -°F
evacuated foam	0.08 BTU-In/Hr-Ft ²
Absorptance of Reflector Surface	0.115
Emittance of Reflector Surface	0.192
End cap only:	
(Gas Bag) Material	Mylar
Reflectance	0.05
Absorptance	0.10
Solar Transmittance	0.85
Emittance and Infrared Absorptance	0.60
Infrared Transmittance	0.35

The vehicle receives thermal radiation as solar energy directly from the sun, solar energy reflected from the earth, and planetary radiation. These terms may be computed from the system parameters. Figures A-1 and A-2 present these heat fluxes on the concentrator external and internal surfaces, the latter with the gas bag attached. A slight variation of heat fluxes and temperatures will occur with radial distance from the hub; for simplicity all values presented herein are average values over the indicated surfaces.

Radiation equilibrium temperatures are more readily computed than transient temperatures and will indicate the types of coatings and orientations required. Table A-1 presents a summary of these computations.

The following surface coatings were considered:

Aluminized Mylar	$\alpha = 0.12, \epsilon = 0.05$
Alodine	$\alpha = \epsilon = 0.35$

Black surface	$\alpha = \epsilon = 0.9$
Cr-Ni-V	$\alpha = 0.94, \epsilon = 0.40$
Cobalt oxide	$\alpha = 0.93, \epsilon = 0.24$

As observed from Table A-1, the critical temperature of 195°F cannot be attained in the normal orientation with any coating other than possibly a selective solar absorber, and then only in an orbit that passes through or near the earth-sun line. In the reversed orientation both the black and selective solar absorbers seem to be adequate with very little dependence on the type of orbit. The reversed orientation should therefore be used for the paste heating and initial cooling periods.

In order to accomplish a transient temperature analysis, a type of orbit must be assumed. All orbits lie within two extremes, i. e. a day-night orbit that passes through the earth-sun line and a twilight orbit wherein the vehicle remains 90° from the earth-sun line. These two orbits were selected since they present the thermal extremes for design purposes. An IBM 1410 electronic computer was used for all transient temperature computations.

Figure A-3 presents the foam paste temperature vs time provided no chemical energy is liberated. In the day-night orbit the vehicle is presumed to be deployed ten minutes before the vehicle passes through the earth-sun line. The black surface meets the heating requirements very well.

Figures A-4 and A-5 present the foam temperatures vs time following leavening. The gas bag is presumed to be attached to the concentrator for these curves. In the day-night orbit the vehicle is presumed to be initially on the earth-sun line. The black surface seems to meet the requirements but its temperature decays more rapidly than desired; the Cr - Ni - V surface meets these objections.

The orbital temperatures with a black surface were also computed and are shown in Figures A-6 and A-7 for a day-night orbit. The foam temperatures with a normal orientation and without the gas bag vary from -130°F to 130°F.

APPENDIX A

In summary, the concentrator should have a reversed orientation during the foaming and stabilization process. The back surface should be black or coated with a selective solar absorber. The black surface may be located either above or below a transparent back flap but the selective solar absorber would have to be located on the surface of the back flap.

Table A-1. Radiation Equilibrium Temperature (End Cap Attached)

Concentrator Orientation	Angle From Earth-Sun Line ~ Degrees	Solar Absorptance	Emittance	Temperature °F
Reversed	0	0.12	0.05	189
		0.35	0.35	192
		0.9	0.9	218
		0.94	0.40	339
		0.93	0.24	403
Reversed	90	0.12	0.05	146
		0.35	0.35	180
		0.9	0.9	217
		0.94	0.40	333
		0.93	0.24	395
Normal	0	0.12	0.05	173
		0.35	0.35	133
		0.9	0.9	128
		0.94	0.40	208
		0.93	0.24	254
Normal	90	0.12	0.05	121
		0.35	0.35	27
		0.9	0.9	-35
		0.94	0.40	18
		0.93	0.24	51
Normal	180	0.12	0.05	-121
		0.35	0.35	-183
		0.9	0.9	-228
		0.94	0.40	-189
		0.93	0.24	-167

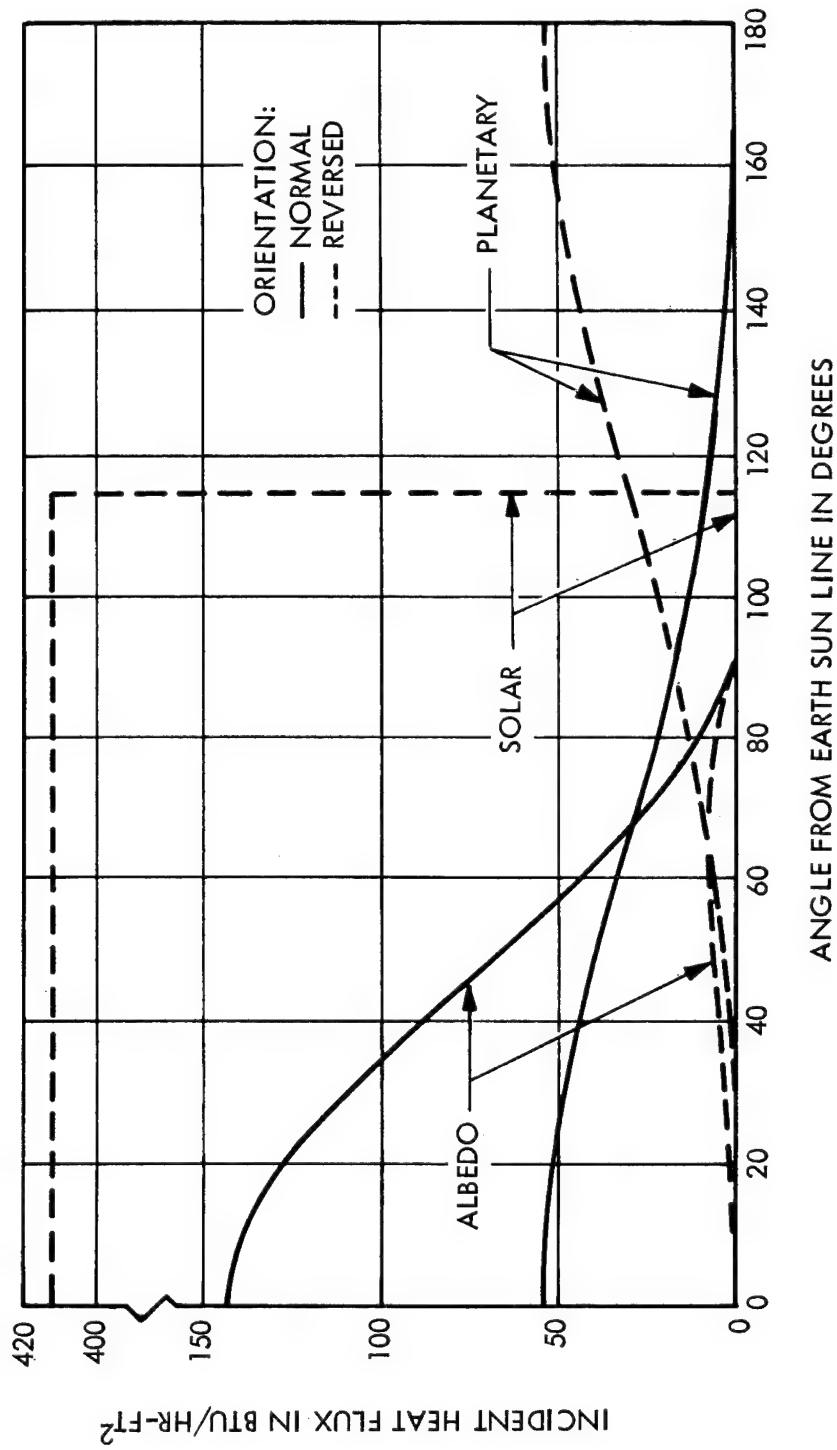


Figure A-1. Heat Fluxes on Concentrator External Surface

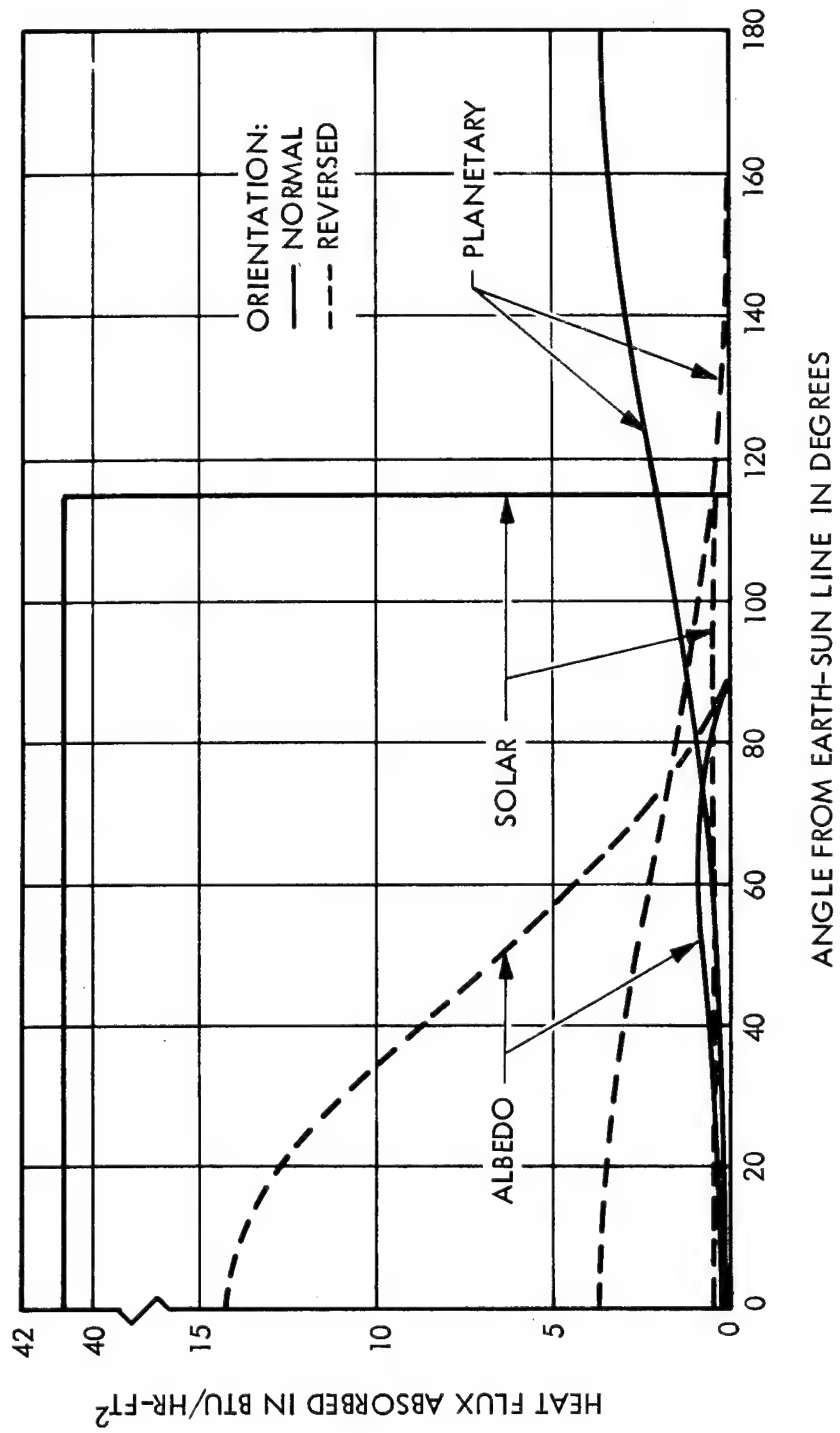


Figure A-2. Heat Fluxes on Concentrator Internal Surface (End Cap Attached)

APPENDIX A

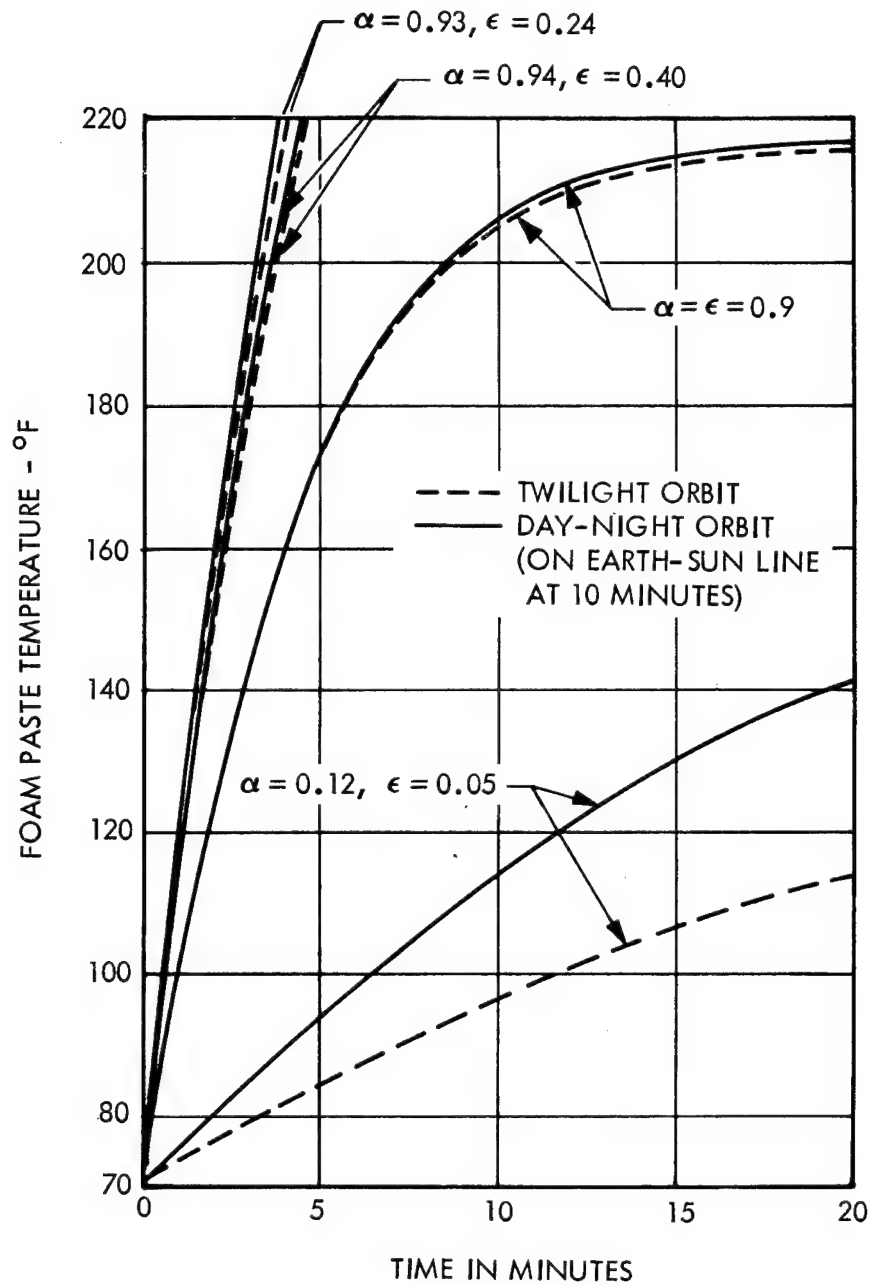


Figure A-3. Precoat Surface Temperatures Versus Time (Reversed Orientation)

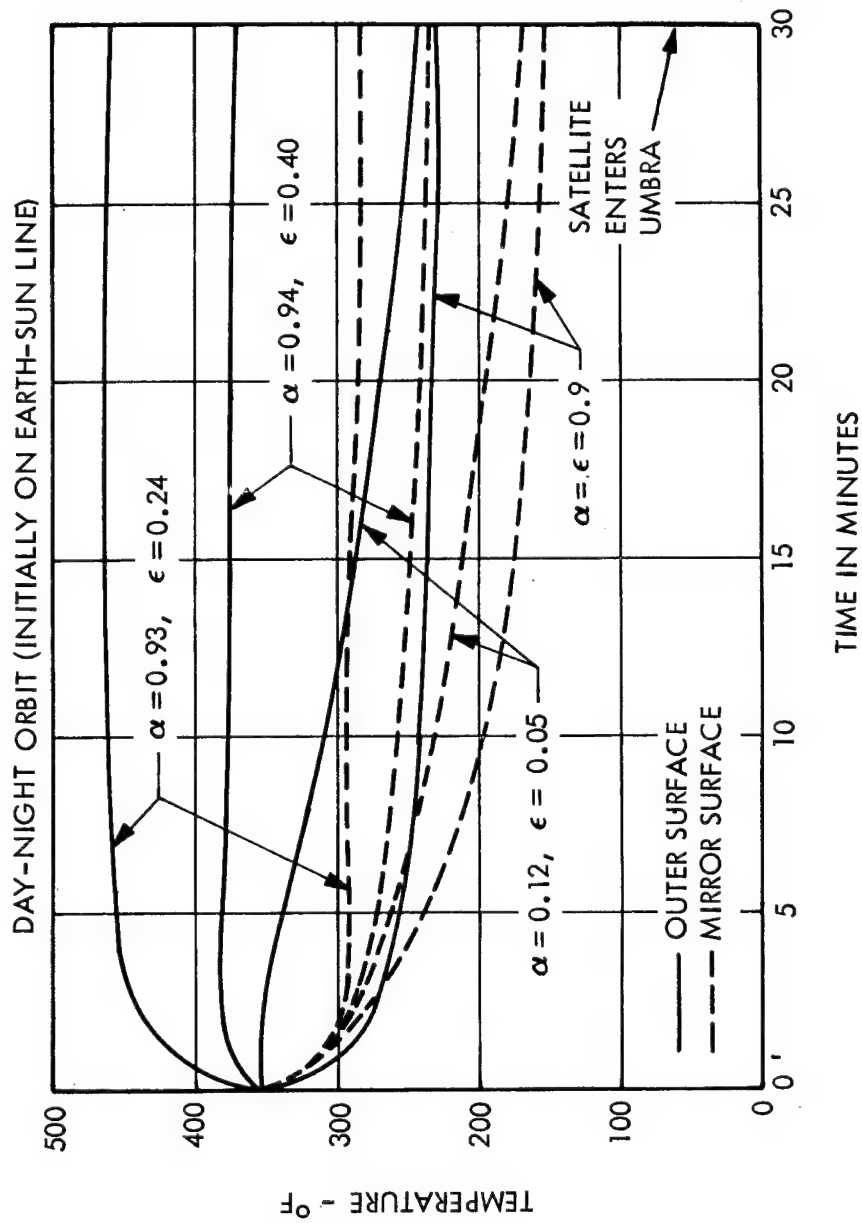


Figure A-4. Foam Temperatures Versus Time (Reversed Orientation)

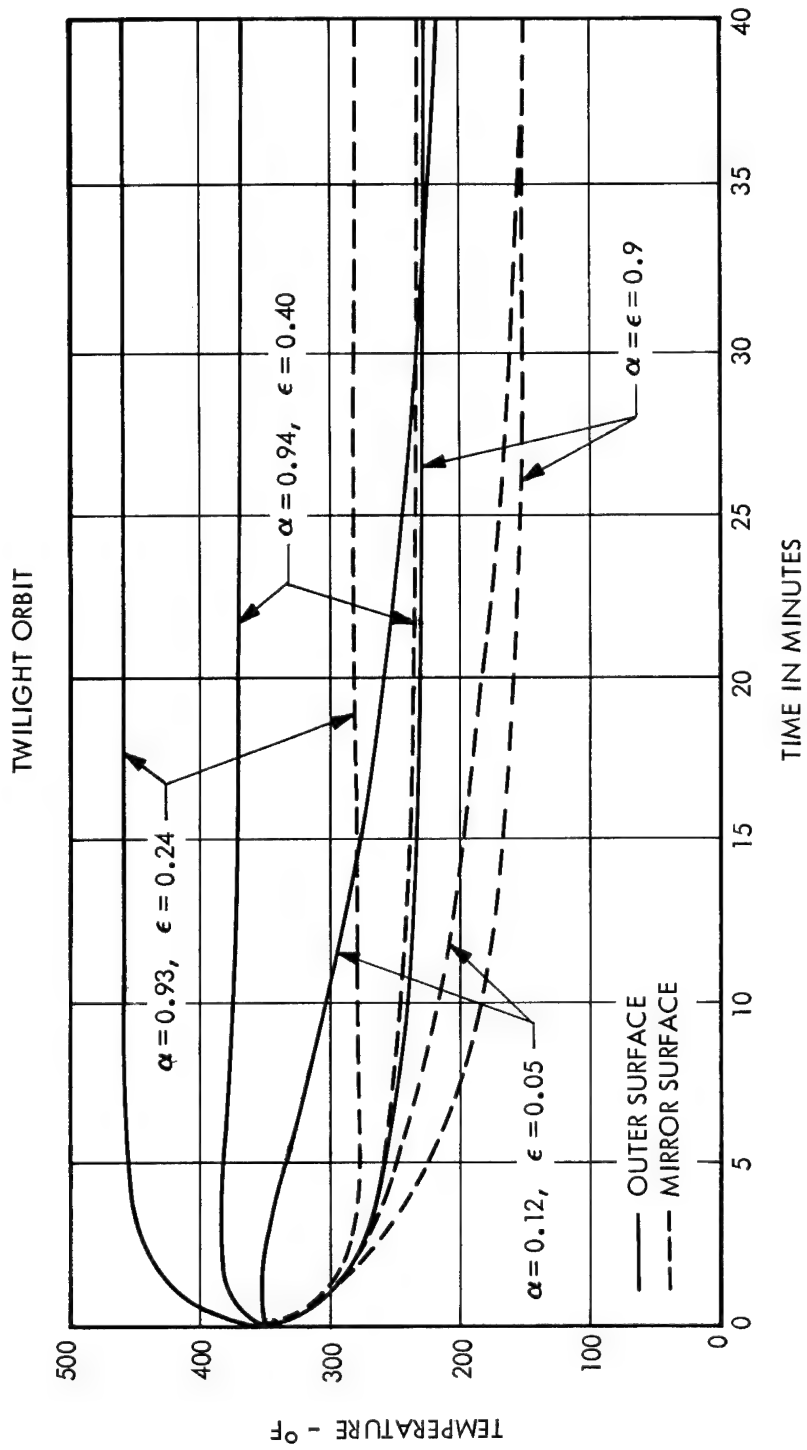


Figure A-5. Foam Temperatures Versus Time (Reversed Orientation)

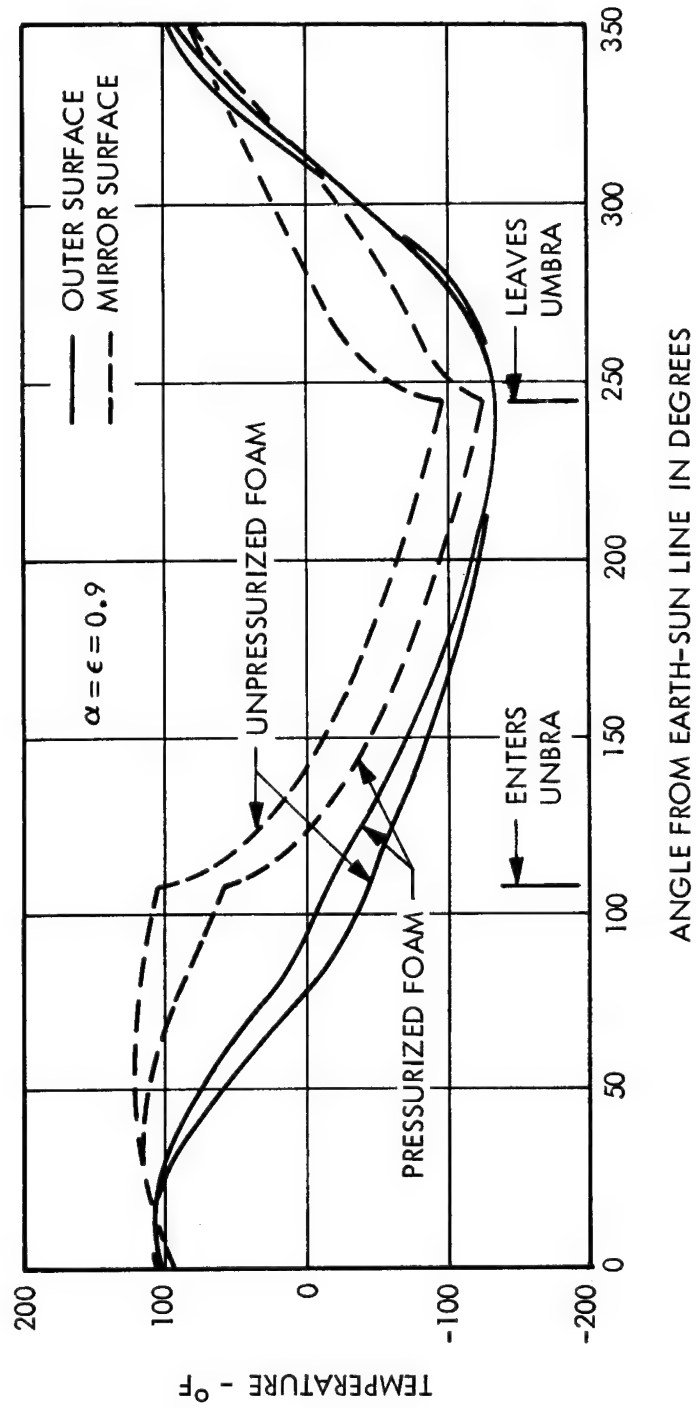


Figure A-6. Orbital Temperatures (Normal Orientation, End Cap Attached)

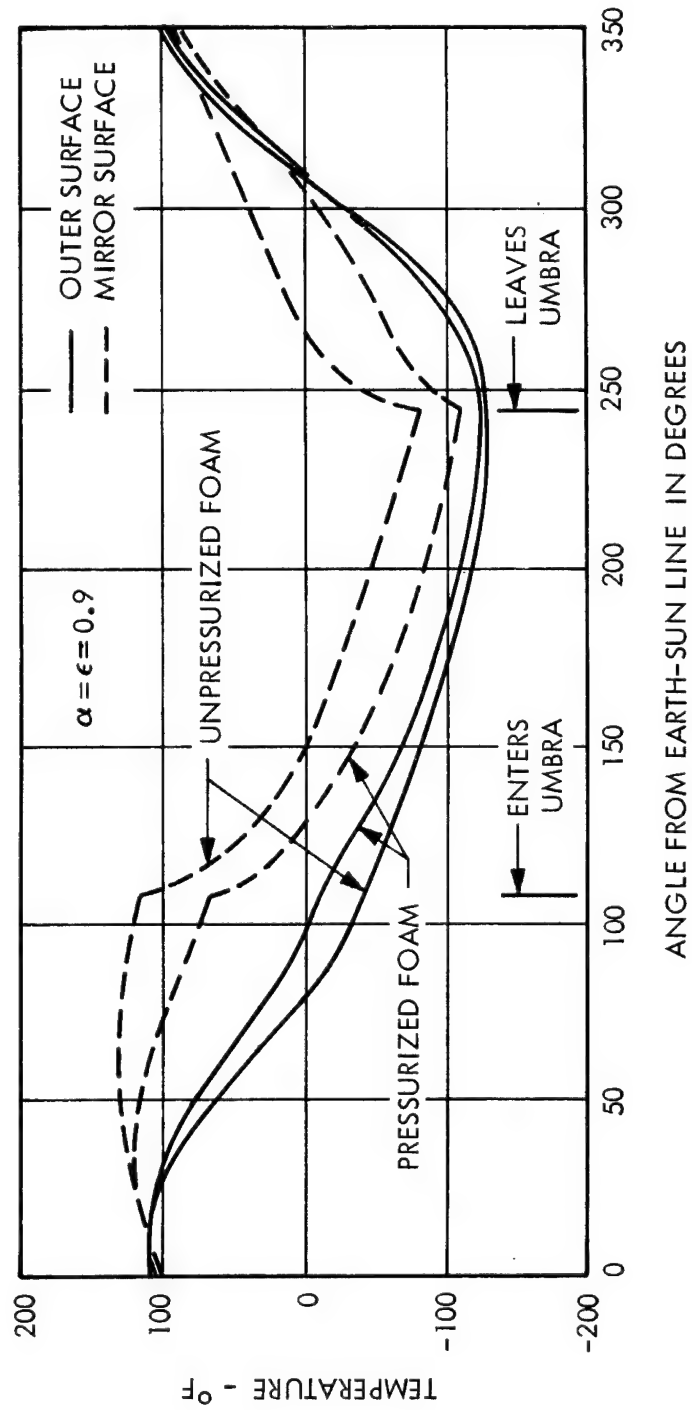


Figure A-7. Orbital Temperatures (Normal Orientation, End Cap Detached)

APPENDIX B. AZOTOMETER TEST AND ANALYSIS

The azotometer*(similar to a nitrometer) apparatus is shown in Figures B-1 and B-2. It is used to measure the volume of nitrogen evolved during the rearrangement of an organic compound, the azide material. A description of its operation follows.

One hundred milligrams of azide material and 0.5 to 1.0 gram of unreactive paraffin oil (for heat transfer) are placed in the bottom of the reaction tube. The gas burette contains a potassium hydroxide solution with a layer of mercury at the bottom extending to about one-half inch above the entrance tube. The system is already purged with CO₂, and the CO₂ is allowed to flow continuously at a rate of approximately one bubble per second or 5 cc/minute. Blank runs are made to determine the volume of insoluble gas collected; this represents impurities in the CO₂.

The sample of azide placed in the reaction tube is maintained at room temperature until the start of the run, which is initiated by raising a preheated, thermostated water bath around the reaction tube. Nitrogen gas, which then begins to be evolved by the azide, is swept in the flowing CO₂ stream to the gas collection burette, and there its rate of collection versus time is observed. Appropriate corrections for temperature, barometric pressure, and water vapor over the KOH solution are made to the nitrogen volume. The amount of nitrogen evolved is determined by the following calculation:

$$N = \left(\frac{V}{22,400} \right) \frac{N_{MW} \times 100}{S_W}, \quad (1)$$

*S. Siggia, "Quantitative Organic Analysis via Functional Groups," Third Edition. John Wiley and Sons, Inc, New York, 1963, p 545.

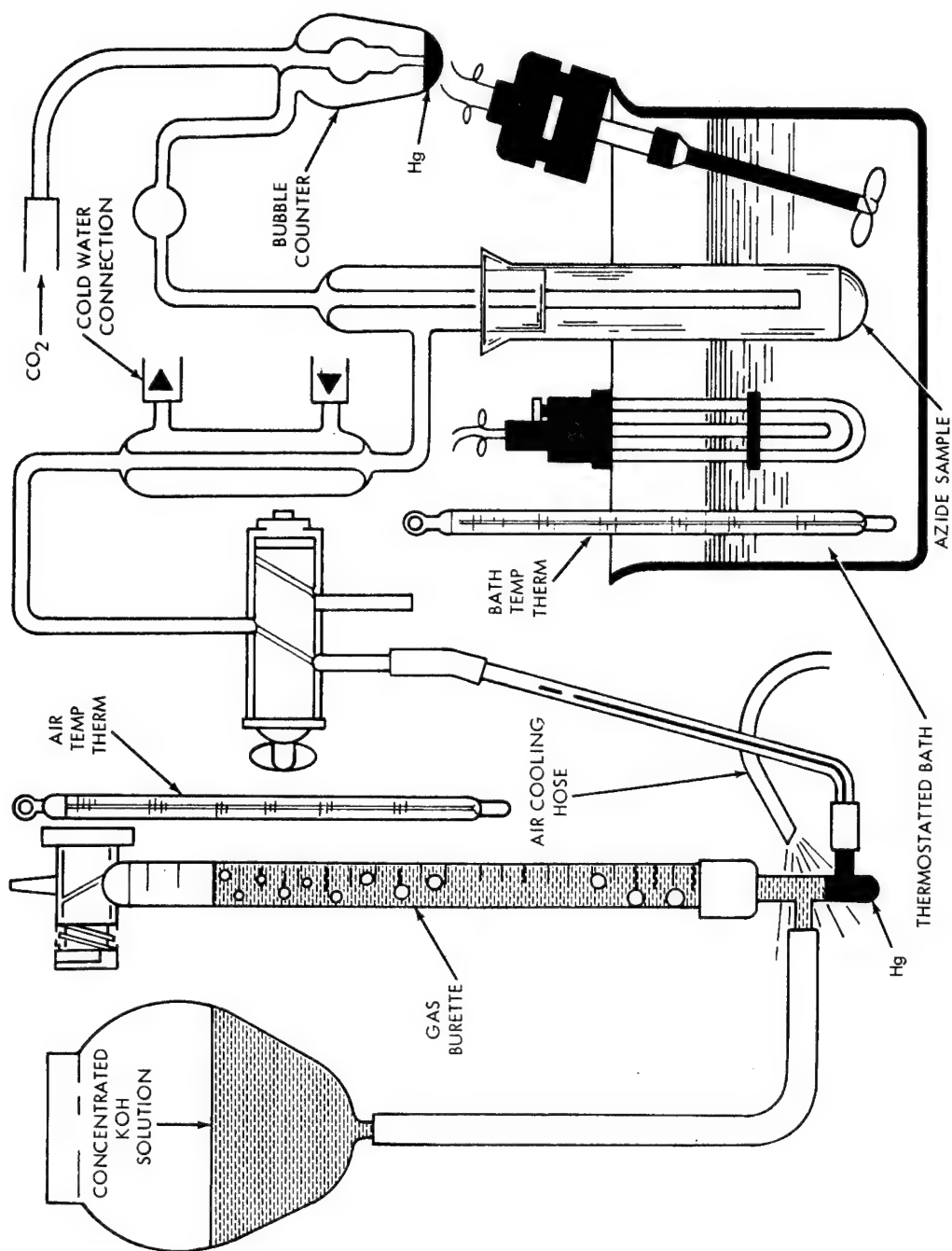


Figure B-1. Sketch of Azotometer Apparatus

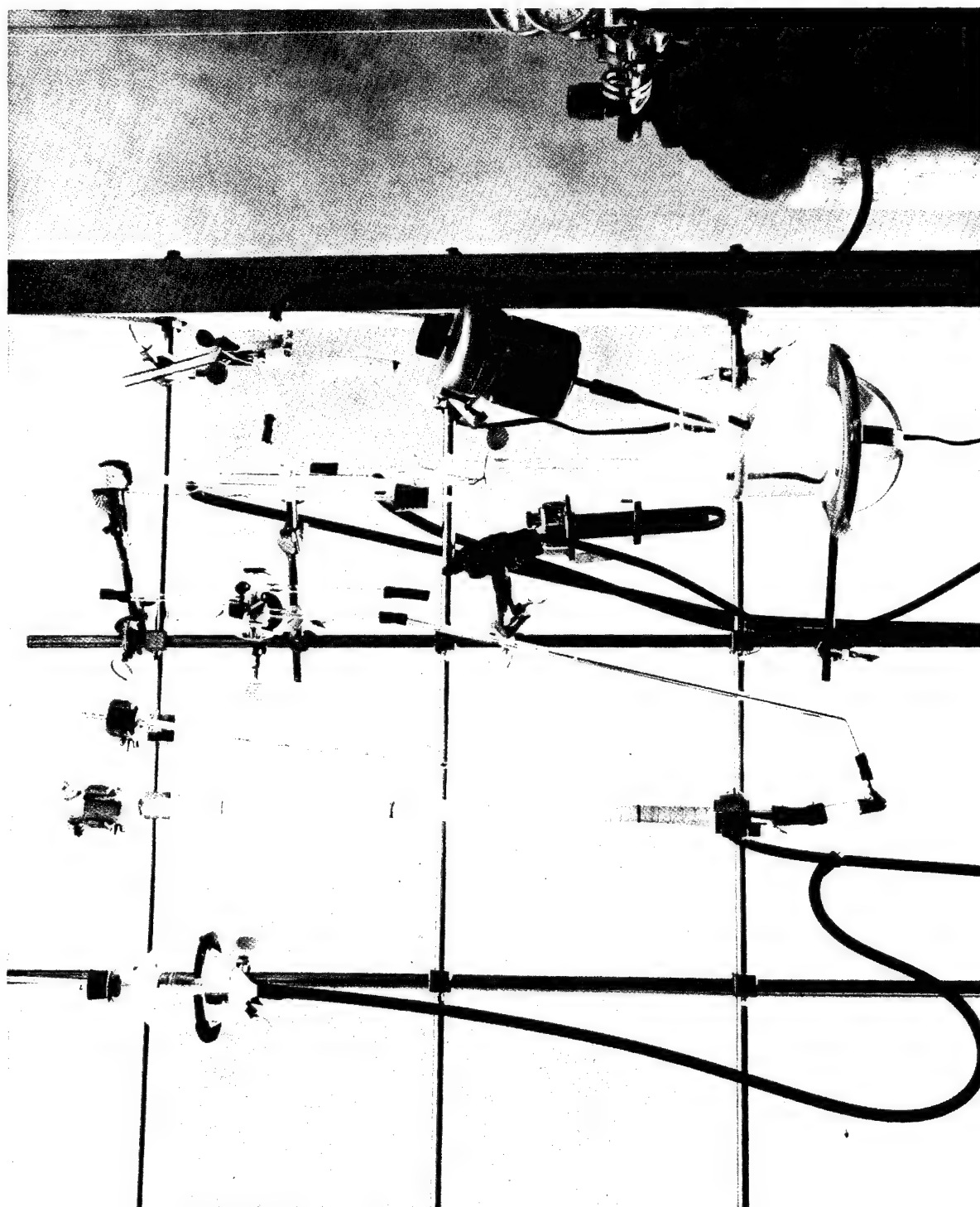


Figure B-2. Photograph of Azotometer Apparatus

APPENDIX B.

where

N = amount of nitrogen evolved in percent of azide compound by weight,

V = volume of gas collected - corrected for CO_2 blank and for NTP in cm^3 ,

N_{MW} = molecular weight of the nitrogen,

S_W = weight of the azide sample in gms.

The determination is accurate and precise to better than ± 1 percent.

Azotometer information gives the rate and amount of nitrogen evolved when the azide is exposed to a specific temperature. From these runs a value "k" for the reaction velocity of azide rearrangement (as a unimolecular reaction) can be determined. Then from Equation 2, the azide rate of decomposition can be determined for any time period. A typical analytical run is given in the following paragraphs (see Table B-1):

Table B-1. Azotometer Run of Structure X

① Clock Time	② Elapsed Min	③ Accumulated Gas Vol	④ Blank	⑤ Volume of Nitrogen ③ - ④	⑥ Correction for Normal Temp and Press. ⑤ x 0.871	⑦ Conversion to Weight in Mg ⑥ x 1.25 mg/cc	⑧ Percent of Azide Decomposed 100 x ⑦/18.3
2:47	0	0	0	0	0	0	0
3:10	23	5.35	0.4	4.95	4.31	5.37	29.3
3:25	38	9.25	0.8	8.45	7.36	9.18	50.2
3:40	53	11.75	1.2	10.55	9.19	11.55	62.8
3:55	68	13.80	1.6	12.20	10.63	13.15	71.9
4:10	83	15.50	2.0	13.50	11.76	14.65	80.1

The effect of the starting time of 8 minutes (see Figure B-3) is minimized by the determination of k on the basis of the half life of azide rearrangement:

$$\frac{dx}{dt} = -kx \quad (2)$$

where

x = amount of azide in grams,

t = time after start of azotometer run,

k = reaction velocity of azide rearrangement.

$$\frac{dx}{x} = -kdt$$

$$\int_x^0 \frac{dx}{x} = -k \int_0^t dt \quad (3)$$

$$\ln x \Big|_x^0 = -kt \Big|_0^t .$$

when $t = 0$, $x = 1$; when $x = 0$, $t = \infty$.

For half life:

$$\ln x \Big|_x^{\frac{x}{2}} = -kt \Big|_0^{\frac{t}{2}}$$

$$\ln \frac{x}{2} - \ln x = -k \left(\frac{t}{2} \right)$$

APPENDIX B.

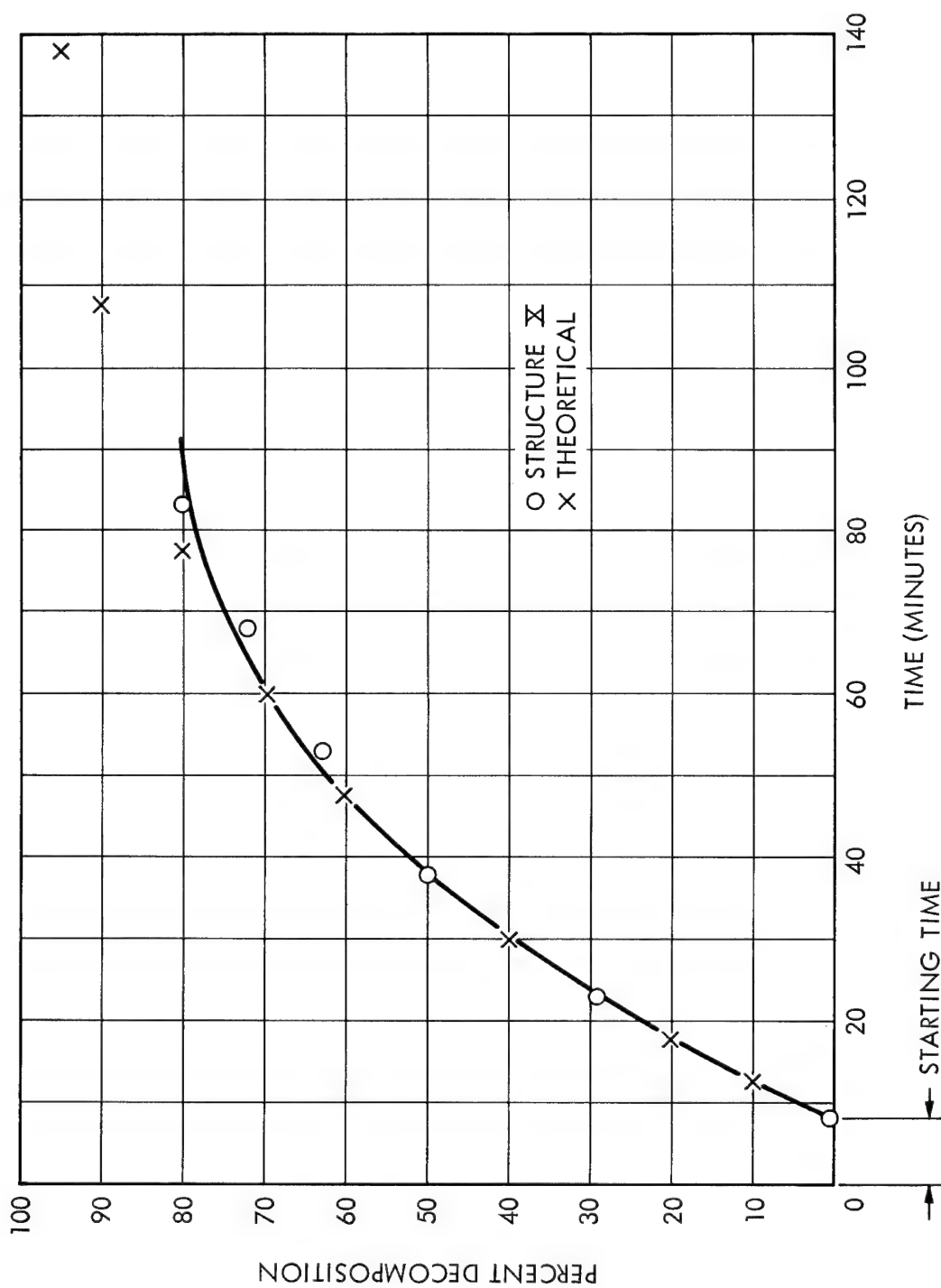


Figure B-3. Percent of Azide Decomposition against Time
(Azide Structure X at 193°F)

$$\ln \left(\frac{1}{2} \right) = -k \left(\frac{t}{2} \right)$$

$$-0.693 = -k \left(\frac{t}{2} \right).$$

If $\left(\frac{t}{2} \right) = (38-8) = 30$ (see Figure 8),

$$k = \frac{0.693}{30} = 2.31 \times 10^{-2}.$$

The ordinate values for Figure 8 are obtained by solving for N_1 in the following expression:

$$\int_0^{N_1} \frac{dn}{n} = -k \int_0^{t_1} dt,$$

where

N_1 = the value N from Equation 1

$$k = 2.31 \times 10^{-2}$$

t_1 = actual time minus starting time

and subtracting from 100, e.g., percent decomposition = $(100 - N_1)$.

The separation of experimental values from theoretical values at the higher percentage of decomposition is considered as possibly due to the impurities in the azide structure.

APPENDIX C. MEASUREMENT OF HEAT RELEASE FROM AZIDE REARRANGEMENT

A test apparatus has been assembled and calibrated to determine the heat of decomposition of candidate azide materials (see Figures C-1, C-2, and C-3). The assembly is essentially a calorimeter which provides a means for controlling the initial or "triggering" temperature for the test material. The apparatus consists of a thin-walled glass test tube enclosed in a glass Dewar. Thermocouples placed in the test tube are connected to a chart recorder. The Dewar is connected to a vacuum pump. The space between the test tube and the Dewar inner wall is evacuated. The test tube surrounded by radiation shields (aluminized Mylar) and vacuum results in a low heat loss system.

Calibration of the system was accomplished by the method of mixtures. A solid specimen of known mass and specific heat was heated and lowered into the test tube containing an inert liquid (paraffin oil). The equivalent specific heat of the system is calculated by use of the following equation:

$$c_{cu} m_{cu} \Delta t_{cu} = c_s m_s \Delta t_s$$

(Heat lost by copper) = (Heat gained by system),

or

$$c_s = \frac{c_{cu} m_{cu} \Delta t_{cu}}{m_s \Delta t_s},$$

where

c_s = equivalent specific heat of calorimeter (cal/gm °C),

m_s = mass of inert fluid (grams),

Δt_s = temperature change of fluid (°C),

c_{cu} = specific heat of copper (cal/gm °C),

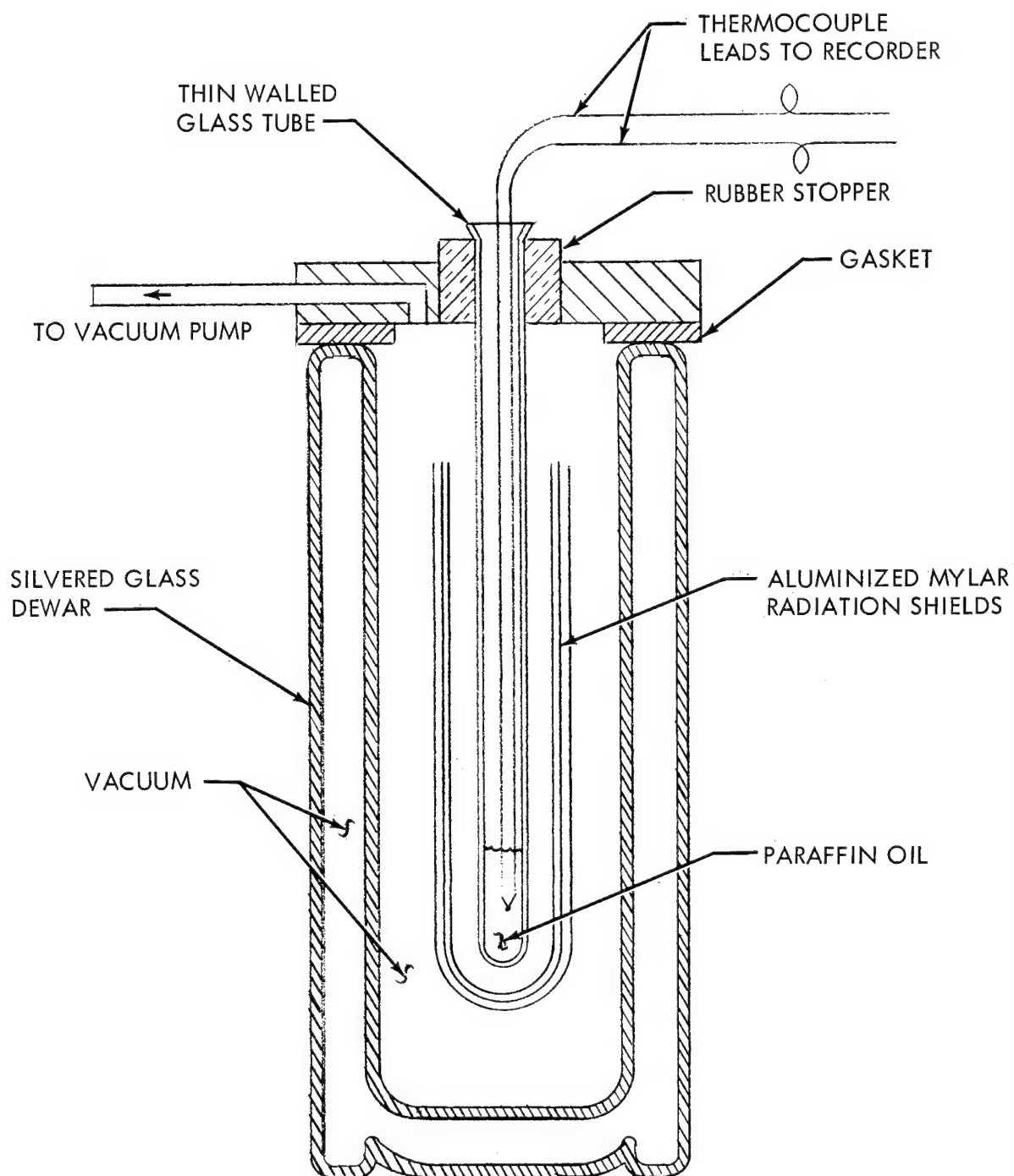


Figure C-1. Sketch of Heat of Decomposition Apparatus

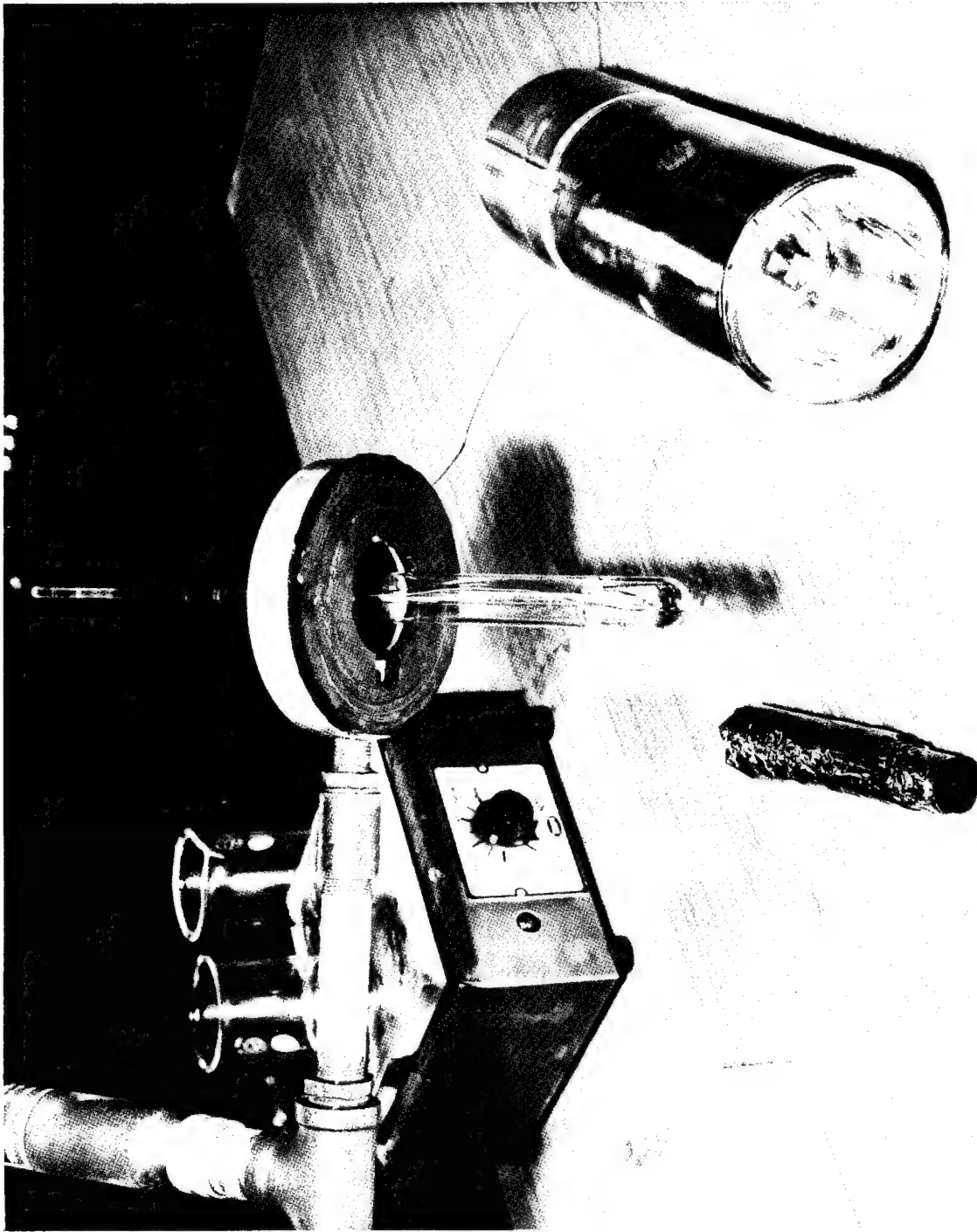


Figure C-2. Heat of Decomposition Apparatus - Disassembled

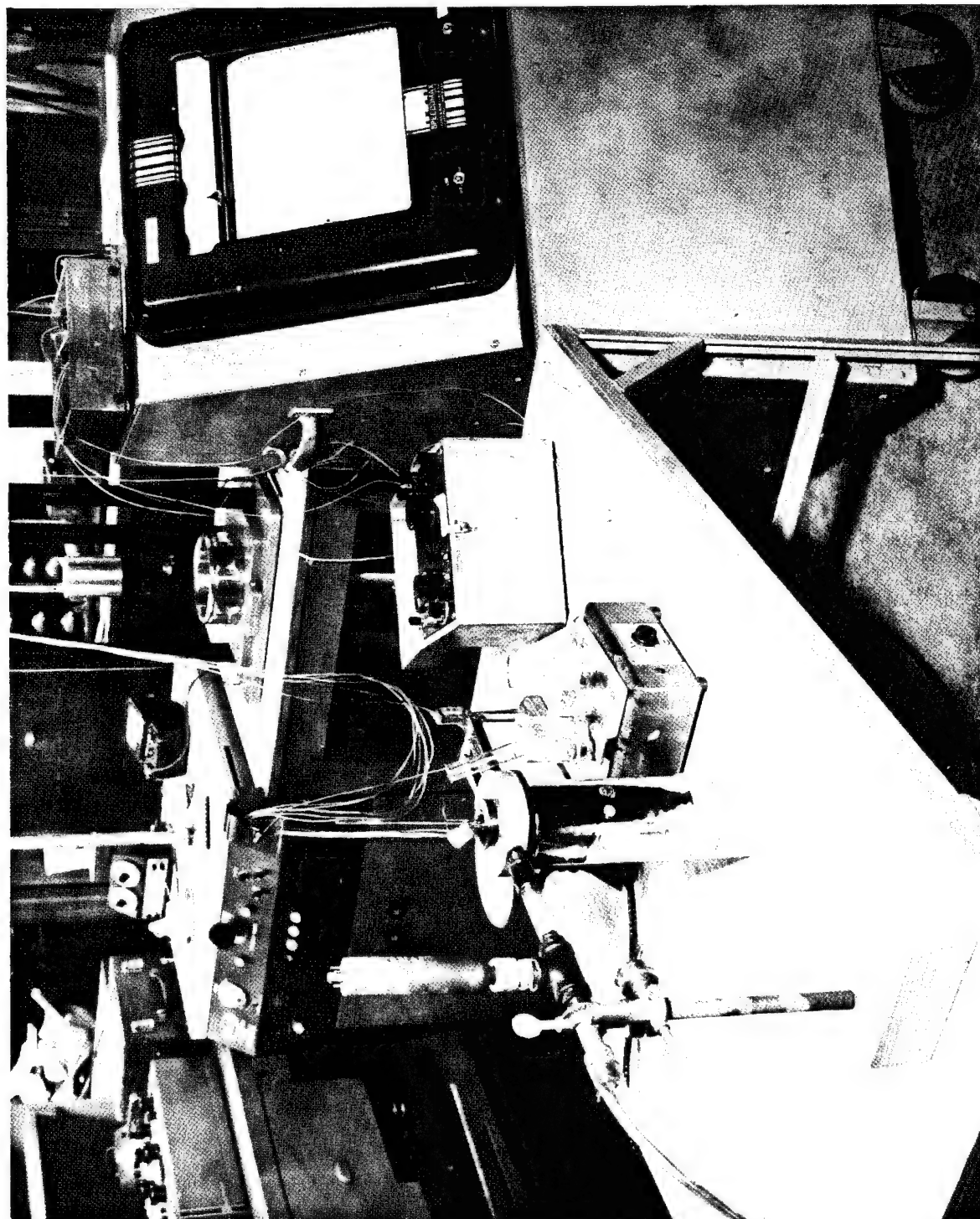


Figure C-3. Heat of Decomposition Apparatus - Assembled

m_{Cu} = mass of copper specimen (grams),

Δt_{Cu} = temperature change of copper specimen ($^{\circ}\text{C}$)

The inert liquid (paraffin oil) was then heated and poured into the test tube. The cooling rate of the liquid was determined by the thermocouple and the recorder. When the temperature of the liquid dropped to the desired level, a copper specimen was lowered into the liquid. Temperature changes of the liquid and the copper specimen were recorded.

The determination of the heat of decomposition of the azide materials is conducted basically the same as described for the calibration except that a known quantity of azide supplies the added heat to the inert liquid instead of the copper specimen.

APPENDIX D. SUBLIMATION TESTS

The sublimation tendency of the candidate precoat foam materials was determined by the weight loss method. Precoat foam formulations are prepared and applied to the cups of the apparatus shown in Figures D-1, D-2, and D-3. The cups are then subjected to a high-vacuum environment for a specified time interval after which one cup is removed and the weight loss determined with a minimum exposure to the atmosphere. The remaining cups are returned to the high-vacuum environment. After a specified time exposure, a second cup is removed and the weight loss determined. This procedure continues until a curve can be established for the rate of sublimation of the material.

Initial tests were performed at room temperature. More severe tests are performed with the material subjected to heat approaching the azide reacting temperature as well as the high vacuum.

A 4-inch diameter by 1/2-inch thick copper plate contains seven wells in which the copper specimen cups are placed. Temperature control is obtained manually for short-time runs by adjusting power to the electric heater with a variac. For long-duration tests, temperature is automatically controlled with a "Simplytrol" temperature controller. Temperature of the copper plate is sensed by thermocouples and is recorded on a strip chart recorder. Calibration tests were conducted to determine if the specimen cup temperature is the same as that of the copper plate. Since the tests are performed in a vacuum, good mechanical contact must exist to permit proper heat transfer. This has been accomplished by means of stainless steel wires (anchored to screws on the copper plate) acting as springs and exerting a small force against the specimen cups. Tests have shown that

APPENDIX D

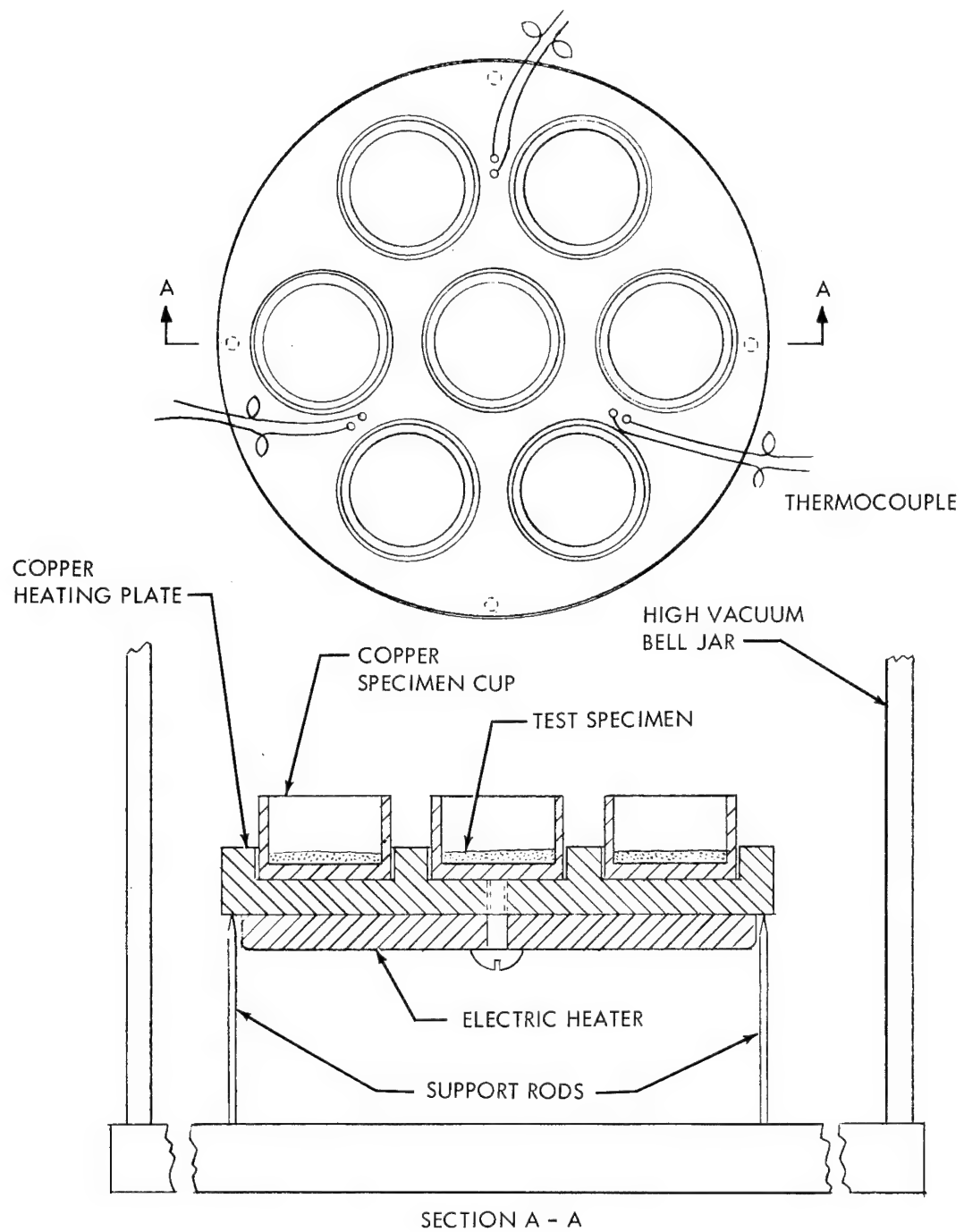


Figure D-1. Sketch of Sublimation Test Apparatus



Figure D-2. Closeup of Sublimation Test Apparatus

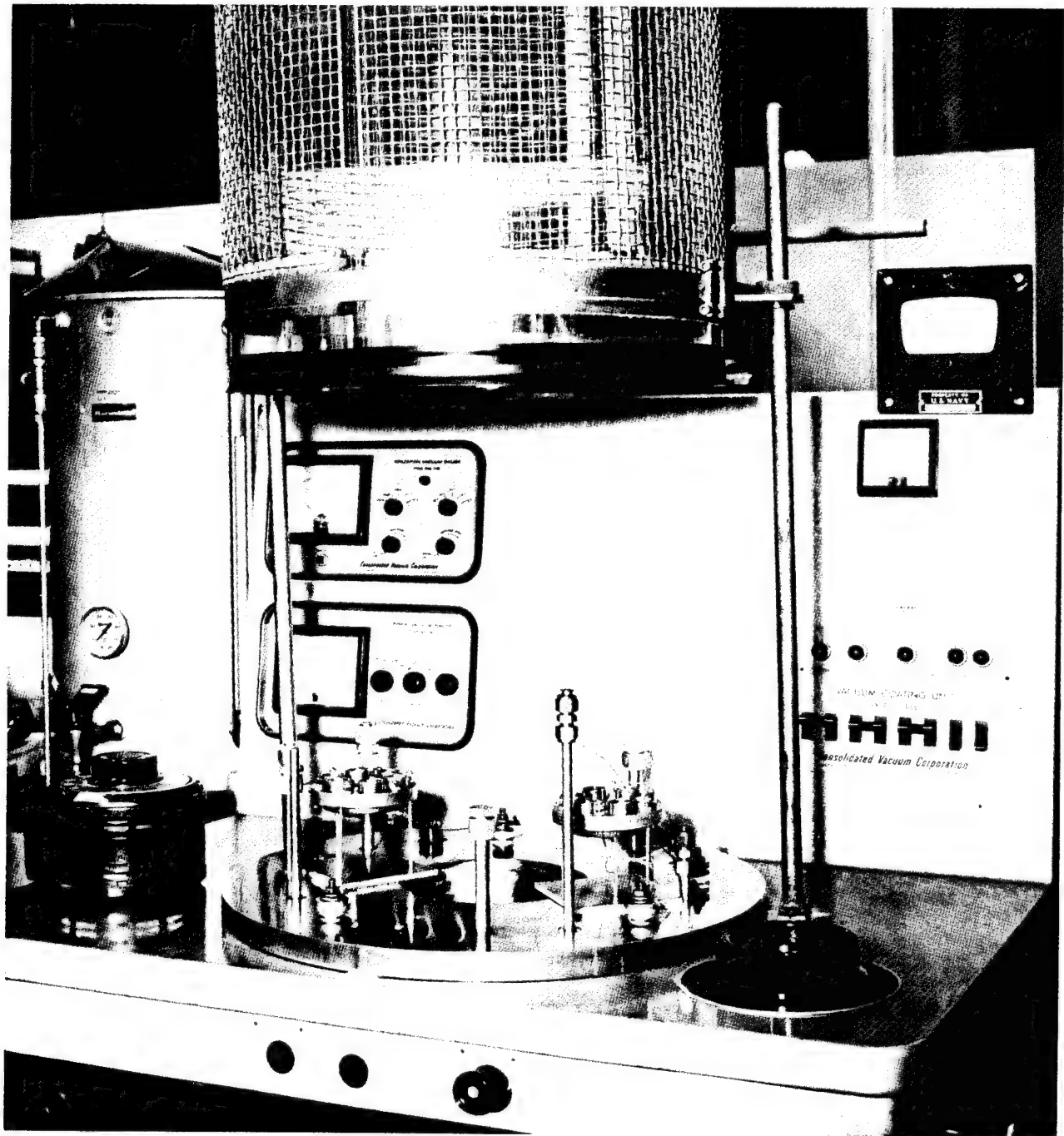


Figure D-3. Sublimation Test Apparatus in Bell Jar Installation

specimen cup temperatures are within 2 °F of the copper plate temperature.

The procedure followed for conducting a sublimation test is as follows:

- (1) Weigh empty cups.
- (2) Weigh cups with sample material.
- (3) Condition in bell jar overnight at a pressure of from 10 to 50 microns.
- (4) Weigh samples.
- (5) Evacuate bell jar to 10^{-5} torr.
- (6) Apply heat and retain pressure $\leq 10^{-2}$ torr.
- (7) Weigh first sample after two hours.
- (8) If difference in weight is significant, weigh succeeding samples in one-hour intervals. If weight difference is not significant, weigh succeeding samples in intervals of \geq two hours.

APPENDIX E

ORGANIC AZID TEST RESULTS

U. S. NAVAL AMMUNITION DEPOT LETTER

APPENDIX F. ORGANIC AZIDE TEST RESULTS
FOR SHIPPING CLASSIFICATION

The Bureau of Explosives refusal to classify the organic azides (refer to the following pages) does not close the door to obtaining a classification by which these azides can be shipped in accordance with ICC Regulations. Paragraph 73.51(q) of T. C. George's Tariff No. 15, Interstate Commerce Commission Regulations for transportation of explosives and other dangerous articles by land and water in Rail Freight Service and by motor vehicle (highway), is as follows:

"New explosives except samples for laboratory examination and military explosives approved by the Chief of Ordnance, Department of the Army; Chief Bureau of Naval Weapons, Department of the Navy; or Commander, Air Force Systems Command, and Commander, Air Force Logistics Command, Department of the Air Force. All other new explosives must be approved for transportation by the Bureau of Explosives."

The above regulation delegates responsibility to the various Departments of the Department of Defense for approving shipments of new explosives designed and manufactured by or for the Departments of the Navy, Army or Air Force.

The procedure and test methods performed by the various departments of Defense are not available at the present time. An investigation into the parameters necessary to obtain an ICC Shipping Classification for the Organic Azides from the Departments of the Navy, Army, or Air Force should be considered.

APPENDIX F

BUREAU OF EXPLOSIVES

ASSOCIATION OF AMERICAN RAILROADS

63 VESSEY STREET

NEW YORK, N. Y. 10007

FILE NUMBER

T. C. GEORGE, DIRECTOR AND CHIEF INSPECTOR

25-16-

CAG-S

December 21, 1964

Goodyear Aerospace Corporation
Akron 15
Ohio

Gentlemen:

Attention: Mr. J.E. Seagraves
Senior Engineer
Test Operations
Department 486 - Plant G

This will reference your telephone conversation with my Assistant, Mr. C.A. Garland, Jr. and your Purchase Order No. 69084 YX dated November 13, 1964 which deals with the testing of an organic azide being produced at your installation.

I am attaching for your information, two copies of the laboratory report covering the examination of this material.

You will note where Dr. McKenna states the shipment of this sample is not considered advisable under the Interstate Commerce Commission Regulations.

This aspect was discussed with you in detail in the referenced phone call.

Attached you will find invoice to cover costs of examining the sample.

Yours truly,

H. George
Chief Inspector

58113

BUREAU OF EXPLOSIVES

ASSOCIATION OF AMERICAN RAILROADS

**REPORT FROM CHEMICAL
LABORATORY**

25-16-

T. C. GEORGE, DIRECTOR AND CHIEF INSPECTOR

WILLIAM G. MCKENNA, CHIEF CHEMIST

SOUTH AMBOY, N. J., December 15 196⁴

ORGANIC AZIDES

GOODYEAR AEROSPACE CORPORATION

Samples of a material identified as "organic azides" were received from Goodyear Aerospace Corporation of Akron, Ohio.

The sample consists of a free-flowing, buff colored powder.

The composition is given in chemical symbols.

The sample does not withstand incubation at 75°C. for 48 hours.

The sample explodes when a container with a loosened closure was placed in a mass of wood, paper, etc. and a fire kindled.

The sample decomposes instantly but does not detonate when subjected to initiation by a #8 Blasting Cap.

Small portions of the sample decompose consistently when subjected to 6 inch and 3-3/4 inch drops in the Impact Apparatus.

The shipment of this sample is not considered advisable under the Interstate Commerce Commission Regulations.

W.G. McKenna
Chief Chemist

(ps)

APPENDIX G

CONTOUR MEASUREMENTS

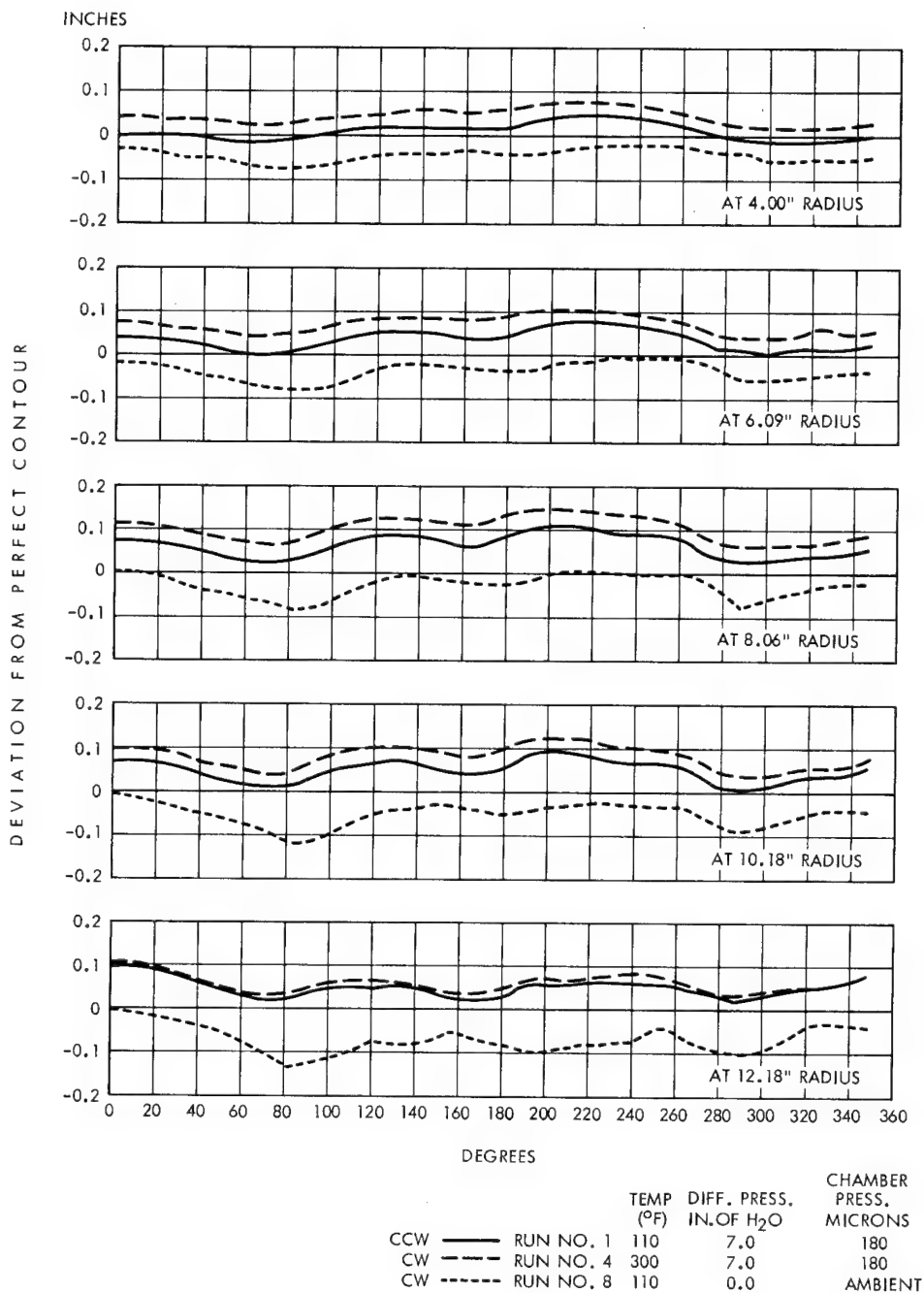


Figure G-1. Contour Comparisons from all Stations Before, During and After Rigidizing - Mirror No. 1 (RISEC 918)

APPENDIX G

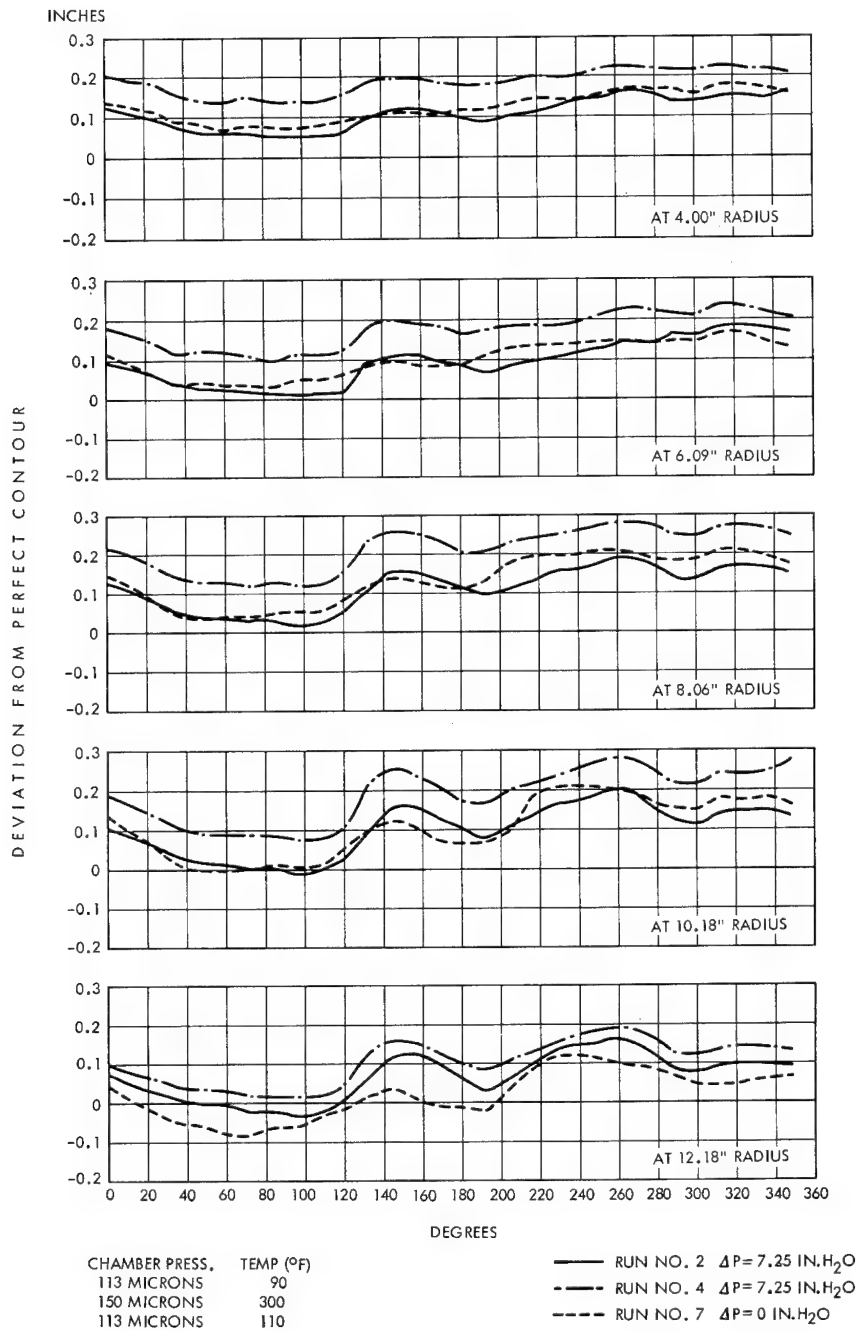
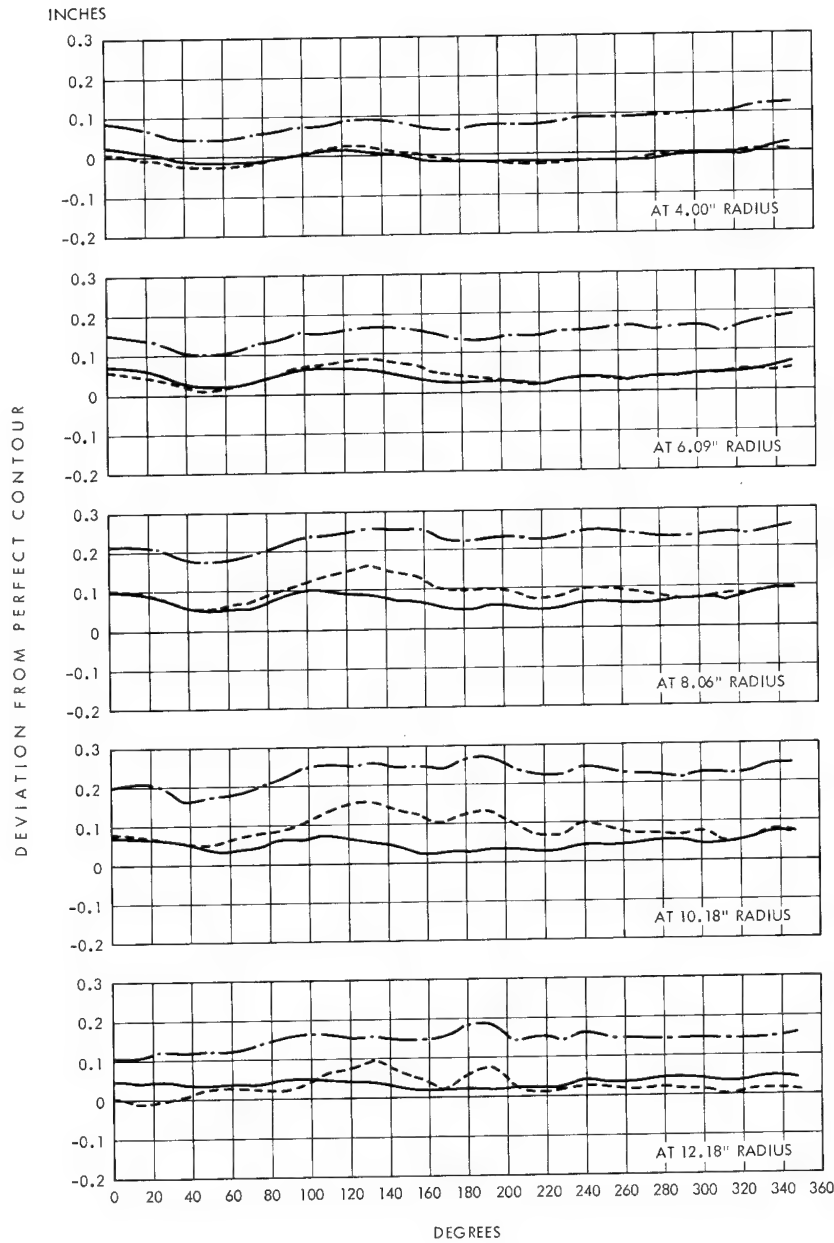


Figure G-2. Contour Comparisons from all Stations, Before, During and After Rigidizing - Mirror No. 3 (RISEC 929)

APPENDIX G



	TEMP °F	DIFF. PRESS.	CHAMBER PRESS.
— RUN NO. 1	90	7.5 IN. H ₂ O	AMBIENT
- - - RUN NO. 4	300	6.0 IN. H ₂ O	110 MICRONS
- · - RUN NO. 8	125	0 IN. H ₂ O	AMBIENT

Figure G-3. Contour Comparisons from all Stations Before, During, and After Rigidizing - Mirror No. 4 (RISEC 1014)

APPENDIX G

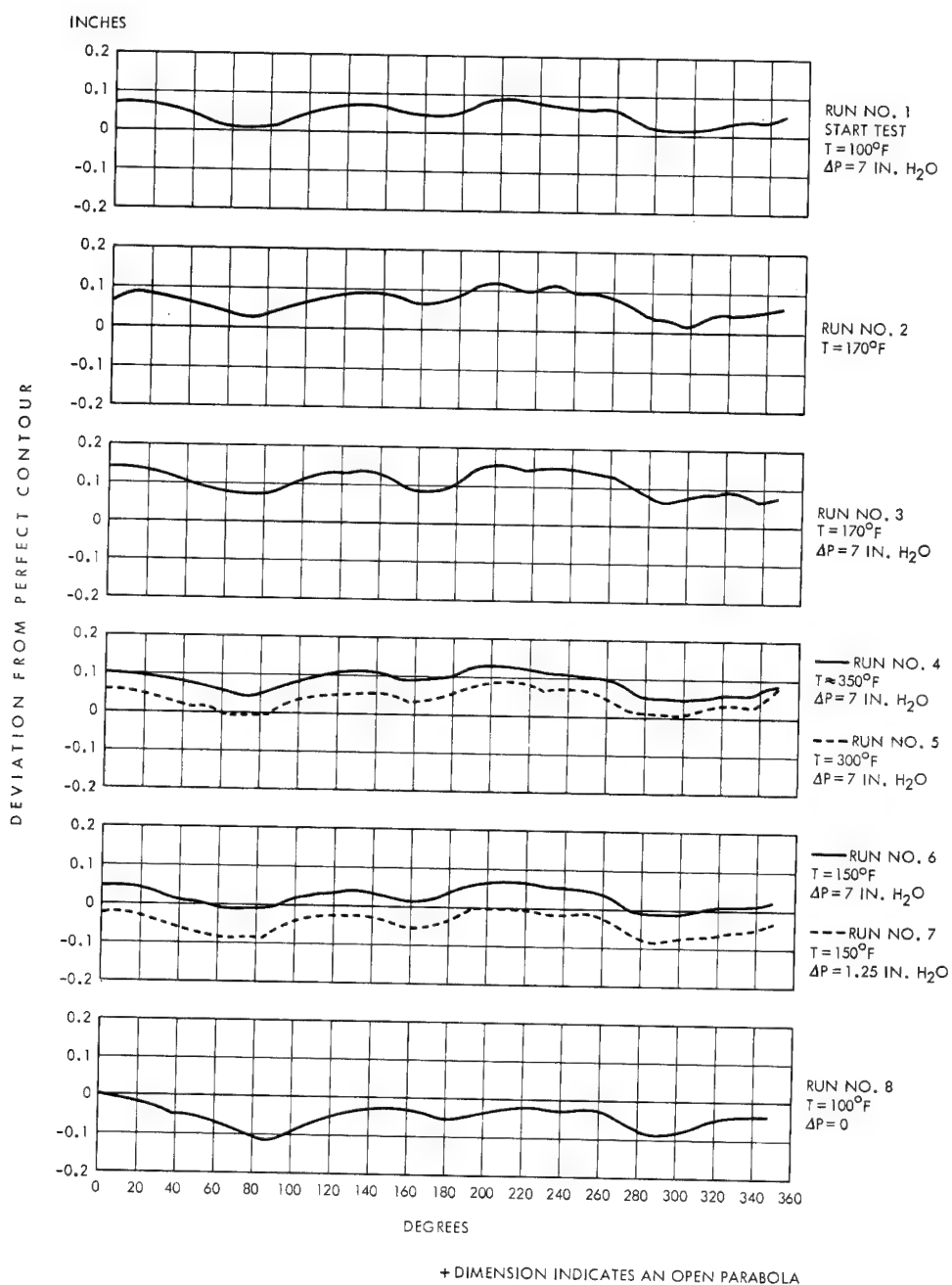


Figure G-4. Contour Comparisons of Various Runs from one Station - 10.18 Inch Radius - Mirror No. 1 (RISEC 918)

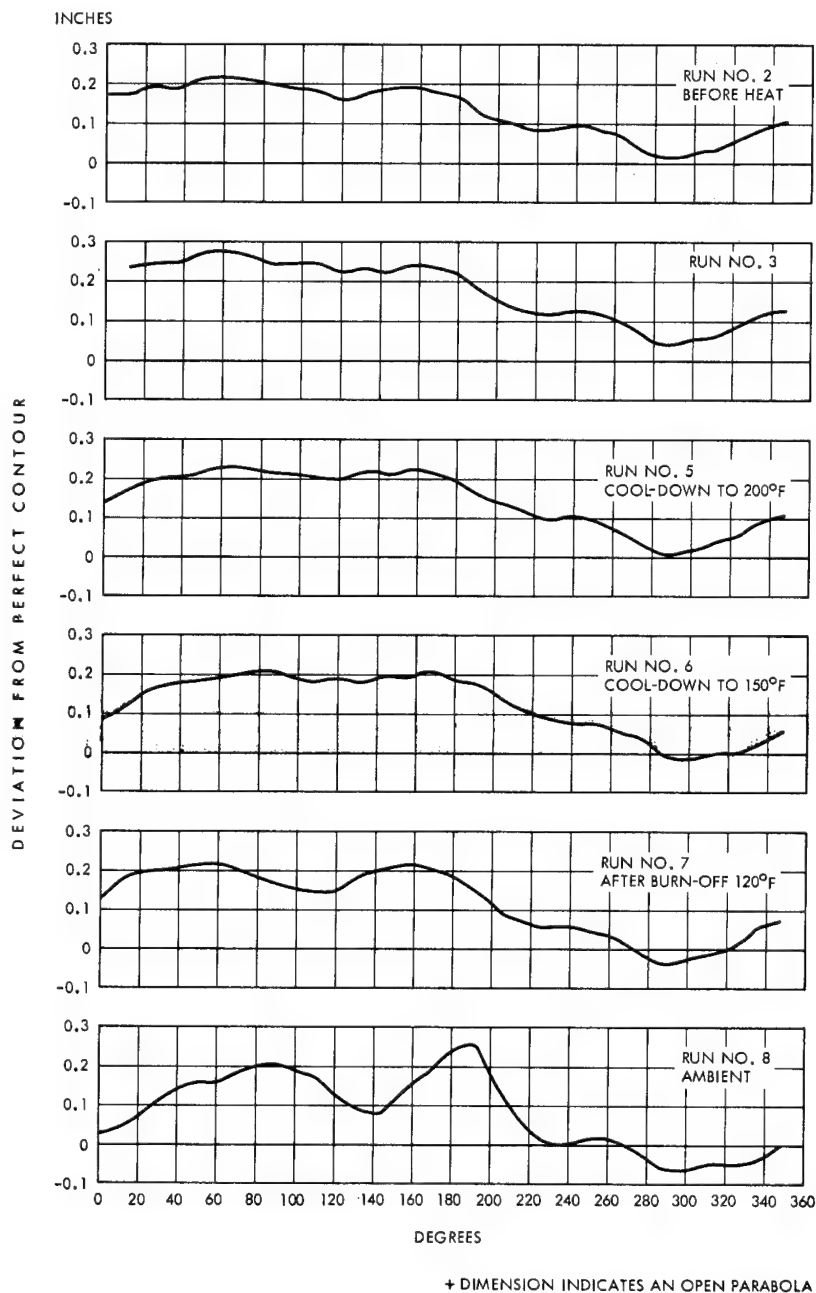


Figure G-5. Contour Comparisons of Various Runs from one Station - 10.18 Inch Radius - Mirror No. 2 (RISEC 924)

APPENDIX G

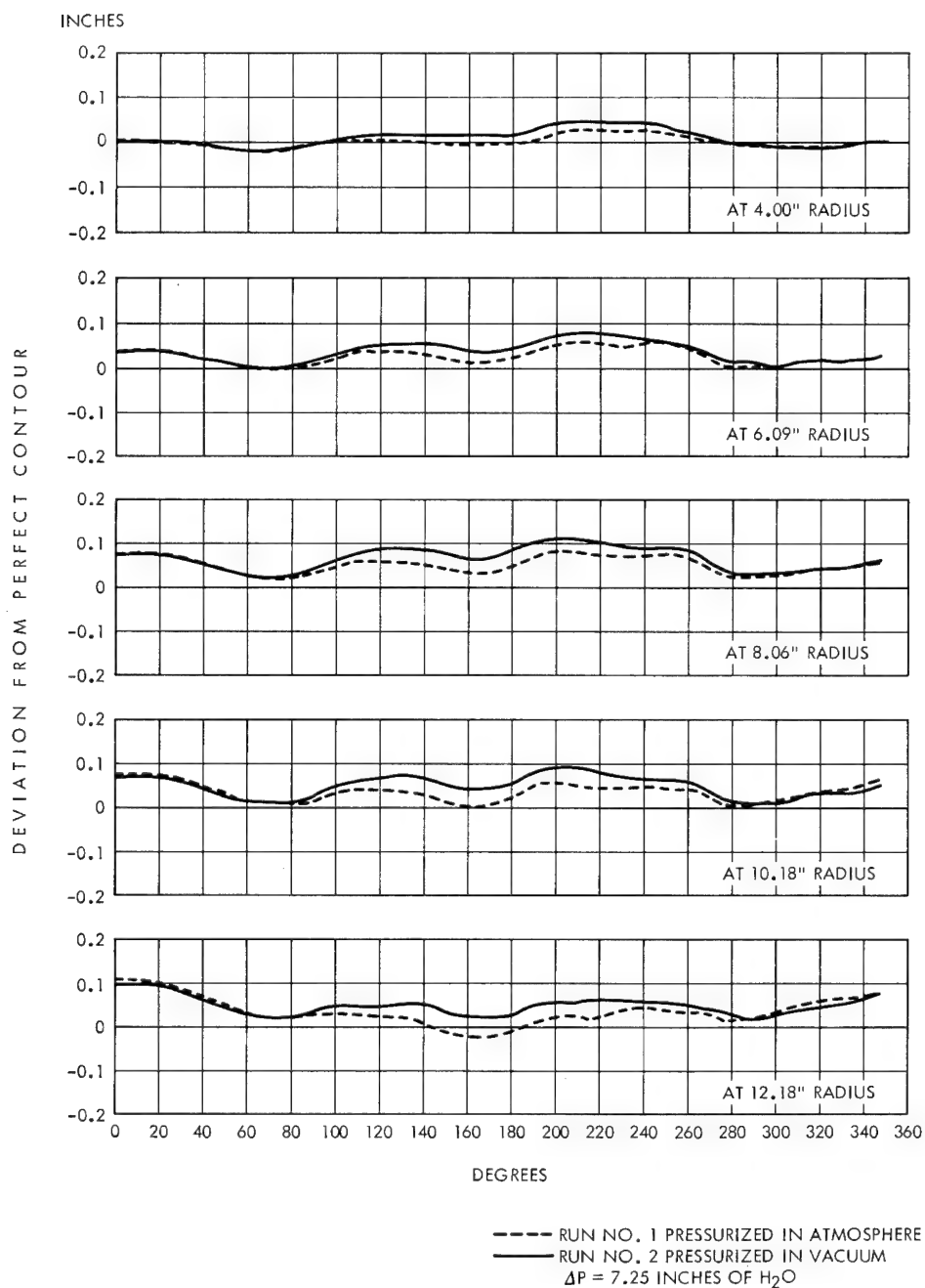


Figure G-6. Contour Comparison of Membrane from all Stations in Atmosphere and in Vacuum - Mirror No. 1 (RISEC 918)

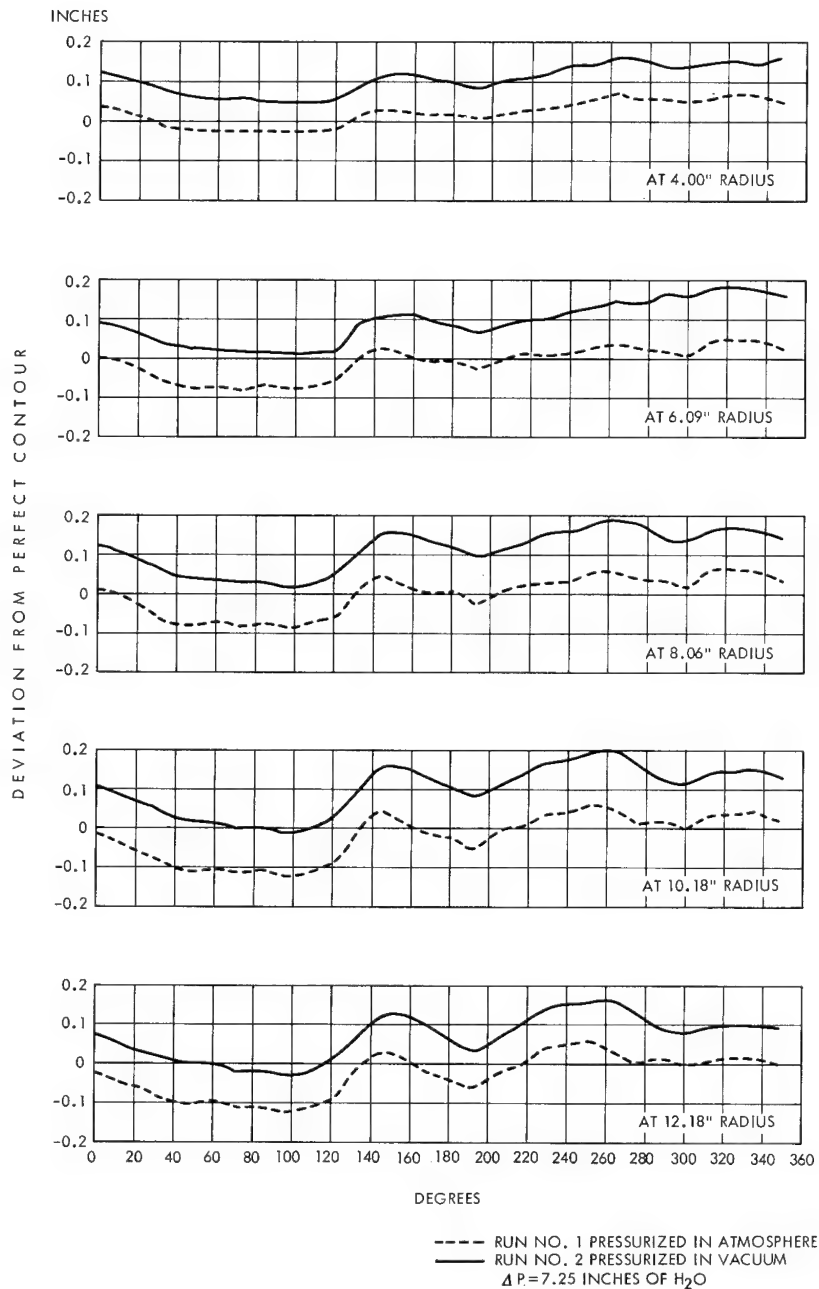


Figure G-7. Contour Comparison of Membrane from all Stations in Atmosphere and in Vacuum - Mirror No. 3 (RISEC 929)

APPENDIX G

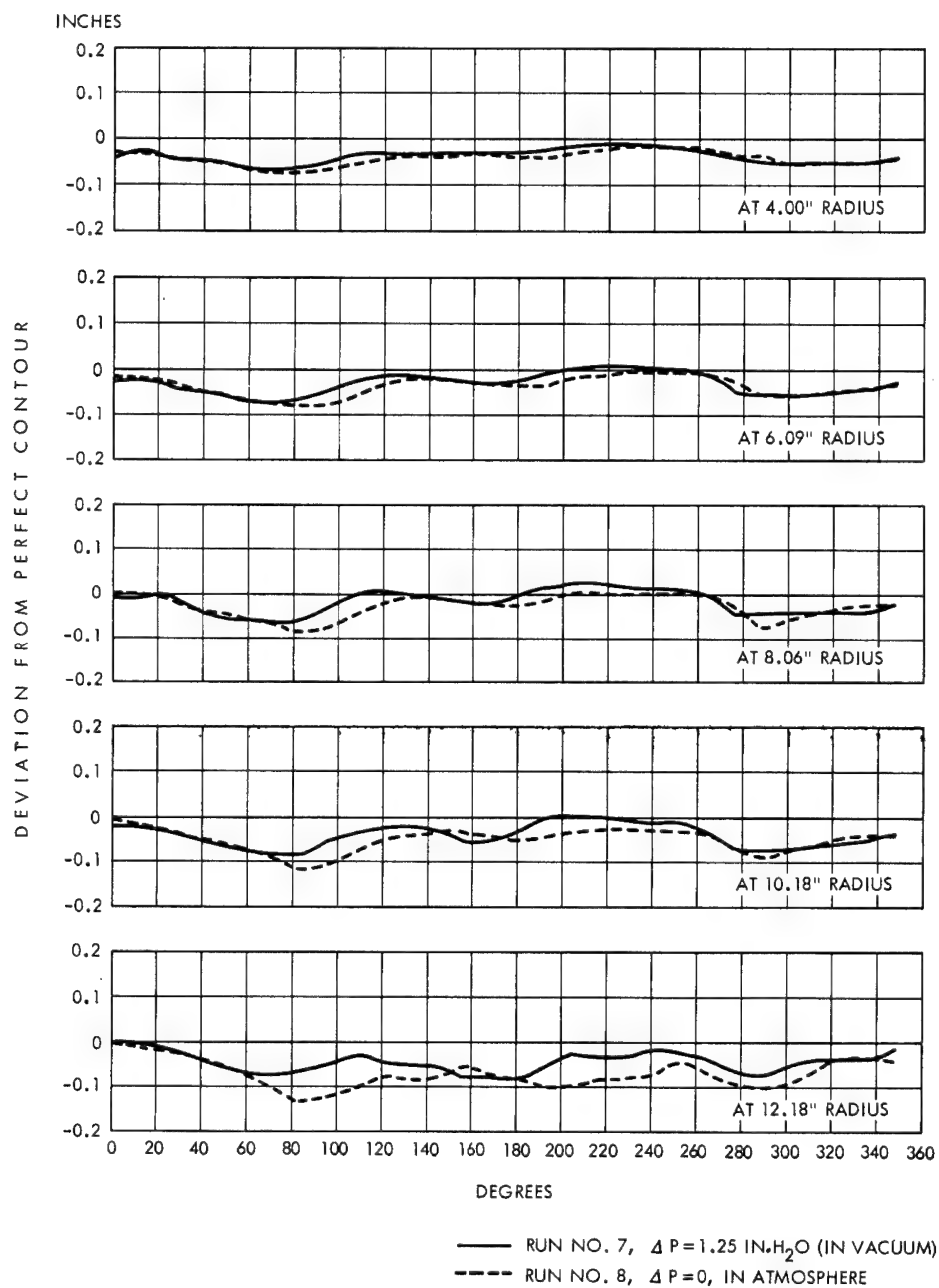


Figure G-8. Contour Comparison of Rigidized Mirror from all Stations in Vacuum and in Atmosphere - Mirror No. 1 (RISEC 918)

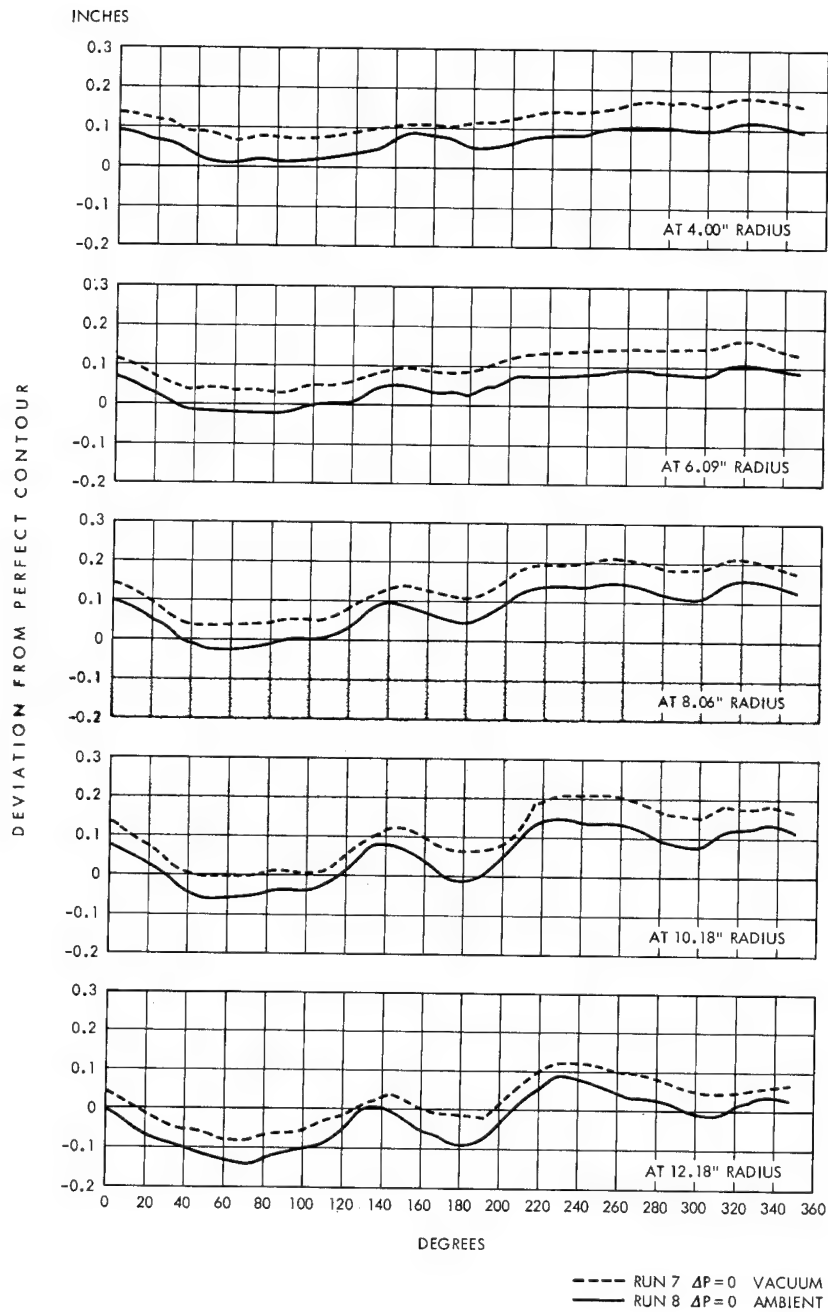


Figure G-9. Contour Comparison of Rigidized Mirror from all Stations in Vacuum and in Atmosphere - Mirror No. 3 (RISEC 929)

APPENDIX H. GEOMETRIC CONTOUR MEASURING FIXTURE

SECTION I. INTRODUCTION AND DESCRIPTION

A. INTRODUCTION

This manual contains test operation instructions for the Geometric Contour Measuring Fixture, fabricated by Goodyear Aerospace Corporation, Akron, Ohio, under Contract AF33(657)-10165, Task No. 314502. The instructions are prepared for personnel of the Aero Propulsion Laboratory, Research and Technology Division, Air Force Systems Command, Wright-Patterson Air Force Base, Ohio.

The fixture measures the accuracy of the 10-ft rigidized mirrors being produced under the solar concentrator research and development program.

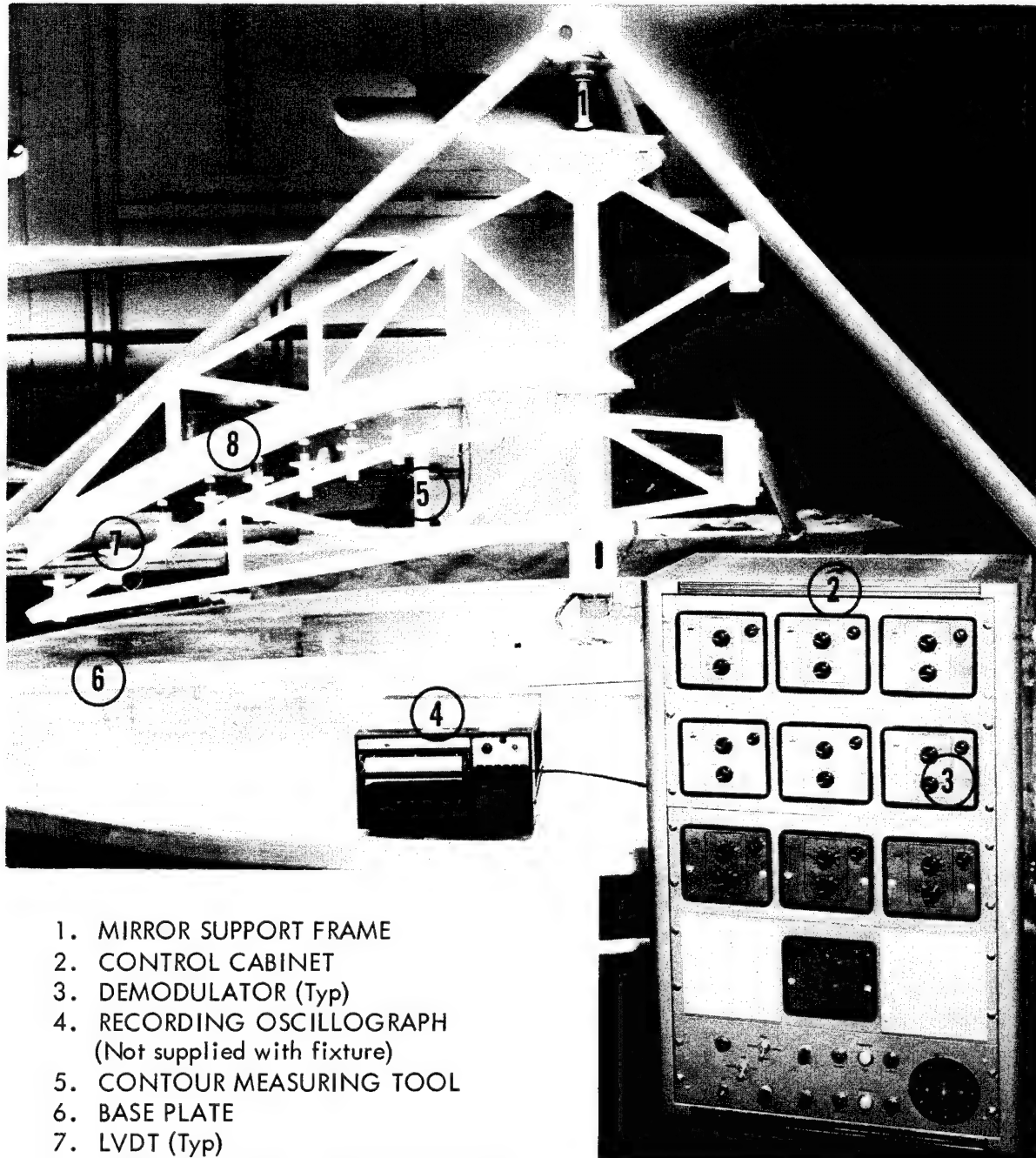
The contour of the mirror is compared with the design parabola. The highest possible mirror accuracy results when the calibrated fixture matches the mirror contour as nearly as possible with the design parabola contour.

B. LEADING PARTICULARS

- | | |
|--|---|
| 1. Length | 15 ft (approx) |
| 2. Width | 13.5 ft (approx) |
| 3. Height | 9 ft (approx) |
| 4. Weight | 500 lb (approx) |
| 5. Power Requirements | 115V, 60-cycle, a-c;
6 VDC at 1600 cps |
| 6. Environmental conditions limiting use | Designed for use in
a vacuum chamber. |

C. DESCRIPTION

The fixture (Figure H-1) consists basically of a mirror support frame, contour calibration fixture, contour measuring tool, base plate, and a control cabinet.



1. MIRROR SUPPORT FRAME
2. CONTROL CABINET
3. DEMODULATOR (Typ)
4. RECORDING OSCILLOGRAPH
(Not supplied with fixture)
5. CONTOUR MEASURING TOOL
6. BASE PLATE
7. LVDT (Typ)
8. CONTOUR CALIBRATION FIXTURE

Figure H-1. Geometric Contour Measuring Fixture with
Contour Calibration Fixture Installed

A recording oscillograph, not supplied with the fixture, is required for the test operation.

1. Mirror Support Frame

The tubular aluminum, tripod support frame receives the contour calibration fixture or mirror hub.

2. Contour Calibration Fixture

The face of the calibration fixture is machined to the design parabolic shape. When mounted on the support frame with the contour measuring tool, the calibration fixture adjusts the linear variable differential transformers (LVDT's) to electrical center.

3. Contour Measuring Tool

A drive motor at the base rotates the measuring tool over the mirror contour. The LVDT's on the tool produce an a-c voltage output proportional to the displacement of its moving element from electrical center.

4. Base Plate

The base plate serves as a mounting base for the mirror and permits mirror pressurization. Windows through the base plate provide pressure-tight connectors for the electrical circuitry and provide access to the contour measuring tool when the mirror is in place.

5. CONTROL CABINET

The control cabinet contains control switches for fixture operation and houses demodulators. The demodulators convert LVDT output to a direct signal for oscillograph operation.

APPENDIX H

D. CIRCUIT DESCRIPTION (See Figure H-2)

When connected to a 115 VAC, 60-cycle external power source, the control cabinet supplies a-c power to the LVDT's, the contour measuring tool drive motor, and the oscillograph.

The LVDT's receive power from the MAIN POWER switch through chamber wall connectors and base plate window connectors. The LVDT's measure electrical centers as indicated by the contour calibration fixture. Deviations from electrical center as the contour measuring arm sweeps the mirror contour are transformed into a-c voltage changes. The voltage changes are fed to the input of the demodulators where the signal is boosted through a transistorized amplifier, rectified with phase sensitivity, filtered, and converted to a current output.

The d-c voltage from the demodulators is recorded on the oscillograph paper.

The drive motor receives power from the MAIN POWER switch through the DRIVE MOTOR switch, chamber wall connectors, and base plate window connectors.



SECTION 2. PREPARATION FOR USE

Perform the following procedure to prepare the fixture for use. (See Figures H-1 and H-2.)

- a. Make certain that 115V 60-cycle, a-c power is connected to the control cabinet (2, Figure H-1).
- b. Move the ANGLE POS. switch to OFF.
- c. Move the DRIVE MOTOR switch to STOP.
- d. Move the MAIN POWER switch to ON.
- e. On the face of all demodulators (3, Figure H-1) turn the RANGE knob to REC. ZERO.
- f. On the recording oscillograph (4, Figure H-1), move the POWER switch to ON.

CAUTION

Allow the equipment to warm up for one-half hour.

SECTION 3. CALIBRATION

Zero calibration of the LVDT's is required before each mirror measurement. Perform the following procedure to calibrate the LVDT's. (See Figure H-1.)

CAUTION

Before starting calibration, perform the procedures in Section 2 to assure accuracy.

- a. Bolt the contour calibration fixture (8) to the mirror support frame (1) with 16 bolts, washers, and nuts.
- b. Tape down the plungers of LVDT's (7) on the contour measuring tool (5) as follows:
 - (1) Depress the Teflon button (1, figure H-3) on the tip of the rod to within approximately one-half inch of the nylon guide bushing (2, Figure H-3).

CAUTION

Do not completely compress the plunger spring (4, Figure H-3).

- (2) While holding the button in the depressed position, place masking tape over the button and secure to flange (3, Figure H-3) of the transformer support.

- c. Bolt the contour measuring tool to the contour calibration fixture.

CAUTION

Pushing the installed contour measuring tool to cause rotation may result in damage to the motor gear mechanism. Though the tool is easily rotated by hand, electrical operation only is recommended.

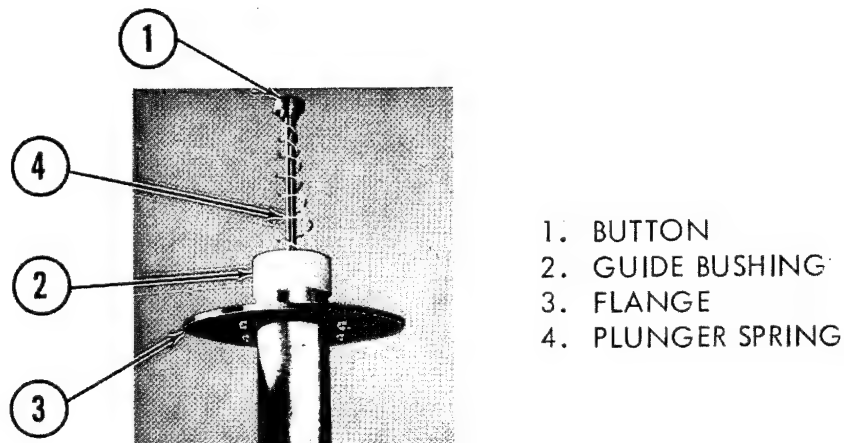


Figure H-3. Typical LVDT

d. Connect the plugs of cables No. 1 and 2 from the contour measuring tool to the similarly numbered receptacles in the top of the window in the support structure base plate (6).

NOTE: See Figure H-2 for electrical schematic.

e. Connect the plugs of the cable from the control cabinet (2) to the receptacles on the bottom of the window.

CAUTION

Make certain that No. 1 plug is connected to No. 1 receptacle.

f. Rotate the contour measuring tool to center the LVDT's under the contour calibration fixture, as follows:

- (1) Move the DRIVE MOTOR switch on the control cabinet panel to RUN.

NOTE: If the control cabinet motor is at 0 or 360 degrees as indicated on the POSITION indicator, the contour measuring tool will remain stationary until the PUSH TO START switch is pushed. If the control cabinet motor was stopped by the DRIVE MOTOR switch between the 0- and 360-degree limits, the contour measuring tool will begin to rotate (refer to NOTE following step 2).

(2) If the contour measuring tool is not rotating, push the PUSH TO START switch to override the limit switches of the system.

NOTE: From the 0-degree indication on the POSITION indicator, the motor, indicators, and contour measuring tool turn clockwise (FORWARD). From the 360-degree indication, the system rotates counterclockwise (REVERSE).

(3) Push the FWD or REV switch, as required, to change the rotation direction of the contour measuring tool.

(4) Move the DRIVE MOTOR switch to STOP to stop rotation of the contour measuring tool.

NOTE: Rotation automatically stops when the POSITION indicator is at 0 or 360-degrees.

g. Make certain that the demodulator RANGE knobs are at REC ZERO; then adjust the recording oscillograph galvanometers to give equal spacing between traces.

h. Adjust each LVDT as follows:

APPENDIX H

(1) Remove the tape and permit the button (1, Figure H-3) to seat against the contour measuring tool (5).

(2) Move the RANGE knob of matching numbered demodulator to ZERO SET.

NOTE: See Figure H-2 for electrical schematic.

(3) Rotate the demodulator ZERO ADJUST knob until the oscillograph trace returns to record zero position.

NOTE: If the ZERO ADJUST range is insufficient, adjust the LVDT position in the clamp as required.

(4) Mark the position of the ZERO ADJUST knob with tape or a marking pencil.

(5) Return the RANGE knob to REC ZERO.

(6) Retape the LVDT.

(7) Repeat steps (1) through (6) for each LVDT.

i. Remove the contour measuring tool (5) from the contour calibration fixture (8) and place the tool on the base plate (6).

j. Remove the contour calibration fixture (8) from the mirror support frame

(1). Remove the fixture from immediate area.

SECTION 4. TEST PROCEDURE

Perform the following procedure to test the mirror contour. (See Fig. H-1 and H-2.)

- a. Perform the procedures in Sections 2 and 3.

NOTE: Zero calibration is recommended once daily.

- b. Check electrical connections for security (see Figure H-2 for wiring schematic).

- c. Make certain that the recording oscillograph galvanometers are moving in the correct direction.

- d. Fix the mirror in place as shown in Figure H-1).

- e. Through the window in the base plate (6, Figure H-1), bolt the contour measuring tool (5, Figure 1) to the mirror hub.

- f. Remove tape from each LVDT (7, Figure H-1).

- g. Make certain that the ZERO ADJUST knob on each demodulator has not been moved.

NOTE: Knob must be at position marked during calibration.

- h. Gain access to REMOTE MOTOR switch through the back of the control cabinet (2, Figure H-1).

- i. Move the REMOTE MOTOR switch to OFF.

- j. On the control panel of the control cabinet, move the DRIVE MOTOR switch to RUN and make certain that the motor and POSITION indicator are functioning.

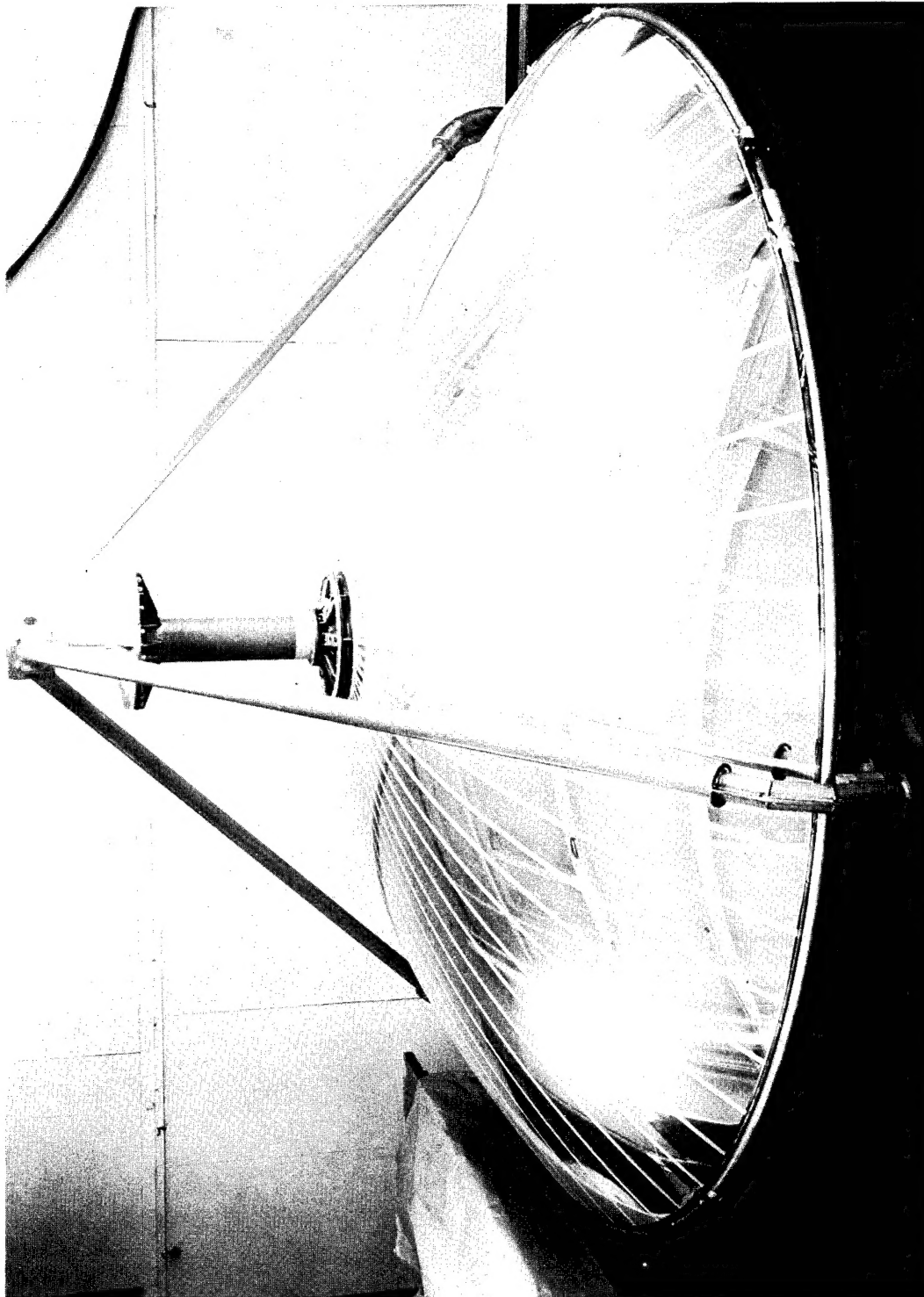


Figure H-4. Mirror Ready for Rigidization on Geometric
Contour Measuring Fixture

NOTE: With the REMOTE MOTOR switch in OFF, the control cabinet motor and POSITION indicator will normally function but the contour measuring tool drive will not operate.

- k. Return POSITION indicator to either 0 or 360 degrees; then move the DRIVE MOTOR switch to STOP.

NOTE: The control cabinet motor, POSITION indicator, and contour measuring tool are in alignment.

- l. Move the REMOTE MOTOR switch in back of the control cabinet to ON.
- m. While watching the oscillograph, place the ANGLE POS switch in the ON and OFF positions several times to make certain that the switch is functioning; then leave the switch in the OFF position.
- n. Inflate the mirror; then move the ANGLE POS switch to ON.
- o. With the demodulator RANGE knob in REC ZERO, run about 15 inches of oscillograph paper as a lead.
- p. Move the RANGE knob to the 250 setting.
- q. Start and run the oscillograph paper at the slowest possible speed.
- r. Move the MOTOR DRIVE switch to RUN.
- s. Rotate the contour measuring tool through 360 degrees and move the MOTOR DRIVE switch to STOP.
- t. Stop the oscillograph paper run.
- u. Rotate the demodulator RANGE knob to REC ZERO.
- v. Run about 15 inches of oscillograph paper.

APPENDIX H

- w. Move the ANGLE POS switch to OFF.
- x. Remove the trace from the oscillograph and check the mirror alignment.

NOTE: Read oscillograph paper from left to right as the paper comes from the oscillograph. Test run traces above record zero indicate high mirror; those below indicate low mirror.

- y. Repeat steps "n" through "x" each time a mirror measurement is made.

NOTE: Normally a 360-degree sweep is sufficient, and the contour measuring tool need not be returned to original position. When the sweep is made in the opposite direction, the traces on the oscillograph paper must be read the opposite way.

- z. When the runs are completed, move demodulator RANGE knob to OFF, and move MAIN POWER switch to OFF.

"The aeronautical and space activities of the United States shall be conducted so as to contribute . . . to the expansion of human knowledge of phenomena in the atmosphere and space. The Administration shall provide for the widest practicable and appropriate dissemination of information concerning its activities and the results thereof."

—NATIONAL AERONAUTICS AND SPACE ACT OF 1958

NASA SCIENTIFIC AND TECHNICAL PUBLICATIONS

TECHNICAL REPORTS: Scientific and technical information considered important, complete, and a lasting contribution to existing knowledge.

TECHNICAL NOTES: Information less broad in scope but nevertheless of importance as a contribution to existing knowledge.

TECHNICAL MEMORANDUMS: Information receiving limited distribution because of preliminary data, security classification, or other reasons.

CONTRACTOR REPORTS: Technical information generated in connection with a NASA contract or grant and released under NASA auspices.

TECHNICAL TRANSLATIONS: Information published in a foreign language considered to merit NASA distribution in English.

TECHNICAL REPRINTS: Information derived from NASA activities and initially published in the form of journal articles.

SPECIAL PUBLICATIONS: Information derived from or of value to NASA activities but not necessarily reporting the results of individual NASA-programmed scientific efforts. Publications include conference proceedings, monographs, data compilations, handbooks, sourcebooks, and special bibliographies.

Details on the availability of these publications may be obtained from:

SCIENTIFIC AND TECHNICAL INFORMATION DIVISION
NATIONAL AERONAUTICS AND SPACE ADMINISTRATION

Washington, D.C. 20546